Dynamics of *Shigella* intracellular replication and plasmid maintenance



Jessica E Martyn

Sir William Dunn School of Pathology

Exeter College

University of Oxford

A thesis in fulfilment of the requirements for

the degree of Doctor of Philosophy

Trinity Term 2018

Dynamics of *Shigella* intracellular replication and plasmid maintenance

Jessica E Martyn

DPhil Pathology, Trinity Term 2018, Exeter College

Abstract

Shigella spp. are human specific bacterial pathogens that are an important cause of diarrhoeal disease worldwide. *Shigella flexneri* can invade into epithelial cells, and survive within the intracellular compartment. Escape from the vacuole and replication in the host cell cytosol are critical for *S. flexneri* virulence. However, little is known about the basis of bacterial replication inside host cells. There are significant limitations with current methods to study intracellular replication, so fluorescence dilution, which has been developed for studying intracellular salmonellosis was applied to understand the dynamics of *S. flexneri* survival at a single cell level. Limitations of fluorescence dilution became apparent when it was used to examine interactions of bacteria with non-phagocytic cells.

All species of *Shigella* express a Type III secretion system (T3SS) which is essential for virulence and encoded on a pathogenicity island (PAI). The T3SS PAI is located on a large > 210 kb virulence plasmid, pINV, which is present as single copy in the bacterium. *S. flexneri* loses pINV during growth in the laboratory, but the mechanisms governing its maintenance are largely unaffected by environmental conditions except the ambient temperature. *Shigella sonnei* is increasingly becoming an emerging pathogen, which loses pINV at a higher rate than *S. flexneri*. Toxin-antitoxin systems on *S. flexneri* and *S. sonnei* contribute to the vertical transmission of pINV in *Shigella* populations by mediating post-segregational killing (PSK).

Single nucleotide polymorphisms in the Toxin-Antitoxin (TA) system, VapBC, from *S. sonnei* and *S. flexneri* have a profound effect on plasmid retention. Additionally, I demonstrated that the genetic background influences the ability of TA systems to mediate PSK and therefore plasmid maintenance. This is due to the different profiles of the target of VapC, $tRNA^{fMet}$, in *Shigella* spp. and *E. coli*. Subtle differences in plasmid maintenance systems and the targets of TA systems can have profound effects on plasmid biology.

Acknowledgments

As everyone knows nothing in life is achieved alone. I am ever grateful for the people around me. I would first like to thank Prof. Christoph Tang for his supervision. I would not have been here or completed this thesis without the vision and tenacious faith of Chris. I am eternally grateful for the opportunity and the privilege to do a DPhil in his lab.

I would like to say thank you to Tang lab members past and present. I would like to thank; Dr. Sarah Hollingshead who solved the structure of VapBC from *S. sonnei* and helped me with the analysis; Guangyu Liu and Dr. Gareth McVicker for the use of plasmids and strains used in this study; and Dr. Lindsay Stimson for proofreading this work. In particular I would like to thank Giulia Pilla and Dr. Emeline Lawarée for their daily support and encouragement. Without Giulia and Emeline, I don't think I would be here writing these words.

I would especially like to thank Prof. Tracy Palmer who encouraged me from undergraduate to pursue a PhD. Tracy not only recognised my love of science but also my total lack of self-confidence, and without Tracy's guidance and continued mentorship I wouldn't be at Oxford or have finished my DPhil.

I would like to thank my family who have patiently and lovingly listened and supported me these past four years. My parents set by example the kind of person I wanted to become. They showed me not to be afraid to try things and choose courage over comfort. I would not be the person I am or have achieved this DPhil without them. I would like to thank both of them individually for steadfastly loving and supporting me.

Finally, I would like to thank John for his patience and his love these four years.

Words are never enough but words are what I have, so thank you. Thank you all so much.

Jessica

Table of Contents

ABSTRACT 2

1 ..... CHAPTER ONE INTRODUCTION 16

1.1 Microbiology of *Shigella* spp. 16

1.2 Evolution of *Shigella* spp. from *E. coli* 17

1.3 Epidemiology of shigellosis 18

1.4 Symptoms of shigellosis 20

1.5 Treatment of shigellosis 21

1.6 *Shigella* virulence 21

1.7 The large *Shigella* virulence plasmid, pINV 22

1.8 Chromosomal virulence genes 26

1.9 Regulation of virulence 27

1.10 Pathogenesis 30

1.10.1 Transit in the gastrointestinal tract 30

1.10.2 M cells and intracellular survival of *Shigella* spp. in phagocytes. 32

1.10.3 Epithelial intracellular survival and replication 33

1.10.4 *Shigella* spp. manipulates host immune responses 35

1.11 Intracellular nutrition 37

1.12 Measuring intracellular replication 39

1.13 Biology of the large *Shigella* spp. virulence plasmid (pINV) 42

1.13.1 pINV replication and copy number 43
1.13.2 *S. flexneri* pINV plasmid stability 44
1.13.3 Partitioning systems 46
1.13.4 Toxin-Antitoxin systems 46
1.13.5 pINV maintenance 50
1.14 CcdAB 51
1.15 VapBC 52
1.16 Type II Toxin-Antitoxin systems with GNAT fold toxins 55
1.17 Aims 56

2 CHAPTER TWO MATERIALS AND METHODS 57

2.1 Bacterial strains and growth 57
2.2 Antibiotics 57
2.3 Bacterial strains and plasmids 58
2.4 Bacterial growth 60
2.5 Bacterial growth measured by flow cytometry 60
2.6 *Shigella sacB-kan*^{r} marker loss assay 61
2.7 Tissue culture cell lines and growth conditions 61
2.8 Infection of eukaryotic cells with *Shigella flexneri* 62
2.8.1 Infection of HeLa cells 62
2.8.2 Infection of THP-1 cells 63
2.9 Intracellular replication measured by flow cytometry 63
2.10 Isolation of DNA 64
2.11 Polymerase chain reaction (PCR) 64
2.12 Restriction endonuclease digestion of DNA 68
2.13 DNA ligations 68

2.14 NEBuilder® HiFi DNA Assembly 68
2.15 Transformation of *E. coli* 68
2.16 Transformation of *S. flexneri* 69
2.17 Genetic manipulation 70
2.17.1 Lambda red-based recombination 70
2.17.2 Conjugation 71
2.18 Transduction 72
2.19 DNA sequencing 72
2.20 Analysis of nucleotide and amino acid sequences 72
2.21 Statistics 72

3 CHAPTER THREE DETERMINING THE DYNAMICS OF *S. FLEXNERI* INTRACELLULAR REPLICATION AT THE SINGLE-CELL LEVEL 73

3.1 Validation of fluorescence dilution (FD) in *S. flexneri* pDiGc *in vitro* 74
3.2 Validation of FD of *S. flexneri* pDiGc *in vivo* 81
3.3 Construction of pDiGc^{cam} as a new fluorescence dilution tool to measure *in vivo* replication 85
3.4 Assessment of growth conditions for *S. flexneri* pDiGc^{cam} 86
3.5 Validation of FD in *S. flexneri* pDiGc^{cam} *in vitro* 88
3.6 Use of β-lactam antibiotics to eliminate extracellular bacteria 94
3.7 DsRed reduces the sensitivity of fluorescence dilution 103
3.8 Discussion 107

4 CHAPTER FOUR INVESTIGATION OF PINV MAINTENANCE 113

4.1 VapBC is important for pINV stability 115
4.2 The role of TA systems on pINV stability is not altered at 42°C 117

4.3 The role of VapBC on pINV stability is affected by amino acid limitation..119

4.4 The role of VapBC is altered during anaerobic growth conditions 122

4.5 The role of TA systems on pINV stability is not altered in acidic conditions124

4.6 The role of TA systems during replication of *S. flexneri* in THP-1 cells 127

4.7 *S. flexneri* requires a functional T3SS to replicate inside THP-1 cells 130

4.8 Construction of *S. flexneri* with *sacB-kan*^{r} in an intergenic region of pINV (Ig::*sk*) 132

4.9 Validation of Ig::*sk* for measuring plasmid loss *in vivo*.....134

4.10 The *sacB-kan*^{r} marker in the *virB-ipaJ* intergenic region does not impede *S. flexneri* replication in THP-1 cells. 138

4.11 VapBC is not required to stabilise pINV in THP-1 cells. 140

4.12 Discussion 142

5..... CHAPTER FIVE INVESTIGATION OF THE INFLUENCE OF GENETIC BACKGROUND IN PLASMID MAINTENANCE.....148

5.1 pSTAB2 a plasmid to study the role of individual elements on plasmid maintenance.....149

5.2 VapBC^{Sf} reduces pSTAB2 loss in *S. flexneri* but not *E. coli* DH5α.....151

5.3 VapC cleavage sites and analysis of tRNA^{fMet} alleles.....153

5.4 tRNA^{fMet} profiles affects the impact of VapBC on pSTAB2 loss 155

5.5 tRNA^{fMet2} reduces the impact of VapBC^{Sf} on pSTAB2 loss 157

5.6 Introduction of tRNA^{fMet2} into *S. flexneri* reduces the impact of VapBC^{Sf} on pSTAB2 loss 159

5.7 Generation of *E. coli* MG1655 expressing only tRNA^{fMet2} 161

5.8 Comparison of VapBC from *S. flexneri* and *S. sonnei* 163

5.9 VapBC^{Ss} is less efficient at reducing pSTAB2 loss than VapBC^{Sf} 167

5.10 VapC^{Ss} is sufficient to increase pSTAB2 loss 168

5.11 Background *Shigella* spp. effects impact of VapBC^{Ss} on pSTAB2 loss 170

5.12 VapBC^{Ss} is not effective at maintaining pSTAB2 in *E. coli.* 172

5.13 Discussion 174

6 ..... CONCLUSION 183

List of Figures

Figure 1.1 Circular map of *S. flexneri* pINV 23

Figure 1.2 Map of part of *S. flexneri* pINV 25

Figure 1.3 Environmental regulation of virulence 29

Figure 1.4 *Shigella* spp. host pathogen interaction 32

Figure 1.5 Carbon energy sources used by *S. flexneri* in epithelial cells..... 38

Figure 1.6 Schematic of Fluoresence Dilution, pDiGc 40

Figure 1.7 Schematic of the bacterial TIMER, pBR322 41

Figure 1.8 Schematic *M. Tuberculosis Erdman* chromosomal TIMER 42

Figure 1.9 Mechanism of antisense RNA-mediated plasmid copy number control.44

Figure 1.10 Schematic representation of potential plasmid maintenance systems on *Shigella* spp. pINV. 45

Figure 1.11 Toxin-Antitoxin types 48

Figure 1.12 Model for DNA binding and activation of VapBC TA systems. 54

Figure 3.1 The FD plasmid, pDiGc 75

Figure 3.2 Fluorescence conferred by pDiGc in *S. flexneri.* 76

Figure 3.3 Stability of DsRed from pDiGc in *S. flexneri.* 78

Figure 3.4 Use of FD to assess growth of *S. flexneri in vitro* 80

Figure 3.5 Invasive and intracellular replication capacity of *S. flexneri* pDiGc..... 82

Figure 3.6 Intracellular replication of *S. flexneri* pDiGc in HeLa cells detected by FD. 84

Figure 3.7 Maintenance of pINV and pDiGc^{cam} in *S. flexneri*. 87

Figure 3.8 Fluorescence conferred by pDiGc^{cam} in *S. flexneri*. 89

Figure 3.9 Stability of DsRed from pDiGc^{cam} in *S. flexneri.* 91

Figure 3.10 Use of pDiGc^{cam} to assess growth of *S. flexneri in vitro* 93

Figure 3.11 Sensitivity of *S. flexneri* to penicillin G. 95
Figure 3.12 Invasion assays using penicillin G to remove extracellular bacteria ... 97
Figure 3.13 Invasion assays using cefsulodin to remove extracellular bacteria 99
Figure 3.14 Intracellular replication of *S. flexneri* pDiGc^{cam} in HeLa cells using FD102
Figure 3.15 Fluorescence from DsRed is affected by growth conditions. 104
Figure 3.16 Invasion and intracellular replication comparing stationary and mid-log bacteria. 106
Figure 3.17 Schematic of ChromFD 111
Figure 4.1 VapBC is important for pINV stability at 37°C. 116
Figure 4.2 The role of TA systems on pINV stability at 37°C and 42°C. 118
Figure 4.3 The role of VapBC on pINV stability is affected by availability of amino acids. 121
Figure 4.4 The role of TA systems on pINV stability altered in anaerobic growth conditions. 123
Figure 4.5 The role of TA systems on pINV stability at pH 7, pH 6 and pH 5. 126
Figure 4.6 Effect of TA systems on plasmid marker loss in THP-1 cells. 129
Figure 4.7 *Shigella* require a functional T3SS to replicate inside THP-1 derived macrophages 131
Figure 4.8 Schematic of *sacB-kan*^{r} in the *virB*/*ipaJ* intergenic region 133
Figure 4.9 The *sacB-kan*^{r} marker in the *virB/ipaJ* intergenic region does not affect bacterial growth in TSB. 135
Figure 4.10 The effect of position of the *sacB-kan*^{r} marker on pINV stability 137
Figure 4.11 The dual marker in *S. flexneri* (Ig::*sk*) does not impede replication in THP-1 macrophages. 139
Figure 4.12 VapBC is not required to stabilise pINV in THP-1 cells. 141

Figure 5.1 pSTAB2, a vector to measure plasmid maintenance/loss 150

Figure 5.2 VapBC^{Sf} reduces pSTAB2 loss in *S. flexneri* but not *E. coli* DH5α 152

Figure 5.3 VapC cleavage site and tRNA^{fMet} alleles 154

Figure 5.4 tRNA^{fMet} profile affects the impact of VapBC^{Sf} on pSTAB2 loss 156

Figure 5.5 tRNA^{fMet2} reduces the impact of VapBC^{Sf} on pSTAB2 loss 158

Figure 5.6 Introduction of tRNA^{fMet2} into *S. flexneri* reduces the impact of VapBC^{Sf} on pSTAB2 loss 160

Figure 5.7 The effect of four tRNA^{fMet2} on the impact of VapBC^{Sf} pSTAB2 loss ... 162

Figure 5.8 Nucleotide and protein alignments of VapBC^{Sf} and VapBC^{Ss} 164

Figure 5.9 Superimposition of VapBC^{Sf} on VapBC$^{Ss.}$ 166

Figure 5.10 VapBC^{Sf} is more effective in reducing pSTAB2 loss than VapBC^{Ss}.. 167

Figure 5.11 VapC^{Ss} is sufficient to increase pSTAB2 loss..... 169

Figure 5.12 VapBC^{Sf} is more effective in reducing pSTAB2 loss than VapBC^{Ss} in *S. sonnei* 171

Figure 5.13 VapBC^{Ss} is not effective at maintaining pSTAB2 in *E. coli* 173

Figure 5.14 tRNA tertiary structure interactions 175

Figure 5.15 VapBC amino acid sequence alignments from EIEC and *Shigella* spp. 180

Figure 5.16 Nucleotide alignment highlighting polymorphisms in tRNA^{fMet} in *Shigella* spp. 181

List of Tables

Table 2.1 Bacterial strains used in this study 58

Table 2.2 Bacterial strains and plasmids used in this study 59

Table 2.3 List of primers used for PCR 66

Table 5.1 $tRNA^{fMet}$ profile in *E. coli* and *Shigella* spp. 178

Table 5.2 $tRNA^{fMet}$ polymorphism profile in different *Shigella* spp. 181

List of Appendices

Appendix 1 Geometric mean fluorescence of GFP and DsRed from HeLa infection with *S. flexneri* pDiGc 188

Appendix 2 Geometric mean fluorescence of DsRed from HeLa infection with *S. flexneri* $pDiGc^{cam}$ 189

Appendix 3 Geometric mean fluorescence of DsRed from THP-1 infection with *S. flexneri* $pDiGc^{cam}$ 190

Appendix 4 Geometric mean fluorescence of DsRed from Ig::*sk* THP-1 infection with *S. flexneri* $pDiGc^{cam}$ 191

Abbreviations

amp	ampicillin
carb	carbenicillin
cam	chloramphenicol
Ccd.	coupling cell division system
CFU	Colony forming units
CR	Congo red
DAP	diaminopimelic acid
DsRed	Discosoma red
FD	fluorescence dilution
FCS	Foetal bovine calf serum
fMet	formylated methionine
HeLa	Henrietta Lacks cells
GFP	green fluorescent protein
GNAT	GNC5 related N acetyltransferase
GmvAT	GNAT maintenance of virulence Antitoxin Toxin
hr	hour
IS	Insertion sequence

kan	kanamycin
kb	kilobase
K_M	Michaelis constant in Michaelis–Menten kinetics
LB	Lennox L Broth Base
LPS	Lipopolysaccharide
MCS	Multiple cloning site
min	minutes
MOI	Multiplicity of infection
Mxi	Membrane expression of invasion plasmid antigens
OD	Optical density
ORF	Open reading frame
PAI	Pathogenicity Island
PFA	paraformaldehyde
pINV	*Shigella* virulence plasmid
PMN	polymorphonuclear neutrophil
pen	penicillin G
PBS	phosphate buffered saline
PCR	polymerase chain reaction

RT	room temperature
RNA	Ribonucleic acid
rRNA	ribosomal RNA
mRNA	messenger RNA
sec	seconds
SD	Standard deviation
Spa	Surface presentation of antigen
T3SS	Type III secretion system
TA	Toxin-Antitoxin
THP-1	Monocyte
tRNA	Transfer RNA
TSB	Tryptic Soy Broth
tet	tetracycline
VapBC	Virulence associated protein B/C

1 Chapter One Introduction

Shigellosis is an acute intestinal disease caused by members of the genus *Shigella*. Infection is characterised by bacterial invasion of the intestinal epithelial cells lining the terminal ileum and colon (1, 2). Bacterial invasion results in inflammation in the sub-epithelial tissue and destruction of the mucosal layer. The symptoms of shigellosis range from mild watery diarrhoea to severe dysentery (3). Infection with *Shigella* spp. is estimated to cause 188 million cases worldwide each year with 164,300 deaths particularly in young children in regions with low income (4, 5). Factors that promote the transmission of *Shigella* include its low infectious dose (10-100 bacteria (6)), poor sanitation and hygiene, and the lack of available treatment (3). First-line therapy with antibiotics is increasingly ineffective with the rise in antimicrobial resistance (AMR) in *Shigella* spp. (7, 8). The continuing human cost of shigellosis and the threat posed by AMR have prompted increased efforts to understand its mechanisms of pathogenesis and to discover novel approaches for therapy and vaccine targets.

1.1 Microbiology of *Shigella* spp.

Shigella spp. are facultative anaerobic, Gram-negative, non-motile, non-sporulating, ~1 to 3 µM long bacilli belonging to the Enterobacteriaceae family (2). The genus *Shigella* is composed of four species (also referred to as groups or subgroups), *Shigella flexneri*, *Shigella sonnei*, *Shigella dysenteriae*, and *Shigella boydii* (2). In contrast to *Escherichia coli*, *Shigella* spp. are non-lactose fermenters, with the exception of *S. sonnei* which is a late lactose fermenter (9). Additionally *Shigella* do not decarboxylate lysine (10).

Each species is subdivided into serotypes and sub-serotypes based on the composition of the O-antigen portion of lipopolysaccharide (LPS). *S. dysenteriae*

(Group A) was the first species recognised, and characteristically expresses the Shiga toxin; this species has 15 serotypes. *S. flexneri* (Group B) has 14 serotypes, while *S. boydii* (Group C) has been classified into 20 serotypes; there is a single serotype of *S. sonnei* (Group D) (11).

Andre Chantemesse and Fernand Widal first described bacillary dysentery in 1888 (12). However, Kiyoshi Shiga first cultured the causative agent from faeces using alkaline media in 1898 during an outbreak in Japan (13). This strain, which Shiga called *Bacillus dysenteriae* is now referred to as *S. dysenteriae* serotype 1. Two years later Simon Flexner isolated *Shigella flexneri* (14), then in 1915 Carl Sonne isolated a lactose late fermenter as the main causative agent of dysentery in Denmark (15). *S. sonnei* resembled *S. flexneri*, but it did not agglutinate in the presence of anti-*S. flexneri* or anti-*S. dysenteriae* serum (15). In the 1930s, J.S.K. Boyd discovered another species in Bangalore which was named *S. boydii* (16).

1.2 Evolution of *Shigella* spp. from *E. coli*

The emergence of *Shigella* spp. is an example of convergent evolution, as members of the genus have evolved from *E. coli* on four independent occasions resulting in the four *Shigella* species (9). *S. dysenteriae*, *S*. *flexneri* and *S*. *boydii* are estimated to have diverged from *E. coli* between 35,000 to 270,000 years ago (9). However, *S. sonnei* is thought to have arisen more recently, diverging around 10,000 years ago (17). Overall the genomes of *E. coli* and *Shigella* spp. have a sequence difference of around 1.5 % and are highly syntenic (9). The horizontal acquisition of genetic elements such as the large virulence plasmid, pINV, and several chromosomal pathogenicity islands have had a pivotal role in the evolution of *Shigella* (9).

In addition to gaining genetic information, many pathogens, including *Shigella* spp., have undergone genome reduction and lost non-essential genes which are dispensable or detrimental for their survival (10). On average, 726 genes have been deleted from *Shigella* spp. compared to *E. coli*, with a further 200 pseudogenes (18, 19). The inability of *Shigella* spp. to ferment lactose is due to the inactivation of a large proportion of the genes necessary for this activity (19). Additionally, genes that inhibit virulence have been lost. For example *Shigella* spp. are unable to decarboxylate lysine and produce cadaverine, because *cadA*, which encodes lysine decarboxylase 1, has been deleted by different events; cadaverine attenuates *Shigella* virulence by inhibiting the activity of *Shigella* enterotoxins (10). *Shigella* spp. infection promotes polymorphonuclear leukocyte (PMN) migration which subsequently destroy the integrity of the epithelial lining, allowing more bacteria to reach the submucosal layer (2). Cadaverine also acts on intestinal epithelial cells to abolish signalling to PMN, attenuating inflammatory responses (20). Another example of gene inactivation affects the synthesis of nicotinamide adenine dinucleotide (NAD) in *Shigella* spp.; the NAD precursor quinolinate inhibits virulence (21, 22). Additionally in comparison to *E. coli*, *Shigella* spp. do not express functional flagella (23). The genetic defect responsible for loss of flagella varies between strains and is an example of convergent evolution leading to loss of motility (23). A possible reason for this is that the absence of flagellin prevents recognition *via* host Toll-like receptor 5 ,TLR-5 (23).

1.3 Epidemiology of shigellosis

Humans are the only natural host for *Shigella* spp. which is transmitted by the faecal-oral route through the consumption of contaminated food or water (3). Transmission is promoted in conditions where sanitation and hygiene are poor, and there is limited access to clean water (3); *Shigella* can persist in water for several months (24).

Additionally, monsoons and tsunamis are associated with epidemics of shigellosis, by compromising water supply and sanitation (25). *Shigella* is also spread by direct person to person contact (3). As few as 10 bacteria of *S. dysenteriae* type I, and < 200 colony forming units (CFU) of *S. flexneri* or *S. sonnei* are sufficient to produce symptomatic infection in human volunteers (6).

Shigella spp. have their own global burden and epidemiological profile (26). The distinct geographical distribution is, in part, related to the level of economic development and poverty (27). *S. flexneri* is the leading cause of shigellosis in economically developing countries, whereas *S. sonnei* is the predominant pathogen in more wealthy countries (27). When China underwent rapid industrialisation, there was a five-fold increase in *S. sonnei* infections between 2003 and 2013 (28, 29). Recently there has been a significant rise in cases caused by *S. sonnei* in Bangladesh, probably due to improvements in sanitation (30). *S. flexneri* and *S. sonnei* account for the majority of shigellosis (26) while *S. boydii* and *S. dysenteriae* infrequently cause dysentery (26). Infection with *S. dysenteriae* type I is infrequent, causing sporadic outbreaks in settings such as refugee camps and among other displaced individuals living in impoverished circumstances (3, 26). The last major outbreak of *S. dysenteriae* type I was in 1999 in Sierra Leone during the civil war, which killed around 4000 people (31). As global public health improves, it is likely that *S. sonnei* will increase in global importance.

Children under five are particularly susceptible to shigellosis. Indeed *Shigella* spp. are a leading cause of childhood morbidity and mortality in low and middle-income countries (32). The case-control, Global Enteric Multicentre Study (GEMS) examined the causes of acute, medically treated moderate-severe diarrhoeal disease among

children younger than five living in sub-Saharan Africa and South East Asia (33). *Shigella* spp. were the most common aetiological agent in children aged 24-59 months and the second most common aetiological agent in children aged between 12-23 months; when samples from this study were reanalysed using quantitative PCR, the attributable incidence of *Shigella* doubled (5).

In the 1970s, shigellosis was increasingly observed among men who have sex with men (MSM) (3). Behaviours such as unprotected anal sex, oro-anal contact, and multiple sexual partners are thought to have led to the increase (3). In 2009, an outbreak of *S. flexneri* 3a occurred among MSM in England and Wales (34). Those with HIV and who were immunocompromised experienced persistent and/or relapsing shigellosis (34).

Shigellosis is also associated with travel. Around 536 million people travel from richer to low- or middle-income countries annually, and 10-40 % develop a diarrhoeal illness, 3-9 % of which are caused by *Shigella* spp. (35) Additionally, outbreaks of shigellosis have occurred in residential institutions such as prisons and care homes, as well as among children in day care (36).

1.4 Symptoms of shigellosis

The incubation period of shigellosis is typically one to four days but can be up to six days with *S. dysenteriae* type I (37). Initial symptoms include fever, headache and vomiting, followed several hours later by the abrupt onset of watery or blood stained diarrhoea (3). Symptoms can vary depending on age, immune status, and nutrition. In previously healthy individuals, symptoms are usually mild and subside in a few days (3). However, some people suffer from the sudden onset of dysentery, characterised by frequent bloody stools with fever and abdominal cramps (3). In young or

immunocompromised patients, *Shigella* spp. can cause a systemic infection, resulting in meningitis, osteomyelitis, arthritis, or splenic abscess (38). Shigellosis in young infants can mimic intussusception or necrotising enterocolitis (39). Further complications depend on the infecting species, inoculum, and host human leukocyte antigen (HLA) subtype, and include Haemolytic-Uremic Syndrome (HUS). HUS is caused by the Shiga toxin attaching to glycosphingolipid Gb3 on endothelial cells and activating platelets which also adhere to the endothelium and occlude blood vessels. This leads to microangiopathic haemolysis renal failure, and thrombocytopaenia, with an overall mortality rate of 35% (40). Further complications with *S. dysenteriae* type I infection include rectal prolapse, intestinal obstruction, toxic megacolon, and intestinal perforation (3).

1.5 Treatment of shigellosis

In contrast to other enteric infections such as cholera, bacillary dysentery does not benefit from oral rehydration alone. Antibiotics have been shown to reduce the duration of fever and diarrhoea by 1-2 days, and pathogen spread is interrupted, reducing the risk of person-to-person transmission (3). The emergence of AMR is reducing the efficacy of treatment, while the only rational approach for prevention would be vaccination. Over the past 60 years, multiple *Shigella* vaccine candidates have been explored, but there are no currently licensed vaccines against this bacterium.

1.6 *Shigella* virulence

Shigella spp. are characterised by their ability to invade into epithelial cells and replicate within the intracellular compartment. The first description of *Shigella* spp.

invading epithelial cells was in 1964 (1). Before this, dysentery caused by *Shigella* spp. was thought to be mediated by secreted bacterial exotoxins (41).

Initial studies to define genes necessary for virulence in *Shigella* were focused on the chromosome, but were relatively unrevealing (42). Instead, the main genetic element responsible for virulence in all *Shigella* spp. has been identified as the large virulence plasmid (43, 44).

1.7 The large *Shigella* virulence plasmid, pINV

Plasmids are extrachromosomal DNA molecules, which can carry genes that provide fitness benefits to their host, such as virulence or AMR. Studies in 1980 first indicated that a plasmid was responsible for *Shigella* virulence (43, 44). *S. sonnei* was found to have two colony morphologies. Phase I colonies were smooth small colonies that were virulent. During growth, phase II colonies, which were large and had a rough morphology, arose spontaneously and did not revert to phase I colonies. The differences between the two phases was the presence in virulent bacteria or absence in avirulent bacteria of a large plasmid, pINV (43, 44). This was also observed in *S. flexneri* (45). Transfer of pINV from *S. flexneri* into *E. coli* was sufficient to confer invasion of mammalian cells (46).

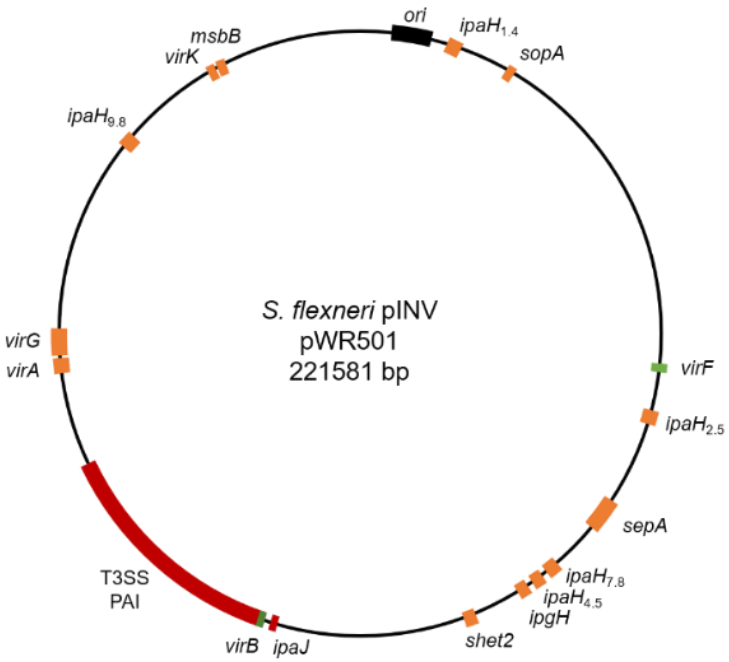


Figure 1.1 Circular map of *S. flexneri* pINV

The map shows the origin of replication (black) and the T3SS PAI (red) and genes encoding transcriptional regulators (in green) and other virulence associated genes (in orange). Schematic representation of genomic description from Vankatesan *et al*. 2001 (48)**.**

All known pathogenic strains of *Shigella* harbour pINV. The most characterised example is pWR100 from *S. flexneri* M90T (Figure 1.1), a serotype 5a strain (47). Subsequently, a 31 kb pathogenicity island (PAI) was found on pINV which restored invasion to plasmid-less *S. flexneri*. (49). The PAI encodes a Type III Secretion System (T3SS) as well as several secreted effectors (2). The T3SS is a molecular syringe that allows bacteria to deliver protein effectors across eukaryotic cellular membrane (50). The T3SS is essential for *Shigella* spp. invasion of epithelial cells, intracellular replication, and inducing pyroptosis, a pro-inflammatory form of programmed cell death, driven by stimulation of the pore-forming activity of gasdermin D and

accompanied by the release of pro-inflammatory cytokines, such as IL-1β and IL-18 (49, 51-53).

A total of 286 open reading frames have been identified on *S. flexneri* pINV. 58 kb of the plasmid is homologous to known or putative insertion sequences (ISs), suggesting a history of IS-mediated acquisition of DNA (48, 54). Insertion sequences are short transposable DNA elements that can move within the same DNA molecule or between different DNA molecules. They are composed only of genes encoding proteins involved in mobility, such as transposases and regulatory elements. Analysis of the GC content, position and function of genes in pINV indicates that the plasmid contains blocks of genes from various origins (47). The T3SS PAI is flanked by IS*100* and IS*600*, but does not contain any IS elements (unlike the remainder of the plasmid) indicating that it was acquired by *Shigella* spp. from a common ancestor (48).

The T3SS PAI contains 34 genes that are organised into two clusters (Figure 1.2), transcribed in opposite directions (2). One cluster includes the *ipa* (Invasion plasmid antigen) genes which encode secreted effectors, including IpaA, IpaD, IpaC, IpgB, IscB and IpgD, which target eukaryotic cell functions (2). The second cluster of genes in the PAI are the *mxi* (Membrane expression of *ipa*) and *spa* (Surface presentation of antigen) genes which are responsible for the assembly and activity of the T3SS (2). A third gene cluster on the PAI include two transcriptional activators, VirB and MxiE (2). Another cluster of genes in the PAI encode other chaperones, IpgA, IpgC, IpgE and Spa15 (2).

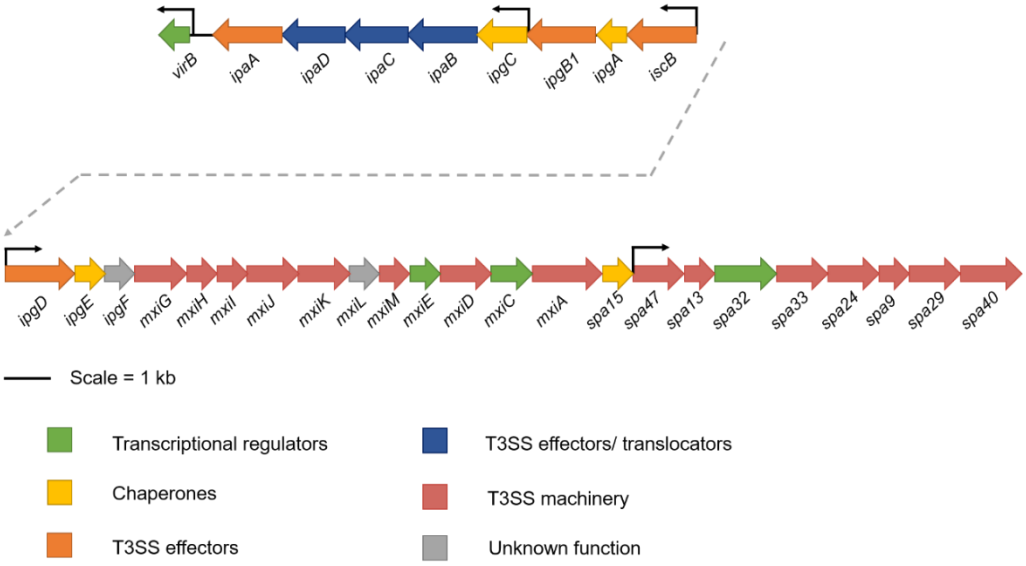


Figure 1.2 Map of part of *S. flexneri* pINV

Schematic of the 31 kb entry region on the *S. flexneri* pINV, which is essential for invasion of epithelial cells and pyroptosis of macrophages. Genes are shown which encode the structural components of the T3SS apparatus (in red), secreted translocon and effectors (in orange), chaperones (in yellow) and transcriptional regulators (in green). Schematic adapted from Schroeder *et al.* 2008 (2).

The secretion of effectors is temporally regulated. Secretion of a second set of effectors, regulated by MxiE, is dependent on secretion of first the set (55). The activation of effectors is controlled by an “anti-activator” complex composed of the effector OspD1, the chaperone IpgC, and MxiE. The secretion of OspD1 with other first line effectors releases their cognate chaperone IpgC, MxiE then associates with IpgC and this upregulates the second line effectors (56).

There are also virulence genes on pINV which are located outside the PAI. These included genes encoding T3SS effectors belonging to the outer *Shigella* protein (Osp) family *i.e.* OspB, OspC1, OspD2, OspE2, OspF, and OspG (57). Additionally genes

for five IpaH effectors are on the pINV but not in the PAI (57), as are genes involved in *Shigella* actin mediated intracellular motility (*e.g. iscA*, *iscP*, *virA* and *phoN2*); VirA is secreted *via* the T3SS, while IscA and SepA are Serine protease autotransposters (SPATE) proteins.

1.8 Chromosomal virulence genes

In addition to pINV, there are chromosomal genes which influence virulence. For example, LPS is a major surface antigen and an important virulence factor. The O-antigen of LPS contributes to the ability of the bacterium to evade complement and antimicrobial peptides (58). Furthermore, adaptive immune responses following shigellosis are specifically directed to the O-antigen. Therefore, natural immunity conferred by infection with one serotype of *Shigella* does not confer protection against other serotypes (27, 59). Additionally, the length and conformation of the O-antigen are important for *S. flexneri* invasion and virulence (58). *Shigella* serotypes are defined by the structure of the O-antigen repeating unit. Differences in serotype can result from O-antigen glucosylation or *O*-acetylation (60) performed by enzymes encoded on chromosomally integrated bacteriophages. Glucosylation of the O-antigen can cause a conformational change which facilitates bacterial invasion without compromising the ability of the O-antigen to resist complement-mediated killing (58).

Shigella spp. have acquired virulence genes by horizontal gene transfer, with many genes located on chromosomal PAIs. PAIs have several features: they i) contain virulence genes, ii) are between 10-200 kb in size, iii) differ in base and codon usage from the core genome, iv) are frequently adjacent to tRNA genes, v) are often associated with mobile genetic elements, and vi) exhibit instability and may have a mosaic structure (61). *Shigella* chromosomal PAI are as follows:

A 46 kb chromosomal PAI, SHI-1, is located downstream of *pheV* tRNA, and encodes ShET1 enterotoxin and three serine protease autotransporters (SPATEs), which are not present in all species of *Shigella*. ShET1 induces intestinal fluid accumulation (62), while the SPATEs have different activities which aid intestinal penetration. For example, Pic is a mucinase (63), while SigA can destabilise focal adhesions and contribute to enterotoxicity and fluid accumulation (64).

SHI-2 is a 23.8 kb PAI inserted at the *selC* tRNA locus, and encodes a siderophore as well as ShiA which suppresses T cell signalling (65, 66). The SHI-3 PAI is a 21 kb region found in *S. boydii*, located downstream of *pheU* tRNA and encodes a different siderophore from SHI-2 (67).

A 66 kb PAI downstream of *serX* tRNA has been designated the *Shigella* resistance locus (SRL) as it confers resistance to a range of antibiotics; streptomycin, ampicillin, chloramphenicol and tetracycline in *S. flexneri* (68). Additionally it harbours genes for a ferric dicitrate uptake system (68).

1.9 Regulation of virulence

Expression of the T3SS and secretion are carefully regulated. Environmental conditions such as temperature, pH and osmolarity affect T3SS expression and secretion. One of the main environmental factors that affect T3SS regulation is temperature. Initially, it was first noted that *Shigella* is non-invasive and does not elicit a positive Sereny test when grown at 30°C compared to 37°C (69). The Sereny test is a commonly used model for measuring the invasive capacity of *Shigella* spp., and detects the ability of bacteria to elicit keratoconjunctivitis in guinea pigs (70). Subsequent studies demonstrated that the T3SS is specifically expressed at 37°C (71).

The molecular mechanisms by which *Shigella* regulates its virulence genes involve two pINV encoded transcriptional activators, VirF and VirB, and a chromosomally encoded transcriptional repressor, H-NS (Figure 1.3) (72). *virF* is located outside the PAI on pINV, while *virB* is within the PAI. The promoters of *virF* and *virB* are strongly repressed at 30°C and in the presence of low osmolarity, due to changes in DNA topology induced by binding of the chromosomally encoded H-NS, a nucleoid-structuring protein (73, 74). Following a shift in temperature to 37°C, repression of VirF and VirB by H-NS is relieved (73, 74). VirF acts as an “anti-silencer” and is synthesised, relieving H-NS mediated repression of *virB* (75). Furthermore VirF acts as a DNA binding protein capable of activating *virB* expression and a threshold level of VirF is required for this activation (76). The expression of VirB leads to the expression of many virulence-associated genes, including those in the *mxi* , *spa*, and *ipa* operons (76).

Fis and IHF which have growth phase dependent expression at early and late stages of growth respectively and these two factors positively regulate expression of VirF (76). VirF expression is also affected by other environmental conditions such as low pH and osmolality (76). H-NS is involved in the repression of *virF* under low osmotic conditions (74, 77). Expression of VirF is also controlled by pH *via* the CpxA/CpxR two-component system (78).

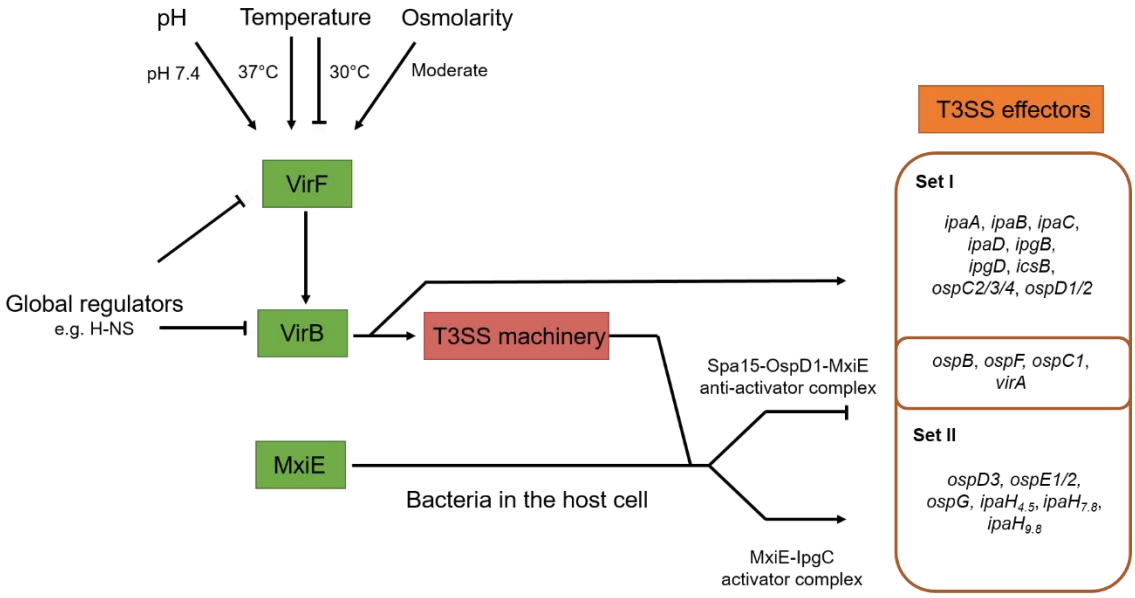


Figure 1.3 Environmental regulation of virulence

The transcriptional activator VirF is regulated by environmental stimuli such as temperature, osmolality and pH. VirF induces the expression of the transcriptional regulator VirB. Global regulators such as H-NS, also contribute to virulence gene expression. VirB induces the expression of the *Shigella* T3SS and effectors on pINV. T3SS effectors can be characterised on their regulation. Some are regulated by VirB, while others are regulated by MxiE; some are regulated by VirB and MxiE. Furthermore there are distinct sets of effectors. Set I are stored in the bacterial cytoplasm and produced independently of the T3SS. Set II effectors are induced following activation of the T3SS when *Shigella* is in the host cytosol. Genes encoding the structural components of the T3SS machinery (in red), secreted translocon and effectors (in orange) and transcriptional regulators (in green). Schematic adapted from Schroeder *et al.* 2008 (2).

Virulence and T3SS expression is also controlled *via* other mechanisms than the expression of VirF. At environmental temperatures (21°C) by pINV integration into the chromosome *via* IS*1294*; this leads to downregulation of the expression of T3SS genes (79). The T3SS is also regulated by the anaerobic transcriptional regulator fumarate and nitrate reductase (FNR) (80). As *Shigella* approaches the epithelium it is exposed to increased oxygen tension. While the central lumen of the colon is anaerobic, oxygen in delivered to the mucosal surface by the vascular supply. When bacteria are in close proximity to the epithelium, the oxygen concentration rises, alleviating FNR repression, resulting in activation of the T3SS (80). Furthermore the T3SS is activated or repressed during bacterial entry, inhibited in the host cytoplasm and reactivated for cell to cell movement (81).

1.10 Pathogenesis

1.10.1 Transit in the gastrointestinal tract

Shigella spp. are spread through the faeco-oral route. *Shigella* colonises the large intestine and is a highly contagious pathogen; ingestion of 10-100 bacteria can be sufficient to cause disease (6).

The acidic pH *Shigella* spp. encounters in the stomach activates RpoS sigma factor-dependent expression of periplasmic chaperone-like proteins, which allows survival in acidic conditions (82). Once in the intestine *Shigella* has to compete with other members of the microbiome. The influence of the microbiome in protecting against *Shigella* infection has been highlighted in animal models of shigellosis (83). Depletion of the host flora with streptomycin is necessary for colonisation of the murine intestine with *Shigella* spp. Furthermore *Shigella* competes with other bacteria in the gut by secreting small molecules such as colicins which are bacteriocidal (11). Additionally,

S. sonnei possess a Type VI secretion system which is highly effective at killing other species in the microbiome (84).

A complex layer of mucus overlays the epithelium in the gastrointestinal tract. Mucus is mainly composed of mucins, which are either oligomeric, soluble and secreted or are membrane tethered (85). The mucus layer prevents direct interaction between bacteria and epithelial cells, and reduces stimulation of the immune system by the microbiome (85). Commensal bacteria colonize and adhere to O-glycans in the outer mucus layer (85). The inner mucus layer is thought to be relatively sterile because epithelial cells and phagocytes act at mucosal surfaces and secrete chemokines that recruit, activate, and regulate immune cells such as dendritic cells (DCs), resident macrophages, and PMNs which migrate through the epithelium and clear bacteria (85).

Shigella is able to degrade the mucus layer by secreting mucinases and neuraminidases (86). Chromosomally encoded Pic is a mucinase belonging to the SPATE family (63). Additionally, SepA is encoded on pINV and acts as a mucinase. When *Shigella* is in contact with the apical surface of the epithelium it down-regulates production of antimicrobial peptides (AMPs) such as human β-defensin *via* MxiE-dependent *S. flexneri* effectors (87). Additionally, the production of the chemokine CCL20 is also downregulated which reduces DC recruitment (87).

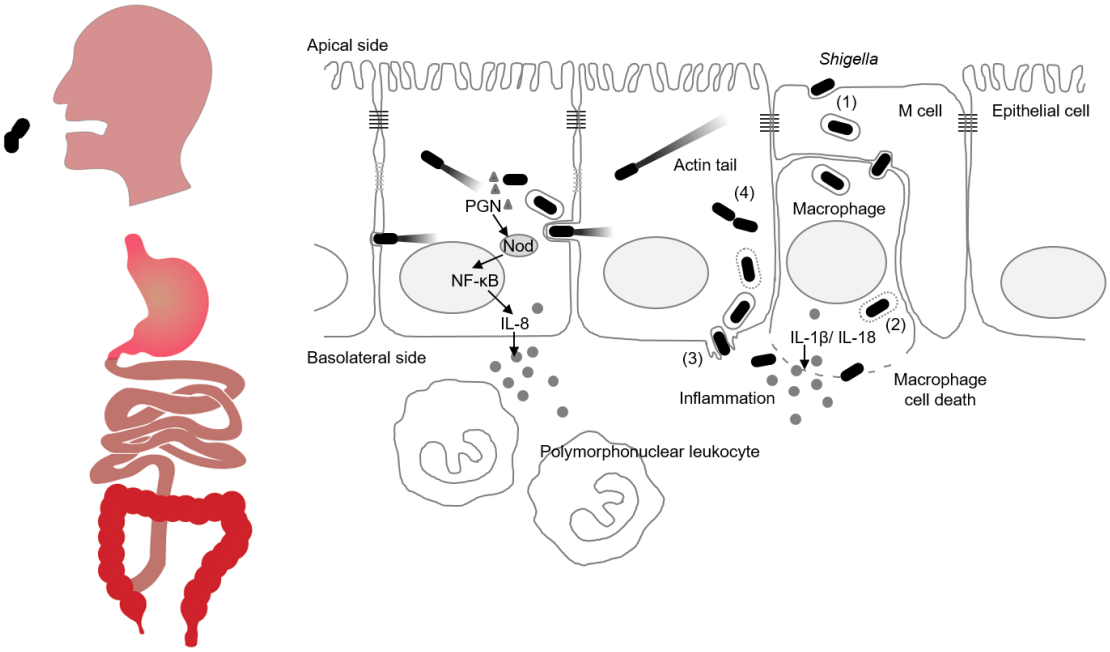


Figure 1.4 *Shigella* spp. host pathogen interaction

The life cycle of *Shigella* spp. is divided into four stages (numbered in the diagram): (1) entry into the host *via* M cells (2) escape from the vacuole of macrophages following phagocytosis, (3) entry into epithelial cells, and (4) replication within the cytosol. Figure adapted from Sasakawa, 2010 (88).

1.10.2 M cells and intracellular survival of *Shigella* spp. in phagocytes.

Shigella is unable to invade the apical side of the intestinal epithelial layer (89). Instead, the bacterium gains access to and invades through the baso-lateral aspect of epithelial cells following uptake by microfold (M) cells (Figure 1.4) (90). M cells are specialised epithelial cells that sample antigens in the intestinal lumen and present them to immune cells in mucosal associated lymphoid tissue.

Once *Shigella* crosses the intestinal epithelial barrier *via* M cells, it encounters phagocytic cells, such as macrophages and DCs, which are resident in Peyer's patches which are small masses of lymphatic tissue found throughout the ileum region of the small intestine (91). Following uptake by phagocytes, the T3SS tip complex

(formed by IpaB and IpaC) interacts with and inserts into the lipid membranes of nascent phagosomes (92). IpaB forms ion channels in eukaryotic membranes that are selective for monovalent cations (93). *Shigella* is able to escape the phagosome in a T3SS-dependent manner, either because pore formation leads to destabilisation of the membrane, or there is translocation of an unidentified membranolytic effector (93).

Shigella enters into the cytosol of phagocytes, where it promotes the activation of the Nucleotide-binding oligomerisation domain (Nod)-like receptor (NLR) family caspase recruitment domain (CARD)-containing protein 4 (NLRC4) inflammasome (94, 95). This leads to activation of Caspase-1 and subsequent pyroptosis of *Shigella* infected macrophages (51, 96). Macrophage pyroptosis leads to the release the pro-inflammatory cytokines, interleukin 1β (IL-1β) and IL-18, which trigger inflammatory responses and symptoms of shigellosis (97).

1.10.3 Epithelial intracellular survival and replication

Once *Shigella* reaches the sub-epithelial compartment, the bacterium invades epithelial cells through their basolateral surface (98). IscA is a VirF regulated autotransporter that is necessary and sufficient to promote contact with host cells (99). T3SS effectors have many roles to allow invasion to occur. Invasion of the epithelial cells is mainly mediated by the IpaB effector. IpaB interacts with CD44, a glycoprotein located within lipid rafts and involved in binding ezrin, radixin and moesin which act as linkers of the membrane to the actin cytoskeleton (100). IpaD is also involved in invasion as it acts as a scaffold at the tip of the T3SS needle to support IpaB and helps the delivery of the IpaB-C translocon into host cell membranes (92). IpaB and IpaD are thought to “sense” contact with host cell membranes and signal the activation of the T3SS (101).

A series of bacterial effectors induce changes in host cells which promote uptake of *Shigella* by non-phagocytic cells. *Shigella* invasion of epithelial cells is associated with the formation of actin-rich “membrane ruffles” at the site of bacterial contact that engulf the bacterium by macropinocytosis (a form of endocytosis). Invasion is triggered by the cell-contact-dependent injection of T3SS effectors acting together to reorganise the actin cytoskeleton. Insertion of IpaC into the membrane, triggers cytoskeletal rearrangements by inducing actin polymerisation involving the recruitment and activation of the Src tyrosine kinase, which allows further amplification of actin polymerisation and membrane ruffling (102, 103). IpgB1 and IpgB2 induce Rac dependent actin polymerisation (103). IpaD also participates in the induction of membrane ruffling, although its precise function is unclear. Phosphatidylinositol 4,5-bisphosphate (PIP_2)-binding proteins are involved in the anchoring of cortical actin to the plasma membrane. IpgD mediates PIP_2 hydrolysis which is thought to free cortical actin to favour *de novo* polymerisation at invasion sites (104). Moreover the phosphotidylinositol 5-monophosphate recruits ADP ribosylation factor (ARF) nucleotide binding site opener (ARNO), which activates ARF6 GTPase, promoting Rac dependent actin remodelling (105). Although Rac and actin polymerisation are required for ruffle formation and the initiation of *Shigella* invasion, Rho activation is required for the recruitment of components such as ezrin, involved in later stages of invasion. IpaA interacts with vinculin which is involved in focal adhesion structures, allowing anchorage of bacteria within the membrane ruffle (106). IpaA also enables depolymerisation of actin filaments during the completion of the invasion process (107).

Shigella entry into non-phagocytic cells produces membrane ruffling which produces a large number of macropinosomes. Macropinosome contact with the *Shigella*

containing vacuole is required for efficient vacuole rupture. The *Shigella* effector IpgD is thought to regulate Rab-11 (a marker for the recycling endosomal pathway) recruitment to macropinosomes (108, 109). VirA and IscB are also involved in lysis of the vacuole, which *Shigella* escapes in ~15 min (52, 110). Escape from the vacuole has not been well studied as mutants, such as Δ*ipaB*, are unable to invade non-phagocytic cells.

In the cytoplasm, *Shigella* can replicate every 37 min (111). To allow the intracellular spread of bacteria, *Shigella* undergoes motility which is mediated by the polymerisation of actin at one pole of the bacterium, propelling *Shigella* through the cytosol (112-114). Actin mediated motility occurs through the *Shigella* effector IscA which acts as a mimic of Cdc42 to recruit and activate N-WASP and Arp2/3 (115). This promotes actin assembly and filament growth at the N terminus of N-WASP providing the force to move the bacterium through the host cell (115). Other factors such as LPS and IscP are required for localising IcsA at one of the bacterial poles (115). The transmembrane proteins VpsABC and VacJ are ABC transporters that are required for lysis of the double membrane vacuole during intracellular spread although it is not sufficient for lysis (116).

1.10.4 *Shigella* spp. manipulates host immune responses

Host cells cope with cytosolic stress through mechanisms such as autophagy which breaks down defective cellular complexes through lysosome/vacuole-dependent turnover. Once in the cytosol *Shigella* is targeted by ATG8/LC3 which promotes the generation of autophagosomes (117). Furthermore, IscA can be recognised by ATG5 and entrapped in septin filament cage-like structures, thereby targeting bacteria to autophagic degradation (118). The *Shigella* effector IscB prevents autophagy by

masking the ATG5 binding site on IscA, preventing ATG5 initiating the formation of an autophagosome (117). Furthermore, IcsB recruits Toca-1 which prevents LC3-mediated autophagy (119). Additionally, VirA interferes with autophagy and ER-to-Golgi trafficking by stabilising Rab1, a GTPase which regulates membrane traffic, in its inactive form (120). The *Shigella* effector IpaJ inhibits vesicular intracellular traffic (121). IpaJ is a cysteine protease which preferentially cleaves N-myristoylated proteins such as ADP-ribosylation factors (121). IpaJ cleaves the myristoyl on ARF1 (121) which plays a role in ER-Golgi transport (121).

Death of *Shigella* infected phagocytic and non-phagocytic cells is an intrinsic immune defence strategy. Pyroptosis is a form of programed cell death that is accompanied by activation of caspase 1 or caspase 11 (human homologues caspase-4/5) inflammasomes, leading to the production of pro-inflammatory cytokines such as IL-1β, IL-18 and IL-8. When *Shigella* invades and replicates in the host, it releases bacterial molecules such as peptidoglycan, LPS and T3SS components (122). These pathogen associated molecular patterns (PAMPs) are detected by host pattern recognition receptors (PRRs), which activate signalling pathways and inflammatory responses (122). Intracellular PRRs include NLRs such as NLRC4 and Nod proteins (described above). NLRs and Nod form inflammasomes, which are multi-protein signalling complexes composed of NLR, the adaptor protein ASC, and an inflammatory caspase, such as caspase-1 (in canonical inflammasomes) and caspase-11 (in non-canonical inflammasomes) (122).

Bacterial toxins contribute to the symptoms of shigellosis. The chromosomally encoded ShET1 and plasmid encoded ShET2 (also OspD3) induce fluid secretion in the intestine by irreversibly binding to uncharacterised epithelial receptors (62, 123).

ShET2 also promotes an increase in IL-8 secretion by epithelial cells which induces PMN migration (124).

S. dysenteriae serotype 1 possesses Shiga toxin (Stx) which is an exotoxin encoded on a bacteriophage. Stx is cytotoxic for a variety of cell types and responsible for the development of vascular lesions in the colon, kidney, and central nervous system (40). The Stx is an AB5 toxin, composed of five B subunits which bind to globotriasylceramide (Gb3) on eukaryotic cells allowing delivery of the A subunit into cells (40). The A subunit acts as a N-glycosidase and cleaves a single adenine in the 28S ribosomal RNA component of 60S ribosomal subunit, inactivating it. Shiga toxin inhibition of protein synthesis and induction of host cell apoptosis results in tissue damage (40).

1.11 Intracellular nutrition

Shigella replicates efficiently within the host cell cytosol (111) suggesting that the host cytosol provides sufficient nutrients for bacterial division.

The mammalian cytosol consists mostly of water, dissolved ions, small molecules and large water soluble molecules such as proteins (125). The intracellular concentrations of ions such as magnesium (0.5 mM), sodium (5-15 mM), calcium (10-4 mM) and chloride ions (5-15 mM) are low compared with the extracellular compartment. In contrast, intracellular potassium concentrations are high (140 mM) (125). The host cell cytosol is rich in carbon and other energy sources which are derived from host cell catabolic and anabolic pathways (126). Glycolysis and the pentose-phosphate pathway occur within the host cell cytosol (126). The tricarboxylic acid (TCA) cycle and β-oxidation of fatty acids occur in mitochondria, but the resulting metabolites can

enter the cytosol (126). The catabolic intermediates produced by these pathways can be used by bacteria for the synthesis of amino acids, nucleotides, and fatty acids (126).

The metabolic requirements of *S. flexneri* in the host cytosol have been studied (111, 127). Infection of epithelial cells with *S. flexneri* does not affect uptake or catabolism of glucose through the Embden-Meyerhof and pentose phosphate pathways. Other host cell metabolic enzymes remain largely unaltered during infection, suggesting there is no reprogramming of metabolism (128) .

S. flexneri utilises host cell pyruvate and converts it to acetate from acetyl CoA using the phospho-transacetylase-acetate kinase pathway (PTA-ACKA) Figure 1.5 (111). Although this process generates less ATP than the TCA cycle, the PTA-ACKA pathway operates at a much faster rate and can sustain bacterial replication (111). However, *Shigella* must also synthesise asparagine, proline and purine nucleosides for intracellular growth (111).

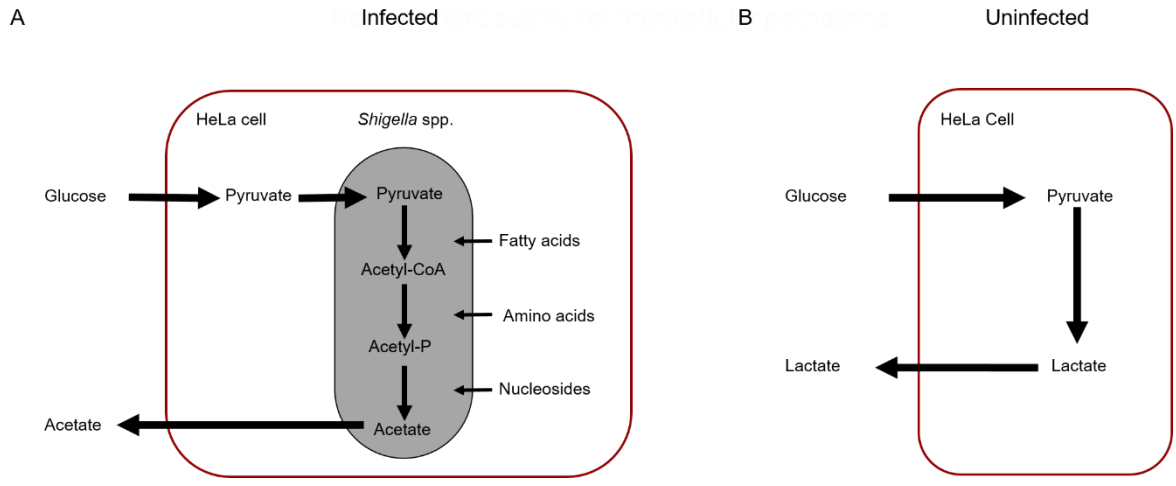


Figure 1.5 Carbon energy sources used by *S. flexneri* in epithelial cells.

Schematic showing the fate of glucose in epithelial cell infected with *S. flexneri*, and in uninfected cells. Intracellular bacteria scavenge host cell pyruvate, and convert it to acetate by the PTA-ACK pathway. Schematic adapted from Kentner *et al.* 2014 (111).

1.12 Measuring intracellular replication

Previous studies on the intracellular replication of *Shigella* have measured net bacterial growth by recovering live bacteria from cells. However, the number of CFU bacteria recovered from cells is influenced both by replication and killing by host factors. Methods have been recently developed to measure intracellular bacterial replication at the single cell level which circumvent this issue (Figure 1.6) (129-131).

Fluorescence dilution (FD) (Figure 1.6) allows quantification of bacterial replication based on the reduction in fluorescence during growth. Expression of a fluorescent protein (DsRed) is induced in bacteria prior to infection of cells, then the fluorescence intensity decreases with each division in the absence of the inducer, as the protein is diluted in daughter cells. A second constitutive fluorescent protein (GFP) allows the detection of bacteria. This technique allows measurement of replication for several divisions, until the dilution results in a low signal-to-noise ratio. This approach revealed a non-proliferating *Salmonella* population in macrophages and in mesenteric lymph nodes of orally infected mice (129).

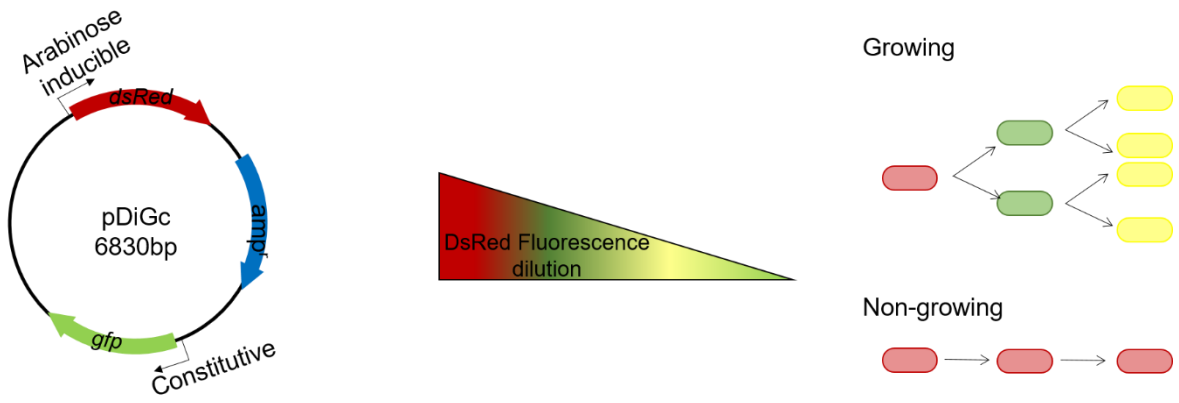


Figure 1.6 Schematic of Fluoresence Dilution, pDiGc

Fluorescence dilution (FD) is a plasmid approach to measure intracellular growth and heterogeneity and employs a plasmid (pDiGc) which encodes a constitutively expressed fluorophore (to allow detection of bacteria), and a different, inducible fluorophore the signal from which reduces during replication in non-inducing conditions) (129).

A similar method to FD is based on the maturation of the fluorescent TIMER protein (Figure 1.7), which combines two fluorophores in a single protein (132). This results in

different ratio of green:orange fluorescence depending on the rate of division. If a bacterial cell replicates then new TIMER protein is continually produced, and the population remains green. If a bacterial cell does not divide, the TIMER protein matures and bacteria appear orange. Differences in *Salmonella* growth rates during systemic infection were revealed by TIMER fluorescence (130). With this approach, it was possible to show that fast growing *Salmonella* (GFP positive) showed high expression of ribosomal proteins, consistent with the ribosome being regulated by growth rate (130). This technique allows measurement of bacterial heterogeneity for five to six hours post-infection.

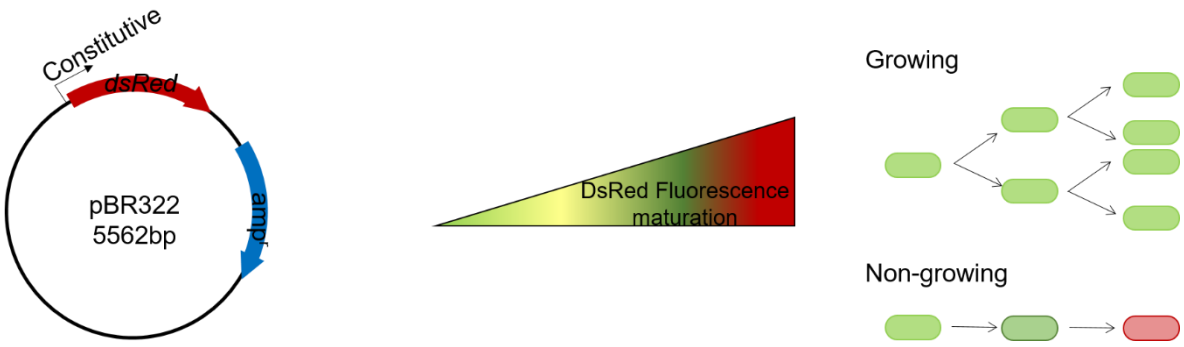


Figure 1.7 Schematic of the bacterial TIMER, pBR322

Bacterial TIMER is a plasmid approach to measure intracellular growth and heterogeneity, based on the alteration of the properties of a fluorophore over time after it has been translated (130).

The TIMER protein has also been combined with a biomarker to demonstrate that metabolic activity, and abundance of ribosomal RNA (rRNA) is closely correlated with growth (Figure 1.8) (131) . A green fluorescent protein (GFPdeg) was inserted at the rRNA locus with a TIMER protein expressed from a separate chromosomal locus in

Mycobacterium tuberculosis (131). The degradable GFP allowed distinction of non-growing bacteria from the replicating, metabolically inactive population (131).

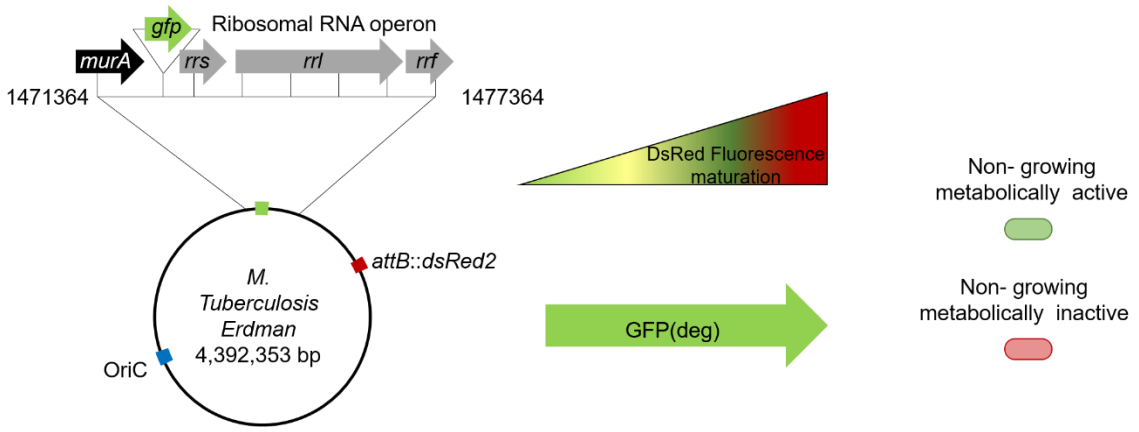


Figure 1.8 Schematic *M. Tuberculosis Erdman* chromosomal TIMER

A chromosomal bacterial TIMER in *M. tuberculosis* to measure intracellular replication and heterogeneity. This has a degradable green fluorescent protein (GFPdeg) at the ribosomal RNA (rRNA) locus which is reports transcription and translation. Figure adapted from Manina *et al.* 2015 (131).

1.13 Biology of the large *Shigella* spp. virulence plasmid (pINV)

Subsequent chapters in my thesis concern the maintenance of the virulence plasmid, pINV, in *Shigella* spp. This episomal element was acquired during the emergence of *Shigella* from *E. coli* (133). pINV is essential for virulence as it encodes a T3SS and a number of effectors. However, during growth in the laboratory, strains emerge that have lost the ability to express the T3SS. These avirulent strains grow faster than strains containing pINV, indicating that expressing a T3SS has a fitness cost (134).

1.13.1 pINV replication and copy number

Plasmids can impose a significant burden on their bacterial host, so many plasmids are present in low copy number. pINV is a non-conjugative, single copy plasmid (47), and has a RepFIIA origin of replication where replication occurs unidirectionally according to theta replication model (135). The replicon of *Shigella* pINV has not been extensively studied, but it is closely related to the replicon of the R100 and R1 resistance plasmids (136). The pWR501 replicon is more than 75 % identical to the R100 replicon at both nucleotide and amino acid levels (48).

The RepFIIA replicon is composed of a origin of replication (*ori*), a replication initiation protein RepA, CopB, and an untranslated RNA, *copA* (Figure 1.9) (135). Initiation of replication of RepFIIA replicon plasmids is dependent on RepA (135). When RepA binds, the DNA relaxes and becomes single stranded, proteins for DNA replication such as the DNA polymerase III holoenzyme, DnaB helicase and primase are recruited (135). Once initiation of leading strand synthesis occurs, replication continues until completion.

Plasmid replication and copy number is controlled mainly at the level of the initiation of replication through negative regulatory circuits (136). Replication of RepFIIA replicon is controlled by an unstable and constitutively produced antisense RNA, *copA* (136). The *copA* the antisense RNA binds to CopT, its complementary target RNA found upstream of *repA* mRNA, inhibiting translation (Figure 1.9) (136). Copy number of RepFIIA plasmids is further controlled by CopB repressing the *repA* promoter (136). CopB is continually expressed so if the plasmid copy number decreases, the CopB concentration will decrease also (Figure 1.9) (136).

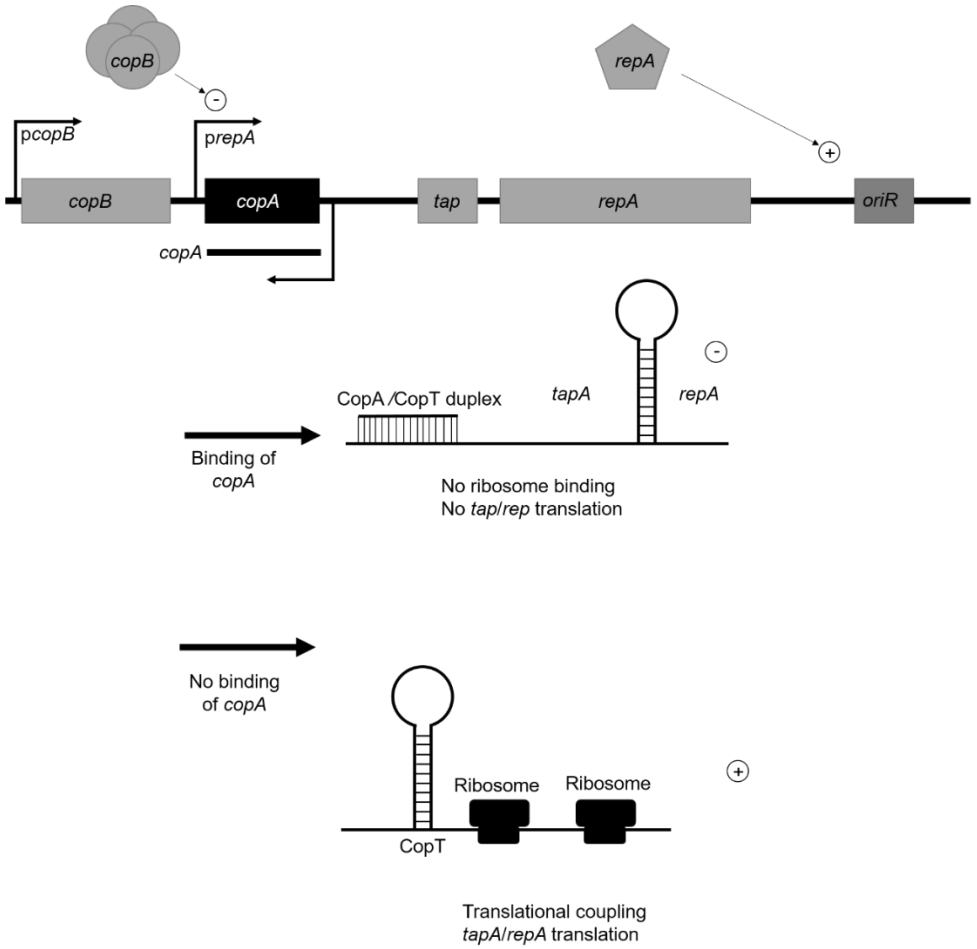


Figure 1.9 Mechanism of antisense RNA-mediated plasmid copy number control.

Translational inhibition. Inhibition of RepA translation: plasmid R1. The RepFIIA replicon is composed of a replication origin (*ori*), a replication initiation protein RepA, CopB, and an untranslated RNA, *copA.* Plasmid replication and copy number is controlled mainly by copA. *copA* antisense RNA binds to CopT, its complementary target RNA found upstream of *repA* mRNA, inhibiting translation. Copy number of RepFIIA plasmids is further controlled by CopB repressing the *repA* promoter. Figure modified from Brantl, 2004 (137).

1.13.2 *S. flexneri* pINV plasmid stability

Plasmid stability refers to the maintenance of a plasmid within a bacterial population. *S. flexneri* pINV instability can be caused by i) loss of the entire plasmid, ii)

deletions/rearrangements of the plasmid and iii) integration of the plasmid into the chromosome (79). pINV has two distinct mechanisms for its maintenance, partitioning systems and Toxin-Antitoxin (TA) systems (Figure 1.10).

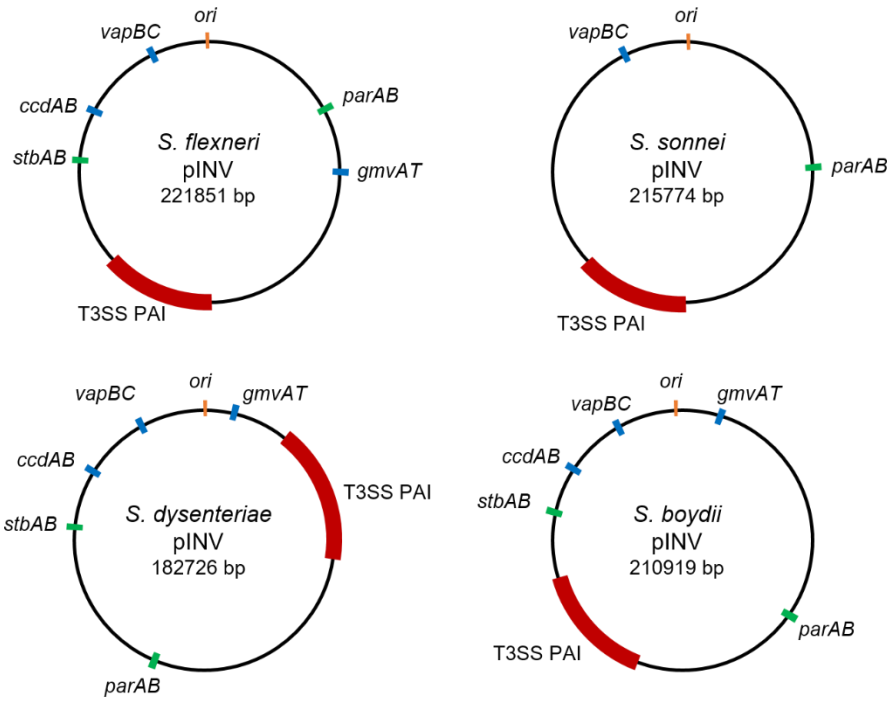


Figure 1.10 Schematic representation of potential plasmid maintenance systems on *Shigella* spp. pINV.

Labelled are the key maintenance features of *Shigella* spp. pINV relative to the origin (orange). The partitioning systems are labelled in green and the TA systems are labelled in blue. Figure adapted from Pilla and Tang, 2018 (135).

1.13.3 Partitioning systems

Partitioning systems position low copy plasmids in different daughter cells during bacterial replication and division. Partitioning systems are typically composed of three elements, an nucleoside triphosphatase (NTPase), centromere-like *par* sites, and a centromere binding protein (CBP) which interacts with the *par* sites (135). The NTPase uses the energy of the nucleotide binding and hydrolysis to move the plasmid (138). Two types of partitioning systems Type I and II are found on virulence plasmids (135). Type I partitioning systems have a Walker ATPase, while Type II systems have an actin-like ATPase. Type I have a "pulling" mechanism, drawing plasmids into separate daughter cells, while Type II have a "pushing" mechanism (135). *S. flexneri* pINV is predicted to contain two partitioning systems. ParAB is a Type I system found in all species of *Shigella*, and is The ParA proteins of pWR501 and P1 The ParA proteins of pWR501 and P1 are 75 % identical and the ParB proteins are 59 % identical over most of their lengths (48). StbAB is a Type II system (47), which is present on *S. flexneri* pINV but not *S. sonnei* (unpublished). StbAB is 43 and 29 % identical to R100 StbA and StbB over more than 80 % of the target sequences (48). Neither partitioning system has been characterised in *Shigella* pINV.

1.13.4 Toxin-Antitoxin systems

TA systems are almost ubiquitous in prokaryotes (139), and consist of a toxin and an antitoxin. Toxins of TA systems interfere with cell growth or viability, and target a variety of key cellular processes (140). Toxins are usually expressed along with their cognate antitoxin which neutralises the toxin (140). TA systems were initially described as addiction systems, which promote the retention of mobile genetic elements such as plasmids (*e.g*. *ccdAB* on the F plasmid and *relBE* on p307), prophages (*e.g phd-doc* on P1) through a process termed post-segregational killing (PSK) (141-145). In PSK,

if a daughter cell fails to receive genes encoding the TA system, lack of *de novo* antitoxin production leads to the unopposed action of the toxin, resulting in growth arrest and/or death. Additionally PSK has been found to maintain regions in bacterial chromosomes such as superintegrons which contain a group of genes flanked by a recombination sequence targeted by the integron integrase (*e.g.* the *higBA* TA system in the *Vibrio cholerae* superintegron) (144, 146).

There are six different types of TA system, depending on the nature of the antitoxin and the mechanism of its action (140). The toxin is usually a protein while the antitoxin can be a non-coding RNA (Types I and III) or a protein (Types II, IV, V and VI) (Figure 1.11) (140).

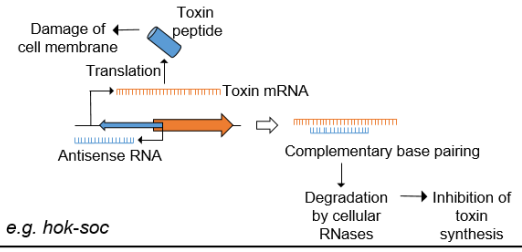
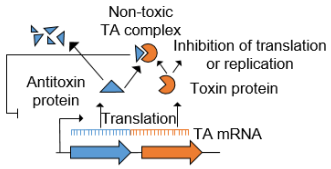
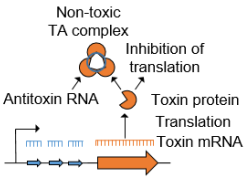
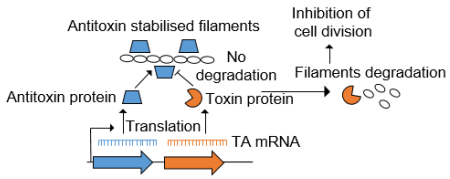
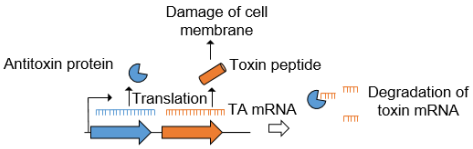
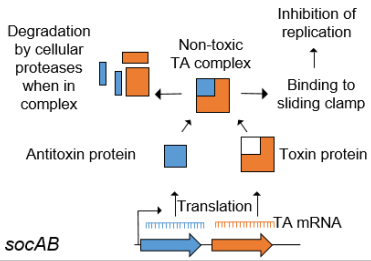
Type I	 *e.g. hok-soc*	Antitoxin is a antisense RNA
Type II	 *e.g. ccdAB*	Antitoxin is a labile protein that interacts with the toxin
Type III	 *e.g. toxIN*	Antitoxin is a labile protein
Type IV	 *e.g. cbtE/cbeA*	Antitoxin is a protein that does not interact with toxin
Type V	 *e.g. ghoST*	Antitoxin is a stable Rnase protein
Type VI	 *e.g. socAB*	Antitoxin is a protein which is an adaptor that promotes degradation

Figure 1.11 Toxin-Antitoxin types

Different types of TA systems with a schematic of the mechanism of action of the antitoxin and examples of TA systems belonging to each type (middle column), and the nature of the antitoxin (right sided column). Figure adapted from Lee and Lee, 2016 (147).

In Type I TA systems, the antitoxin is a small regulatory antisense RNA which can base-pair with the mRNA of the toxin and inhibit its translation. The most characterised Type I TA systems is the *hok-soc* system on the R1 plasmid (148, 149). The *soc* antitoxin bind *hok* mRNA, generating an RNA heteroduplex that is degraded by RNase III. (140).

In Type II TA systems, the toxin and the antitoxin are proteins. Type II antitoxins usually have two domains. Typically, the N-terminal domain binds the promoter of the TA system, leading to autoregulation. The second domain is usually at the C terminus, and interacts with and neutralises the toxin by preventing the toxin binding to its target. Examples include VapBC, RelBE, and CcdAB (150-152).

Type II TA systems are typically expressed from a single promoter upstream of the two genes (153). Activation of Type II TA systems is triggered by cellular proteases that degrade the antitoxin to release the toxin. In *E. coli*, several Type II antitoxins are degraded by Lon, but some are processed by ClpP (154). Type II TA systems are involved in plasmid maintenance as well as tolerance to antibiotics (155).

In Type III TA systems, the antitoxin is a small non-coding RNA which forms a pseudoknot that binds directly to the toxin preventing its activity (156, 157). All known Type III toxins are mRNA endonucleases with a fold related to MazF/CcdB family proteins. Type III TA systems have been observed to be involved with abortive phage infection and can confer plasmid maintenance (156, 157).

Type IV TA systems contain protein toxins and antitoxins which do not interact. The first recognised Type IV TA system, CbtA/CbeA, was found on the cryptic prophage CP4-44 in *E. coli*. CbtA prevents growth by binding and inhibiting the polymerisation of the bacterial cytoskeletal proteins MreB and FtsZ (158). CbeA stabilises MreB and

FtsZ polymers, and thereby counteracts the activity of CbtA and other MreB/FtsZ polymerisation inhibitors (158). Type IV TA systems can stabilise model plasmids and protect against phage infection (159).

There are two further types of TA system. Type V TA systems are similar to Type II TA systems as both components are proteins, but the antitoxin is stable and not a transcriptional regulator of its own operon. Instead, the antitoxin is an RNase that cleaves the toxin mRNA (160). In Type VI systems both components are also proteins, but the antitoxin is an adaptor protein that promotes the degradation of the toxin (161). Some TA systems such as DarTG are a mixture of Type II and Type IV and have not been classified separately (162).

1.13.5 pINV maintenance

S. flexneri pINV has three functional TA systems: VapBC, GmvAT, and CcdAB (163), while *S. sonnei* pINV has two functional TA systems, VapBC and RelAB (unpublished). Only VapBC and GmvAT have been shown to play a role in plasmid maintenance in *Shigella* (163). The reason why a single plasmid has more than one TA system is unclear. However, VapBC maintains pINV during growth at temperatures found in the human body, while GmvAT promotes pINV maintenance at temperatures in the external environment (163). Another potential role for multiple TA systems is to prevent loss of nearby sequences (79). VapBC is near the origin of replication on pINV, while GmvAT is located close to *virF*, a transcriptional activator which controls the expression of genes on the PAI. Recent evidence demonstrates that TA systems can prevent the loss of adjacent sequences (79).

Despite these strategies to maintain pINV, avirulent colonies arise during growth of *Shigella* spp. in the laboratory (79). Indeed the discovery of pINV was based on the

identification of *S. sonnei* colonies that were non-invasive and had lost a large plasmid (43, 44). Subsequently, the T3SS was shown to be encoded on pINV.

In *S. flexneri* the majority of events that lead to the spontaneous loss of the T3SS result from internal deletions of pINV due to intra-molecular events between ISs flanking the PAI or *virF* (79, 164). *Shigella* which are avirulent through loss of the T3SS (either through loss of the plasmid or plasmid re-arrangements) can be distinguished from wild-type bacteria by colony morphology on a plates containing the indicator dye, Congo Red (CR) (165). Bacteria expressing a T3SS bind Congo Red (CR) and appear as red colonies (CR^+), while colonies from avirulent, $T3SS^-$ strains are white (CR^-)(69, 166). This simple method can distinguish between colonies of virulent and avirulent bacteria, but is not suitable for detecting rare events. An alternative method has been established to quantify plasmid instability in *Shigella* (163) by introducing a *sacB-kan*^{r} marker into *mxiH* which encodes the T3SS needle subunit. Bacteria which retain *mxiH* in the T3SS PAI can be selected by resistance to kanamycin, while those which have lost the PAI (either through plasmid loss or re-arrangements) are resistant to growth in the presence of sucrose. Insertion of the *sacB-kan*^{r} also eliminates any growth differential between strains with or without the T3SS PAI, as the presence of the cassette in *mxiH* results in a T3SS-negative phenotype (163).

1.14 CcdAB

CcdAB has been found on the chromosome and plasmids in bacteria and archaea (139). CcdAB can stabilise plasmids *via* PSK (141). The role of chromosomal CcdAB is unclear, but has been proposed to be linked to survival during stress (167). *S. flexneri* pINV has a CcdAB TA system that is 86 to 96 % protein identity) to the well characterised CcdAB system on the F plasmid.

The CcdA antitoxin neutralises CcdB by forming a noncovalent complex which also acts as a repressor of the *ccdAB* operon (153, 168, 169). PSK hinges on the differential degradation of the antitoxin compared to the toxin (170). CcdA is a substrate for the Lon protease and is a dimeric, two-domain protein (170). The N-terminal CcdA dimerization/DNA-binding domain adopts a ribbon-helix-helix fold, while the C-terminal domain, which interacts with CcdB, is intrinsically disordered until it binds the toxin (171). CcdB targets DNA gyrase, an essential topoisomerase II (172, 173), which is responsible for disassociating DNA during replication and transcription. Dimeric CcdB engages and physically locks GyrA in its open confirmation (174). CcdA can remove CcdB complexed to gyrase (152).

1.15 VapBC

The Virulence associated protein (Vap) VapBC system is the most prevalent TA module and is abundant on the chromosomes of many prokaryotes and archaea (139). For example, *M. tuberculosis* harbours 45 *vapBC* operons (167), while non-pathogenic *Mycobacterium smegmatis* and *Mycobacterium avium* have a single *vapBC* TA operon (175). VapBC was originally identified on the *Salmonella* Dublin virulence plasmid pSLT (176), and contributes to intracellular survival in non-phagocytic cells as well as plasmid stabilisation (177, 178). A VapBC homologue, termed Maintenance of virulence plasmid (Mvp) MvpAT, is located on *S. flexneri* pINV and is important for maintaining pINV *via* PSK (179, 180); I refer to this system as VapBC in my thesis. The *S. typhimurium* VapB antitoxin is degraded by the Lon protease to release a free VapC, which inhibits cell growth by preventing protein translation (181, 182).

VapC has a PilT N-terminal (PIN) domain with an RNase H-like fold (183). PIN domains contain a conserved fold consisting of a central β-sheet comprising five

parallel β-strands, sandwiched by seven α-helices at both sides that results in the clustering of four conserved acidic residues that form the active site (151). In *S. flexneri* VapC these residues include Asp^{7}, Glu^{42} and Asp^{98} (151). The position of the fourth acidic residue in PIN domains can vary. In *S. flexneri* VapBC the fourth acidic residue is Glu^{120}. The cleavage mechanism of PIN domains is unknown but involves co-ordination of a Mg^{2+} or Mn^{2+} ion at the active site (184). The molecular targets of most prokaryotic VapCs are unknown. However, VapC from *E. coli*, *S. Typhimurium* and *S. flexneri* cleaves the initiator tRNA in its anticodon loop, inhibiting translation initiation (182). Currently there are no structures of a PIN domain protein bound to its cognate RNA target that would shed light on the mechanism of RNA recognition and cleavage. VapB has an N-terminal domain consisting of four *β*-strands (residues 1–45), which forms a homodimer that binds DNA. The extended C-terminal tail of VapB (residues 46–67) wraps around VapC, engaging the active site and the putative substrate binding site (151). In examples studied so far, VapC and VapB interact to form a heterooctameric complex. The VapBC complex is stabilised through interactions between the VapB N-terminal domains (151), and between the C-terminal region of VapB and the VapC PIN domain (Figure 1.12).

VapBC expression is regulated at the transcriptional level through direct binding of the antitoxin to palindromic AT rich sequences on the operator DNA. The VapBC heterooctomer complex specifically binds to two sites in the *vapBC* promoter which results in transcriptional repression (151).

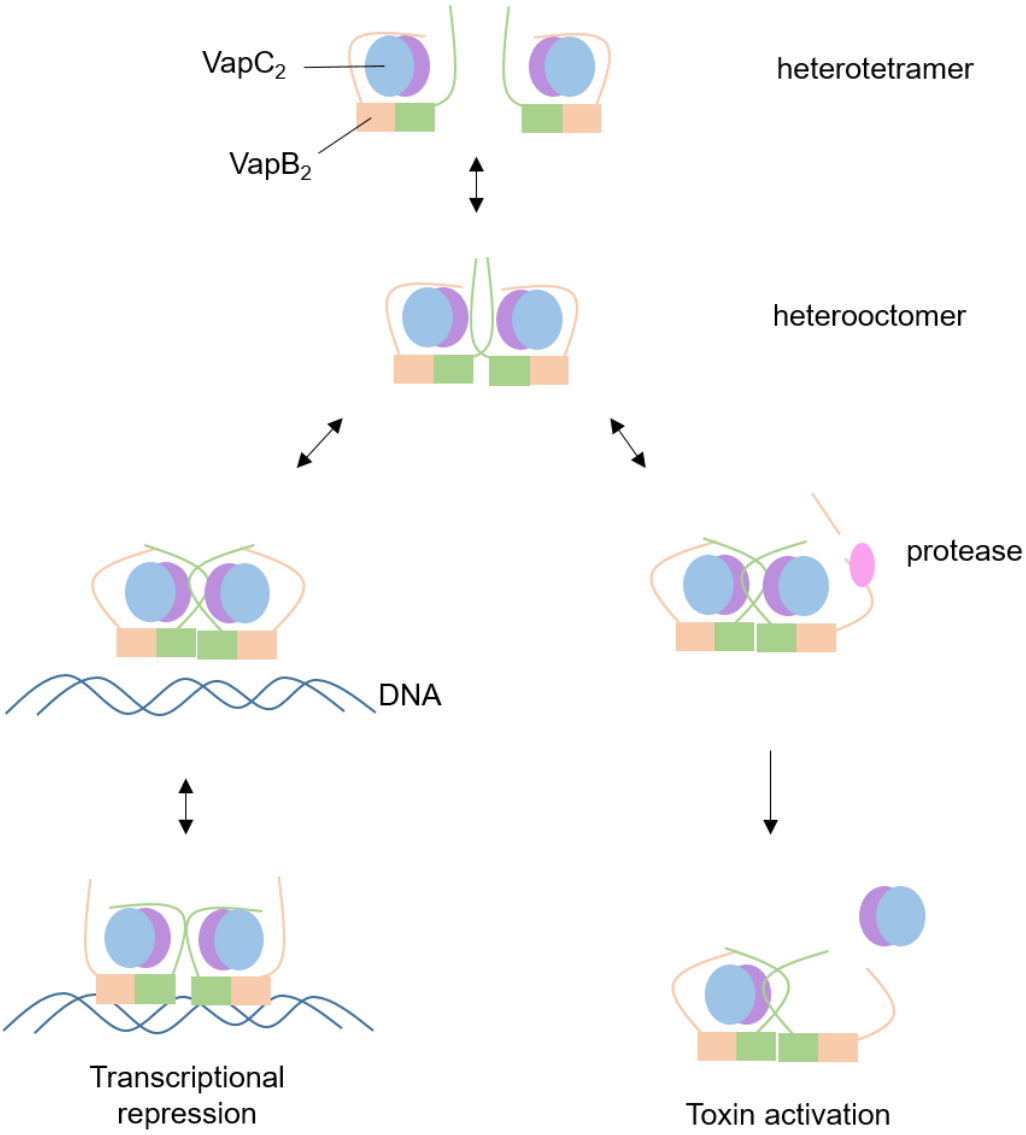


Figure 1.12 Model for DNA binding and activation of VapBC TA systems.

VapB and VapC associate as heterooctamers that bind DNA, causing the extended C-termini of VapB to stabilise the complex while bound to operator DNA in the promoter region. Protease cleavage destabilises the complex leading to toxin activation. Schematic adapted from Bendtsen *et al.* 2017 (185).

1.16 Type II Toxin-Antitoxin systems with GNAT fold toxins

GmvAT is a member of a recently described family of Type II TA systems, in which the toxin has a GNAT fold (GCN5 related N acetyltransferase) while the antitoxins have a ribbon-helix-helix fold (163). GNAT fold TA systems are found on the chromosome, superintegrons, and plasmids (186). GmvAT is sufficient to stabilise *S. flexneri* pINV stability at environmental temperatures (*i.e.* 21°C) (163). Unpublished work demonstrates that GmvA is subject to Lon degradation, suggesting GmvAT stabilises plasmids in a similar way to CcdAB and VapBC. In *S. typhimurium*, TacAT has been shown to contribute to intracellular persistence in macrophages (187, 188).

GNATs are a large family of enzymes in prokaryotes and eukaryotes that mainly utilise acetyl-CoA as the acetyl donor in acetylation reactions (186). The term GNAT is derived from yeast GCN5 (general control non-repressible 5), which is a histone acetyl transferase (186). Protein acetylation by GNATs usually occurs at the ε-amine group of lysines or the α-amine group of the first amino acid in a peptide chain (186)

GNAT family toxins described so far acetylate and inactivate tRNAs, subsequently inhibiting translation. GmvT from *Shigella* pINV blocks mRNA translation in an acetyl-CoA dependent manner (163). TacT of *S. typhimurium* targets a wide range of tRNAs by directly acetylating the primary amine group of charged tRNAs (187). This modification is hypothesised to arrest bacterial growth by blocking translation thus preventing the charged tRNA from interacting with EF-Tu (187). The toxin TacT from *S. Typhimurium* can also acetylate a lysine residue of TacA, providing the first example of a system in which the toxin recognises a protein and non-proteinaceous substrate (189). AtaT from *E. coli* O157:H7 was found to arrest translation by transferring the acetyl group from acetyl-CoA to the free amine group of $tRNA^{fMet}$ (190). GNAT TA

systems auto-regulate their transcription as their antitoxins act as transcriptional repressors by binding to their own promoters (189, 191).

1.17 Aims

The aim of the work in the first results chapter of this thesis was to further understand the basis of intracellular replication by *S. flexneri*. My goals were to establish a method for determining the rate of bacterial division inside epithelial cells, based on FD and use this techinique to screen individual mutants in a Tn5 transposon library and examine their capacity to survive and replicate within epithelial cells. Additionally I wanted to determine if heterogeneity is observed in intracellular *S. flexneri*, as has been established in *Salmonella* (128).

In the fourth chapter of my thesis, I aimed to understand further why *S. flexneri* pINV has multiple TA systems. A hallmark of *Shigella* pathogenesis is its regulation by temperature, which also influences the role of TA systems on pINV stability (163). My goal was to establish if other stresses such as low pH, oxygen tension and intracellular life also affected the role of TA systems on pINV stability. The aim of chapter five was to examine the influence of the genetic background of different *Shigella* and *E. coli* spp. on plasmid maintenance by VapBC from *S. flexneri* and *S. sonnei.*

2 Chapter Two Materials and methods

2.1 Bacterial strains and growth

Unless otherwise stated, *Shigella* was grown in Tryptic Soy Broth (TSB, Sigma), and *E. coli* was grown in Lennox L Broth Base (LB, Invitrogen); for solid media, agar (1.5 % w/v) Oxoid) was added to the media. Congo red (0.01 % w/v, final concentration) was added to TSB agar as an indicator of activity of the T3SS. Specialised media included M9 minimal media (25 mM $Na_2HPO_4 \cdot 7H_2O$, 22 mM KH_2PO_4, 18.8 mM NH_4Cl, 8.55 mM NaCl) supplemented with 0.4 % (w/v) glucose (VWR International), 2 µM $MgSO_4$, 0.1 mM nicotinic acid and agar (1.6 % w/v) is denoted as M9+ agar). For anaerobic growth, LB agar was supplemented with KNO_3 100 mM (192). Bacteria were grown in a Whitley A35 Anaerobic work station in the presence of 10 % H2, 10 % CO2 and 80 % N2. For acidic agar 1M HCl was added dropwise to agar, which was subsequently tested using pH strips (VWR). For selection with sucrose, 1 % (w/v) tryptone (Sigma), 0.5 % (w/v) yeast extract (Sigma), and 1.5 % (w/v) agar were autoclaved in water, and filter sterilised sucrose was added to a final concentration of 10 % (w/v)(4).

For growth of *E. coli* λ pir donor strain for conjugation liquid media was supplemented with 300 µM diaminopimelic acid (DAP).

2.2 Antibiotics

Antibiotics were used at the following concentrations: apramycin (apra, 30 µg/ml) carbenicillin (carb, 100 µg/ml), cefsulodin (cef, 600 µg/ml), chloramphenicol (cam, 20 µg/ml), erythromycin (erm, 200 µg/ml), gentamicin (gent, 50 µg/ml), kanamycin (kan, 50 µg/ml), penicillin G (pen, 600 µg/ml) tetracycline (0.2 µg/ml), and zeocin (zeo, 50 µg/ml). Antibiotic stock solutions were prepared in ddH_2O, filter sterilised using a 0.22

µm pore sized filter, and stored at -20°C. Chloramphenicol and tetracycline were prepared in ethanol and stored -20°C.

2.3 Bacterial strains and plasmids

The bacterial strains and plasmids used in this study are shown in Tables 2.1 and 2.2, respectively.

Table 2.1 Bacterial strains used in this study

Species	Relevant genotype/description	Ref.
S. flexneri		
M90T	Wild-type *S. flexneri* serotype 5a	(49)
BS176	Non-invasive M90T	(53)
mxiH::*sk*	M90T with *sacB-kan*^{r} in *mxiH*	(4)
mxiH::*sk* Δ*vapBC*	M90T with *sacB-kan*^{r} in *mxiH*, deletion of *vapBC*	(4)
mxiH::*sk* Δ*gmvAT*	M90T with *sacB-kan*^{r} in *mxiH*, deletion of *gmvAT*	(4)
mxiH::*sk* Δ*ccdAB*	M90T with *sacB-kan*^{r} in *mxiH*, deletion of *ccdAB*	(4)
Ig::*sk*	M90T with *sacB-kan*^{r} in an intergenic locus between *virB* and *ipaJ* on pINV	This study
Ig::*sk* Δ*vapBC*	M90T with *sacB-kan*^{r}, deletion of *vapBC*	This study
Ig::*sk* Δ*gmvAT*	M90T with *sacB-kan*^{r}, deletion of *gmvAT*	This study
Ig::*sk* Δ*ccdAB*	M90T with *sacB-kan*^{r} in an, deletion of *ccdAB*	This study
S. flexneri fMet2^{x1}	M90T with tRNA^{fMet2} in *metY* locus	This study
E. coli		
MG1655	Wild-type *E. coli* K-12	
MRE600	Wild-type *E. coli* B strain	(193)
MG1655 Δ*metY*	MG1655 lacking *metY*	This study
MG1655fMet1^{x4}	MG1655 with *metV* (tRNA^{fMet1}) in the *metY* (tRNA^{fMet2}) locus	This study
MG1655fMet2^{x4}	MG1655 with tRNA^{fMet1} in the *metY* locus and insertion of three tRNA^{fMet2} in the *metZWV* locus	This study

Table 2.2 Bacterial strains and plasmids used in this study

Strain or plasmid	Relevant genotype or description	Antibiotic Selection	Ref.
Strains			
E. coli DH5α	*fhuA*2 Δ(*argF-lacZ*) *U169 phoA glnV44* Φ*80* Δ(*lacZ*)*M15 gyrA96 recA1 relA1 endA1 thi-1 hsdR17*	-	(194)
E. coli SM10	*thi thr leu tonA l*acY *supE recA*::RP4-2-Tc::Mu Km λpir	kan^r	(195)
E. coli λ pir	λpir Δ*dapA* Δ*recA*	$apra^r$ zeo^r erm^r	(196, 197)
Plasmids			
pUC19	Cloning vector	amp^r	(198)
pBAD33	Cloning vector	cam^r	(199)
pKD46	Derivative of pINT-ts which contains *araC*-P*araB* and γ β *exo* (with tL3).	amp^r	(8)
pCP20	Temperature sensitive plasmid encoding FLP recombinase	amp^r	(8)
pKD4	Plasmid with FRT-sites flanking and kan^r cassette.	kan^r	(8)
pCONJ4s	Plasmid with R6Kγ origin on a pKNG101 vector which harbours *sacB* and s*fgfp*	amp^r	GL from (200)
pDiGc	Inducible expression of *dsRed* and constitutive expression of *gfp*	amp^r	(9)
$pDiGc^{cam}$	Inducible expression of *dsRed* and constitutive expression of *gfp*	cam^r	This study
pSTAB2	6.3 kb plasmid containing the pINV *ori* and *sacB-kan*^{r}	kan^r	GM
pSTAB2 $VapBC^{Sf}$	pSTAB2 with $VapBC^{Sf}$	kan^r	GM
pSTAB2 $VapBC^{Ss}$	pSTAB2 with $VapBC^{Ss}$	kan^r	GM
pSTAB2 $VapB^{Ss}C^{Sf}$	pSTAB2 with $VapB^{Ss}C^{Sf}$	kan^r	This study
pSTAB2 $VapB^{Sf}C^{Ss}$	pSTAB2 with $VapB^{Sf}C^{Ss}$	kan^r	This study
pOK-synthesised $tRNA^{fMet2(3)}$	pOK-synthesised $fMet2^{x4}$	kan^r	GeneArt Thermofisher

2.4 Bacterial growth

Liquid media (TSB), 5 ml was inoculated with a single bacterial colony, and incubated at 37°C with shaking at 180 r.p.m. overnight. The next day, cultures were diluted in fresh media to an optical density (OD) (A_{600}) of 0.03, then incubated at 37°C with shaking at 180 r.p.m.; measurements of the OD were taken at hourly intervals. The number of viable bacteria was enumerated by plating serial dilutions of cultures to solid media, and incubating at 37°C overnight prior to counting the number of colony forming units (CFU).

2.5 Bacterial growth measured by flow cytometry

The fluorescence of bacteria harbouring dual fluorescence reporter plasmids was monitored by flow cytometry. Bacteria were grown with or without 0.2 % (w/v) arabinose induction overnight in 1:4 diluted TSB liquid media. The following day bacteria were sub-cultured 1:100 into 1:4 diluted TSB. Following this bacteria were pelleted by centrifugation at 3000 *x g,* washed three times in phosphate buffered saline (PBS) and re-suspended in 1:4 diluted TSB and monitored for growth over time. Tetracycline (0.2 µg/ ml) was added to cultures to prevent replication. At each time point samples were centrifuged at 3000 *x g*, then re-suspended in 200 µl 3 % (w/v) paraformaldehyde (PFA) for fixation. Samples were fixed for 30 min, centrifuged at 3000 x *g* and re-suspended in 200 µl PBS.

Samples were analysed using a FACSCalibur™ (Becton Dickinson Biosciences). The gating strategy was as follows: first, forward scatter (FSC) and side scatter (SSC) was used to separate bacteria and cell debris. GFP fluorescence intensity was captured by excitation at 488 nm, using a 530/30 filter, and DsRed fluorescence intensity was captured by excitation at 488 nm, using a 585/42 filter. For each experiment,

compensation was performed using unlabelled and single-colour controls. Around 30,000 events were captured per sample. Data were captured using Cell Quest Pro and analysed using FlowJo software V.10 (Treestar).

Bacterial generations were determined as outlined by Helaine *et al.* (2010) and detailed below (129). To determine dilution of DsRed, the fold replication of the population (F) was first equated to the geometric mean of DsRed fluorescence (Y), as follows; F=Y0/Yt, where the geometric mean of DsRed fluorescence was taken at time zero (Y0) and time t (Yt; generally 1, 3 or 5 hours). This was then related to the number of generations (N), using the equation; $F=2^N$. Taken together, the number of generations at a specific time could be calculated as the difference between the natural logs of Y0 and Yt over the natural log of 2, as follows; N= (ln (Y0) - ln (Yt)/ (ln2).

2.6 *Shigella sacB-kan*^{r} marker loss assay

The *sacB-kan*^{r} marker was employed to assess plasmid stability (4). *sacB* confers sensitivity to sucrose, allowing positive selection for loss of the *sacB-kan*^{r} marker. The *kan*^{r} cassette confers resistance to kanamycin, allowing positive selection for retention of the *sacB-kan*^{r} marker.

Bacteria were plated onto solid media and incubated at the temperatures specified, and grown for ~25 generations. Individual colonies were then suspended in PBS, serially diluted and plated onto LB plates containing either kanamycin or sucrose.

2.7 Tissue culture cell lines and growth conditions

Cell culture reagents were purchased from Gibco-Invitrogen (UK) unless otherwise stated. HeLa cells were maintained in Dulbecco's modified Eagle's medium (DMEM D6429) supplemented with 10 % (v/v) heat inactivated foetal calf serum (FCS) at 37°C

in the presence of 5 % CO_2. HeLa infection assays were routinely performed in DMEM supplemented with 15 mM HEPES buffer (pH 7.4) with cells at a passage number of between 16 and 30.

THP-1 cells are a human acute monocytic leukaemia cell line established from the peripheral blood of a child with acute monocytic leukaemia (201). THP-1 cells were maintained in Roswell Park Memorial Institute (RPMI) medium supplemented with 10 % (v/v) heat inactivated foetal calf serum (FCS) at 37°C in the presence of 5 % CO_2. THP-1 cells were differentiated into macrophages in six-well plates containing 3 ml RPMI 1640 medium with 100 ng/ml 12-phorbol 13-myristate acetate (PMA) for 72 hr. THP-1 infection assays were routinely performed in RPMI 1640 with 15 mM HEPES (pH 7.4) with THP-1 cells at were used between passage number 6 to 15.

2.8 Infection of eukaryotic cells with *Shigella flexneri*

2.8.1 Infection of HeLa cells

HeLa cells were seeded into 6 well plates at a density of $5x10^5$ cells/well. Cells were infected with *S. flexneri* at a multiplicity of infection (MOI) of 10. Bacteria were spun onto HeLa cells by centrifugation at 6000 *x g* to synchronise invasion, then incubated for 30 min at 37°C. Cells were washed three times with PBS, and media containing gentamicin (100 µg/ml), penicillin G (600 µg/ml), or cefsulodin (600 µg/ml) was added to kill extracellular bacteria, and incubated for 1 to 3 hr.

To recover bacteria, cells were washed three times with PBS to remove gentamicin, then lysed by adding 1 % (w/v) saponin (MP Biomedicals UK) for 10 min. Serial dilutions of lysates were plated onto TSB plates. Plates were incubated at 37°C overnight and the CFU counted. The difference between the number of bacteria in the input and the number recovered following cell invasion at 1 hr was used to calculate

the invasion percentage ([no. at T1÷T0] x 100). The difference between the bacteria recovered at 3 hr and the number of bacteria recovered after 1 hr of incubation was used to calculate the replication index ([no. at T3÷T1] x 100).

2.8.2 Infection of THP-1 cells

THP-1 cells were seeded into six well plates at a density of $1x10^6$ cells/well. Cells were infected with *S. flexneri* at an MOI of 5. Bacteria were spun onto THP-1 cells by centrifugation at 3000 *x g* to synchronise invasion, and incubated for 30 min at 37°C. Cells were washed three times with PBS then incubated in media containing gentamicin (100 µg/ml) or penicillin G (600 µg/ml) or cefsulodin (600 µg/ml), then left for 1 hr. To recover bacteria, cells were washed three times with PBS to remove gentamicin, and lysed by adding saponin (final concentration, 0.5 % w/v) for 10 min. Serial dilutions of lysates were plated on solid media with kanamycin or sucrose. Plates were incubated at 37°C overnight, before CFU were counted.

2.9 Intracellular replication measured by flow cytometry

Flow cytometry analysis was performed as previously (129). Bacteria were grown with or without 0.2 % (w/v) arabinose induction overnight in 1:4 diluted TSB. The following day bacteria were sub-cultured 1:100 into 1:4 diluted TSB and grown to mid-log (OD_{A600} ~0.3) for 2-3 hr in the presence or absence of 0.2 % (w/v) arabinose. Following this, bacteria were pelleted by centrifugation at 3000 *x g,* washed three times in PBS, and re-suspended in DMEM or RPMI 1640 comtaining 15 mM HEPES. Next bacterial invasion was performed as described above in section 2.8. The fluorescence of bacteria harbouring dual fluorescence reporter plasmids was monitored at time points after invasion of HeLa or THP-1 cells. At 1, 3, 5 hr and sometimes 16 hr post infection, infected cells were lysed by addition of saponin (final concentration, 0.5 % w/v) for 10

min. Following lysis, the lysate was pelleted by centrifugation at 3000 x *g*, then re-suspended in 200 µl 3 % (w/v) PFA for fixation for 30 min, pelleted and re-suspended in 500 µl PBS. Samples were then analysed using a FACSCalibur™ (Becton Dickinson Biosciences) as in section 2.5. Around 10,000 events were captured for each bacterial sample recovered from HeLa or THP-1 cells.

2.10 Isolation of DNA

Genomic DNA was prepared using a Genomic DNA Purification Kit (Promega) according to the manufacturer's protocol. PCR products and gel fragments were purified using Wizard SV Gel and PCR Clean-up System (Promega). Plasmid DNA was extracted using GenElute Plasmid Miniprep Kit (Sigma).

2.11 Polymerase chain reaction (PCR)

The nucleotide sequences of primers used in this study are shown in Table 2.3. PCRs were performed using an Eppendorf mastercycler.

Reaction mixtures contained 1 µL of DNA template, 0.2 µM of each primer, 200 µM of dNTPs, 1x Q5® High-Fidelity DNA Polymerase, 5x Q5® High-Fidelity DNA Polymerase buffer and 5 x GC enhancer in a final volume of 50 µL. Control reactions contained no target DNA. Typical cycling conditions were as follows: i) denaturation at 98°C for 2 min, ii) 35 cycles [98°C for 10 sec, 60°C for 30 sec, 72°C for 1-3 min (1 min/kb)] and iii) a final extension step at 72°C for 2 min.

For colony PCR, bacterial colonies were mixed into the reaction instead of the DNA template.

Multiplex PCR was performed with primers (Table 2.3) to amplify *virF*, *virB*, *vapBC*, and *mxiM* to generate products of distinct sizes; *h-ns*, a chromosomal gene, was included as a control.

Multiplex reaction mixtures contained, 1 µM of each primer, 200 µM of dNTPs, 1x Taq polymerase, 5x Taq DNA Polymerase buffer in a final volume of 50 µL. Control reactions contained no target DNA. Typical cycling conditions were as follows: i) denaturation at 94°C for 5 min, ii) followed by 25 cycles [94°C for 30 sec, 51.2°C for 45 sec, 72°C for 1.5 min and iii) a final extension step at 72°C for 7 min].

pGEMT-easy (PROMEGA) is a commercial vector which has 3′ poly-T overhangs. To ligate a fragment of interest to the vector, a DNA fragment with a poly-A tail is required. PCRs were performed using Eppendorf mastercycler. Reaction mixtures contained 7.8 µL DNA template, 200 µM of dATP, 1x Taq DNA Polymerase, and 2 µL 10x Taq DNA polymerase buffer final volume of 20 µL.

Table 2.3 List of primers used for PCR

F =forward primer and R =reverse

Primer	Primer sequence (5' - 3')	Use of the primer
JM085	CTGTCAGACCAAGTTTACTC	pDiGc backbone (F)
JM086	AGAGTTTGTAGAAACGCAAAAAG	PDiGc backbone (R)
JM089	TTTGCGTTTCTACAAACTCTTGTGTAGGCTGGAGCTGC	Add cam cassette into pDiGc (F)
JM090	GAGTAAACTTGGTCTGACAGATGGGAATTAGCCATGGTCC	Add cam cassette into pDiGc (R)
GM043	GCCCATGGCTTTAAAGTCATCATCT	Multiplex *mxiM* (F)
GM044	AGGCGAAGCGGCATGCTGCAGACATAACCCCATC	Multiplex *mxiM* (R)
GM053	CCTGCGCGATACTCATCATAAACG	Multiplex *vapBC*(F)
GM054	GTTGAGCCGGGAGATGATTTCTG	Multiplex *vapBC* (R)
GM055	GCTTGTTGCACAGAGAAATAGAAGC	Multiplex *virF* (F)
GM068	GCGATGGGCTATGAAGCATTTAA	Multiplex *virF*(R)
GM065	GCCACAGGCCCTCAATGATATG	Multiplex *H-NS* (F)
GM066	GCATATGGCGTTGTGGATTGC	Multiplex *H-NS*(R)
GP13	ACGGCCAGTGAATTCGAGCTCTGGATGGCACTCGTAGAAG	Ig::*sk* upstream (F)
JM179	GCAGGTATATGTGTAAAAGCGTTGACTGCTAATC	Ig::*sk* upstream (R)
JM180	AAAAATTGAGTAGCACATATACCTGCCGTTC	*sacB-kan*^{r} (F)
JM181	GTCAACGCTTTTATCAGAAGAACTCGTCAAG	*sacB-kan*^{r} (F)
JM212	CATATGTCAGAAGAACTCGTCAAGAAGGCGATAGAA	Ig::*sk* upstream and *sk* (R)
JM213	CATATGCTACTCAATTTTTTTACATGGTGATAAACA	Ig::*sk* downstream (F)
GP17	CTATGACCATGATTACGCCAAGCTTATGCCTGATAAGATAGTCATG	Ig::*sk* downstream (R)
JM172	AGCATGTTGGAGTCTGTGGA	Upstream *metY* (F)
JM173	GGTCGACGGATCCCCGGAATGCGCCTGAAACGTGGCAAAT	Upstream *metY* (R)
LB001	ATTCCGGGGATCCGTCGACC	FRT kan^r (F)
LB002	TGTAGGCTGGAGCTGCTTCG	FRT kan^r (R)
JM174	CGAAGCAGCTCCAGCCTACACAAATCCGGCCCCCGCAACCA	Downstream *metY* (F)
JM175	CTAACCAGCGACGGAAAGTG	downstream *metY* (R)
JM176	CTATGACCATGATTACGCCAAGCATGTTGGAGTCTGTG	Overlap *metY*::kan^r (F)

JM177	ACGGCCAGTGAATTCGAGCTAGCTTCTAACCAGCGACG	Overlap *metY*::kan^{r} (R)
JM304	CGGAGTATAGTAAAACGACGGCCAGTGTTTCCCAGTTCAT CAATAAAGTCAGTATCAAGC	Upstream *metY* (F)
JM261	ACTCGTTTTGGGTAAAAAATGCAAATACTGCTG	Upstream *metY* *S. flexneri* (R)
JM262	ATTTGCATTTTTTACCCAAAACGAGTAGAATTTG	tRNA^{fMet2} insert (F)
JM263	GGCCGAAGTCTTCACAGTATATTTGAAAAAGGACTC	tRNA^{fMet2} insert (R)
JM264	TCAAATATACTGTGAAGACTTCGGCCTTCGTAG	Downstream *metY* *S. flexneri* (F)
JM303	CTATACTAGCAGGAAACAGCTATGACGTTTGCTTTCCAAT GCTTCGAAAATCTTCTCGCG	Downstream *metY* (R)
JM273	ACTCGTTTTGGGTAAAAAATGCAAATACTGCTG	Upstream *metY* MG1655 (R)
JM274	ATTTGCATTTTTTACCCAAAACGAGTAGAATTTG	tRNA^{fMet1} insert (F)
JM275	GGCCGAAGTCTTCACAGTATATTTGAAAAAGGACTC	tRNA^{fMet1} insert (R)
JM276	GCTCCACCCCGCGTCCGTGGATGCGCACTATAC	Upstream *metY* MG1655 (F)
JM326	CGGAGTATAGTAAAACGACGGCCAGTGTTTCCAGTGACG AATCGCCTGCATCGACATATC	Insert MG1655::tRNA$^{fMet2(3)}$ (F)
JM327	CTATACTAGCAGGAAACAGCTATGACGTTTCTGCTGGAGG ATTACAACAAAGGCGACCTC	Insert MG1655::tRNA$^{fMet2(3)}$ (R)
GM393	CCATATGGCTAGCATGAGCGGATCCGTAATTATCCTTGTC GGTATAATAATTACC	VapBC insert into pSTAB2 (F)
GM394	GGTGCTCGAGTGCGGCCGCAAGCTTGAACAGGTCAGCTC CAG	VapBC insert into pSTAB2 (R)

2.12 Restriction endonuclease digestion of DNA

Restriction digests contained 1 µg DNA, 1 U enzyme (New England Biolabs (NEB)), enzyme buffer and ddH_2O to a final volume of 50 µl. DNA was digested for at least 1 hr at 37°C.

2.13 DNA ligations

DNA ligation reactions contained purified vector and insert DNA in ratios of 1:1, 2:1 or 3:1 ratio, 1 µl of Quickstick ligase (Bioline), 5 µl 4x buffer and ddH_2O to a final volume of 20 µl. Reactions were incubated at room temperature for 10 min.

For pGEM T-easy ligation (Promega), reactions included 1 µl vector, 1 µl T4 ligase, 1 µl PCR product, 5 µl 2X ligase buffer, with 2 µl MilliQ water, and were incubated overnight at 4°C.

2.14 NEBuilder® HiFi DNA Assembly

For one step plasmid assembly, which joins multiple fragments in a single isothermal reaction (NEB), 20 ng of vector and insert DNA in a ratio of 2:1 were combined in reaction buffer. Reactions were incubated at 50°C for 1 hr.

2.15 Transformation of *E. coli*

Chemically competent *E. coli* was prepared as follows. Bacteria were grown overnight in 5 ml LB at 37°C with shaking at 180 r.p.m. The culture was diluted 1:100 into 120 ml of LB which was incubated at 37°C with shaking until the OD_{600} reached between 0.4 and 0.6. Bacteria were left on ice for 10 min, then pelleted by centrifugation at 3000 *x g* for 10 min at 4°C. The supernatant was discarded and the pellet re-suspended in 40 ml of RF1 (15 % w/v glycerol, 100 mM RbCl, 50 mM $MnCl_2$, 30 mM KCH_3COO, 10 mM $CaCl_2$, adjusted to pH 5.8, then filter sterilised), and incubated on ice for 60 min.

Bacteria were pelleted by centrifugation at 3000 x *g* for 10 min at 4°C, and the pellet re-suspended in 9.6 ml of RF2 (15 % w/v glycerol, 100 mM RbCl ,10 mM MOPS, 75 mM KCH_3COO, 10 mM $CaCl_2$, adjusted to pH 6.8, filter sterilised) and incubated on ice for 15 min. Bacteria were then immediately aliquoted, frozen in dry ice and stocked at -80°C.

Between 1-10 µl of DNA (up to 500 ng) was added to 50 µl of chemically competent *E. coli*, then incubated on ice for 30 min. Bacteria were heat shocked at 42ºC for 45 sec, then incubated on ice for 2 min. LB (1 ml) was added to the bacteria which were incubated at 37°C for 1 hr. The bacteria were pelleted by centrifugation, re-suspended in 50 µl of LB and plated to solid media with appropriate antibiotics and incubated overnight at 37°C.

2.16 Transformation of *S. flexneri*

Electro-competent *Shigella* was prepared as follows. *Shigella* was grown overnight in 5 ml TSB at 37°C then 1:100 diluted into 25 ml of TSB, and incubated 37°C with shaking at 180 r.p.m. until the culture reached an OD_{600} of between 0.4 and 0.6. Bacteria were then left on ice for 10 min, then pelleted by centrifugation at 3000 x *g* for 10 min at 4°C. The supernatant was removed and the pellet was re-suspended in ice-cold water; this was repeated twice. Bacteria were finally re-suspended in 10 % (v/v) glycerol and centrifuged for a further 5 min. The supernatant was removed and bacteria were re-suspended in 500 µl 10 % glycerol; 50 µl was used for each electroporation.

Cells were incubated with up to 5 µg of DNA for 10 min on ice. Bacteria were then electroporated in 2 mM gap cuvettes (Fisher) at 2.5 kV (Biorad Gene pulser II, UK), then transferred to ice. LB (1 ml) was added and bacteria were incubated at 37°C for

1 to 3 hr (Lambda red recombineering recovery step), before they were centrifuged 3000 x *g* and re-suspended them in 50 µl of TSB. Bacteria were plated onto solid media with antibiotics as required.

2.17 Genetic manipulation

Two methods were employed for genetic manipulation. The first used the Lambda red system derived from the Lambda red bacteriophage (202). The second method was developed by Guangyu Liu (unpublished), and is based on conjugation.

2.17.1 Lambda red-based recombination

The Lambda Red recombinase was employed to insert the *sacB-kan*^{r} marker in the intergenic region between *virB* and *ipaJ* (Chapter 4, Figure 4.8) and make Ig::*sk*. Additionally it was used to individually delete the *vapBC*, *ccdAB* and *gmvAT* from Ig::*sk* parental background and to delete *metY* from *E. coli* MG1655.

For the insertion the *sacB-kan*^{r} cassette. ~ 1000 bp upstream and ~ 1000 bp downstream of the insertion site were amplified from *S. flexneri* M90T by PCR. Overlap PCR was performed to anneal the upstream region (*virB*) with the *sacB-kan*^{r} cassette. To obtain the full linear fragment, this fragment and the downstream region were inserted into pGEMT-easy (Promega). Following insertion, restriction digest was performed, and the full length construct was ligated into pUC19. The plasmid was used at the target to amplify the insert by PCR.

To generate *E. coli* MG1655 Δ*metY* and *S. flexneri* Ig::*sk* with TA deletions the gene was replaced with a kanamycin resistance cassette flanked with flippase recognition target (FRT) sites, with only the start and stop codon remaining. Upstream and downstream fragments (each ~ 1000 bp) were amplified, and the products included in

an overlap PCR with the kan^r cassette flanked by FRT sites. The DNA construct was introduced into pUC19 with theNEBuilder® HiFi DNA Assembly. The plasmid was used at the target to amplify the insert by PCR.

Electro-competent *E. coli* or *Shigella* harbouring pKD46 were prepared. Expression of the Lambda recombinase was induced during growth by adding arabinose (final concentration, 0.3 % w/v) when the OD_{A600} of cultures reached ~ 0.2. Strains were checked by PCR and sequencing; constructs were transduced into a wild-type strain using P1 (2.16).

pCP20 was introduced into strains by electroporation to remove the kanamycin marker. Bacteria containing pCP20 were then grown at 42°C to eliminate plasmid which has a temperature-sensitive replicon. Strains were checked by PCR and sequencing.

2.17.2 Conjugation

To construct strains by conjugation, regions of ~ 800 bp upstream and downstream of the gene of interest were amplified. An overlap PCR was performed with resistance cassette or inserted gene, and the upstream and downstream regions, then assembled into pCONJ4s (kind gift, Guangyu Liu) using NEBuilder® HiFi DNA Assembly and transformed into *E. coli* SM10. This plasmid was transformed into *E.coli* λpir, which is auxotrophic for DAP. The *ori* of pCONJ4s is only functional in the presence of the Pir protein. *E.coli* λpir harbouring pCONJ4s with the insertion of interest was grown overnight in LB with 300 µM DAP, as well as the recipient strains. The donor and the recipient were mixed in a 1:1 ratio, and plated on an LB plate supplemented with 300 µM DAP for 4 hr at 37°C, after which bacteria were plated on LB with carbenicillin to eliminate the donor strain. Bacteria were picked from plates,

and grown for 4 hr in liquid LB to remove the plasmid. Bacteria which had lost the *sacB* gene in pCONJ4s were selected for by plating onto agar with 10 % (v/v) sucrose. Strains were checked by PCR and sequencing.

2.18 Transduction

P1 lysates were prepared from donor strains according to published protocols (203). Cells of the recipient strain were pelleted following overnight growth, and re-suspension in 750 µl P1 salts solution (10 mM $CaCl_2$, 5 mM $MgSO_4$). An aliquot (100 µl) of the cell suspension was incubated with 1, 10, or 100 µl of P1 lysate for 30 min at 37°C. After incubation, 1 ml of LB/0.2 M sodium citrate was added and the samples grown for 1 hr at 37°C with shaking. Cells were harvested by centrifugation 3000 *x g* then re-suspended in 50 µl LB/0.2 M sodium citrate and transductants selected by growth on LB agar containing appropriate antibiotics.

2.19 DNA sequencing

All sequencing was performed by Source Bioscience with typical reactions containing 3.2 pmol of primer and 100 ng plasmid DNA or 10 ng PCR product. Sequence reads were analysed using Snapgene (GSL Biotech LLC).

2.20 Analysis of nucleotide and amino acid sequences

Clustal OMEGA searches were performed to compare DNA or protein sequences with the following database: https://www.ebi.ac.uk/Tools/msa/clustalo/

2.21 Statistics

Statistical analysis was carried out using GraphPad Prism v7 software. Plasmid loss data were log-transformed (normally-distributed) and analysed using one-way or two-way ANOVA with Tukey's multiple comparisons tests as indicated in Figure legends.

3 Chapter Three Determining the dynamics of *S. flexneri* intracellular replication at the single-cell level

The ability to survive and replicate in an intracellular niche is critical for the virulence of several pathogenic bacteria including *S. flexneri*, the leading cause of bacillary dysentery (204). *S. flexneri* invades non-phagocytic intestinal epithelial cells in a T3SS-dependent manner (204). Following rupture of the nascent phagosome membrane surrounding the bacterium (52), progression to clinical disease is dependent on the capacity of the bacterium to proliferate rapidly within the host cell cytosol, and undergo cell-to-cell spread (113). While the mechanisms of cell entry by *S. flexneri* have received extensive attention (205), the strategies employed by *Shigella* to replicate in the intracellular environment remain poorly understood. Previous studies on intracellular replication of *Shigella* have measured the net bacterial growth by plating cell lysates to determine the number of CFU. Recently methods using fluorescent reporters, have begun to look at intracellular bacterial replication and heterogeneity at the single cell level in other bacteria (129-131, 206). The first aim of work in this chapter was to develop a single cell-based assay to examine intracellular replication of *Shigella* and characterise any *S. flexneri* heterogeneity within the same cell and in different cell types.

Bacterial growth in the laboratory is usually measured by either assessing changes in the turbidity of media, or determining the number of viable bacteria by counting CFU after plating samples to solid media. As alterations in turbidity cannot be used to observe bacteria replicating in an intracellular environment, previous studies have measured intracellular growth of bacteria by counting CFU. The number of intracellular bacteria is usually assessed by treating invaded cells with a non-cell penetrating antibiotic such as gentamicin to kill extracellular bacteria (53). However the number of

CFU (representing the number of bacteria recovered) is influenced by both replication and killing by the host immune system (207). Therefore, other approaches are required to measure the rate of bacterial replication during this critical phase in pathogenesis.

An FD system, employing two fluorescent proteins, has been established to quantify intracellular bacterial replication (Figure 3.1) (129, 206). In an early version of FD, the plasmid (pDiGc) encodes GFP under the control of a constitutive promoter (allowing detection of bacteria by flow cytometry or fluorescence microscopy), while expression of DsRed is regulated by an inducible promoter. Following removal of the inducer (arabinose for pDiGc), bacterial cell division is assessed by the rate of dilution of fluorescence from DsRed. The use of flow cytometry or fluorescence microscopy allows the fate of individual bacteria to be followed in real-time.

3.1 Validation of fluorescence dilution (FD) in *S. flexneri* pDiGc *in vitro*

The plasmid pDiGc has been successfully used to monitor the growth of *Salmonella* both *in vitro* and *in vivo* (129). Initial experiments were performed to validate its use in *S. flexneri*. pDiGc was introduced into *S. flexneri* by transformation, generating *S. flexneri* pDiGc. The plasmid harbours a gene encoding β-lactamase (and hence ampicillin/penicillin G resistance), as well as genes encoding two fluorescent proteins, GFP and DsRed (Figure 3.1).

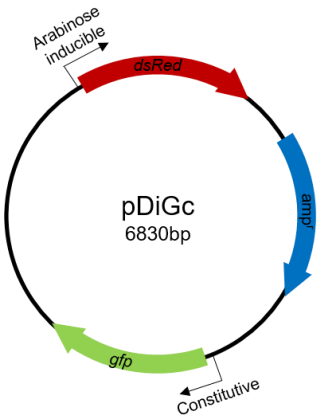


Figure 3.1 The FD plasmid, pDiGc

pDiGc encodes GFP under the control of a constitutive promoter (p*rpsM*) to allow detection of bacteria. pDiGc also encodes DsRed under an arabinose inducible promoter (p*araBAD*) the signal from which reduces during replication in non-inducing conditions. The plasmid also includes a β lactamase (amp^r) to allow for selection.

To establish whether pDiGc allows for inducible expression of DsRed in *S. flexneri*, fluorescence of *S. flexneri* pDiGc was measured by flow cytometry following growth overnight (16 hr) in 1:4 TSB, in the presence or absence of the inducer, arabinose (0.2 % w/v, final concentration). Fluorescence from GFP was excited at 488 nm and emission was measured at 510 nm, while the corresponding wavelengths were 488 nm and 585 nm for DsRed. As expected in the absence of arabinose, pDiGc carrying *S. flexneri* demonstrated green fluorescence only, and there was no significant DsRed geometric mean fluorescence detected above levels found in untransformed *S. flexneri* ($p > 0.9999$, one-way ANOVA, Figure 3.2). Furthermore, it was confirmed that addition of 0.2 % arabinose to *S. flexneri* pDiGc growth media resulted in significant DsRed geometric mean fluorescence compared to non-induced *S. flexneri* pDiGc ($p = 0.0294$, one-way ANOVA, Figure 3.2). Therefore, results demonstrate that pDiGc confers constitutive GFP expression and arabinose inducible DsRed in *S. flexneri*.

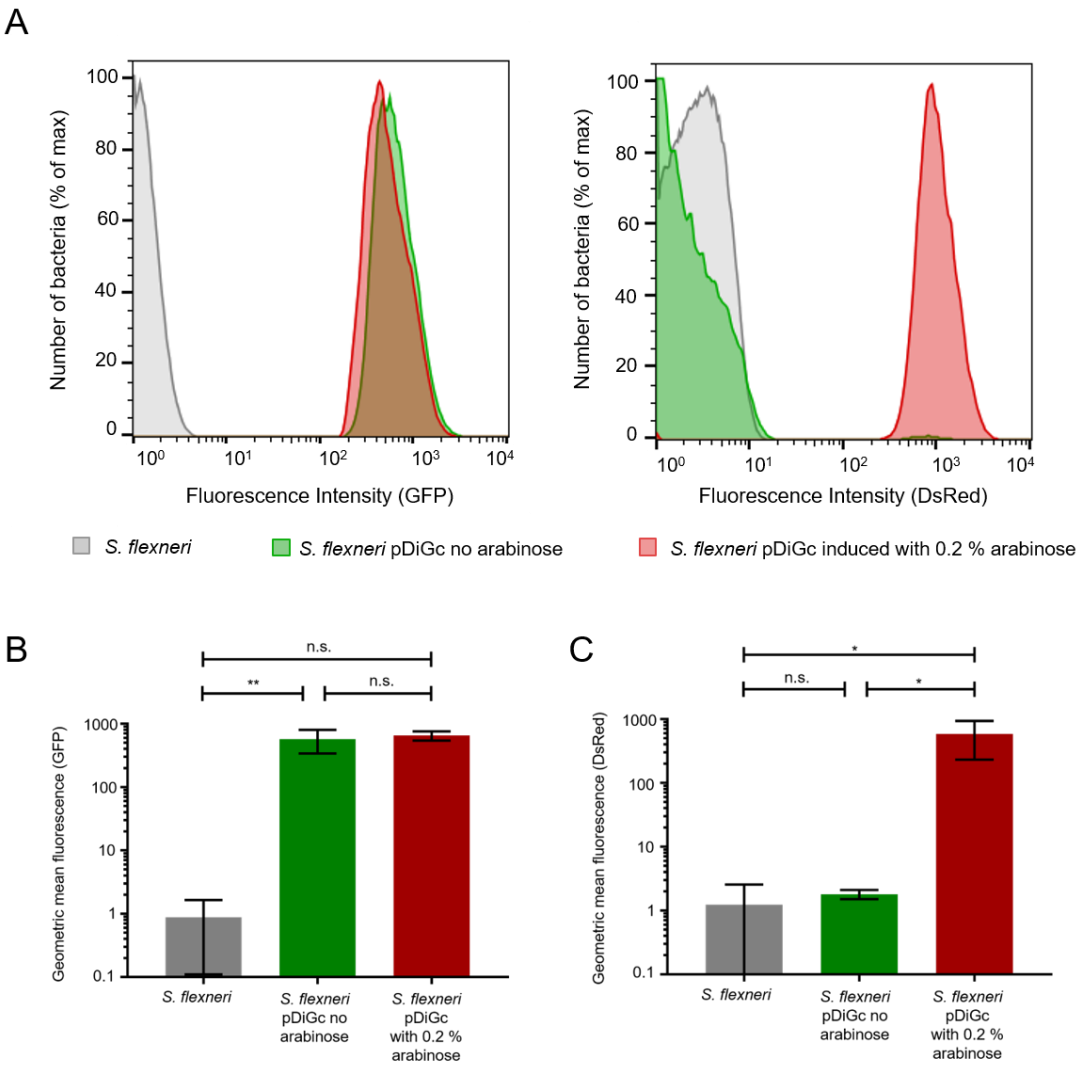


Figure 3.2 Fluorescence conferred by pDiGc in *S. flexneri.*

(A) *S. flexneri* pDiGc was grown in the presence (0.2 %, red trace) or absence (green trace) of arabinose. Flow cytometric detection of GFP and DsRed. Fluorescence intensity was measured of at least 30,000 events. The traces show one of three independent experiments. (B) Geometric mean fluorescence of GFP; mean shown +/- S.D. of three independent experiments. (C) Geometric mean fluorescence of DsRed; mean shown +/- S.D. of three independent experiments. One-way ANOVA statistical analysis with Tukey's multiple comparisons was performed. *, $p < 0.05$, **, $p < 0.01$ and n.s., non-significant.

An important requirement for the successful application of FD is that the reporter proteins should be stable within the bacterium. In pDiGc, DsRed acts as the reporter for replication, so the protein needs to have a sufficiently long half-life so that only bacterial division, and not protein degradation, will cause the reduction of signal over time. To determine the stability of DsRed and GFP in *S. flexneri*, fluorescence of this protein in non-replicating bacteria was measured over 6 hr. *S. flexneri* pDiGc was grown in 1:4 TSB liquid media overnight in the presence of inducer (0.2 % arabinose), then transferred to fresh media 1:100 without arabinose but containing tetracycline (0.2 µg/ml). This is a bacteriostatic concentration of tetracycline that blocks *de novo* protein synthesis (208). The DsRed geometric mean fluorescence of *S. flexneri* pDiGc did not significantly change over 6 hr (p = 0.2322, one-way ANOVA, Figure 3.3). The GFP geometric mean fluorescence intensity of *S. flexneri* pDiGc did not significantly change over 6 hr (p = 0.7225, one-way ANOVA, Figure 3.3). The results show that DsRed is sufficiently stable and can be used as a marker for *S. flexneri* replication over 6 hr (Figure 3.3).

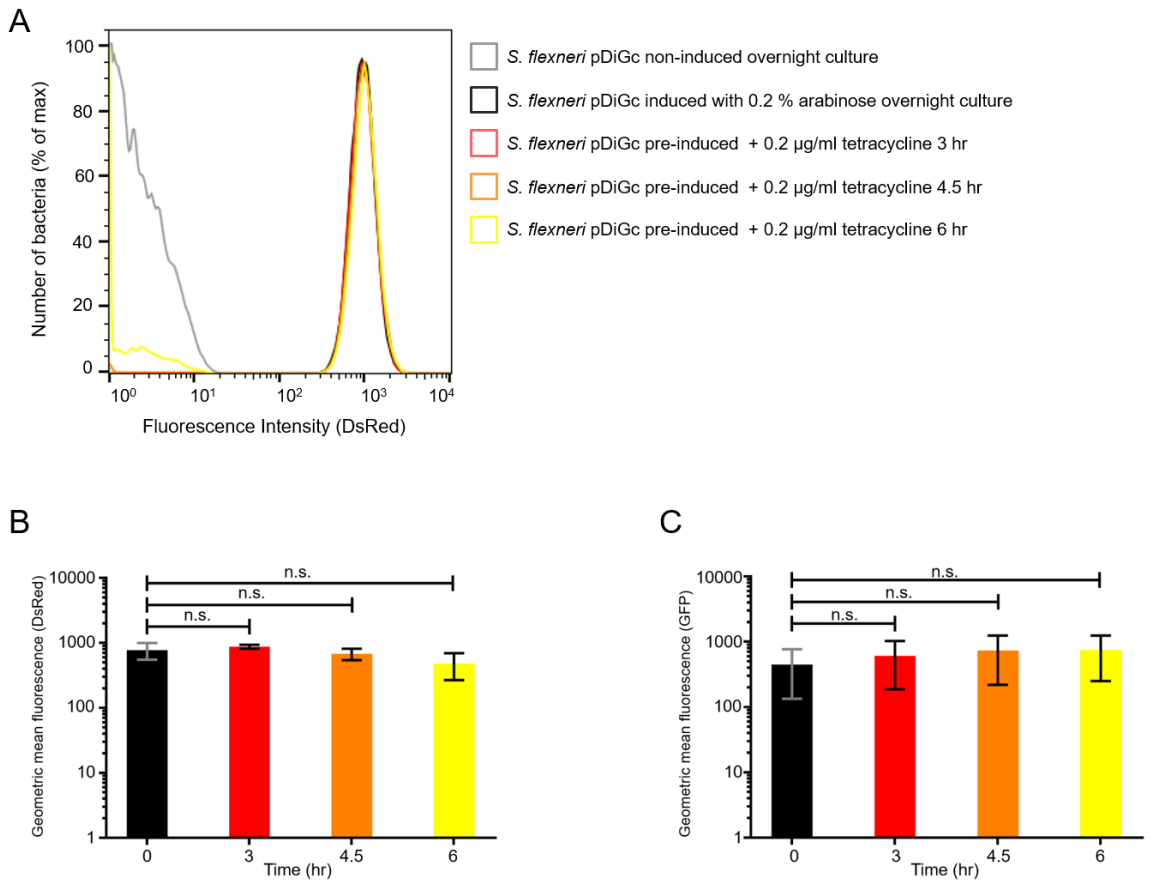


Figure 3.3 Stability of DsRed from pDiGc in *S. flexneri.*

(A) Flow cytometric detection of DsRed fluorescence intensity of *S. flexneri* pDiGc induced with 0.2 % arabinose overnight, washed and subcultured in the presence of a bacteriostatic concentration (0.2 µg/ml) of tetracycline without arabinose. The colours of traces are shown in the key, and indicate the duration of incubation in media containing tetracycline. The trace shown is one of three independent experiments. (B) Geometric mean fluorescence of DsRed; mean shown +/- S.D. of three independent experiments. (C) Geometric mean fluorescence of GFP; mean shown +/- S.D. of three independent experiments. Fluorescence was measured of at least 30,000 events. One-way ANOVA statistical analysis with Tukey's multiple comparisons was performed. n.s., non-significant.

Next, I determined whether FD could provide a reliable measure of *S. flexneri* replication compared with commonly used methods such as following the optical density (OD) of bacterial cultures. Expression of DsRed was induced in *S. flexneri* pDiGc by growth overnight in 1:4 media in the presence of 0.2 % (w/v) arabinose, then bacteria were transferred into fresh media lacking arabinose by diluting the culture 1:100, followed by growth with shaking at 37°C. Samples of bacteria were removed at hourly intervals, and the fluorescence of bacteria, number of CFU, and OD (A_{600}) of cultures were measured (Figure 3.4). Bacteria were then analysed by flow cytometry, gating around GFP positive bacteria, then DsRed fluorescence intensity was measured to assess replication. The results of flow cytometry indicate that the signal from DsRed diminished during the course of growth over 6 hr (Figure 3.4). The change in the geometric mean fluorescence from DsRed was used to estimate the number of bacterial generations by each time point; the results with FD were compared with the number of generations calculated by recovering CFU and by measuring the OD of cultures. There was a significant correlation obtained measuring growth using the OD, CFU, and FD over seven generations for *S. flexneri* pDiGc (Figure 3.4). Pearson correlation tests demonstrate statistically significant correlations between the number of generations calculated on the basis of OD and FD for *S. flexneri* pDiGc ($R=0.995$, two-tailed *p* value, $p < 0.0001$) as well as between the CFU and FD ($R=0.975$, two-tailed *p* value, $p < 0.0001$). Therefore, the data confirm that FD can be reliably used to monitor *S. flexneri* replication *in vitro* for at least seven generations.

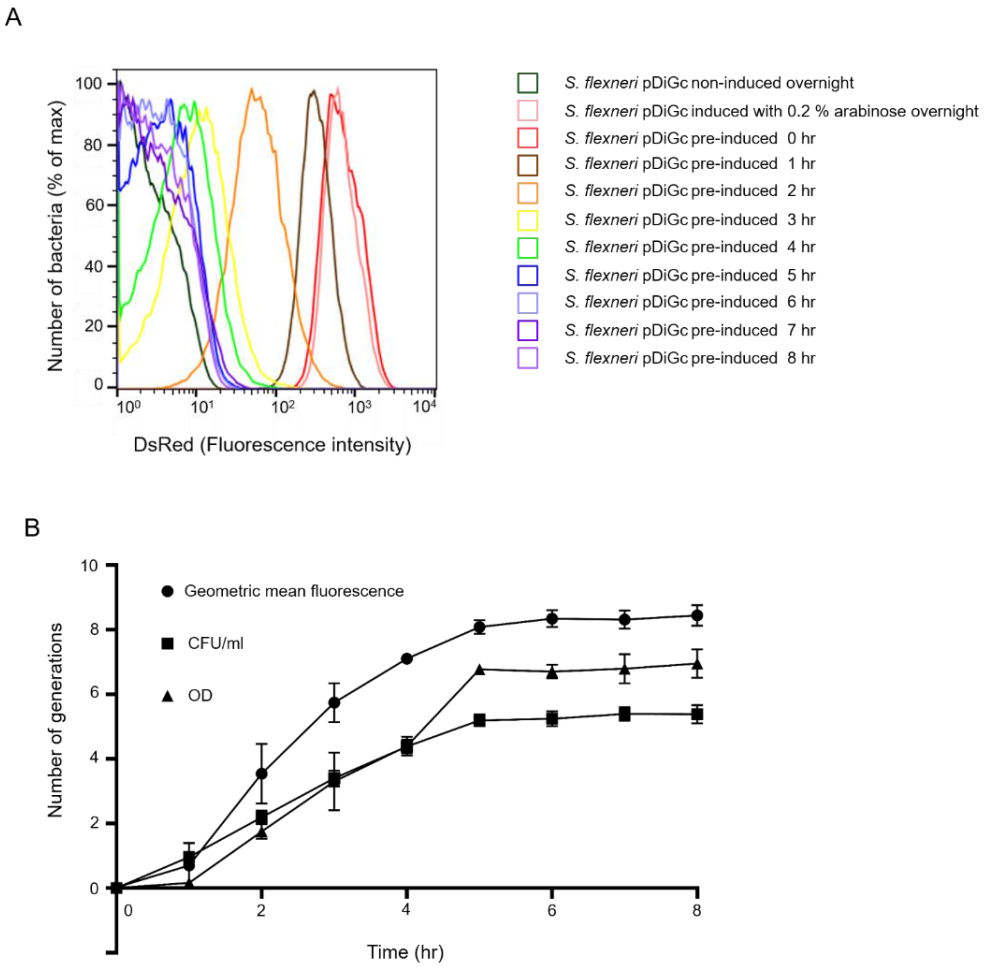


Figure 3.4 Use of FD to assess growth of *S. flexneri in vitro*

(A) Flow cytometric detection of DsRed fluorescence intensity from *S. flexneri* pDiGc grown in liquid media at hourly intervals. The trace shown is one of three independent experiments (with three technical repeats). Cytometry results are of at least 30,000 bacteria at each time point. (B) Number of bacterial generations determined by FD (filled circles), CFU/ml (filled squares) and OD (filled triangles). For fluorescence dilution replication of the population was calculated by the ratio: Yo/Yt (Y being the geometric mean of DsRed at specific times). The number of generations, N, is deduced from the formula F = 2 N. A total of 7-8 generations could be followed by FD. Results for recovery of bacteria and OD show the average +/- S.D. of three independent experiments (each with three technical repeats performed).

3.2 Validation of FD of *S. flexneri* pDiGc *in vivo*

As FD can measure the replication of *S. flexneri* pDiGc *in vitro*, I next examined the ability of FD to assess the intracellular replication of *S. flexneri*. HeLa epithelial cells were challenged at an MOI of 100:1 with *S. flexneri* pDiGc that had been grown overnight (16 hr) in 1:4 TSB in the presence of 0.2 % (w/v) arabinose. This MOI was chosen as *S. flexneri* has a low invasive capacity (~0.01 % of the inoculum), and I wanted to maximise the number of intracellular bacteria to enable detection by flow cytometery. After 30 min to allow the bacterial invasion, gentamicin (100 µg/ml) was added to kill extracellular bacteria and prevent further bacterial entry. HeLa cells were incubated until 1 hr (T1) and 3 hr (T3) after the addition of gentamicin, then they were washed, and lysed by the addition of 1 % (w/v) saponin in PBS to release intracellular *Shigella*. Bacterial recovery at these times was quantified by plating and counting CFU to assess the net growth of the bacterial population. There was no significant difference in invasive capacity of *S. flexneri* pDiGc compared to *S. flexneri* ($p = 0.3216$, one-way ANOVA, Figure 3.5). Furthermore, there was no significant difference in intracellular replication capacity of *S. flexneri* pDiGc compared to *S. flexneri* as assessed by recovery from cells ($p = 0.1974$, one-way ANOVA, Figure 3.5).

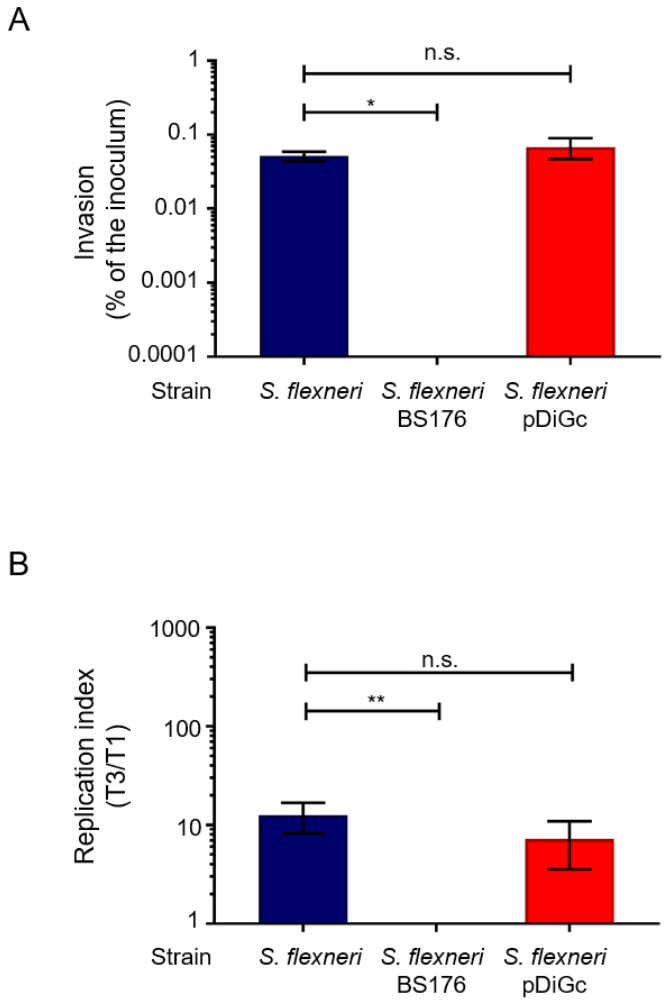


Figure 3.5 Invasive and intracellular replication capacity of *S. flexneri* pDiGc

(A) HeLa cells were infected with *S. flexneri*, *S. flexneri* BS176 a non-invasive strain and *S. flexneri* pDiGc at an MOI of 100:1. Percentage invasion was determined by comparing the bacteria recovered from cells at 1 hr (T1) after gentamicin treatment to the input (T0) x 100 (B) Replication index following invasion. Replication index represents the fold increase in bacteria recovered between 1hr (T1) and 3hr (T3). Results show mean +/- S.D. of three independent experiments (each with three technical replicates). One-way ANOVA with Tukey's multiple comparisons was performed. *, $p < 0.05$, **, $p < 0.01$, n.s., non-significant.

As FD can measure the replication of *S. flexneri* pDiGc *in vitro*, and the strain is able to invade and replicate, I examined the ability of FD to assess the intracellular replication and heterogeneity of *S. flexneri*. Infection of HeLa cells was repeated and recovered intracellular *S. flexneri* pDiGc were analysed by flow cytometry by gating on GFP-positive bacteria, then measuring fluorescence intensity generated by DsRed. The cytometric trace indicates that there are two bacterial populations following *S. flexneri* infection at the end of the experiment, a sub-population where the DsRed fluorescence intensity has reduced (replicated), and a larger DsRed positive non-replicating population (Figure 3.6). However, there was no overall reduction in the geometric mean of fluorescence from DsRed and GFP from *S. flexneri* pDiGc following invasion between 1 hr and 3 hr (Appendix 1). Furthermore, replication could not be detected as had been detected *in vitro.* An average of -0.1669 (+/-1.0201 S.D.) generations were observed by FD for *S. flexneri*. This suggests that *S. flexneri* intracellular replication cannot be measured using FD.

A potential source of non-replicating bacteria is extracellular bacteria that have been exposed to gentamicin. Gentamicin is an aminoglycoside, irreversibly binds to the 30S subunit of the bacterial ribosome, interrupting protein synthesis (209). This mode of action is bactericidal but not does not cause lysis. Therefore, the bacteria detected in this assay could be gentamicin-treated extracellular bacteria. Consistent with this, infection of cells with *S. flexneri* BS176 pDiGc, which is non-invasive due to lack of the virulence plasmid (49), also leads to a DsRed positive (non-replicating population) detected by flow cytometry (Figure 3.6).

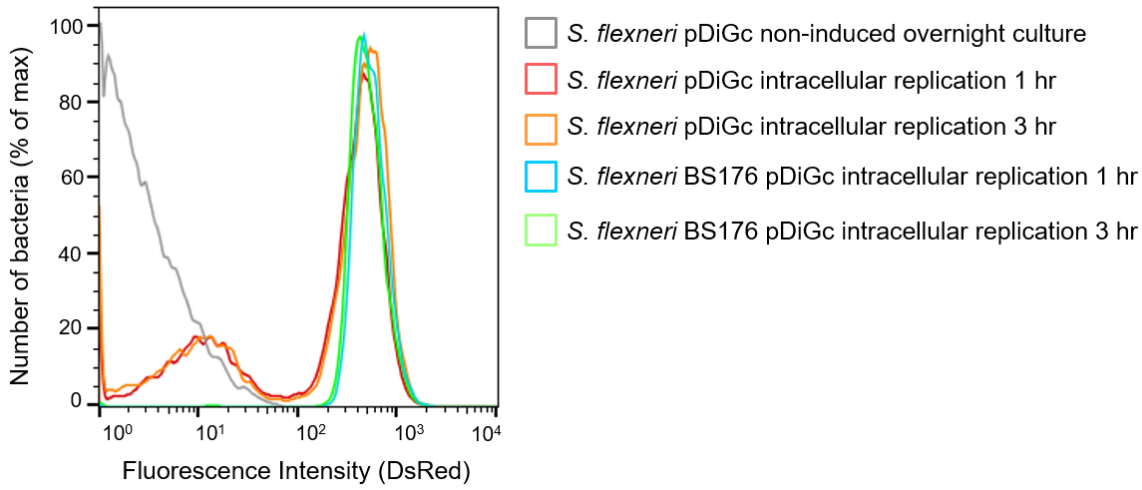


Figure 3.6 Intracellular replication of *S. flexneri* pDiGc in HeLa cells detected by FD.

HeLa cells were infected with *S. flexneri* pDiGc or *S. flexneri* BS176 pDiGc at a MOI of 100:1. Cells were incubated for 30 min to allow invasion, after which gentamicin was added to remove extracellular bacteria. Traces show the DsRed fluorescent intensity for arabinose induced and non-induced *S. flexneri* pDiGc as positive and negative controls respectively, and bacteria recovered after T1 (1 hr) or T3 (3 hr) following addition of gentamicin. Results show one of two independent experiments. Cytometry results are of at least 30,000 bacteria.

3.3 Construction of pDiGc^{cam} as a new fluorescence dilution tool to measure *in vivo* replication

Intracellular replication assays have been established in other pathogens, such as *Burkholderia cepacia*, which are inherently resistant to gentamicin. Instead of gentamicin, ceftazidime alone was used to eliminate extracellular bacteria (210). Furthermore, a recent version of FD developed to measure replication of *Mycobacterium tuberculosis in vitro* and *in vivo* used a combination of penicillin G and streptomycin (206).

To prevent extracellular bacteria from being detected by flow cytometry, this population needs to be killed and eliminated. β-lactam antibiotics would be suitable as they cause bacterial lysis, and some antibiotics of this class do not penetrate eukaryotic cells (210, 211). However, β-lactams cannot be used with pDiGc as it harbours a β-lactamase (ampicillin resistance) (Figure 3.1). Therefore, pDiGc was modified by replacing the ampicillin resistance cassette with a gene (*cam*) encoding Chloramphenicol acetyltransferase. In brief, the 530 bp *cam* gene was amplified from pBAD33 and then assembled into pDiGc replacing amp^r using NEBuilder® HiFi DNA Assembly. The resulting plasmid, pDiGc^{cam}, was introduced into *S. flexneri* by electroporation generating *S. flexneri* pDiGc^{cam}.

3.4 Assessment of growth conditions for *S. flexneri* pDiGc^{cam}

S. flexneri pDiGc was virulent when struck out on Congo red plates (an indicator dye which can detect virulent *Shigella* spp.) (165). However, following overnight growth of *S. flexneri* pDiGc^{cam} in the presence of chloramphenicol (5 µg/ml), a high proportion of bacteria (approximately 50 %) gave rise to white colonies after growth on media containing Congo red. To further understand the basis of this observation, white *S. flexneri* pDiGc colonies were analysed by multiplex PCR (Figure 3.7) to detect whether they retained genes on the virulence plasmid. Multiplex PCR targets key genes on pINV (*virF*, *vapBC* and *mxiM*), with *h-ns* included as a chromosomal control. Multiplex PCR confirmed that bacteria in the white colonies had lost *mxiM* which is located in the T3SS PAI but did not lose other plasmid genes. Unfortunately attempts to change the antibiotic resistance cassette were unsuccessful due to the plasmid failing to assemble (tetracycline or spectinomycin). Kanamycin could not be used as it was incompatible with future project plans as I wanted to screen a transposon (Tn*5*) library which harbours a kanamycin resistance cassette.

To find conditions which allowed for the maintenance of both pDiGc^{cam} (as a reporter) and the virulence plasmid (to allow bacterial invasion and intracellular replication) *S. flexneri* pDiGc^{cam} was grown overnight in a range of chloramphenicol concentrations. Following overnight growth, cultures were serially diluted ten-fold and plated onto solid media containing Congo red with and without chloramphenicol (5 µg/ml), to allow enumeration of bacteria expressing the T3SS and/or retaining pDiGc^{cam}. Results demonstrate that growth in no or low concentrations of chloramphenicol (*i.e.* between

0.039 and 0.079 µg/ml, Figure 3.7) was required so that the majority of bacteria retained T3SS expression and pDiGc^{cam} after overnight growth (Figure 3.7).

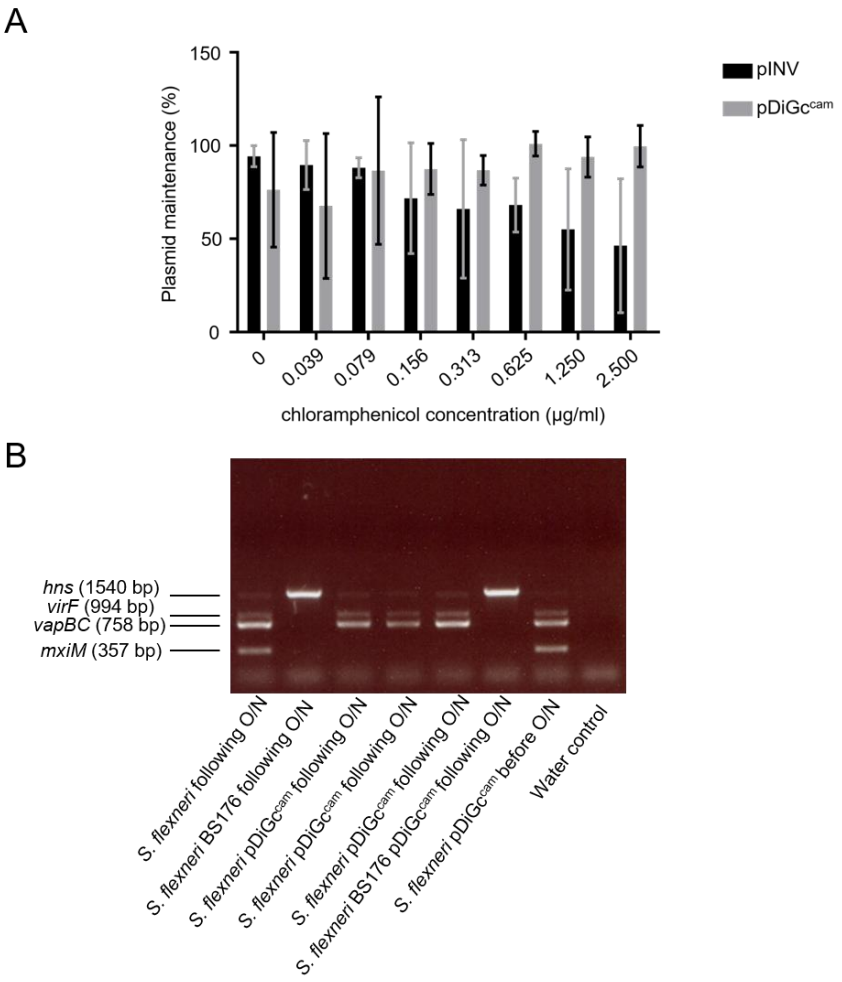


Figure 3.7 Maintenance of pINV and pDiGc^{cam} in *S. flexneri*.

(A) Bacteria were grown overnight in a range of chloramphenicol concentrations, and plated to media containing Congo red (to enumerate bacteria expressing the T3SS) or chloramphenicol (to assess the presence of pDiGc^{cam}). Results for recovery of bacteria show the average +/- S.D. of three independent experiments. (B) Multiplex PCR to determine the nature of pINV instability in *S. flexneri*. Each lane corresponds to a single colony either before or following one passage (growth in TSB 5µg/ml cam media overnight).

3.5 Validation of FD in *S. flexneri* pDiGc^{cam} *in vitro*

To establish if pDiGc^{cam} allows for inducible expression of DsRed similar to pDiGc. *S. flexneri* pDiGc^{cam} was grown overnight (16 hr) without chloramphenicol, with or without arabinose (0.2 %) in 1:4 TSB. As expected, in the absence of the inducer, *S. flexneri* pDiGc^{cam} demonstrated only GFP fluorescence. There was with no significant DsRed geometric mean fluorescence detected above untransformed *S. flexneri* levels (p > 0.9999, one-way ANOVA, Figure 3.8). The presence of arabinose resulted in significant DsRed fluorescence for *S. flexneri* pDiGc^{cam}, showing the plasmid confers inducible DsRed expression in *S. flexneri* (p = 0.0040, one-way ANOVA, Figure 3.8).

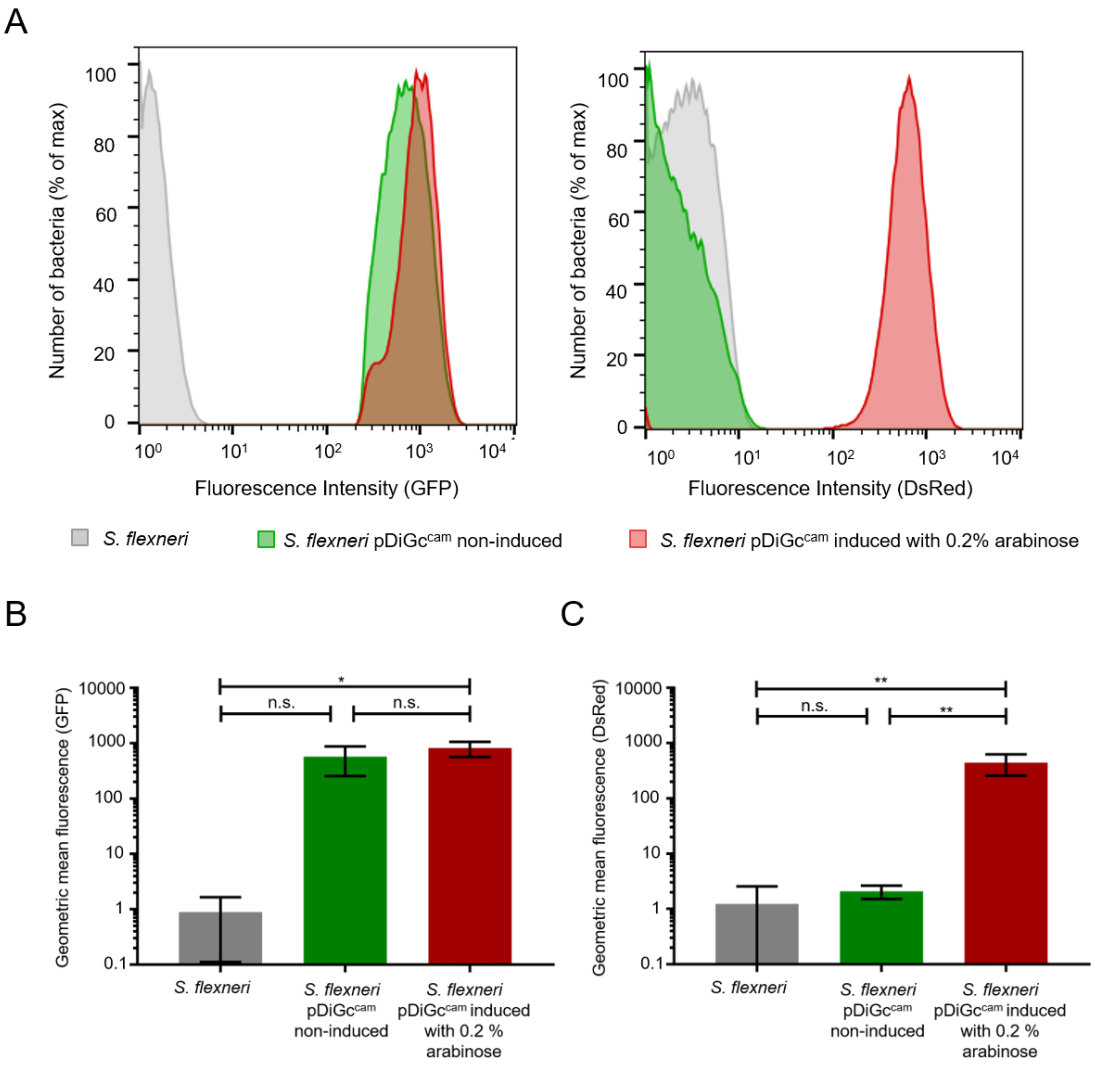


Figure 3.8 Fluorescence conferred by pDiGc^{cam} in *S. flexneri*.

(A) *S. flexneri* pDiGc^{cam} was grown in the presence (0.2 %, red trace) or absence (green trace) of 0.2 % arabinose. Flow cytometric detection of GFP and DsRed fluorescence intensity was measured. The traces show one of three independent biological repeats. (B) Geometric mean fluorescence of GFP mean shown +/- S.D. of three independent experiments. (C) Geometric mean fluorescence of DsRed results mean shown +/- S.D. of three independent experiments. Fluorescence was measured of at least 30,000 events. One-way ANOVA statistical analysis with Tukey's multiple comparisons was performed. *, $p < 0.05$, **, $p < 0.01$ and n.s., non-significant.

Experiments were performed to determine whether DsRed encoded on pDiGc^{cam} is stable in *S. flexneri*. *S. flexneri* pDiGc^{cam} was grown overnight (16 hr) in 1:4 TSB in the presence of 0.2 % arabinose. Then bacteria were washed three times and transferred to media 1:100 dilution containing no arabinose but with a bacteriostatic concentration of tetracycline (0.2 µg/ml) to prevent *de novo* protein synthesis. The intensity of GFP and DsRed fluorescence channels was measured over 6 hr. The DsRed fluorescence intensity of *S. flexneri* pDiGc did not significantly change over 6 hr (p = 0.2894, one-way ANOVA, Figure 3.9). Additionally, the GFP fluorescence intensity of *S. flexneri* pDiGc did not significantly change over 6 hr (p = 0.8408, one-way ANOVA, Figure 3.9). The results show that DsRed is sufficiently stable to be used as a marker for *S. flexneri* replication over 6 hr (Figure 3.9).

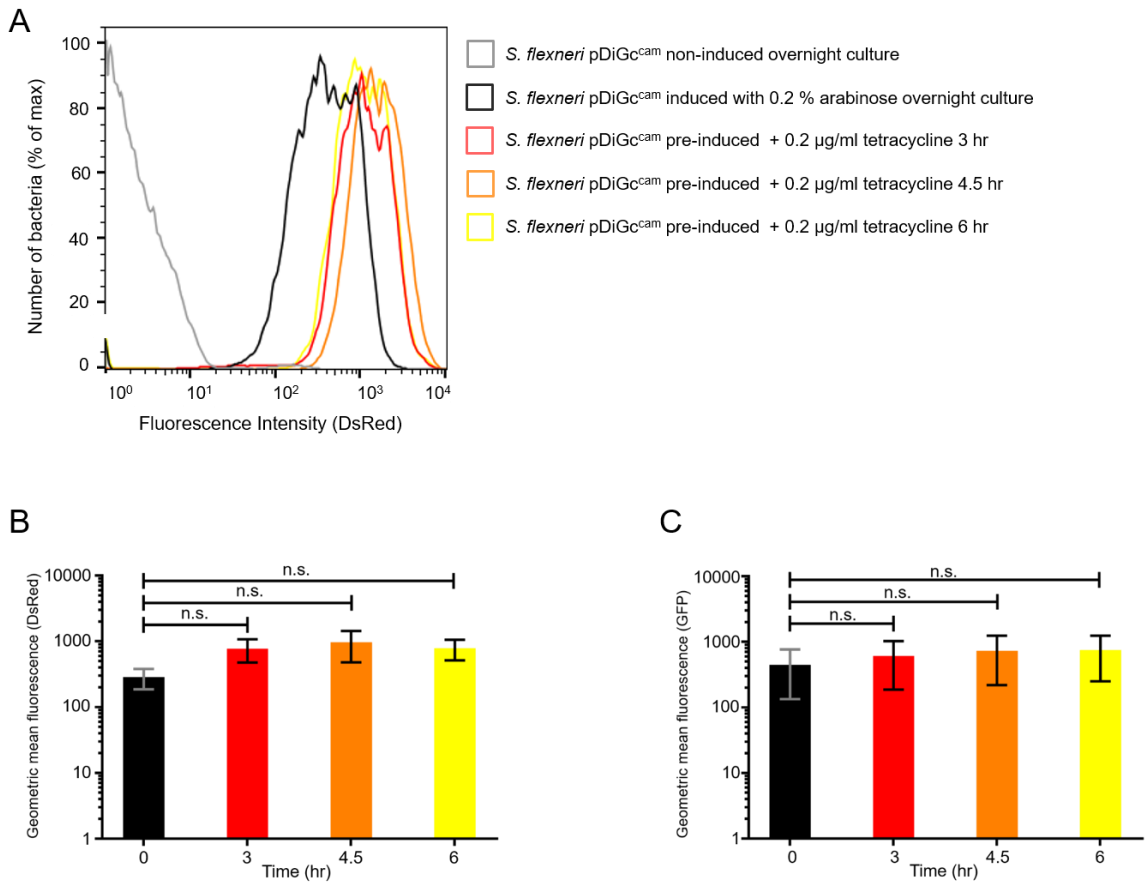
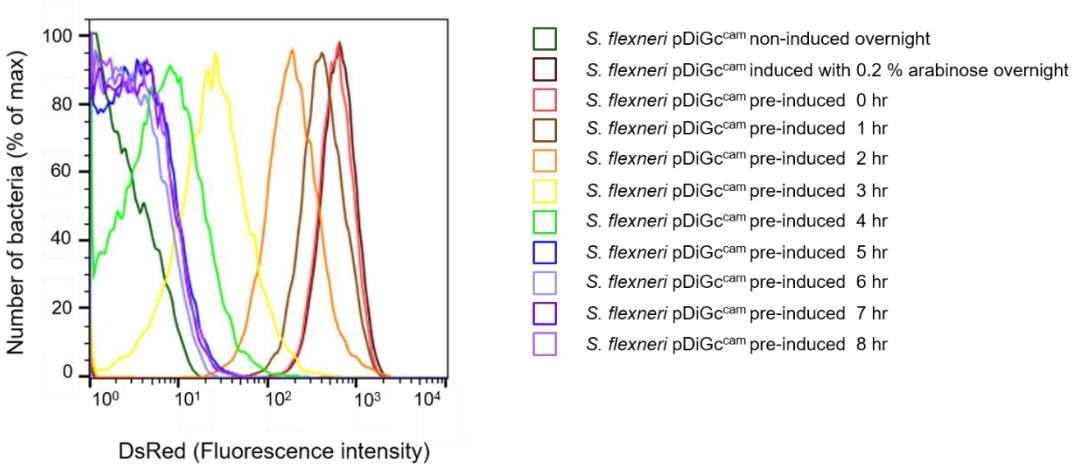


Figure 3.9 Stability of DsRed from pDiGc^{cam} in *S. flexneri.*

(A) Flow cytometric detection of DsRed fluorescence intensity of *S. flexneri* pDiGc induced with 0.2 % arabinose overnight, washed and subcultured in the presence of a bacteriostatic concentration (0.2 µg/ml) of tetracycline without arabinose. The colours of traces are shown in the key, and indicate the duration of incubation in media containing tetracycline. The trace shown is one of three independent experiments. (B) Geometric mean fluorescence of DsRed; mean shown +/- S.D. of three independent experiments. (C) Geometric mean fluorescence of GFP; mean shown +/- S.D. of three independent experiments. Fluorescence was measured of at least 30,000 events. One-way ANOVA statistical analysis with Tukey's multiple comparisons was performed. n.s., non-significant.

To determine whether FD using pDiGc^{cam} provides a reliable measure of *S. flexneri* replication, the expression of DsRed was induced overnight (16 hr) in 1:4 TSB in the presence of arabinose. *S. flexneri* pDiGc^{cam} was then transferred into media 1:100 without arabinose and grown with shaking at 37°C. Samples were taken at hourly intervals to measure OD of cultures, the number of CFU, and for analysing bacteria by flow cytometry (Figure 3.10). Bacteria were analysed by cytometry, gating around GFP positive bacteria, then DsRed fluorescence intensity was measured for replication. Flow cytometry data demonstrate that the DsRed fluorescence intensity diminished during the course of growth. The change in geometric mean fluorescence over time was used to estimate the number of bacterial generations at each time point and the results with FD were compared with the number of generations calculated by recovery of CFU and OD. There was a significant correlation in growth measured by OD, CFU and FD over seven generations for *S. flexneri* pDiGc^{cam}. Pearson correlation tests reveal a statistically significant positive correlation between generations using CFU and FD (R=0.973, two-tailed *p* value, $p < 0.0001$, Figure 3.10), and calculated using OD and FD (R= 0.976, two-tailed *p* value, $p < 0.0001$, Figure 3.10). Therefore, results confirm that FD with pDiGc^{cam} can be used reliably to monitor *Shigella* replication for at least seven generations.

A



B

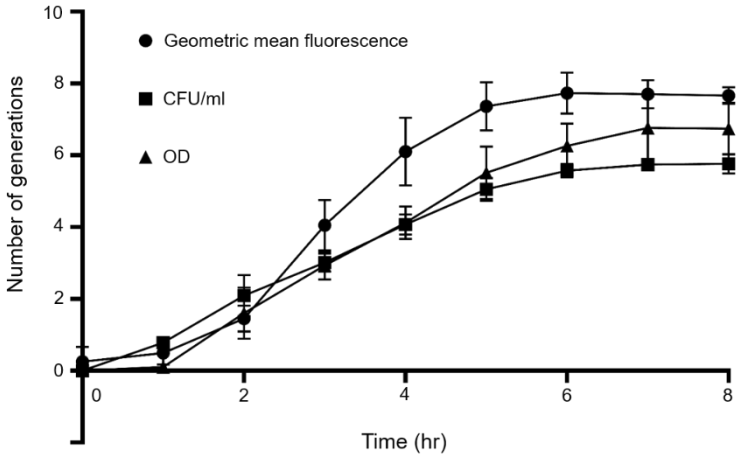


Figure 3.10 Use of pDiGc^{cam} to assess growth of *S. flexneri in vitro*

(A) Flow cytometric detection of DsRed fluorescence intensity from *S. flexneri* pDiGc grown in liquid media at hourly intervals. The trace shown is one of three independent experiments (with three technical repeats). Cytometry results are of at least 30,000 bacteria at each time point. (B) Number of bacterial generations determined by FD (filled circles), CFU/ml (filled squares) and OD (filled triangles). A total of 7-8 generations could be followed by FD. Results for recovery of bacteria and OD show the average +/- S.D. of three independent experiments (each with three technical repeats performed).

3.6 Use of β-lactam antibiotics to eliminate extracellular bacteria

As I wished to use a bacteriolytic antibiotic to reduce the extracellular bacteria detected by the cytometer, the sensitivity of *S. flexneri* to penicillin G was assessed *in vitro.* Bacteria were grown overnight in liquid media and an inoculum of 5 x 10^7 CFU (equivalent to MOI of 100:1) was exposed to a range of concentrations of penicillin G for 1 hr. The killing efficiency of penicillin G was defined as initial inoculum minus recovered bacteria/initial inoculum x 100 (%). Figure 3.11 shows that *S. flexneri* exposed to penicillin G for 1 hr survives, with no significant reduction in viability.

Bacteria have previously been shown to be tolerant of β-lactams when they are in stationary phase (212), which might explain why the majority of bacteria survive exposure to penicillin G following overnight growth. I hypothesised that sub-culturing and growing bacteria, so they are in logarithmic phase, might reduce the population of surviving bacteria following treatment with penicillin G. The sensitivity of *S. flexneri* to penicillin G was re-examined using bacteria in mid-logarithmic (OD_{600} ~0.4) rather than stationary phase. Figure 3.11 shows that exponentially grown bacteria are more sensitive to penicillin G, and the number of CFU recovered reduces by three orders of magnitude when exposed to at least 500 µg/ml of penicillin G.

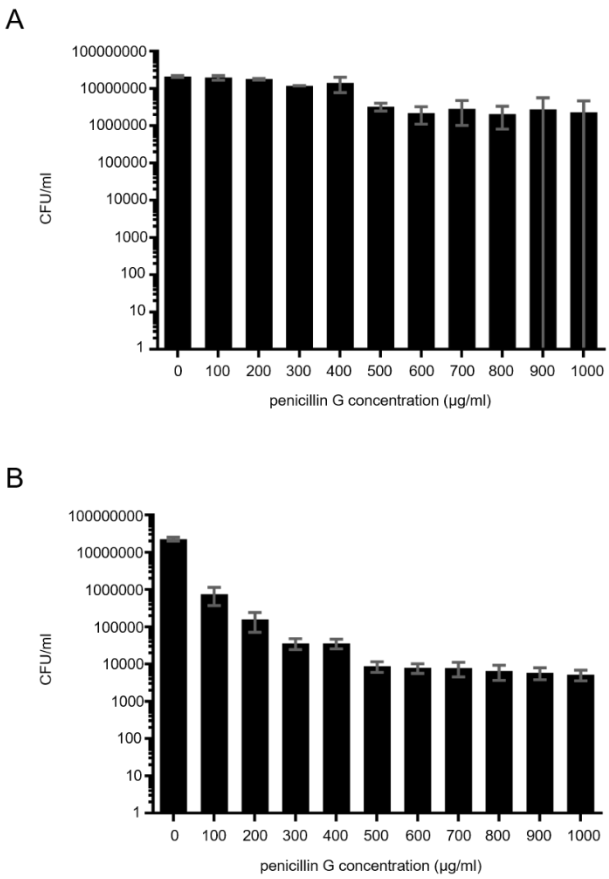


Figure 3.11 Sensitivity of *S. flexneri* to penicillin G.

Killing of *S. flexneri* following exposure for 1 hr to a range of concentrations of penicillin G (indicated) following growth to stationary (A), or mid-logarithmic phase (B). Samples were washed before plating to non-selective media to enumerate surviving bacteria. Results show the mean +/- S.D. of four times independent experiments.

To establish if penicillin G can be used instead of gentamicin to eliminate extracellular bacteria, invasion assays were performed with wild-type *S. flexneri* using either penicillin G (600 µg/ml) or gentamicin (100 µg/ml). As a control, cells were infected with the non-invasive strain, *S. flexneri* BS176. A small amount of the inoculum (0-0.0005 %) of *S. flexneri* BS176 was recovered in assays when cells were incubated with gentamicin or penicillin G. Recovery of *S. flexneri* BS176 was not significantly different from that recovered from gentamicin, validating the use of a β-lactam to recover intracellular bacteria only ($p > 0.9999$, one-way ANOVA, Figure 3.12). There was also no significant difference in the level of recovery of intracellular *S. flexneri* when gentamicin or penicillin G was used, suggesting that penicillin G does not penetrate or affect intracellular bacteria ($p > 0.9999$, one-way ANOVA, Figure 3.12).

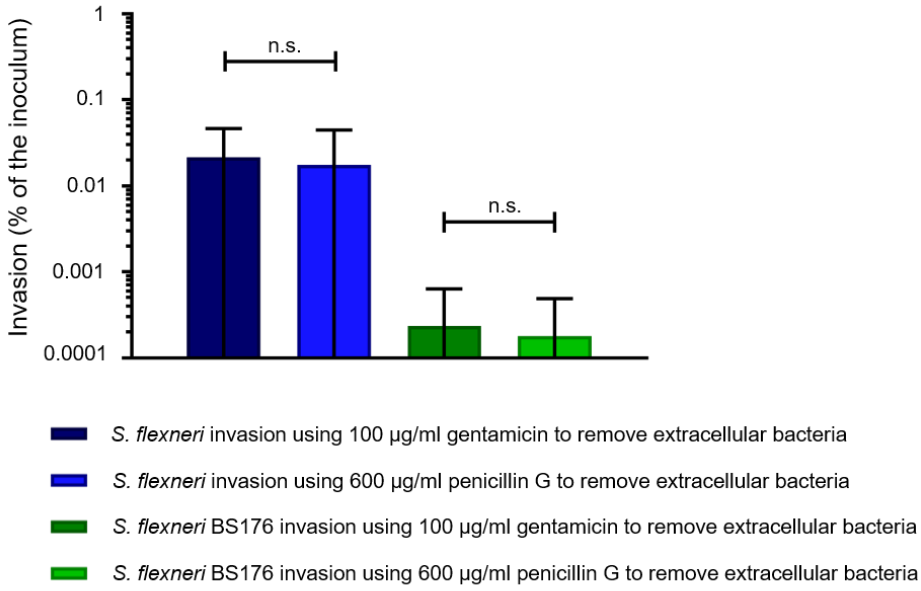


Figure 3.12 Invasion assays using penicillin G to remove extracellular bacteria

HeLa cells were infected with *S. flexneri* or *S. flexneri* BS176 at an MOI of 100:1. Extracellular bacteria were removed as indicated in the key. Results for recovery of bacteria show the average +/- S.D. of three independent experiments (three technical repeats performed). One-way ANOVA with Tukey's multiple comparisons was performed. n.s., non-significant.

To further investigate the use of β-lactam antibiotics, assays were performed with cefsulodin, a β-lactam antibiotic that does not require bacterial replication to lyse them (213). Invasion assays were performed with wild-type *S. flexneri* or *S. flexneri* BS176 as a control. *S. flexneri* BS176 was recovered in assays when cells were incubated with gentamicin or cefsulodin, but not significantly different from one another ($p > 0.9999$, one-way ANOVA, Figure 3.13). Additionally, there was no significant difference in *S. flexneri* invasion assays with gentamicin or cefsulodin, suggesting that cefsulodin could be employed to exclude extracellular bacteria ($p > 0.9999$, one-way ANOVA, Figure 3.13). Taken together these results indicate that *Shigella* invasion and replication assays can be performed with β-lactam antibiotics to remove extracellular bacteria.

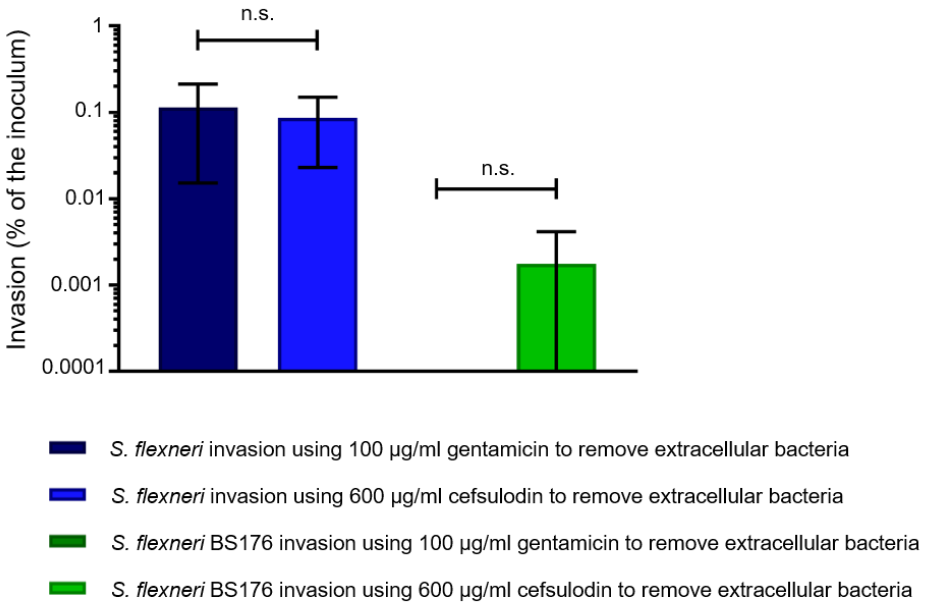


Figure 3.13 Invasion assays using cefsulodin to remove extracellular bacteria

HeLa cells were infected with S. *flexneri* or *S. flexneri* BS176 at an MOI of 100:1. Extracellular bacteria were removed as indicated in the key. Results for recovery of bacteria show the mean +/- S.D. of three independent experiments (three technical repeats performed). One-way ANOVA with Tukey's multiple comparisons was performed. n.s., non-significant.

I assessed if FD could detect the intracellular population of *S. flexneri* pDiGc^{cam} for replication and heterogeneity when cefsulodin was used to remove the extracellular bacteria instead of gentamicin. HeLa invasion was performed as previously described. Following invasion either no antibiotic, gentamicin (100 µg/ml) or cefsulodin (600 µg/ml) was used to remove extracellular bacteria. At 1 hr and 3 hr post-addition of antibiotic, cells were washed then lysed to recover bacteria. The number of CFU was determined by plating to solid media, and bacteria were also analysed by flow cytometry.

When gentamicin was used to remove extracellular bacteria a heterogeneous population of *S. flexneri* was observed (Figure 3.14) as previously (Figure 3.6). On average 1.6119 generations (+/- 0.4409 S.D., Figure 3.14) generations were observed by CFU, and an average of 2.3401 (+/- 1.1904 S.D., Figure 3.14) generations were observed by FD. There was no significant difference between the number of generations observed by either technique (p = 0.8485, two-way ANOVA, Figure 3.14). However, the geometric mean fluorescence of DsRed of *S. flexneri* was not significantly different between 0 hr and 3 hr suggesting that bacterial replication was not occurring (p = 0.9755, two-way ANOVA, Appendix 2). Furthermore, using gentamicin (100 µg/ml) does not stop detection of extracellular bacteria despite killing, as a population of *S. flexneri* BS176 a DsRed positive bacteria was observed at 1 hr and 3 hr that is not significantly different from the 0 hr (p = 0.3534 and p = 0.5256 respectively, two-way ANOVA, Appendix 2). Further evidence that treatment by gentamicin caused this population, was that when no antibiotic was added, no DsRed population was observed in either *S. flexneri* pDiGc^{cam} or *S. flexneri* BS176 pDiGc^{cam} (Figure 3.14).

When cefsulodin was used to remove extracellular bacteria a homogeneous population *S. flexneri* population was observed (Figure 3.14). The geometric mean fluorescence of DsRed of *S. flexneri* was not significantly different between 0 hr and 3 hr suggesting that bacterial replication was not occurring (p > 0.9999, two-way ANOVA, Appendix 2). However, on average 3.07 (+/- S.D. 0.094) generations were observed by CFU, and an average of 3.98 (+/- S.D. 0.835) generations were observed by FD (Figure 3.14). In contrast to using gentamicin to remove extracellular bacteria, when cefsulodin was used, although a DsRed positive population of *S. flexneri* BS176 was observed, there were only a few counts (~500 counts at 1 hr, and ~100 counts at 3 hr) (Figure 3.14). This suggested that most extracellular bacteria had been removed by cefsulodin. With these conditions FD could detect intracellular replication of *S. flexneri* alone. There was no significant difference in the number of *S. flexneri* generations between the two methods of FD and CFU (p = 0.845, two-way ANOVA, Figure 3.14). This suggests that both techniques are equally reliable. Furthermore, using cefsulodin the average replication time was 39 min (+/- 1 min S.D.) when measured by CFU, and 33 min (+/- 3 min S.D.) when measured by FD. There was no significant difference in the generation time measured by CFU or FD (p = 0.9957, two-way ANOVA, Figure 3.14)

An average of four generations was observed following two hours in the HeLa cell (Figure 3.14). Furthermore we can detect 39 min generation time with CFU similar to what had previously been reported (111). With FD the generation time was 33 minutes which suggests that this technique is more sensitive than CFU at measuring bacterial replication (Figure 3.14). However, the level of fluorescence for DsRed reached background levels during this time which might decrease the sensitivity of the technique (Figure 3.14).

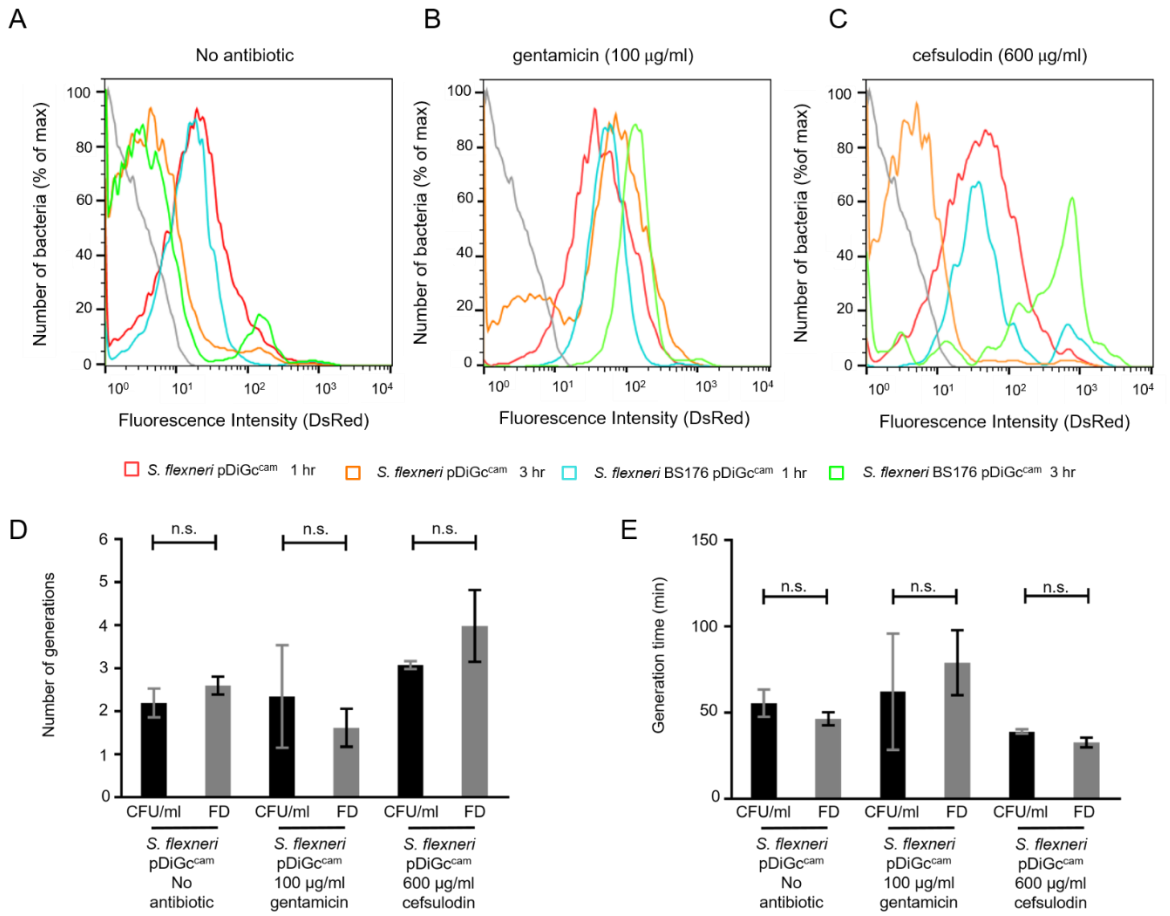


Figure 3.14 Intracellular replication of *S. flexneri* pDiGc^{cam} in HeLa cells using FD

HeLa cells were infected with *S. flexneri* pDiGc^{cam}, and intracellular replication was assessed by measuring fluorescence of bacteria after 1 hr (T1) and 3 hr (T3) invasion Flow cytometry traces of *in vivo* FD when no antibiotic was added to remove extracellular bacteria (A), or when (B) 100 µg/ml gentamicin or (C) 600 µg/ml cefsulodin was added to remove the extracellular population of bacteria (D) The number of generations calculated under each of the above conditions. (E) The generation time determined by each of the methods. Cytometry traces show one of three independent experiments. Fluoresence was measured of at least 10,000 bacteria for each condition, except *S. flexneri* BS176 pDiGc^{cam} where the whole sample was ran. Results for recovery of bacteria show the mean +/- S.D. of three independent experiments (three technical repeats performed). Two-way ANOVA with Tukey's multiple comparisons was performed. n.s., non-significant.

3.7 DsRed reduces the sensitivity of fluorescence dilution

It was observed that fluorescent signal from DsRed was less in *S. flexneri* pDiGc^{cam} when grown to mid-log compared with stationary phase (Figure 3.15). The decrease in DsRed fluorescence following subculture might explain why it was only possible to detect three divisions before the fluorescence of DsRed reached background levels. A possible explanation for this is the maturation time for DsRed T3 S4T. Although the protein is synthesised and detectable by western blot analysis within two hours of growth, the fluorophore does not fully mature until 10-22 hr later (214). pDiGc harbours DsRed T3 S4T, although the maturation of this is 3 hr this is still not ideal (215). In contrast, GFP matures in bacterial growth around 1 hr and the GFP fluorescence was not significantly different following overnight and subculture so would be better to detect replication (p = 0.9643, one-way ANOVA, Figure 3.15) (216).

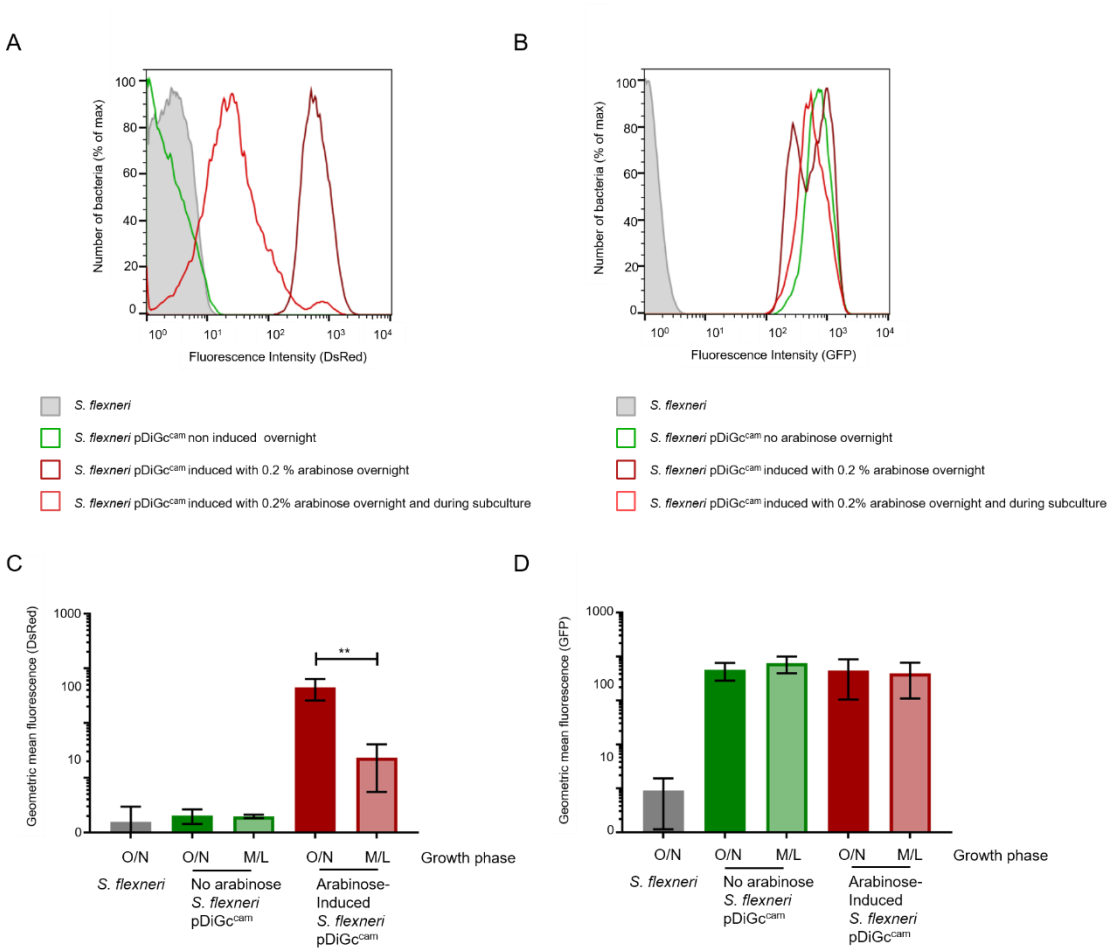


Figure 3.15 Fluorescence from DsRed is affected by growth conditions.

(A) Flow cytometric detection of DsRed fluorescence intensity from a *S. flexneri* pDiGc^{cam} at mid-log or overnight (stationary phase) (B) Flow cytometric detection of GFP fluorescence intensity from a *S. flexneri* pDiGc^{cam} at mid-log or overnight (stationary phase). Trace shows one of three independent experiments (C) Geometric mean of DsRed fluorescence from a *S. flexneri* pDiGc^{cam} after overnight (O/N) and mid-log (M/L). (D) Geometric mean of GFP fluorescence from a *S. flexneri* pDiGc^{cam} after overnight (O/N) and mid-log (M/L). Results for geometric mean show mean +/- S.D. of three independent experiments (three technical repeats performed). One-way ANOVA with Tukey's multiple comparisons was performed **, $p < 0.01$.

The data in Figure 3.15 suggest we could measure intracellular replication following invasion of cells with bacteria grown overnight. However bacteria are usually grown to mid–logarithmic phase before adhesion, invasion and intracellular replication assays (217). Therefore, I compared invasive and replicative capacity of *S. flexneri* or *S. flexneri* pDiGc^{cam} grown overnight or to mid-logarithmic phase; *S. flexneri* BS176 (which lacks pINV) was included as a control. In all conditions *S. flexneri* and *S. flexneri* pDiGc^{cam} behaved similarly. There was no significant difference between *S. flexneri* and *S. flexneri* pDiGc^{cam} in invasion when either mid-log or stationary phase cultures were used to infect cells. There was also no difference in fold replication detected if infected with overnight or mid-log *S. flexneri* (Figure 3.16). However, there was more invasion of HeLa cells by bacteria grown to mid-logarithmic phase (0.05 % of the inoculum +/- 0.006) compared with the same strain grown to stationary phase (0.002 % of the inoculum +/- 0.001) (Figure 3.16). As assays were performed separately statistical comparisons could not be performed.

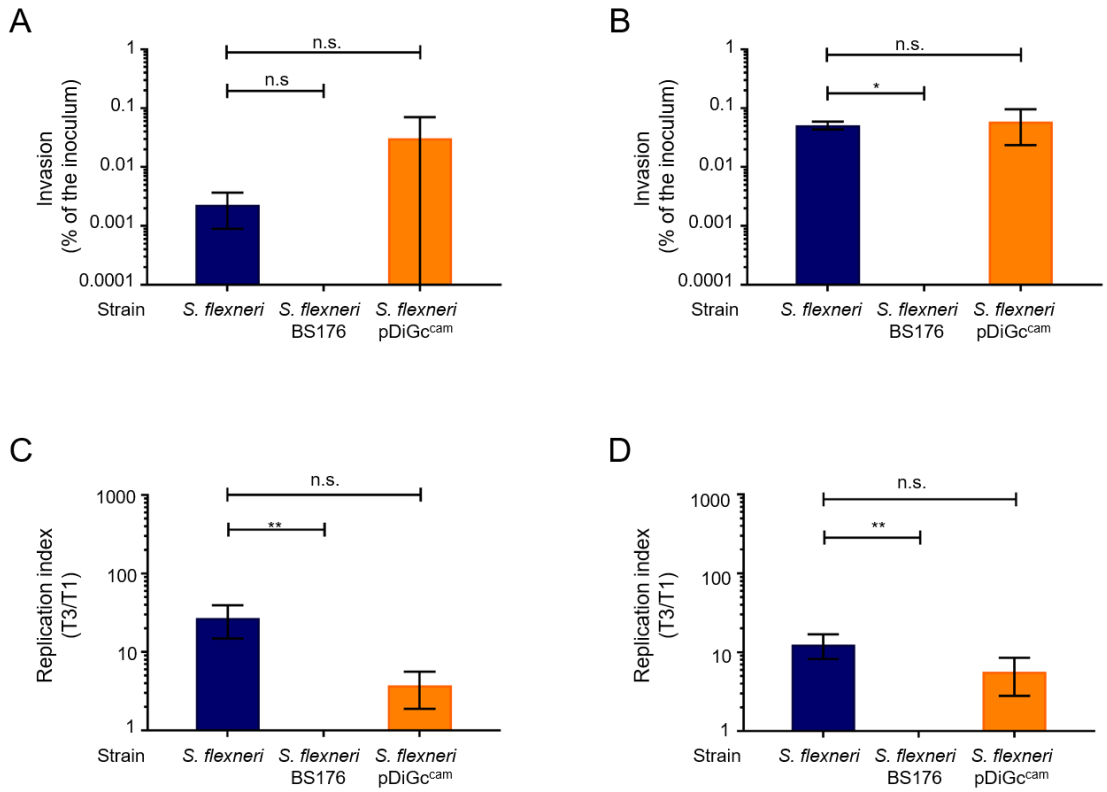


Figure 3.16 Invasion and intracellular replication comparing stationary and mid-log bacteria.

(A) HeLa cells were infected with *S. flexneri*, *S. flexneri* BS176 (non-invasive strain) and *S. flexneri* pDiGc^{cam} at an MOI of 100:1 following growth to stationary phase (overnight). Bacteria were recovered from cells at 1 hr (T1) after gentamicin treatment (to measure bacterial invasion) (B) HeLa cells were infected with *S. flexneri* strains (indicated) grown to mid-logarithmic phase (~OD 0.3) at an MOI of 100:1. (C) Replication index following invasion using overnight (stationary phase) culture. Replication index represents the fold increase in bacteria recovered between 1 hr (T1) and 3 hr (T3). (D) Replication index following invasion using mid-log culture (~OD 0.3) culture. Results show the mean +/- S.D. of three experiments (each with three technical replicates). One-way ANOVA with Tukey's multiple comparisons was performed; *, $p < 0.05$ and **, $p < 0.01$, n.s., non-significant.

3.8 Discussion

One of the defining characteristics of *Shigella* is that it is an invasive, intracellular pathogen (1). The aim of the work in this chapter was to establish a method for determining the rate of bacterial division inside epithelial cells, based on FD. This method has already been established in *Salmonella* to measure replication *in vitro* and *in vivo* (129). Furthermore I wanted to determine if heterogeneity is observed within the population of intracellular *S. flexneri*, as observed in *Salmonella in vivo* (129). Then I wished to screen a transposon library with this tool to assess individual mutants for these properties.

Initially, I demonstrated that FD provides information about bacterial growth and division using laboratory media; my results were validated by comparing findings from measuring the OD of cultures, and recovering viable bacteria by plating. I was able to track up to seven rounds of bacterial replication with FD during growth in liquid media, and the use of a bacteriostatic antibiotic confirmed that the dilution I observed was due to replication, and not to instability of the fluorophore. Of note as previously described FD appears to more sensitively measure replication than other methods (129).

I attempted to establish this method to monitor bacterial replication and heterogeneity inside epithelial cells. However, this proved technically challenging at several levels. Firstly although gentamicin effectively kills extracellular bacteria (which are non-viable and not detected by plating), they can be detected by flow cytometry (Figure 3.6). Evidence for this was provided by examining FD of the non-invasive strain, *S. flexneri* BS176, which showed that after gentamicin treatment, a DsRed population of bacteria could be detected (Figure 3.6). Furthermore the low invasive capacity of *Shigella* into epithelial cells (~0.01 %, Figure 3.5) meant that measuring intracellular bacteria by

flow cytometry post-antibiotic treatment is more difficult than when following *Salmonella* infection in macrophages (129). The extracellular gentamicin exposed population is larger than the intracellular population which only ever reaches ~0.01 % of the inoculum (Figure 3.5).

Therefore, I decided to use alternative antimicrobials, such as β-lactams, which could eliminate extracellular bacteria by lysis. Using β-lactams to remove extracellular bacteria required changing the marker on pDiGc. I replaced the cassette on the plasmid encoding β lactamase (Figure 3.1) with another resistance marker. I utilised a gene encoding chloramphenicol acetyltransferase (*cam*), generating pDiGc^{cam}, thereby allowing use of β-lactams to remove extracellular bacteria. The use of chloramphenicol however had an unexpected effect on the stability of pINV in *S. flexneri* (Figure 3.7). *S. flexneri* pDiGc^{cam} which were grown overnight in selective concentrations of chloramphenicol (5 µg/ml) became avirulent (Figure 3.7). Multiplex PCR revealed that the *mxiM* gene was lost suggesting that growth in chloramphenicol is resulting in loss of the PAI (Figure 3.7). Further investigation would be required to understand if this was IS mediated as has previously been described in the absence of antibiotic (79). This was a critical issue as *S. flexneri* requires pINV to invade epithelial cells (46). The reasons for the effect of pDiGc^{cam} and chloramphenicol on pINV are not clear. The replicon of pINV is RepFIIA while the replicon of pDiGc^{cam} is based on pMB1, so the plasmids are compatible. One possibility is that the function of VapBC, which is the major plasmid maintenance system for pINV at 37°C, is affected by chloramphenicol (181). Both this TA system and the antibiotic target protein translation. This potentially highlights the importance of which antibiotics are used with the study of plasmid maintenance systems. Another potential reason is that the

metabolic cost of maintaining the production of the T3SS and a multi-copy plasmid with two fluorophores was costly, and there was intense selection to lose pINV.

Therefore, I tried to change the antibiotic cassette, however I was unsuccessful. Tetracycline or spectinomycin plasmids failed to assemble. Kanamycin could not be used as it was incompatible with future project plans as I wanted to screen a transposon (Tn*5*) library which harbours a kanamycin cassette. This issue was overcome by not selecting for pDiGc^{cam} (Figure 3.7).

Using β-lactam antibiotics FD measured an average of four generations during two hours in the HeLa cell compared with three generations as could be determined by CFU (Figure 3.14). Furthermore, we can detect 39 min generation time with CFU similar to what had previously been reported (111). With FD the generation time was 33 minutes which suggests that this technique is more sensitive than CFU at measuring bacterial replication (Figure 3.14). However, the level of fluorescence for DsRed reached background levels during this time which might decrease the sensitivity of what we are measuring (Figure 3.14).

It was subsequently found that DsRed is not a robust fluorophore to observe *S. flexneri* intracellular replication for more than four generations. Following growth of bacteria in the presence of the arabinose, the signal from DsRed was significantly higher at stationary phase than after sub-culturing to mid-log phase, even in the presence of arabinose (Figure 3.15). The likely explanation for this finding is the maturation time for DsRed T.3; although the protein is synthesised and detectable by western blot analysis after two hours of growth, the fluorophore does not fully mature until after 10-22 hr growth (214). The duration of growth to reach exponential phase (2-3 hr) probably does not allow enough time for newly synthesised DsRed to mature (Figure

3.15). This may explain why when this technique has been used, infection of macrophages (phagocytic cells) with overnight cultures has been performed (129, 218). This also might explain why subsequent iterations of the plasmid used cherry or TurboFP635 as the fluorophore to track intracellular bacteria (206, 218), which has a maturation time of ~ between 15 min and 1 hr (219, 220), and uses GFP to track replication of bacteria which has a maturation time of ~1 hr (216).

I examined whether it was possible to use bacteria that had been grown overnight for invasion assays as the fluorophore was adequately expressed at this stage (Figure 3.16). This approach however resulted in sub-optimal bacterial invasion of epithelial cells (Figure 3.16). This was a significant problem as it reduces the intracellular population measured as it affects the signal to noise ratio.

It would be possible to circumvent the issues of the chloramphenicol cassette affecting pINV stability and DsRed maturation by a non-plasmid-based approach to perform FD. As a result, I designed and generated a construct with a constitutive fluorophore with a short maturation time, sfmCherry to detect bacteria, together with an inducible fluorophore sfGFP to measure bacterial replication. The exact maturation time of these fluorophores has not been determined because the parent fluorophores have fast maturation times of ~1 hr it was assumed all the derivatives mature quickly. The construct for chromosomal FD (ChromFD) included Rho-independent terminators (Figure 3.17). This was introduced into the *S. flexneri* chromosome in intergenic regions between genes which are transcribed in a tail-to-tail orientation with no predicted transcriptional start site for a sRNA. Furthermore, genetic locations were chosen in which the genes are expressed in all/majority of conditions as one or both

the genes in the pair was essential. Three intergenic regions were identified based on these criteria; those between *ribB*/*ygiE*, *aroG*/*gpmA* and *wzzB*/*hisI*.

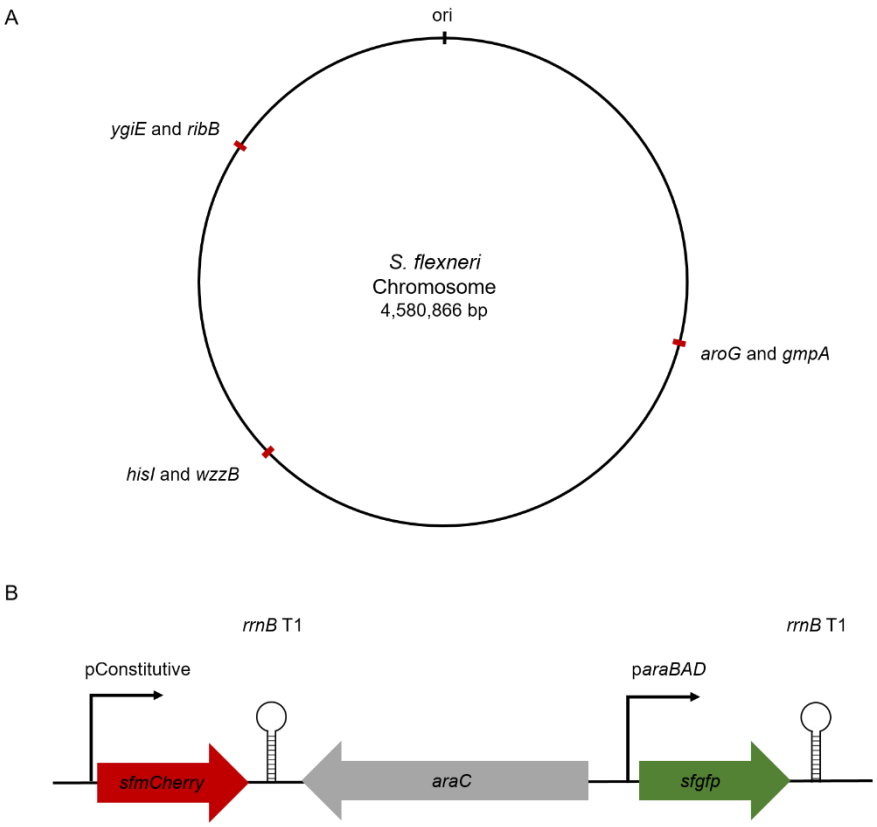


Figure 3.17 Schematic of ChromFD

(A) Schematic of potential chromosomal locations for ChromFD. (B) Schematic of the cassette used for ChromFD, which includes constitutively expressed sfmCherry (to allow detection of bacteria), and a different fluorophore, inducible sfGFP (the signal from which reduces during replication in non-inducing conditions). *araC* encodes the positive and negative regulator of the arabinose promoter.

Preliminary evidence indicates that the ChromFD construct is functional in both the *hisI*/*wzzB* and *aroG*/*gmpA* location *in vitro*. ChromFD is able to measure growth for seven generations like the plasmid versions (Figure 3.4 and 3.10). Furthermore, it maintains pINV during growth. Both sfGFP and sfmCherry mature following subculture to ~OD 0.3 during growth which allowed infection.

However in both epithelia and macrophages, only a small population of intracellular *S. flexneri* was detected and this project was abandoned. If I were to continue these experiments I would need to optimise infection conditions to recover enough bacteria given the poor invasion capacity of *S. flexneri* (0.01 %), to measure > 10,000 counts, such as pooling wells.

ChromFD could easily be applied to study dynamics of bacterial growth *in vitro*. Of particular interest would be to study populations of bacteria that enter a persistent nonreplicating, viable state. Current methods to study persistence measure CFU, however there could be bacteria which are non-replicating but viable which are not measured (221).

4 Chapter Four Investigation of pINV maintenance

The T3SS is a key virulence determinant for *Shigella* spp., and is encoded on a PAI found on the large, single copy plasmid, pINV (135). *Shigella* spp. can spontaneously and irreversibly become avirulent (43-45). During growth *in vitro* at 37°C, pINV or the genes which encode the T3SS of *Shigella* are frequently lost (134). The molecular events which result in loss of the T3SS have been described in *S. flexneri* recently (79). The majority of events that result in loss of virulence are due to the structural instability of pINV, resulting from deletions involving insertion sequences (ISs) flanking the T3SS PAI (79).

As a single copy plasmid, pINV cannot rely on random distribution during cell division to ensure its inheritance, unlike multi-copy plasmids (135). Low copy number plasmids are maintained in bacterial populations by partitioning systems which carefully coordinate plasmid division with chromosomal division. TA systems ensure inheritance in a bacterial population of pINV *via* PSK (135). TA systems that are involved in plasmid maintenance contain two genes in a single operon, encoding a stable toxin and an inherently unstable antitoxin (181). The antitoxin is continuously expressed and able to neutralise the toxin as long as the TA operon is expressed (181). PSK relies on the differential stability of the toxin and antitoxin by causing death of plasmid-free cells as the source of the unstable antitoxin has been lost (140). Strikingly *S. flexneri* pINV possesses two partitioning systems, identified by sequence analysis, ParAB and StbAB and three functional TA systems, VapBC, CcdAB and GmvAT (135). The partitioning systems on *Shigella* pINV have not been well characterised, but the VapBC TA system is important for the maintenance of pINV (163, 179). The focus of the work in chapters four and five was on the TA systems. Recently GmvAT was found to contribute to maintenance of *S. flexneri* pINV at 21°C

(163). CcdAB is a functional TA system but its contribution to *S. flexneri* pINV maintenance is unclear (163) even though CcdAB from the F plasmid has been well characterised (141, 155, 222).

Strains which lack pINV or genes encoding the T3SS grow faster than strains with an intact pINV, indicating that T3SS expression has a fitness cost to the bacterium (134). Despite the apparent fitness cost, *Shigella* is a successful pathogen, suggesting that mechanisms successfully maintain pINV throughout the environments and stresses it encounters in the host. There is some evidence that TA systems can act as response regulators that facilitate changes in gene expression in response to environmental signals (167). Temperature as well as other environmental factors, such as oxygen, nutritional availability and pH, could influence pINV stability. The aim of the work in this chapter was to understand the role of TA systems on pINV stability in different environments including those related to conditions found in the host.

Shigella which fail to express the T3SS can be distinguished from wild-type bacteria by their colony morphology on solid media containing Congo red (165). This method however cannot sensitively detect pINV instability as it does not allow positive selection of bacteria which have lost or retained genes encoding the T3SS (163). To measure pINV instability, a *sacB-kan*^{r} cassette was introduced into *mxiH* which encodes the needle subunit of the T3SS (*mxiH*::*sk*) (163). As the majority of events that result in loss of T3SS expression in *S. flexneri* involve PAI deletions, the *sacB-kan*^{r} cassette was placed within the T3SS PAI (79). The *sacB-kan*^{r} cassette allows positive selection of bacteria which retain (through kanamycin resistance) or lose (through resistance to sucrose) genes encoding the T3SS.

4.1 VapBC is important for pINV stability

To examine the role of TA systems on pINV stability, TA systems were individually deleted in *S. flexneri* carrying *sacB-kan*^{r} in *mxiH* (*mxiH*::*sk*) (163). Bacteria were grown at 37°C on non-selective solid media for 25 generations. Colonies were re-suspended in PBS and plated onto solid media containing kanamycin or sucrose, or LB alone, and the number of CFU/ml counted. Consistent with previous work (163), results demonstrate the absence of GmvAT and CcdAB TA systems has no significant effect in pINV maintenance at 37°C in *mxiH*::*sk* strain ($p = 0.9998$ and $p > 1$, respectively, one-way ANOVA, Figure 4.1). However, VapBC contributes to pINV stability at 37°C; the strain in which this TA system was deleted showed significantly higher loss of the pINV marker compared to the parental *mxiH*::*sk* strain ($p < 0.0001$, one-way ANOVA, Figure 4.1).

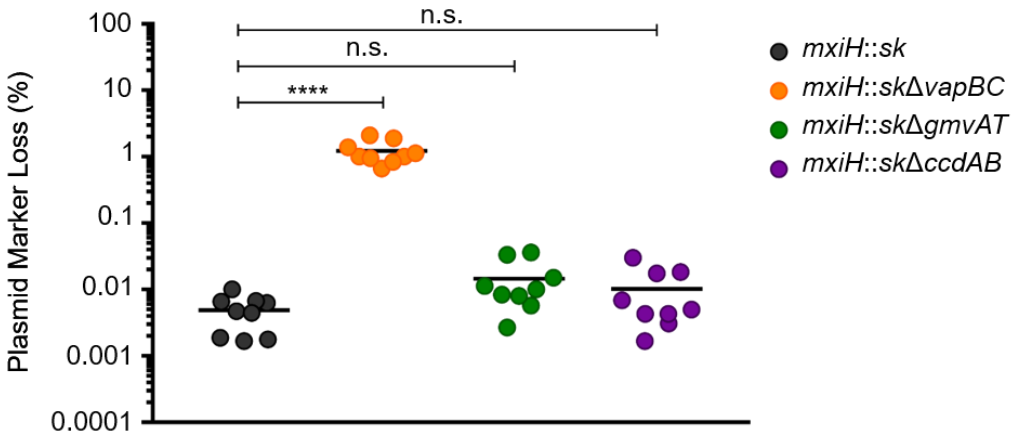


Figure 4.1 VapBC is important for pINV stability at 37°C.

Plasmid marker loss was measured in *mxiH*::*sk* which harbours a dual marker (*sacB-kan*^{r}) in the *mxiH* locus. Results show the percentage of strains that have lost the marker of strains lacking individual TA systems following 25 generations of growth at 37°C. Strains are indicated, and each dot represents results from a single colony (n = 9). Strains were tested on three independent occasions. The horizontal line shows the mean. One-way ANOVA with Tukey's multiple comparisons was performed; ****, $p < 0.0001$, n.s., non-significant.

4.2 The role of TA systems on pINV stability is not altered at 42°C

Different TA systems have different effects on pINV stability at different environmental temperatures (2). The normal body temperature is 37°C, although during inflammation and infection, the temperature can be elevated (223). As 42°C is often used as a temperature to study heat shock in bacteria, I determined the role of TA systems at this temperature, and performed a pINV stability assay at 42°C (223). Deletion of GmvAT and CcdAB TA systems had no significant difference on plasmid marker loss compared to the parental strain at 37°C or 42°C ($p > 0.9999$, respectively, two-way ANOVA, Figure 4.2). Furthermore, plasmid marker loss did not significantly change in deletions of GmvAT and CcdAB when grown at 37°C or 42°C ($p > 0.9999$, two-way ANOVA, Figure 4.2). Strains without VapBC resulted in significant increase in plasmid marker loss relative to *mxiH*::sk at 42°C ($p = 0.0178$, two-way ANOVA, Figure 4.2). There was no significant difference in the role of VapBC on plasmid marker loss at 37°C or 42°C ($p = 0.9965$, two-way ANOVA, Figure 4.2). Overall, there was no difference in the role of TA systems on plasmid stability following bacterial growth at 42°C and 37°C (Figure 4.2).

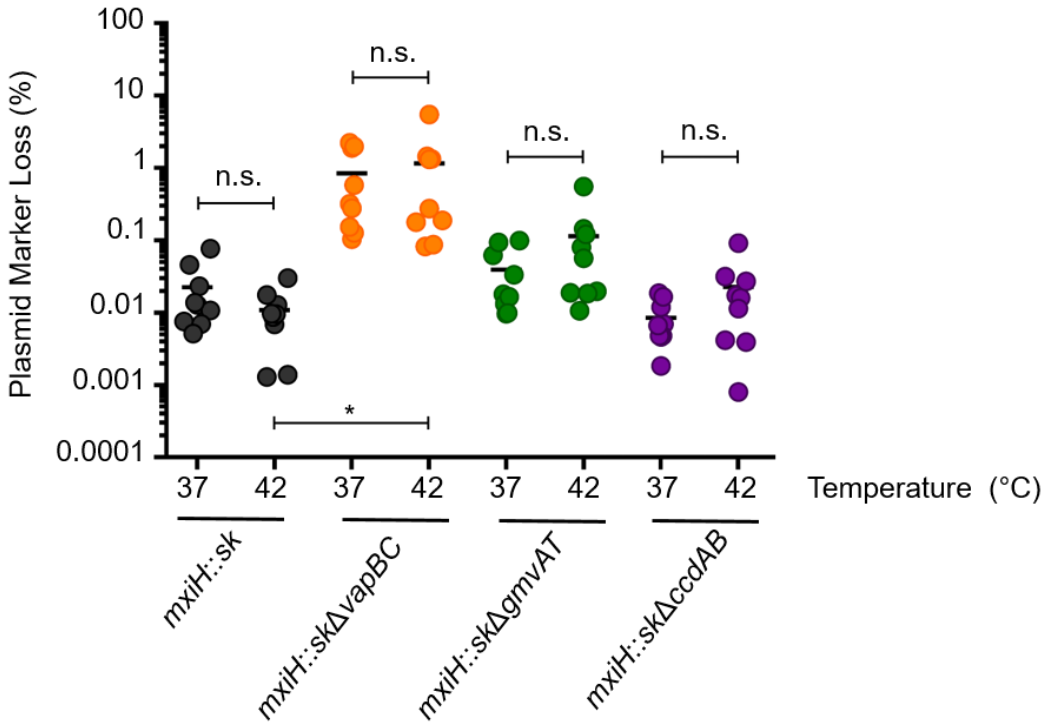


Figure 4.2 The role of TA systems on pINV stability at 37°C and 42°C.

Plasmid marker loss was measured in *mxiH*::*sk* derivatives. Results show the percentage of bacteria that have lost the *sacB-kan*^{r} cassette following 25 generations of growth at 42°C compared to 37ºC. Each dot represents results from a single colony (n = 9). Strains were tested on three independent occasions, and the horizontal lines show the mean. Two-way ANOVA with Tukey's multiple comparison statistical tests was performed; *, $p < 0.05$, n.s., non-significant.

4.3 The role of VapBC on pINV stability is affected by amino acid limitation

Intracellular pathogens encounter a range of nutritional environments while in their host, while competing with the microbiota in the intestine, and in the extracellular compartment (*i.e.* blood or interstitial fluid) where bacteria have access to host glucose and glutamine (224). Intracellular pathogens, such as *Shigella*, experience nutritional stress upon entry into the cytoplasm of host cells, where nutrients can be exhausted as a consequence of bacterial growth (111).

Amino acid starvation leads to the stringent response in bacteria which results in pleiotropic physiological changes (225). The primary result of the stringent response is the inhibition of synthesis of rRNAs and tRNAs, and the upregulation of amino acid biosynthesis (225). The stringent response is dependent on ppGpp (guanosine tetraphosphate) synthesised by RelA, the ppGpp synthetase. ppGpp directly interacts with RNA polymerase leading to down or up- regulation of gene expression (225). TA systems can be activated by amino acid starvation, for example, the HokB-SokB is triggered by (p)ppGpp signalling (140). Furthermore, the degradation of some antitoxins is dependent on Lon which is upregulated during the stringent response (140).

To define the role of TA systems on pINV maintenance under amino acid starvation, strains with *mxiH*::*sk* and individual TA system deletions were examined for pINV marker loss during growth on LB or M9+ (containing 20 % glucose and nicotinic acid) media. Deletion of GmvAT and CcdAB TA systems had no significant difference on plasmid marker loss compared to the parental strain on LB or M9+ ($p > 0.9999$, respectively, two-way ANOVA, Figure 4.3). Furthermore, plasmid marker loss did not

significantly change in deletions of GmvAT and CcdAB when grown at LB or M9+ shown on Figure 4.3 ($p > 0.9999$, two-way ANOVA). While VapBC contributes to pINV maintenance at 37°C on LB ($p < 0.0001$, two-way ANOVA, Figure 4.3), this TA system has no effect during growth on M9+ at 37°C ($p > 0.9999$, two-way ANOVA, Figure 4.3). VapBC is significantly less important in plasmid marker loss during growth on M9+ media ($p < 0.0001$, two-way ANOVA, Figure 4.3). This suggests that during amino acid stress, individual TA systems do not appear to have a major impact on pINV stability.

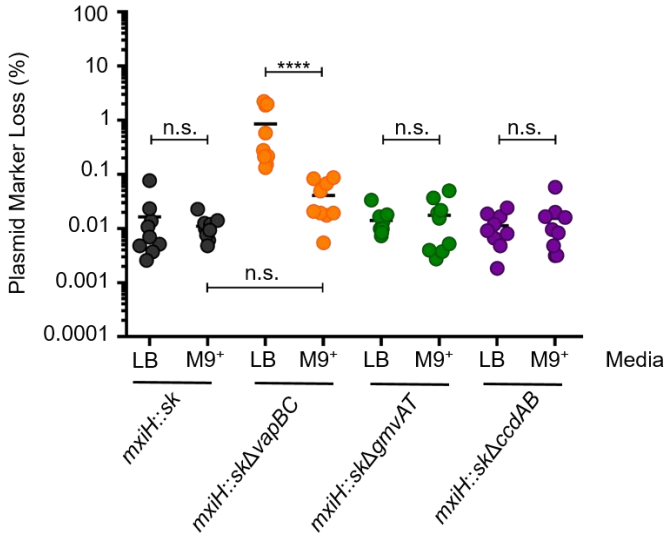


Figure 4.3 The role of VapBC on pINV stability is affected by availability of amino acids.

Plasmid marker loss was measured in *mxiH*::sk derivatives. Results show the percentage of bacteria that have lost the *sacB-kan*^{r} cassette following 25 generations of growth at 37°C on M9^{+} media shown together with results obtained when strains were grown on LB for comparison. Each dot represents results for a single colony (n = 9). Strains were tested on three independent occasions, and the horizontal line represents the mean. Two-way ANOVA with Tukey's multiple comparison statistical tests was performed; ****, $p < 0.0001$, n.s., non-significant.

4.4 The role of VapBC is altered during anaerobic growth conditions

Shigella survives in the colon, which is largely an anaerobic environment (80). The activity of the T3SS is modulated by oxygen availability; the T3SS needle is extended but non-functional in anaerobic environments, but the presence of oxygen close to the epithelial surface triggers activation of the T3SS (80). Given th regulation of T3SS activity by oxygen, the role of TA systems on pINV stability in low oxygen tensions was examined. *mxiH*::*sk* strains with individual TA system deletions were examined for pINV marker loss during growth on LB solid media supplemented with potassium nitrate in aerobic and anaerobic environments. Deletion of GmvAT and CcdAB TA systems had no significant difference on plasmid marker loss compared to the parental strain in aerobic and anaerobic environments ($p > 0.9999$, respectively, two-way ANOVA). Furthermore, plasmid marker loss did not significantly change in deletions of GmvAT and CcdAB when grown in aerobic and anaerobic environments shown on Figure 4.4 ($p > 0.9999$, two-way ANOVA). Deletion of VapBC does not have a significantly different plasmid marker loss than the parental strain in anaerobic conditions ($p > 0.9999$ respectively, two-way ANOVA, Figure 4.4). There was also no difference on plasmid marker loss of *mxiH*::*sk*Δ*vapBC* during aerobic and anaerobic growth at 37°C ($p = 0.0928$ respectively, two-way ANOVA, Figure 4.4). Overall, this data suggests that VapBC plays less of a role in plasmid maintenance in anaerobic conditions (Figure 4.4).

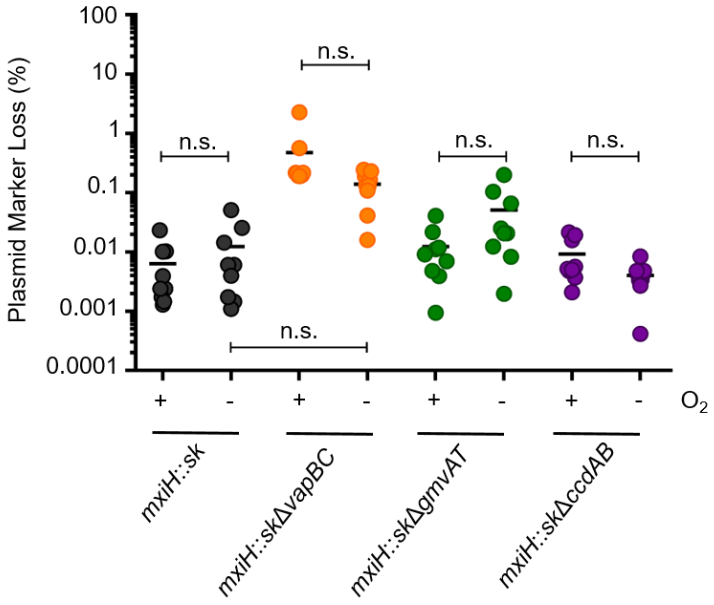


Figure 4.4 The role of TA systems on pINV stability altered in anaerobic growth conditions.

Plasmid marker loss was measured in *mxiH*::sk derivatives. Results show the percentage of bacteria that have lost the *sacB-kan*^{r} cassette following 25 generations of growth at 37°C on LB (100 mM) KNO_3 in anaerobic conditions shown together with results obtained when strains were at 37°C on LB (100 mM) KNO_3 in anaerobic conditions for comparison. Each dot represents results for a single colony (n = 9). Strains were tested on three independent occasions, and the horizontal line represents the mean. Two-way ANOVA with Tukey's multiple comparison statistical tests was performed; n.s., non-significant.

4.5 The role of TA systems on pINV stability is not altered in acidic conditions

Shigella encounters a range of pH stresses in the host, and must pass through the acidic environment of the stomach (pH 2-4), before reaching the ileum which is slightly alkaline. Finally in the large intestine, the bacterium are exposed to short chain fatty acids produced by the microbiota (226). Additionally *Shigella* can be engulfed by professional phagocytes such as macrophages once it crosses the epithelial lining; the vacuole is acidified by the vacuolar-type proton ATPase (V-ATPase) and other hydrogen pumps following fusion with lysosomes (pH approximately 5.5) (227). Enteric bacteria are tolerant to acidic environments, although *S. flexneri* pINV can reduce survival in acidic conditions through unknown mechanisms (228).

To determine the role of TA systems on pINV stability during pH stress, *mxiH*::*sk* strains with individual TA system deletions were examined for pINV marker loss during growth in neutral and acidic conditions on solid media. To increase the acidity of the media, HCl was added to LB and the pH was assessed using strip; media were not buffered. Deletion of GmvAT had no significant difference on plasmid marker loss compared to the parental strain at pH 5, 6 and 7 ($p > 0.9999$, respectively, two-way ANOVA, Figure 5). Furthermore, plasmid marker loss did not significantly change in deletions of GmvAT when grown at pH 5 or pH 6 compared to neutral conditions ($p > 0.9999$, two-way ANOVA, Figure 4.5). Deletion of CcdAB had no significant difference on plasmid marker loss compared to the parental strain when grown at pH5 or pH6 compared to neutral conditions ($p > 0.9999$, respectively, two-way ANOVA, Figure 4.5). Deletion of VapBC also had no significant difference in effect on plasmid marker loss in pH 6 compared to neutral conditions ($p = 0.4069$, two-way ANOVA, Figure 4.5), in contrast at pH 5 there was a significant difference in the plasmid marker loss

compared to neutral conditions (p = 0.0004, two-way ANOVA, Figure 4.5). VapBC however has a significantly higher plasmid marker loss than the parental strain at pH 5, 6 and 7 respectively (p < 0.0001, two-way ANOVA, Figure 4.5). Therefore, VapBC system contributes to plasmid marker loss in both neutral and acidic conditions at 37°C, with no significant difference between the conditions. This indicates that the local pH does not influence the role of TAs on pINV stability.

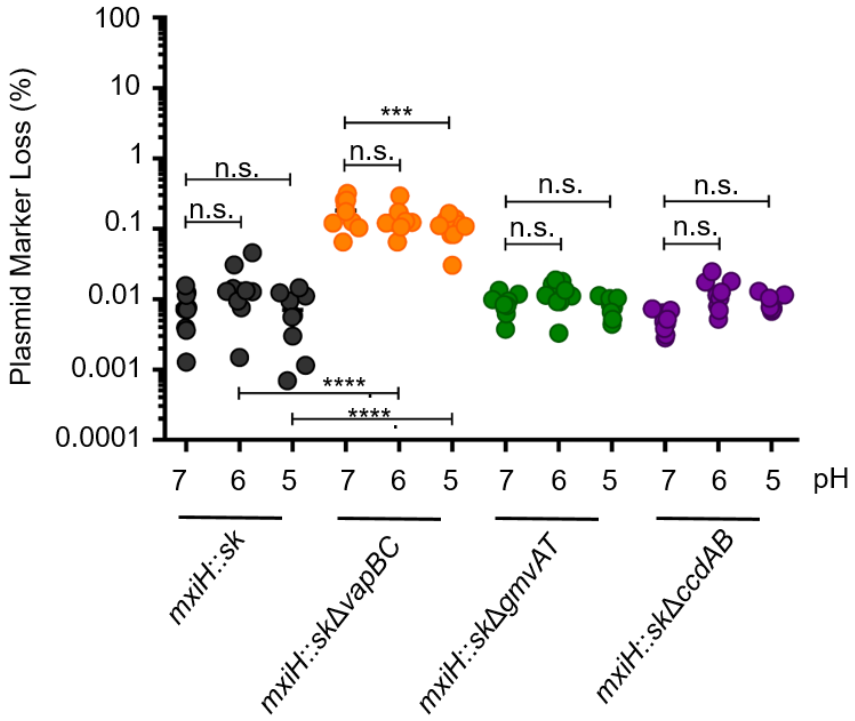


Figure 4.5 The role of TA systems on pINV stability at pH 7, pH 6 and pH 5.

Plasmid marker loss was measured in *mxiH*::sk derivatives. Results show the percentage of bacteria that have lost the *sacB-kan*^{r} cassette following 25 generations of growth at 37°C at the indicated pH with results obtained when strains were at 37°C on LB pH 7 for comparison. Each dot represents results for a single colony (n = 9). Strains were tested on three independent occasions, and the horizontal line represents the mean. Two-way ANOVA with Tukey's multiple comparison statistical tests was performed; ****, p <0.0001 n.s., non-significant.

4.6 The role of TA systems during replication of *S. flexneri* in THP-1 cells

The T3SS PAI is required for invasion of non-phagocytic cells, escape of phagosome and cell-cell spread in non-phagocytic cells and in professional phagocytes. Therefore, pINV must be maintained during each stage of *Shigella* infection. A critical step for pINV maintenance is during intracellular survival and replication in macrophages (51). To determine the role of TA systems in pINV stability during phagocytic cell infection, strains harbouring *mxiH*::*sk* with individual TA system deletions were examined for pINV marker loss during infection of THP-1 derived macrophages.

THP-1 cells are a spontaneously immortalised, human monocytic cell line derived from the blood of a patient with acute monocytic leukemia (201). These cells were chosen for a number of reasons. First, *Shigella* is a human-specific pathogen and THP-1 is a human cell line. Second, primary macrophages cannot be readily expanded for large scale experiments, and use of different donors can introduce variation (229). Finally, as *mxiH*::*sk* does not express a T3SS, I used a phagocytic cell line to ensure efficient uptake of bacteria. Macrophages phagocytose and degrade material such as pathogens, which is the result of increased numbers of lysosomes and mitochondria in differentiated macrophages. THP-1 cells have been shown to produce as many lysosomes and mitochondria as primary macrophages (230)

THP-1 cells (between passage 6 and 15) were differentiated into macrophages in RPMI 1640 + 10 % FCS + 100 ng/ml PMA for 72 hrs. Following this time, the media on the cells were replaced to just RPMI 1640 +10 % FCS. THP-1 cells were then infected with *mxiH*::*sk* at a MOI of 5:1, then left for 30 min to allow invasion. After this time gentamicin (100 µg/ml) was added to kill extracellular bacteria for 1 hr. THP-1 cells either lysed at 1, 2, 3, 5 or 16 hr post-antibiotic treatment. Following lysis, *Shigella*

were plated to selective media to determine the proportion of bacteria retaining the *sacB-kan*^{r} marker. Deletions of individual TA systems did not significantly affect plasmid marker loss following infection (Figure 4.6). At every time point there was no significant defference between plasmid marker loss. As in many cases, the level of plasmid loss was around the limit of detection (l.o.d) of the assay 0.01 % for early 1-5 hrs and 0.1 % for 16 hr post-invasion. The l.o.d. is dependent on the number of bacteria recovered at the end of the experiment, which will be influenced by the number of THP-1, the MOI, and the extent of bacterial growth and killing during the assay.

The results do not provide evidence that TA systems contribute to pINV stability in macrophages. However, the assay is not sensitive enough to detect rare events. Importantly, bacterial replication is required to detect the role of TA systems in PSK. Of note, there was no increase in the number of bacteria recovered from cells over time, although this might not reflect the number of generations.

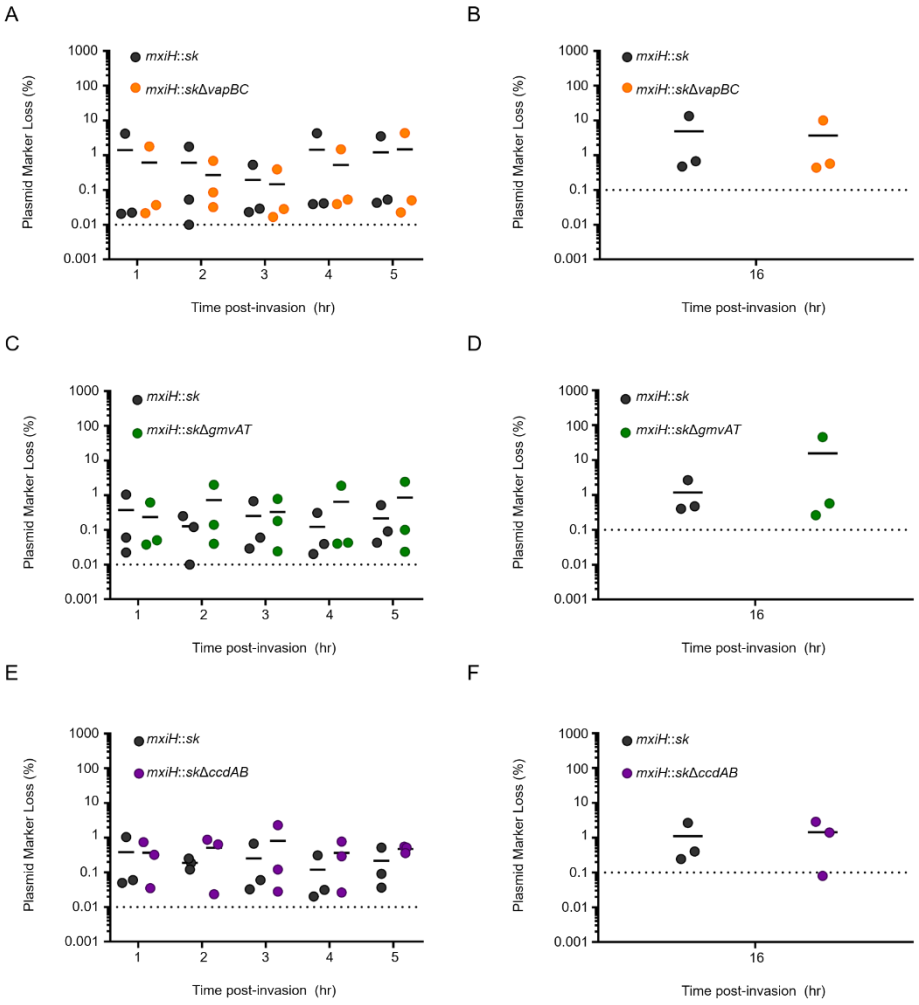


Figure 4.6 Effect of TA systems on plasmid marker loss in THP-1 cells.

Plasmid marker loss was measured in *mxiH*::*sk* derivatives. Results for (A) *mxiH*::*sk* with or without VapBC, (B) *mxiH*::*sk* with or without VapBC after 16 hr post-invasion (C) with or without GmvAT, and (D) *mxiH*::*sk* with or without GmvAT after 16 hr post-invasion (E) *mxiH*::*sk* with or without CcdAB, (F) *mxiH*::*sk* with or without CcdAB after 16 hr post-invasion. Results show the percentage of strains that have lost the *sacB-kan*^{r} cassette following infection of THP-1 cells. THP-1 cells were infected, then lysed at times post-invasion and bacteria were plated onto the appropriate media. The dotted line represents the approximate limit of detection. Each dot represents results for a single well and the mean of technical replicates for plating (n=3). Strains were tested on three independent occasions, and the horizontal line represents the mean. Two-way ANOVA with Tukey's multiple comparison statistical tests was performed; n.s., non-significant.

4.7 *S. flexneri* requires a functional T3SS to replicate inside THP-1 cells

FD was used to examine whether *mxiH*::*sk* replicates within THP-1 macrophages, (129). In Chapter Three, FD of *S. flexneri* and *S. flexneri* BS176 (which lacks pINV) containing pDIGc^{cam} was used to measure bacterial replication *in vivo* (Figure 3.6 and 3.14). Therefore, pDIGc^{cam} was introduced into *mxiH*::*sk* to measure replication in THP-1 macrophages. *mxiH*::*sk*, *S. flexneri* and *S. flexneri* BS176 harbouring pDIGc^{cam} were used to infect THP-1 derived macrophages at an MOI of 5:1. Following invasion for 30 min, infected THP-1 cells were treated with cefsulodin (600 µg/ml) for 1 hr to remove extracellular bacteria. Following treatment bacteria were allowed to replicate for 1, 3 or 5 hrs and then bacteria were recovered. Bacteria were fixed and analysed by flow cytometry for replication by FD (Figure 4.7). Following infection with *S. flexneri* pDIGc^{cam}, a heterogeneous bacterial population was observed with a shift to the left in DsRed intensity over time in a small population detected. The geometric mean of DsRed fluorescence of *S. flexneri* pDIGc^{cam} did not significantly shift between 1hr and 5hr (p = 0.9140, two-way ANOVA, Appendix 3). *S. flexneri* BS176 and *mxiH*::*sk* harbouring pDIGc^{cam} did not exhibit any FD (Figure 4.7). The geometric mean DsRed fluorescence from *S. flexneri* BS176 pDIGc^{cam} and *mxiH*::*sk* pDIGc^{cam} also did not significantly change between 1 hr and 5hr (p > 0.9999, respectively, two-way ANOVA, Appendix 3). Despite an overall non-significant change in fluorescence over time detected, an average of 1.758 (+/- 1.968 S.D.) generations was measured over 5 hrs for *S. flexneri* pDiGc^{cam} compared to *mxiH*::*sk* pDiGc^{cam} and *S. flexneri* BS176 pDiGc^{cam} which had an average of 0.0787 (+/- 1.551 S.D.) and 0.0672 (+/- 0.1508) generations respectively. These data suggest that strains which lack a functional T3SS fail to replicate within macrophages.

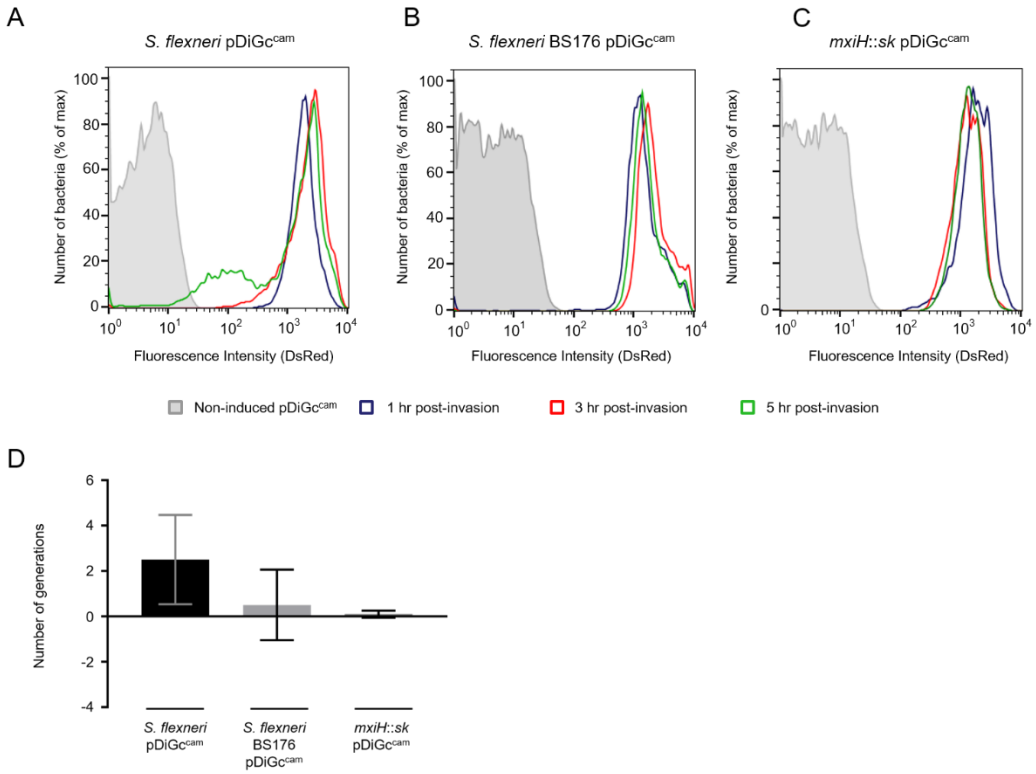


Figure 4.7 *Shigella* require a functional T3SS to replicate inside THP-1 derived macrophages

Flow cytometric detection of DsRed fluorescence intensity of bacteria at time points post invasion (indicated with differently coloured traces). Traces show the fluorescence intensity of (A) *S. flexneri* pDiGc^{cam}, (B) *S. flexneri* BS176 pDiGc^{cam} and (C) *mxiH*::sk pDiGc^{cam}, at times following challenge of THP-1 derived macrophages. Non- induced *S. flexneri*, *S. flexneri* BS176 and *mxiH*::sk pDiGc^{cam} were grown overnight as a negative fluorescence control (grey filled trace). The traces show one of three independent experiments performed. Fluorescence was measured of at least 10,000 bacteria (D) The number of generations +/- S.D measured on the GFP positive population for *S. flexneri*, *S. flexneri mxiH*::*sk* and *S. flexneri* BS176

4.8 Construction of *S. flexneri* with *sacB-kan*^{r} in an intergenic region of pINV (Ig::*sk*)

As *S. flexneri* requires a functional T3SS for intracellular replication in THP-1 macrophages, I decided to generate a new strain. A *S. flexneri* strain was constructed with the *sacB-kan*^{r} marker inserted into pINV at a location that does not affect the T3SS (Figure 4.8). As the majority of events leading to avirulent colonies in *S. flexneri* result from the deletion of the PAI, the *sacB-kan*^{r} cassette was inserted in a 945 bp intergenic region between *virB* and *ipaJ* generating *S. flexneri* Ig::*sk* (Ig::*sk*). This location was chosen as it had been the site of genetic manipulation of pINV previously (79). *virB* and *ipaJ* are organised in a tail-to-tail orientation, so insertion of the dual marker is unlikely to affect the activity of their promoters.

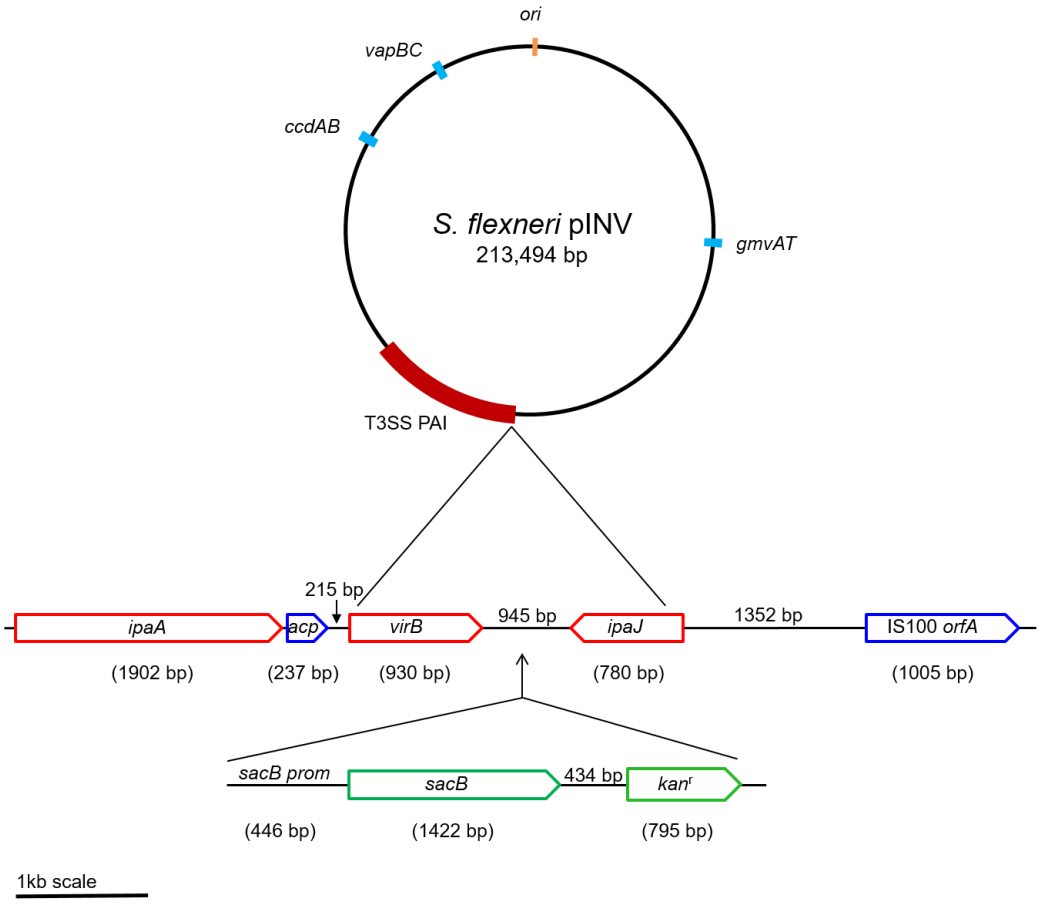


Figure 4.8 Schematic of *sacB-kan*^{r} in the *virB*/*ipaJ* intergenic region

In red are the genes of the PAI, in blue are TA genes and in orange is the pINV ori. Outlined in red are the genes associated with T3SS and in blue are other pINV genes in the region. Outlined in green is the *sacB-kan*^{r} cassette that was inserted into the *virB*/*ipaJ* intergenic region.

4.9 Validation of Ig::*sk* for measuring plasmid loss *in vivo*

Next the growth of Ig::*sk* was compared to wild-type *S. flexneri*. Strains were grown overnight in TSB liquid media, then diluted 1:100 in 25 ml of fresh TSB with or without kanamycin as indicated, and incubated at 37°C with shaking; the optical density of cultures was measured every hour (Figure 4.9). There was no significant difference in the growth between the strain harbouring the *sacB-kan*^{r} marker in the intergenic region and wild-type *S. flexneri* in the presence or absence of kanamycin. Pearson correlation tests reveal a statistically significant positive correlation between growth of *S. flexneri* and Ig::*sk* (R=0.9967, two-tailed *p* value, $p < 0.0001$, Figure 4.9). Furthermore, when grown in antibiotic and the cassette is being selected for, strains also had a statistically significant positive correlation to *S. flexneri* (R=0.9813, two-tailed *p* value, $p < 0.0001$, Figure 4.9). Therefore, the results confirm that the cassette does not affect growth of *S. flexneri*.

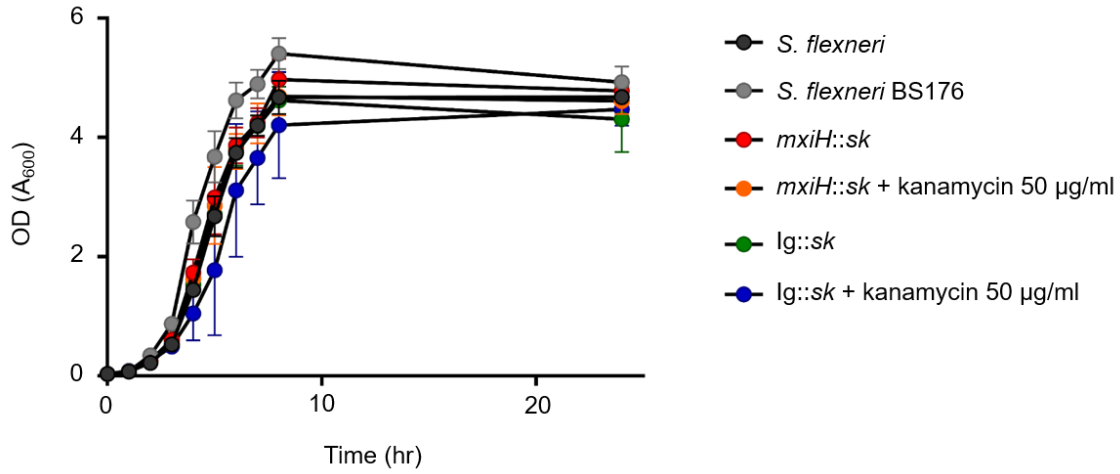


Figure 4.9 The *sacB-kan*^{r} marker in the *virB/ipaJ* intergenic region does not affect bacterial growth in TSB.

Overnight cultures of strains (indicated) were diluted 1:100 into 25 ml of TSB (+/- kanamycin as shown) and grown at 37°C with shaking. The OD of cultures (A_{600}) were measured at time points afterwards. Strains were tested on three independent occasions. Results show the mean +/- S.D.

To examine the effect of individual TA systems on plasmid marker loss in the host, individual TA systems were deleted from pINV in Ig::*sk* parental strain and replaced with an 82 nucleotide scar following lambda red recombination (202). To validate whether Ig::*sk* can be used to measure pINV stability during intracellular replication, the effect of individual TA deletions on pINV marker loss was examined during *in vitro* growth of *S. flexneri* strains with *sacB-kan*^{r} in *mxiH* or in the *virB-ipaJ* intergenic region. There was no significant difference in the VapBC (p = 0.990, two-way ANOVA, Figure 4.10), GmvAT (p > 0.9999, two-way ANOVA), and CcdAB (p > 0.9999, two-way ANOVA, Figure 4.10) to plasmid marker loss in the two genetic backgrounds (Figure 4.10). Taken together, the results indicate that Ig::*sk* can be used to measure plasmid instability.

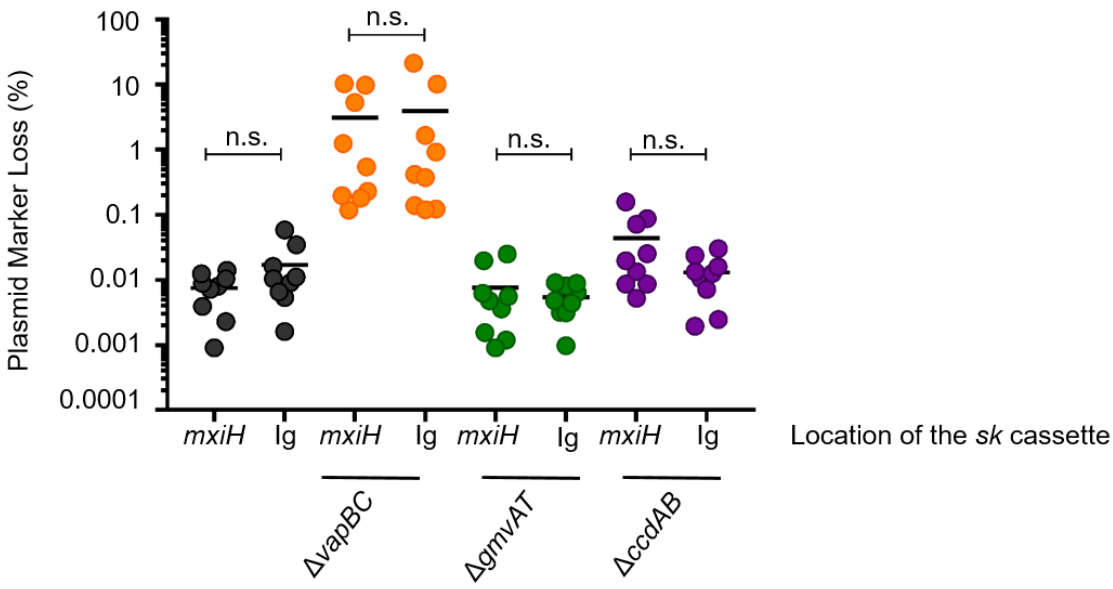


Figure 4.10 The effect of position of the *sacB-kan*^{r} marker on pINV stability

Plasmid marker loss was measured in Ig::*sk* derivatives. Results show the percentage of bacteria that have lost the *sacB-kan*^{r} cassette following 25 generations of growth at 37° C on LB media shown together with results obtained with *mxiH*::*sk*. Each dot represents results for a single colony (n = 9). Strains were tested on three independent occasions. The horizontal line shows the mean. Two-way ANOVA with Tukey's multiple comparison statistical tests was performed; n.s., non-significant.

4.10 The *sacB-kan*^{r} marker in the *virB-ipaJ* intergenic region does not impede *S. flexneri* replication in THP-1 cells.

FD was performed to determine if Ig::*sk* can survive and replicate in THP-1 macrophages; pDiGc^{cam} was introduced into Ig::*sk* by transformation. Differentiated THP-1 cells were then infected at an MOI of 5:1 with Ig::*sk* harbouring pDiGc^{cam}. Following invasion, THP-1 cells were treated with 600 µg/ml of cefsulodin to remove extracellular bacteria for 1 hr. Following treatment bacteria were allowed to replicate for a further 1, 3 or 5 hrs, then cells were recovered; bacteria were analysed by cytometry for changes in DsRed fluorescence intensity. A population of Ig::*sk* pDiGc^{cam} shifted over time during infection of THP-1 cells, similar to *S. flexneri* pDiGc^{cam} (Figure 4.7 and Figure 4.11). This suggests that intracellular replication is occurring in this strain. The geometric mean DsRed fluorescence of Ig::*sk* pDIGc^{cam} did not significantly change over time, but again this is similar to *S. flexneri* (p = 0.5451, one-way ANOVA, Appendix 4). The average number of generations measured by fluorescence dilution in *S. flexneri* Ig::*sk* pDiGc^{cam} was 3.052 (+/-0.4966 S.D.) which is similar to *S. flexneri* pDiGc^{cam}.

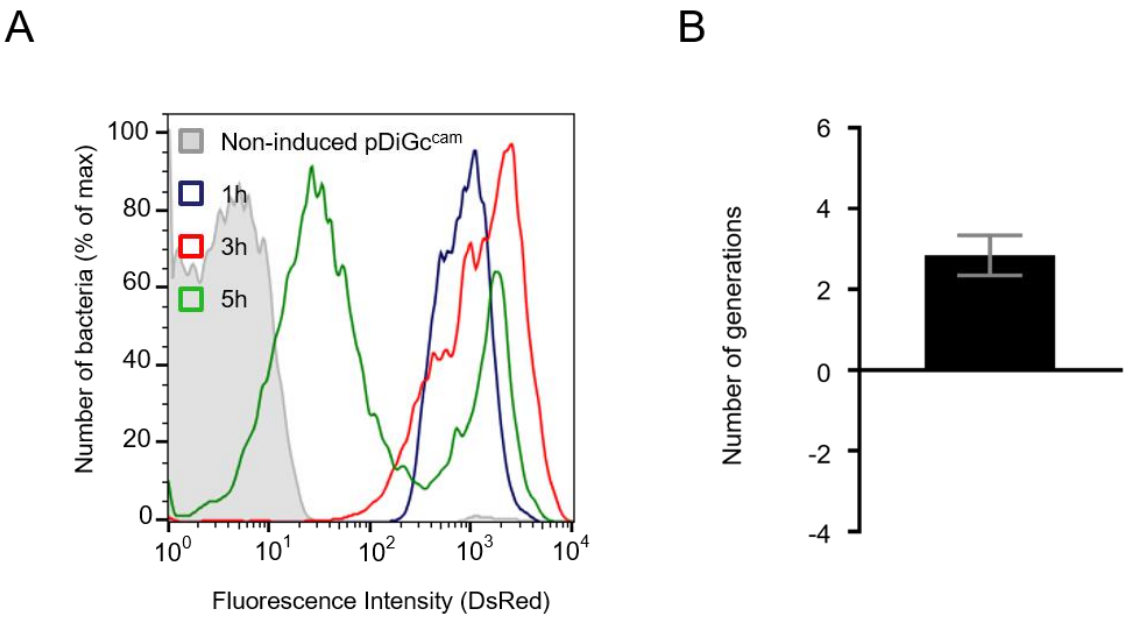


Figure 4.11 The dual marker in *S. flexneri* (Ig::*sk*) does not impede replication in THP-1 macrophages.

(A) Flow cytometric detection of DsRed fluorescence intensity in the intracellular population of Ig::*sk* pDiGc^{cam} at time points post-invasion (indicated with differently coloured traces). (B) The number of generations measured in the GFP positive population +/- S.D.

4.11 VapBC is not required to stabilise pINV in THP-1 cells.

As VapBC has the most prominent role in pINV stability the role of this TA system in pINV stability during macrophage infection was examined in Ig::*sk*. As above THP-1 cells were infected at an MOI of 5:1, treated with cefsulodin to remove extracellular bacteria then lysed at 1, 3 and 5 hr post-antibiotic treatment and bacteria were then plated to media containing kanamycin (to detect bacteria retaining the marker) or sucrose (to select bacteria which had lost the marker). Deletion of VapBC had no effect on marker loss following infection at 1, 3 or 5 hr post-invasion compared to the parental strain ($p > 0.9999$ for 1 hr and 3 hr, and $p = 0.5693$ at 5 hr, two-way ANOVA, Figure 4.12). These data are consistent with VapBC having no role on pINV stability in THP-1 macrophages during this time, although the lack of effect might reflect the low number of generations in the assay.

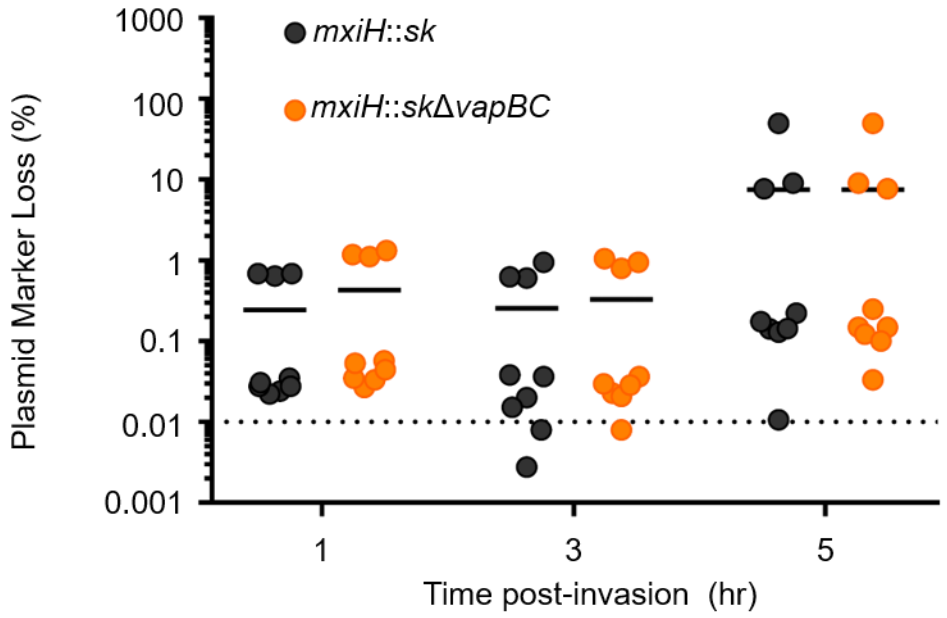


Figure 4.12 VapBC is not required to stabilise pINV in THP-1 cells.

Plasmid marker loss was measured in Ig::*sk* derivatives with or without VapBC. Results show the percentage of strains that have lost the *sacB*-kan^r cassette following infection of THP-1 cells. THP-1 cells were infected, then lysed at times post invasion and bacteria were plated onto the appropriate media. The dotted line represents the approximate limit of detection. Each dot represents results for a single well, and the average of technical replicates for plating is shown (n=9). Strains were tested on three independent occasions, and the horizontal line represents the average. Two-way ANOVA with Tukey's multiple comparison statistical tests was performed; n.s., non-significant.

4.12 Discussion

A striking feature of *Shigella* pINV, and other virulence plasmids is the presence of multiple TA systems on the plasmid (135). One hypothesis for requiring more than one TA system is that they contribute to pINV stability at distinct conditions such as the temperatures found in the external environment and those in the human body (163).

The aim of work in this chapter was to identify further conditions that modulate plasmid stability and the contribution of TA systems in these conditions. A particular emphasis was placed on stresses that *Shigella* could encounter during its lifecycle, such as low pH (such as during exposure to gastric acid), oxygen stress (both anaerobiosis and exposure to reactive oxygen species) and nutritional limitation. The assays performed examined the effects of TA systems on plasmid loss in these environments. Of note in conditions of high temperature, low pH and anaerobiosis only VapBC appeared to affect plasmid stability, while GmvAT and CcdAB seemed to play minor, if undetectable roles. However, these assays failed to include double and triple knockouts of the TA systems so perhaps there is redundancy that is unaccounted for in these conditions. It was only comparing a triple TA pINV knockout and a double knockout of CcdAB and VapBC; that GmvAT was shown to be sufficient for *S. flexneri* pINV stability at 21°C (163).

Of particular interest would be to repeat the experiment assessing the role of TA systems on pINV stability in anaerobic and aerobic conditions. Altering the oxygen availability altered the role VapBC played on plNV stability (Figure 4.4). However, the amount of plasmid marker loss was not significantly different between aerobic and anaerobic conditions. To determine if oxygen availability alters the role of VapBC on plasmid maintenance, this assay should be repeated, and performed with double and

triple knockouts of TA systems to see if other TA systems play a role in these conditions.

Altering the nutritional environment altered the role VapBC played on pINV stability (Figure 4.3). Preliminary data in double and triple knockouts suggest that this is only true for strains where VapBC is absent. It is possible that slowing the rate of division allows segregation systems, ParAB and StbAB, to be more effective. This could be tested using pINV lacking *parAB* and/or *stbAB*. Alternatively, growth conditions might affect post-segregational killing. For example nutritional/amino acid limitation might reduce the half-life of the VapB and VapC, as Lon protease is upregulated in conditions, such as found in M9+ media, as it is regulated by ppGpp, the stress alarmone (231). If the VapC is more readily degraded in these conditions, this will alter the internal VapBC ratio in the cell which is important for regulation of VapBC transcription (151, 181). Low VapBC concentrations will increase transcription and will increase the amount of free VapBC complex in the cell (151, 181). Once high enough VapBC complex represses its own transcription by the binding to two inverted repeat sequences in the *vapBC* promoter (181). Alternatively the target of VapC is $tRNA^{fMet}$, and the stringent response reduces availability of cellular tRNAs (231). Of note, the *metZWV* locus is under the control of the stringent response, while *metY* locus is not (232). This might affect $tRNA^{fMet}$ levels during the stringent response (233). Under these circumstances, VapBC might be more effective at PSK in nutrient limiting conditions as there would be less target to cleave. It would be interesting to replace the (p)ppGpp regulated promoter of *metWV* and see if this affects the action of VapC. Furthermore, VapC toxicity assays could be carried out during growth in LB and in M9+. Equally other maintenance systems, such as the partitioning systems, could compensate for the loss of TA systems. The only observed condition that GmvAT has

demonstrable activity on plasmid stability is at 21°C (163). Therefore, it would be interesting to test the role of GmvAT during nutrient limitation at this temperature.

It is interesting to note that we have not observed a role for CcdAB. CcdAB has been shown to encode a functional toxin and cognate antitoxin (163). *S. flexneri* pINV has a CcdAB TA system that is 86 to 96 % protein identity to the well characterised CcdAB system on the F plasmid (141). GmvAT has been shown to be sufficient for plasmid maintenance at 21°C (163). *S. sonnei* pINV only has VapBC (Figure 1.10), and is less stable than *S. flexneri* pINV (163). When both these TA systems were reintroduced into *S. sonnei* pINV the plasmid was stabilised, suggesting these TA systems play a role (163).

The role of TA systems in PSK is complex. Their function will be affected by several factors: (i) the ratio of toxin to antitoxin in bacteria (153, 234), (ii) the rate of degradation of the antitoxin relative to the toxin once genes encoding the TA have been lost (154, 235), (iii) the activity of the toxin, which will be influenced by the abundance, rate of synthesis and susceptibility of the target to the toxin,(140) (iv) and the ability of the bacterial cell to recover from the action of the toxin (152, 187). Indeed, even when considering the first of these, the ratio of toxin to antitoxin in the cell, this varies at the transcriptional and translational levels.

The reason why we are not observing a role of CcdAB and GmvAT TA systems compared to VapBC, might be due to the assay we are using. The *Shigella* pINV loss assay relies on the recovery of viable bacteria after a certain number of generations. We are unable to detect non-viable bacteria that have lost pINV so if PSK is highly effective, we might miss effects of TA systems. Another approach would be to detect plasmid loss in cells by fluorescence microscopy. Fluorescence dilution (ChromFD)

could be employed to identify replicating and non-replicating populations, and the presence of the plasmid could be detected by fluorescently tagging the origin of replication. Analysis of bacteria by flow cytometry could allow the measurement of plasmid loss at the population level in viable and non-viable bacteria.

Shigella requires pINV for invasion and pathogenesis (43, 44). In the intracellular environment, *Shigella* requires pINV to be maintained as the T3SS is necessary for phagolysosomal escape, and invasion of other cells (51). Assessing plasmid loss during intracellular replication was very challenging, given the short time frame of experiments; within a few hours, virulent *Shigella* causes death of phagocytes (51). Plasmid loss assays are performed over 25 generations during growth in the laboratory, as it is difficult to detect plasmid loss with fewer generations (163). The initial plan was to use the *mxiH*::sk strain to examine the role of TA systems in plasmid stability inside phagocytes, as bacteria were recovered 16 hr post infection. Furthermore, if *Shigella* replicates every 37 min as suggested in the literature ~25 generations could be assessed (111). However, no role of the individual TA systems during infection was observed, even VapBC which plays a role at 37°C (Figure 4.6). There could be three possible explanations for this: (i) is there redundancy in the role of the three TA systems (ii) the bacteria are not replicating in THP-1 macrophages (as bacterial replication needs to occur for plasmid loss to be measured) (iii) there is another method of plasmid maintenance in the host. As VapBC did not play a role in the *in vivo* experiment as it did *in vitro* (Figure 4.1), I first wanted to check the replication and exclude this. However, it became apparent that *mxiH*::sk, which lacks a functional T3SS, fails to replicate in the intracellular compartment, even though there was detectable uptake by phagocytes (Figure 4.7).

I therefore decided to develop a strain to assess plasmid loss in bacteria which expresses the T3SS. Ig::*sk* harbours the same dual marker as *mxiH*::sk, yet has a functional T3SS. With an active T3SS, macrophage viability became compromised at 5 hr following infection. VapBC appeared to have a negative effect on plasmid stability during macrophage infection, however this is a short time frame to measure plasmid loss (Figure 4.12). I did not perform the assay with strains lacking other TA systems as previous work demonstrated that VapBC has a major effect at 37^{o}C, the temperature relevant for work with phagocytes. The limitation measuring *in vivo* plasmid loss using the dual marker *sacB-kan*^{r}, is that this relies on viable counts and may have reduced sensitivity as previously discussed. ChromFD with a tagged origin of replication on pINV would more sensitively assess plasmid loss in these conditions. In the future, similar studies could be performed in an animal model of shigellosis which might give a greater appreciation of the role of TA systems in plasmid maintenance within the mammalian intestine (236, 237).

The striking finding from this work is that *Shigella* requires a T3SS for replication inside THP-1 derived macrophages. BS176 is a strain which lacks the T3SS and showed no fluorescence dilution within macrophages; however replication of *S. flexneri* was detected in these cells. The implication of this is that there is a selection for the T3SS at the step beyond phagocyte escape, but for replication. This may represent a key step in *Shigella* pathogenesis.

Of note, there was a heterogeneous population of wild-type *S. flexneri* inside macrophages. Bacterial interaction with macrophages is a dynamic process, as bacteria can be taken up, escape the cell, and be taken up by other phagocytes. Flow cytometry provides cross sectional snapshots of infection, and is not necessarily the

best method to detect bacterial heterogeneity. Instead, live imaging could be used to follow the fate of bacteria, although this method lacks high throughput offered by flow cytometry. Further work could also be performed to characterise why the T3SS is required for replication. One hypothesis is that *Shigella* is unable to replicate in the vacuole, and requires the T3SS to escape from this environment into the cytosol. This could be assessed by Galectin 3 staining which acts as a marker for vacuole lysis (52). It would be also interesting to determine the nature of the non-replicating bacteria, and whether they are alive or dead by fluorescently tagging their rRNA (131). Understanding why there is a different fluorescence dilution profile between T3SS negative and positive cells might provide insights into why *Shigella* spp. escape the macrophage within 1 hr, while *Salmonella* is able to survive and replicate for days in these cells (51, 129).

5 Chapter Five Investigation of the influence of genetic background in plasmid maintenance

S. sonnei has a rate of higher plasmid instability than *S. flexneri* (163). The main plasmid maintenance mechanism at 37°C is the Type II TA system, VapBC and both *Shigella* species have this maintenance element (163, 179, 180). The aim of work in this chapter was to understand the activity of VapBC and how it is influenced by the genetic background.

Type II TA systems contain two genes in a single operon, encoding a stable toxin and an inherently unstable antitoxin (181). The antitoxin is continuously expressed and able to neutralise the toxin as long as the TA operon is expressed (181). Type II TA systems belonging to the VapBC family are highly prevalent in bacteria and are found both on chromosomes and on plasmids (238). When VapBC is present on the chromosome, it is often present in multiple copies for unknown reasons (238). In enteric VapBC TA systems, VapC and VapB interact to form a heterooctameric complex, which binds to operator sites in the *vapBC* promoter, inhibiting transcription (151, 181). In a VapBC homologue in *Neisseria gonorrhoeae*, FitAB, the toxin acts as a co-repressor by stabilising and increasing the affinity of the antitoxin for DNA (239). When a plasmid harbouring VapBC is lost, the VapB antitoxin is degraded by cellular proteases, such as Lon, to release free VapC, which inhibits cell growth, usually by targeting protein translation (181). VapC toxins are characterised by the presence of a PIN domain with an RNase H-like fold, which is capable of degrading nucleic acids.

VapC from *S. flexneri* 2a and *Salmonella* cleave the initiator $tRNA^{fMet}$ in its anticodon stem loop (182), preventing the initiation of translation (182, 240).

All *Shigella* spp. possess VapBC on pINV, which aids plasmid maintenance (179). The VapBC TA system has been shown to be essential for stability of pINV at 37°C, but has less of a role at 21°C (163, 179, 180). Additionally VapBC in *Shigella* was recently demonstrated to have both a global and local effect on pINV maintenance (79). When VapBC is deleted from the plasmid there is increased loss of the entire pINV during growth *in vitro* demonstrating a global role. When VapBC was moved close to the T3SS PAI, the loss of the PAI was reduced (79). This demonstrates that VapBC plays a key role in plasmid stability. Of interest, VapBC is located close to the *ori* of pINV in all *Shigella* spp., which might explain its crucial role for preventing the loss of pINV (79).

5.1 pSTAB2 a plasmid to study the role of individual elements on plasmid maintenance

In general, virulence plasmids have multiple mechanisms for their maintenance. *S. flexneri* pINV has two putative partitioning systems and three functional TA systems (135). In a large plasmid, studying the role of individual systems on plasmid maintenance can be challenging, as the effects of one system could be masked by redundancy. Furthermore, there could be interactions between maintenance systems, recombination between resident insertion sequences, and chromosomal integration of plasmids which could confound results (79).

To assess the role of VapBC on plasmid maintenance in isolation, a plasmid (pSTAB2) was constructed. pSTAB2 contains the replicon of *S. flexneri* pINV from pWR100 (Figure 5.1), which is a RepFIIA-like element sufficient for plasmid propagation and incompatibility (241). pSTAB2 also harbours a dual marker (*sacB*-*kan*^{r}) to measure loss/retention of the plasmid, and a multiple cloning site for introducing genes encoding maintenance systems (Figure 5.1).

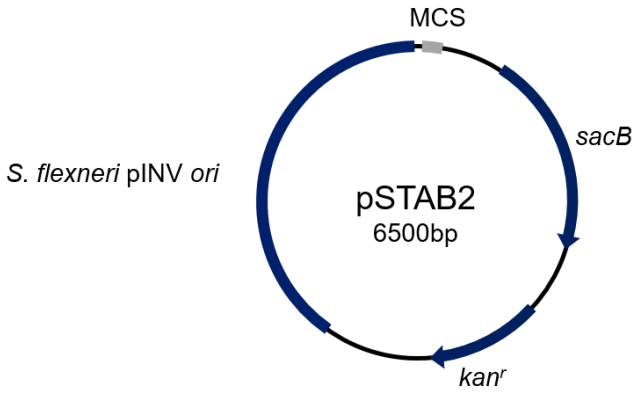


Figure 5.1 pSTAB2, a vector to measure plasmid maintenance/loss

Schematic of the model plasmid, pSTAB2, constructed to assess the impact of individual TA systems on plasmid loss. pSTAB2 contains the *S. flexneri* pINV origin, dual marker (*sacB*-*kan*^{r}) to measure loss/retention of the plasmid, and a multiple cloning site (MCS) for introducing genes encoding maintenance systems

5.2 VapBC^{Sf} reduces pSTAB2 loss in *S. flexneri* but not *E. coli* DH5α

Initially studies with pSTAB2 were performed in *S. flexneri* lacking pINV (*S. flexneri* pINV-) to avoid any interaction with maintenance systems on pINV, and because pSTAB2 is expected to be incompatible with pINV as they contain the same *ori*. VapBC from *S. flexneri* (VapBC^{Sf}) was introduced into the multiple cloning site (MCS) of pSTAB2, and transformed into *S. flexneri* BS176 (pINV-). Individual bacterial colonies were grown on LB agar plates for 25 generations at 37°C, then colonies were re-suspended in PBS and plated onto the appropriate media for quantification of kanamycin or sucrose-resistant colonies (pSTAB2 retaining and minus bacteria, respectively). The presence of VapBC^{Sf} significantly reduced pSTAB2 loss in *S. flexneri* ($p < 0.0001$, two-way ANOVA, Figure 5.2), consistent with its effect on pINV (163). In contrast, introduction of VapBC^{Sf} into pSTAB2 did not significantly reduce pSTAB2 loss in *E. coli* DH5α ($p = 0.1152$, two-way ANOVA, Figure 5.2). There was a significant difference in VapBC capacity to reduce plasmid loss in *S. flexneri* compared with *E. coli* DH5α ($p < 0.0001$, two-way ANOVA, Figure 5.2).

VapC from *S. flexneri* 2a and *Salmonella* cleaves *E. coli* tRNA^{fMet} in its anticodon stem loop, thereby inhibiting translation (182). Despite this evidence that VapC is able to cleave its target in *E. coli*, results demonstrate that VapBC^{Sf} is not as effective in preventing plasmid loss in *E. coli* as in *S. flexneri* ($p < 0.0001$, two-way ANOVA, Figure 5.2).

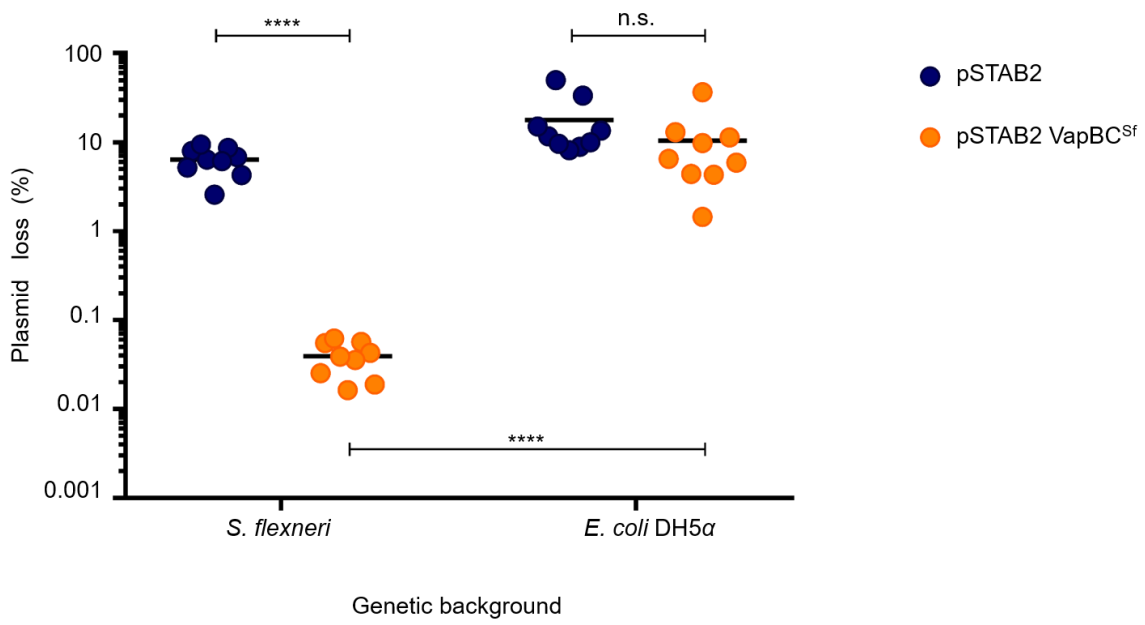


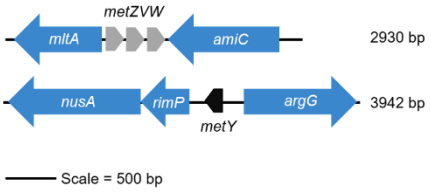
Figure 5.2 VapBC^{Sf} reduces pSTAB2 loss in *S. flexneri* but not *E. coli* DH5α

pSTAB2 loss was measured in *S. flexneri* or *E. coli* DH5α. Results show the percentage of bacteria that have lost the *sacB-kan*^{r} cassette following 25 generations of growth at 37°C on LB media. Each dot represents results for a single colony (n = 9) for each strain. Each strain was tested on three independent occasions. The horizontal line shows the mean. Two-way ANOVA with Tukey's multiple comparison statistical tests was performed; ****, $p < 0.0001$ and n.s., non-significant

5.3 VapC cleavage sites and analysis of tRNA^{fMet} alleles

To understand the different contributions of VapBC to plasmid maintenance in *E. coli* and *S. flexneri*, the profile of the target of VapC, tRNA^{fMet}, was examined. Analysis of available genome sequences revealed that the number and alleles of tRNA^{fMet} is distinct in *S. flexneri* and *E. coli* spp. *E. coli* spp. have four genes encoding tRNA^{fMet} while *S. flexneri* has three. *E. coli* harbours a cluster of three identical tRNA^{fMet} genes, *metZWV,* located between *mltA* and *amiC* (Figure 5.3). In comparison *S. flexneri* only contains two identical tRNA^{fMet} genes at this locus. Additionally, both species have a further gene encoding tRNA^{fMet}, *metY*, which is located at the beginning of the *nusA*/*infB* operon. In *E. coli* B strains and *S. flexneri*, this tRNA^{fMet} is identical to the other tRNA^{fMet} alleles in the genome, and designated here as tRNA^{fMet1}. However, in *E. coli* K strains such as *E. coli* DH5α, there is a polymorphism in the tRNA^{fMet} in *metY*, with a G to A substitution at position 46; this allele is designated as tRNA^{fMet2} (Figure 5.3) (242). Position 46 is in the variable region of tRNA, a five-nucleotide sequence (positions 44 to 48) between the anticodon stem loop and the pseudouridine loop (Figure 5.3). VapC specifically cleaves tRNA^{fMet} between nucleotides 39 and 40 in the anticodon stem loop (182). The polymorphism in tRNA^{fMet} also results in another change. G46 in tRNA^{fMet1} can be methylated, while A46 is not modified (243). The influence of this polymorphism and the associated post-transcriptional modification of tRNA^{fMet} on VapC cleavage is unknown.

A



B

tRNA^{fMet1} CGCGGGGTGGAGCAGCCTGGTAGCTCGTCGGGCTCATAACCCGAAGGTCGTCGGTTCAAATCCGGCCCCCGCAACCA
tRNA^{fMet2} CGCGGGGTGGAGCAGCCTGGTAGCTCGTCGGGCTCATAACCCGAAGATCGTCGGTTCAAATCCGGCCCCCGCAACCA

C

Species	Strain	*metZWV* operon tRNA^{fMet1}	*metZWV* operon tRNA^{fMet2}	*metY* locus tRNA^{fMet1}	*metY* locus tRNA^{fMet2}
E. coli	DH1	3	0	0	1
E. coli	MG1655	3	0	0	1
E. coli	BL21	3	0	1	0
E. coli	MRE600	3	0	1	0
S. flexneri 5a	M90T	2	0	1	0
S. flexneri 2a	2457T	2	0	1	0
S. enteritidis var. Typhimurium	LT2	2	0	1	0

D

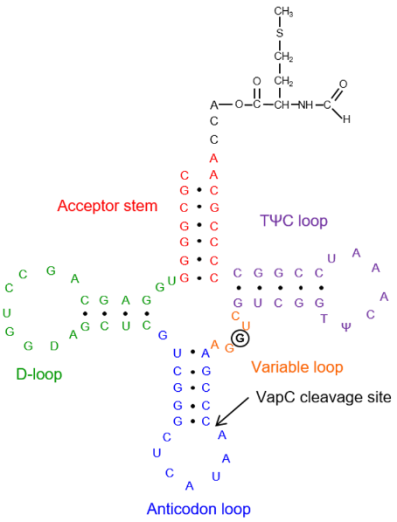


Figure 5.3 VapC cleavage site and tRNA^{fMet} alleles

(A) Schematic representation of tRNA^{fMet} alleles and their genetic organisation in *E. coli* MG1655. (B) Alignment of tRNA^{fMet1} and tRNA^{fMet2} with the polymorphism highlighted in red. (C) Table of the tRNA^{fMet} profiles in different species showing the number of each allele. (D) Secondary structure of *E. coli* tRNA^{fMet1}. Red denotes the acceptor stem. Green denotes the D loop. Blue denotes the anticodon loop. Orange the variable loop and purple is the TΨC loop. The arrow points to the site of VapC cleavage. The black nucleotide circled denotes the nucleotide polymorphism between tRNA^{fMet1} and tRNA^{fMet2} (G->A).

5.4 tRNA^{fMet} profiles affects the impact of VapBC on pSTAB2 loss

Shigella spp. have evolved from *E. coli* on four separate occasions following the aquistion of pINV (244). As a species, *E. coli* is exceptionally diverse and is comprised of multiple strains that are differentiated by their genetic content and physiological properties into groups A, B1 (split into B1a and B1b), B2, D and E (245, 246). Several studies have demonstrated that *Shigella* spp. are closely related to Group A and B1a and B1b *E. coli* (133, 244). Group A contains the commensal strains and their derivatives: the K-12 strains (MG1655, DH1 and DH10B) and B strains (BL21 and REL606) (246). Group A *E. coli* strains have different tRNA^{fMet} profiles (Figure 5.3). Of note, enteric pathogens *S. flexneri* and *S. typhimurium* have a similar tRNA^{fMet} profile to Group A, B strains of *E. coli* such as *E. coli* BL21 rather than K strains such as *E. coli* K-12.

To investigate whether the profile of tRNA^{fMet} alleles in a strain influences VapBC function, pSTAB2 with or without VapBC^{Sf} was introduced into *E. coli* MRE600, a Group A, B strain which carries four tRNA^{fMet1} genes (Figure 5.3) (193). *E. coli* MRE600 has an intermediate phylogeny between *E. coli* DH5α and *Shigella* spp. (193). Plasmid loss in this genetic background was compared with *E. coli* MG1655 which has three tRNA^{fMet1} genes and one tRNA^{fMet2} gene (Figure 5.4).

Of note, the presence of VapBC^{Sf} siginicantly reduced the loss of pSTAB2 in *E. coli* MRE600 ($p < 0.0001$, two-way ANOVA, Figure 5.4) but had no effect in *E. coli* MG1655 ($p = 0.9940$, two-way ANOVA, Figure 5.4). There was a significant difference in the role of VapBC on plasmid maintenace between species ($p < 0.0001$, two-way ANOVA, Figure 5.4). This result is consistent with the presence tRNA^{fMet2} reducing the effect of

VapBC on plasmid maintenance. However, *E. coli* MRE600 and MG1655 are not isogenic, so results do not provide conclusive proof regarding the role of $tRNA^{fMet2}$.

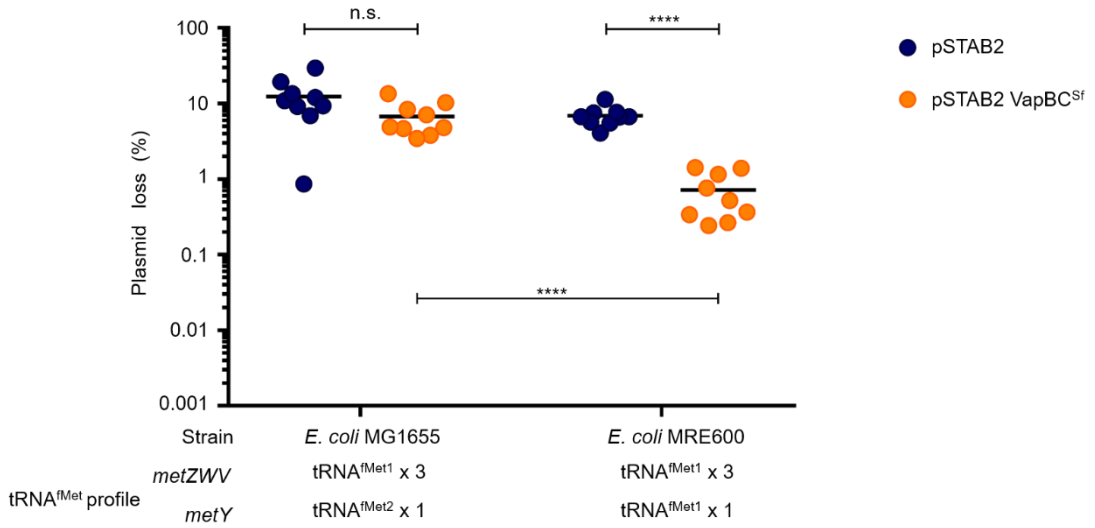


Figure 5.4 $tRNA^{fMet}$ profile affects the impact of $VapBC^{Sf}$ on pSTAB2 loss

The effect of $tRNA^{fMet}$ profiles, on the maintenance of pSTAB2 containing $VapBC^{Sf}$ was evaluated by comparing a K strain of *E. coli* (MG1655) and a B strain of *E. coli* (MRE600). pSTAB2 loss was measured in MG1655 or MRE600 Results show the percentage of bacteria that have lost the *sacB-kan*^{r} cassette following 25 generations of growth at 37^{o}C on LB media. Each dot represents results for a single colony (n = 9) for each strain. Each strain was tested on three independent occasions. The horizontal line shows the mean. Two-way ANOVA with Tukey's multiple comparison statistical tests was performed; ****, $p < 0.0001$, and n.s., non-significant.

5.5 $tRNA^{fMet2}$ reduces the impact of $VapBC^{Sf}$ on pSTAB2 loss

To investigate the role of $tRNA^{fMet2}$ directly, two derivatives of *E. coli* MG1655 were constructed. The first strain was MG1655 with $tRNA^{fMet2}$ deleted (MG1655Δ*metY*); in this strain, 53 of the 77 nucleotide in $tRNA^{fMet2}$ were removed and replaced with an 82 nucleotide scar following lambda red recombination used to generate the deletion (202). In the second strain, the $tRNA^{fMet2}$ in *E. coli* MG1655 was replaced by $tRNA^{fMet1}$ through recombination and conjugation, generating MG1655fMet1^{x4}.

pSTAB2, with or without $VapBC^{Sf}$, was introduced into the strains and plasmid loss was assayed after 25 generations of growth on LB solid media. In MG1655Δ*metY,* the presence of VapBC significantly reduced plasmid loss compared with empty pSTAB2 ($p < 0.0001$, two-way ANOVA, Figure 5.5). However as the amount of $tRNA^{fMet}$ in the cell is proportional to the number of *met* genes (247), so the level as well as the profile of $tRNA^{fMet}$ will be different in MG1655Δ*metY* compared to MG1655. Plasmid loss was therefore examined in MG1655fMet1^{x4} which has the same number of $tRNA^{fMet}$ alleles as the wild-type but lacks $tRNA^{fMet2}$.

In contrast to wild-type MG1655, the presence of $VapBC^{Sf}$ significantly reduced plasmid loss compared to empty pSTAB2 ($p < 0.0001$, two-way ANOVA, Figure 5.5) in MG1655fMet1^{x4}, demonstrating that $tRNA^{fMet2}$ reduces the effect of $VapBC^{Sf}$ on plasmid maintenance in *E. coli* . $VapBC^{Sf}$ is significantly more effective at plasmid maintenance when *metY* is deleted at the beginning of the *nusA*/*infB* operon or replaced with $tRNA^{fMet1}$ ($p < 0.0001$, two-way ANOVA, Figure 5.5).

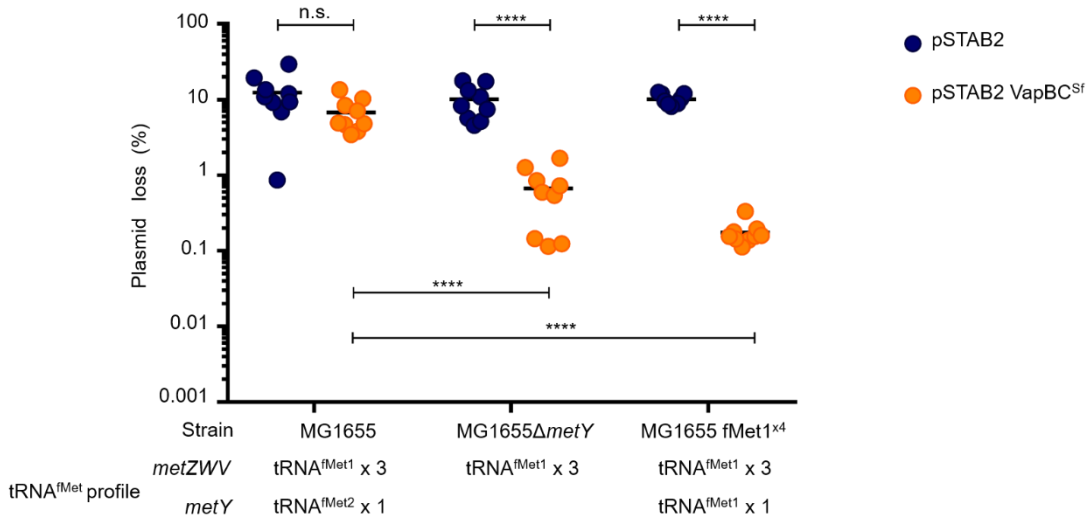


Figure 5.5 tRNA^{fMet2} reduces the impact of VapBC^{Sf} on pSTAB2 loss

The effect of different profiles in tRNA^{fMet} on the maintenance of pSTAB2 containing VapBC^{Sf} was evaluated in isogenic strains of *E. coli* MG1655. pSTAB2 loss was measured in *E. coli* MG1655 lacking tRNA^{fMet2} (MG1655 Δ*metY*) or in MG1655 with tRNA^{fMet2} replaced with tRNA^{fMet1} (MG1655 fMet1^{x4}). Results show the percentage of bacteria that have lost the *sacB-kan*^{r} cassette. Each dot represents results for a single colony (n = 9) for each strain. Each strain was tested on three independent occasions. The horizontal line shows the mean. Two-way ANOVA with Tukey's multiple comparison statistical tests was performed; ****, $p < 0.0001$ and n.s., non-significant

5.6 Introduction of tRNA^{fMet2} into *S. flexneri* reduces the impact of VapBC^{Sf} on pSTAB2 loss

In contrast to *E. coli*, *S. flexneri* has three tRNA^{fMet1} alleles (Figure 5.3). To determine whether introducing tRNA^{fMet2} into *S. flexneri* influences VapBC^{Sf} function, tRNA^{fMet1} in the *metY* locus in *S. flexneri* was replaced by tRNA^{fMet2}, generating *S. flexneri* fMet2^{x1}. A derivative of *S. flexneri* fMet2^{x1} lacking pINV was identified, and pSTAB2 loss assays were performed in this background.

VapBC^{Sf} significantly stabilised pSTAB2 compared to empty pSTAB2 in both backgrounds (p < 0.0001, respectively two-way ANOVA, Figure 5.6), Introducing tRNA^{fMet2} into *S. flexneri* significantly reduced the effect of VapBC^{Sf} on plasmid loss in this background compared to wild-type *S. flexneri* (p = 0.0006, two-way ANOVA, Figure 5.6), consistent with findings in *E. coli* that tRNA^{fMet2} influences the effect of VapBC^{Sf} on PSK. However, the impact of tRNA^{fMet2} in *S. flexneri* was not as marked as in *E. coli*, suggesting other factors contribute to VapBC function in *Shigella*. An alternative explanation is that *S. flexneri* only has two tRNA^{fMet1} alleles in the *metZW*V cluster, while there are three alleles in the corresponding locus in *E. coli.*

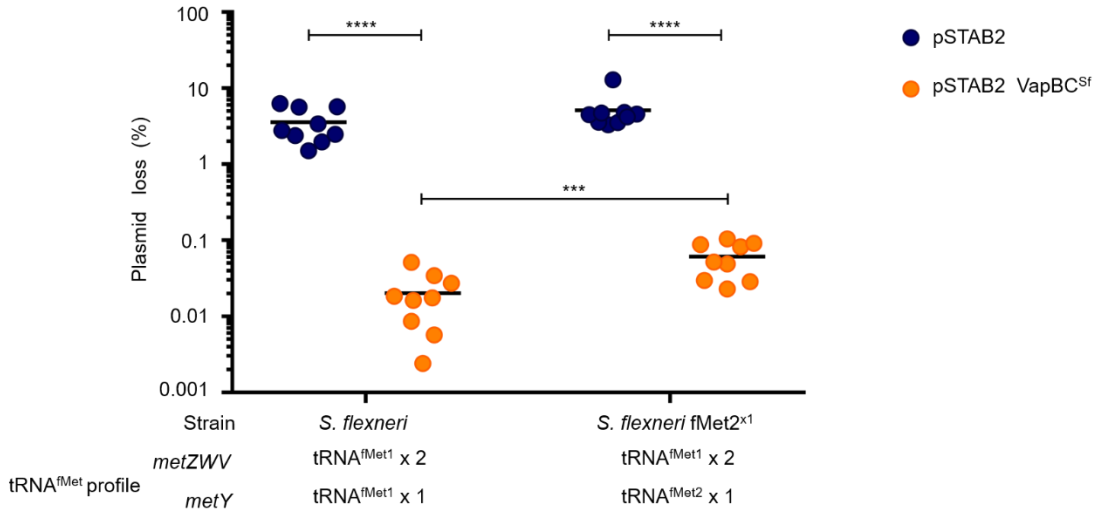


Figure 5.6 Introduction of tRNA^{fMet2} into *S. flexneri* reduces the impact of VapBC^{Sf} on pSTAB2 loss

The effect of different polymorphisms in tRNA^{fMet} on the maintenance of pSTAB2 containing VapBC^{Sf} was evaluated in *S. flexneri*. pSTAB2 loss was measured in of *S. flexneri* in which tRNA^{fMet1} in the *metY* locus was replaced with tRNA^{fMet2} (*S. flexneri* fMet2^{X1}) following 25 generations of growth at 37°C and compared to wild-type *S. flexneri*. Results show the percentage of strains that have lost the *sacB-kan*^{r} cassette. Each dot represents results for a single colony (n = 9) for each strain. Each strain was tested on three independent occasions. The horizontal line shows the mean. Two-way ANOVA with Tukey's multiple comparison statistical tests was performed; **** = $p < 0.0001$ and ***= $p < 0.001$.

5.7 Generation of *E. coli* MG1655 expressing only tRNA^{fMet2}

MG1655 K-12 *E. coli* expressing a single tRNA^{fMet2} in the *metY* locus is viable, suggesting this tRNA^{fMet} is functional (248). Therefore an *E. coli* MG1655 strain was constructed in which all tRNA^{fMet1} alleles were replaced with tRNA^{fMet2} (MG1655 fMet2^{x4}). To do this a fragment with single nucleotide swaps at position (G46A) in each of the tRNA^{fMet} genes in the *metZWV* was synthesised (Geneart, Thermofisher) and introduced into the chromosome of MG1655 by homologous recombination. MG1655::tRNA^{fMet1}, expressing four tRNA^{fMet1} alleles was also constructed by introducing tRNA^{fMet1} into MG1655 at the *metY* locus (MG1655 fMet1^{x4}).

As previously observed there was no significant difference in pSTAB2 loss with or without VapBC in MG1655 on LB (p = 0.9990, two-way ANOVA, Figure 5.7). Furthermore, there was no significant difference in pSTAB2 with or without VapBC loss in MG1655fMet2^{x4} (p > 0.9999, two-way ANOVA, Figure 5.7). This was expected as the upper limit of detection of the plasmid loss assay is reached with wild-type MG1655 which contains a single tRNA^{fMet2} gene (Figure 5.2 and 5.4), so the effect of additional tRNA^{fMet2} alleles would not be obvious (Figure 5.7). In Chapter Three, results demonstrated that VapBC plays a reduced role on pINV maintenance during growth in M9+ media than in LB (Figure 4.3). Therefore, plasmid loss assays were repeated following the growth on M9+. Under these conditions, the impact of tRNA^{fMet2} was observed. In MG1655 there was a significant difference in pSTAB2 loss with or without VapBC in MG1655 on M9+ (p = 0.0057, two-way ANOVA, Figure 5.7). In contrast, there was no significant difference in pSTAB2 loss with or without VapBC in MG1655fMet2^{x4} on M9+ (p = 0.1157, two-way ANOVA, Figure 5.7). There was no significant difference in pSTAB2 loss with VapBC^{Sf} in MG1655 and MG1655fMet2^{x4} (p

> 0.9999, two-way ANOVA, Figure 5.7). These data further suggest the presence of tRNA^{fMet2} reduces the effect of VapBC.

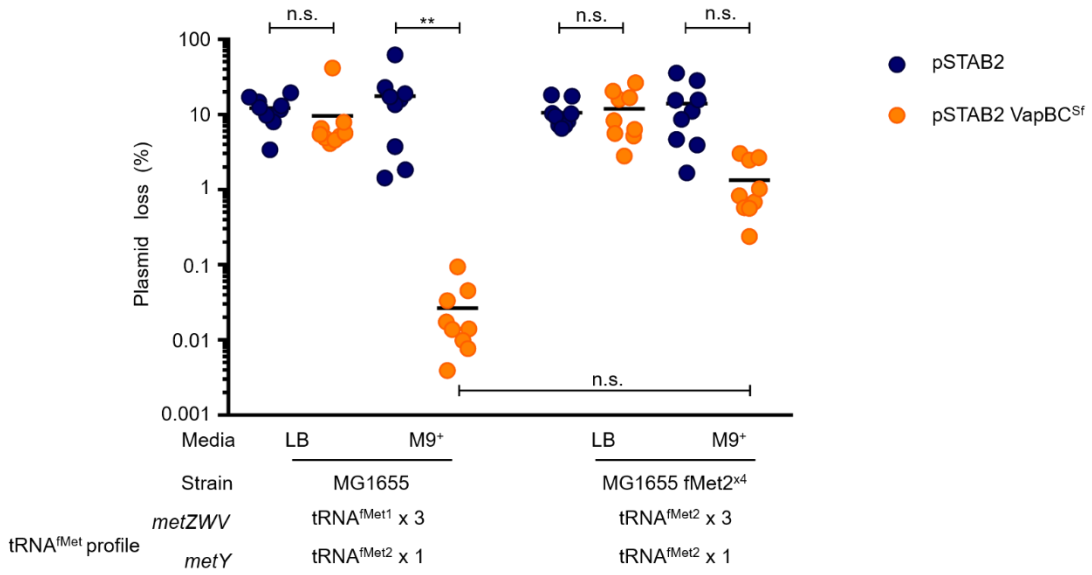


Figure 5.7 The effect of four tRNA^{fMet2} on the impact of VapBC^{Sf} pSTAB2 loss

pSTAB2 loss was measured in *E. coli* MG1655 and MG1655 with all of the tRNA^{fMet} replaced with tRNA^{fMet2}. Results show the percentage of bacteria that have lost the *sacB-kan*^{r} cassette following 25 generations of growth at 37°C on LB or M9+ media. Each dot represents results for a single colony (n = 9) for each strain. Each strain was tested on three independent occasions. The horizontal line shows the mean. Two-way ANOVA with Tukey's multiple comparison statistical tests was performed. ** = p < 0.01 and n.s., non-significant.

5.8 Comparison of VapBC from *S. flexneri* and *S. sonnei*

S. sonnei loses pINV more frequently than *S. flexneri* (163). This can be explained in part by the ancestral loss of GmvAT and CcdAB (163). Both pINV from *S. sonnei* and *S. flexneri* harbour VapBC near their origin of replication, and VapBC is necessary and sufficient for pINV maintenance in *S. flexneri* (163, 179, 180). I next wanted to understand whether VapBC from both species have different effects in plasmid maintenance.

To understand the mechanisms underlying the difference in pINV loss between *S. flexneri* and *S. sonnei*, the nucleotide and predicted amino acid sequences of VapBC from the two species were compared (Figure 5.8). The promoter region is identical in *S. flexneri* and *S. sonnei*. In particular, the putative VapBC binding sites (VapO1 and VapO2) are the same (Figure 5.8) (151, 181). VapBC however was shown to be polymorphic between *Shigella* spp. (Figure 5.8). Both VapB and VapC differ by a single amino acid (Figure 5.8).

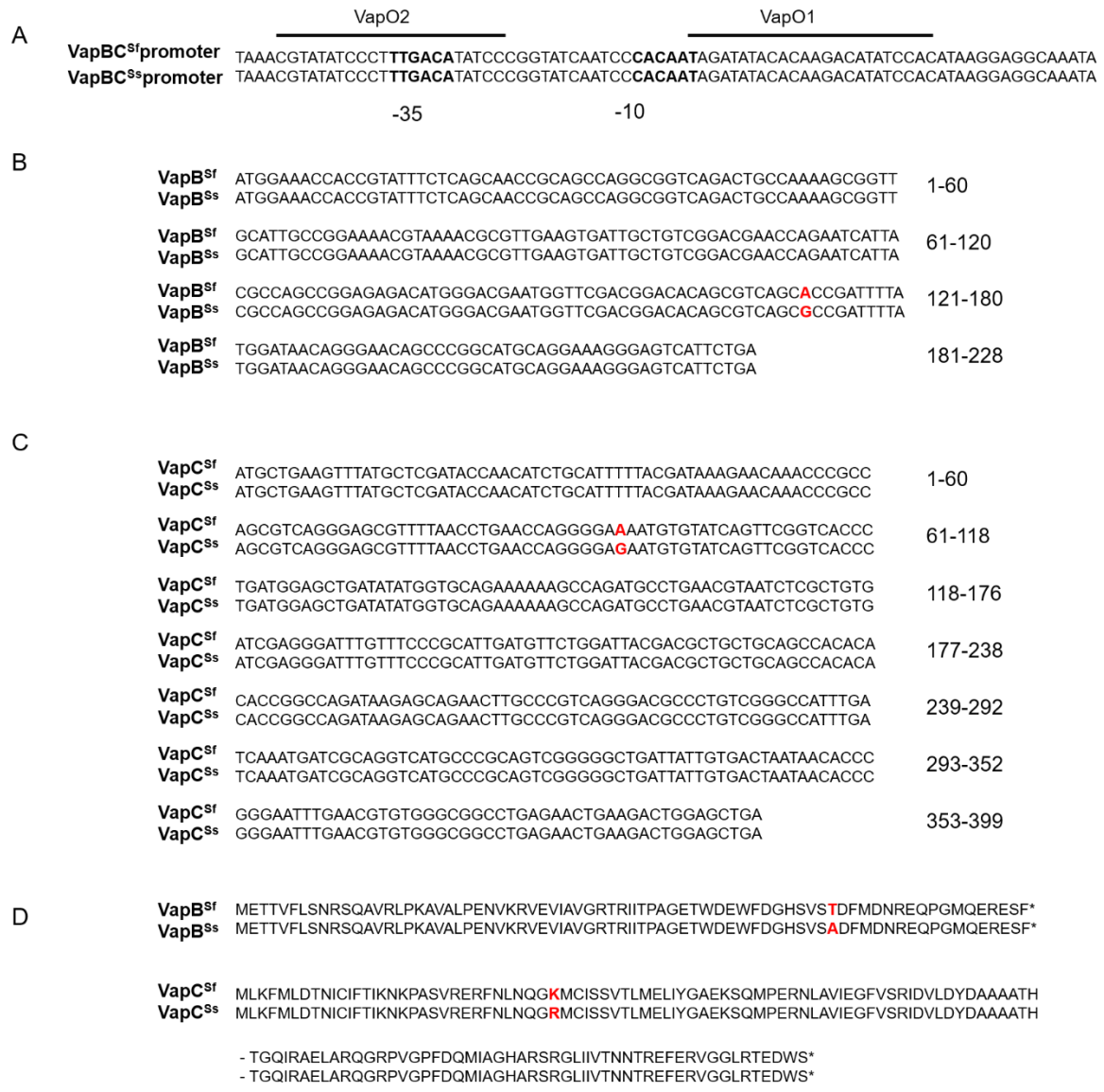


Figure 5.8 Nucleotide and protein alignments of VapBC^{Sf} and VapBC^{Ss}

(A) Nucleotide alignments of the *vapBC* promoter from *S. flexneri* pINV and *S. sonnei* pINV. In bold are the operator sites where VapBC heterooctamers bind. (B) Nucleotide alignment of the open reading frame of the antitoxin, *vapB* from *S. flexneri* pINV and *S. sonnei* pINV. (C) Nucleotide alignment the open reading frame of the toxin, *vapC* from *S. flexneri* pINV and *S. sonnei* pINV.(D) Amino acid alignment of VapB and VapC from *S. flexneri* pINV and *S. sonnei* pINV. Noted in red are nucleotide or amino acid changes between sequences.

The structure of VapBC from *S. sonnei* has been solved by Sarah Hollingshead, unpublished, Figure 5.8. in the lab and in Figure 5.9. Superimposition of the structure of VapBC from *S. sonnei* and *S. flexneri* (PDB 3TND) demonstrate that two heterooctomers are highly similar (RMSD of 0.460 Ă). VapB from *S. sonnei* has a T58A substitution which is located towards its C terminus (Figure 5.9). The C terminus of VapB is important in inhibiting VapC activity, and is the proposed site of protease degradation (151, 249). *S. sonnei* VapC has a K32R substitution compared with the *S. flexneri* protein (Figure 5.9). This substitution is not in the proposed catalytic site of VapC or at its interface with VapB, although it could be involved in VapC binding of $tRNA^{fMet}$ (151).

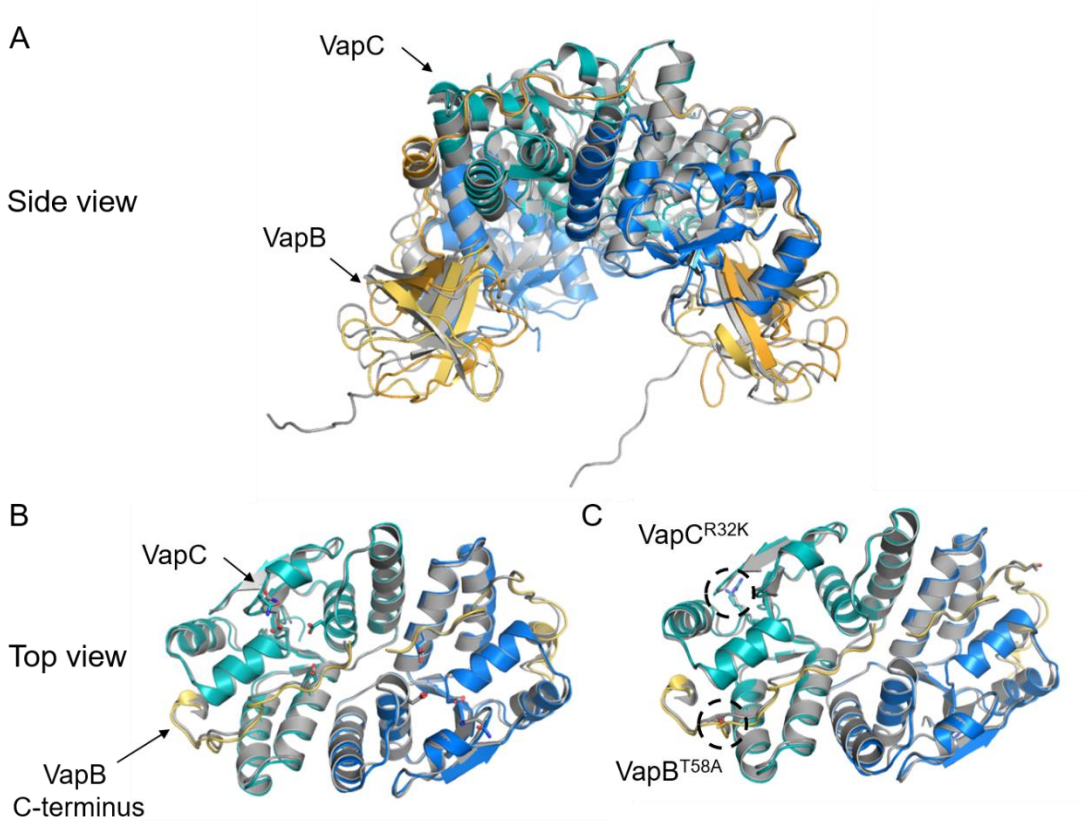


Figure 5.9 Superimposition of VapBC^{Sf} on VapBC^{Ss}.

(A) Superimposition of VapBC heterooctomer from *S. sonnei* (VapBC^{Ss}) and VapBC from *S. flexneri* (VapBC^{Sf}); VapBC^{Sf} is grey, VapB^{Ss} dimers are in yellow or orange and VapC^{Ss} dimers are in blue or teal. VapBC^{Ss} has a RMSD of 0.460Å with the *S. flexneri* complex. (B) Top view of overlay of one VapC^{Sf} dimer (grey) The VapC active site is D7, E42, D98 & E119. The C terminal of VapB is also shown in yellow/ orange (C) The locations of polymorphisms of VapB (T58A) and VapC (R32K) are highlighted.

5.9 VapBC^{Ss} is less efficient at reducing pSTAB2 loss than VapBC^{Sf}

To further investigate the capacity of VapBC^{Ss} in plasmid maintenance, VapBC from *S. sonnei* (VapBC^{Ss}) was introduced into pSTAB2 in the multiple cloning site, and transformed into *S. flexneri* pINV-. The presence of VapBC^{Ss} significantly reduced plasmid loss compared to pSTAB2 without an insert ($p < 0.0001$, one-way ANOVA, Figure 5.10). However, VapBC^{Ss} is less efficient at reducing plasmid loss in *S. flexneri* than VapBC^{Sf} ($p < 0.0001$, one-way ANOVA, Figure 5.10).

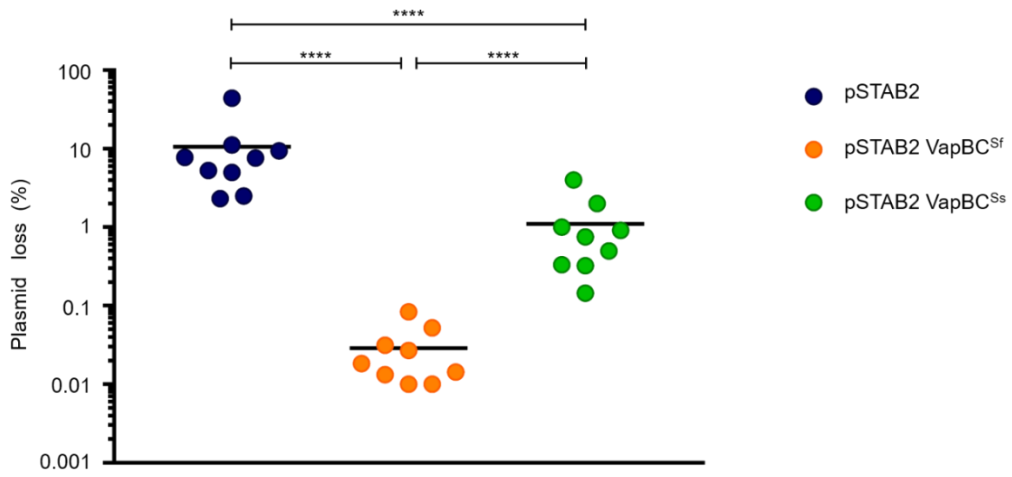


Figure 5.10 VapBC^{Sf} is more effective in reducing pSTAB2 loss than VapBC^{Ss}

The ability of VapBC^{Sf} or VapBC^{Ss} to reduce plasmid loss pSTAB2 in *S. flexneri.* Results show the percentage of bacteria that have lost the *sacB-kan*^{r} cassette. Each dot represents results for a single colony (n = 9). Each strain was tested on three independent occasions. The horizontal line shows the mean. One-way ANOVA with Tukey's multiple comparison statistical tests was performed. ****, $p < 0.0001$.

5.10 VapC^{Ss} is sufficient to increase pSTAB2 loss

To determine whether the polymorphism in VapB, VapC, or both contribute to the differences in the function of VapBC from different *Shigella* spp., chimeric VapBC alleles were generated, with VapB^{Sf} paired with VapC^{Ss} (VapB^{Sf}VapC^{Ss}), and VapB^{Ss} paired with VapC^{Sf} (VapB^{Ss}VapC^{Sf}). These VapBC alleles were inserted into the multiple cloning site of pSTAB2, then transformed into *S. flexneri* pINV-. Interestingly pSTAB2 with VapB^{Sf}VapC^{Ss} did exhibit significantly higher plasmid loss compared with pSTAB2 containing VapBC^{Sf} ($p < 0.0001$, one-way ANOVA Figure 5.11). However, pSTAB2 with VapB^{Sf}VapC^{Ss} did not exhibit significantly higher plasmid loss compared with pSTAB2 containing VapBC^{Ss} ($p = 0.4667$, one-way ANOVA Figure 5.11). Interestingly pSTAB2 VapB^{Ss}VapC^{Sf} did not exhibit significantly different plasmid loss compared with VapBC^{Sf} ($p = 0.0991$, one-way ANOVA, Figure 5.11). However, VapB^{Ss}VapC^{Sf} did exhibit significantly different reduced plasmid loss compared with VapBC^{Ss} ($p < 0.0001$, one-way ANOVA, Figure 5.11). This suggests that the substitution in VapC is responsible for the different capacity of VapBC from *S. sonnei* and *S. flexneri* to mediate plasmid stability.

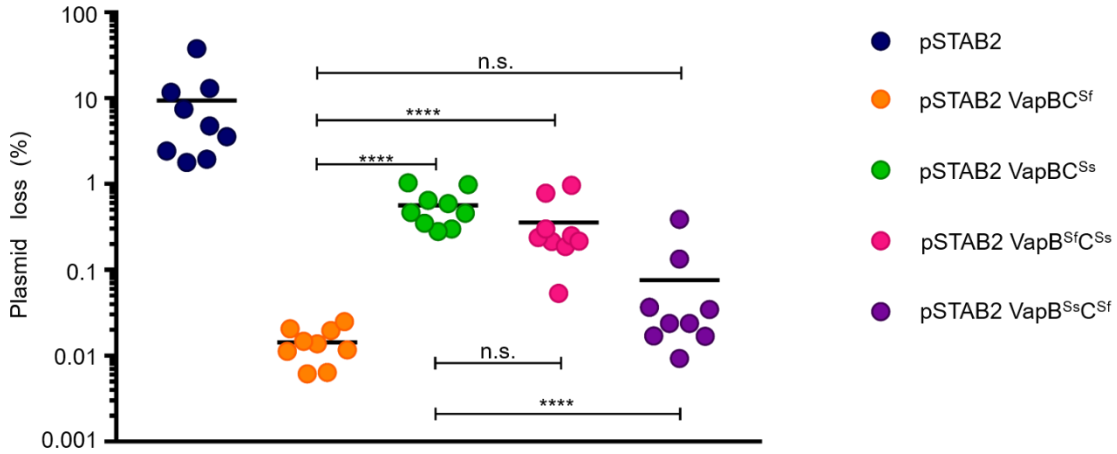


Figure 5.11 VapC^{Ss} is sufficient to increase pSTAB2 loss

The effect of VapB^{Ss} or VapC^{Ss} to stabilise pSTAB2 was evaluated. Results show the percentage of bacteria that have lost the *sacB-kan*^{r} cassette. Each dot represents results for a single colony (n = 9) for each strain. Each strain was tested on three independent occasions. The horizontal line shows the mean. One-way ANOVA with Tukey's multiple comparison statistical test was performed. ****, $p < 0.0001$ and n.s., non-significant.

5.11 Background *Shigella* spp. effects impact of VapBC^{Ss} on pSTAB2 loss

To further investigate the effect of the genetic background in *Shigella* spp., pSTAB2 containing VapBC^{Sf} or VapBC^{Ss} was introduced into *S. sonnei* pINV-. Both VapBC^{Sf} and VapBC^{Ss} significantly reduced plasmid loss compared to empty pSTAB2 in *S. sonnei* ($p < 0.0001$ for both VapBC^{Sf} and VapBC^{Ss}, one-way ANOVA, Figure 5.12). Similar to results obtained in *S. flexneri* (Figure 5.10), VapBC^{Ss} is less effective at reducing plasmid loss than VapBC^{Sf} in *S. sonnei* ($p < 0.0001$, respectively, one-way ANOVA, Figure 5.10 and 5.12). Interestingly VapBC^{Sf} and VapBC^{Ss} appears less efficient at reducing plasmid loss in *S. sonnei* than in *S. flexneri*. After 25 generations, the percentage of bacteria lacking pSTAB2 containing VapBC^{Sf} was 0.0290 % (S.D. +/- 0.0247) in *S. flexneri* (Figure 5.10) compared with 0.4011 % (S.D. +/- 0.1926) in *S. sonnei* (Figure 5.12). The percentage of bacteria lacking VapBC^{Ss} pSTAB2 in *S. flexneri* was 0.8414% (S.D. +/- 1.217, Figure 5.10), but in a *S. sonnei* background is 1.7443% (S.D. +/- 1.941, Figure 5.12). This suggests that the genetic background, affects plasmid maintenance.

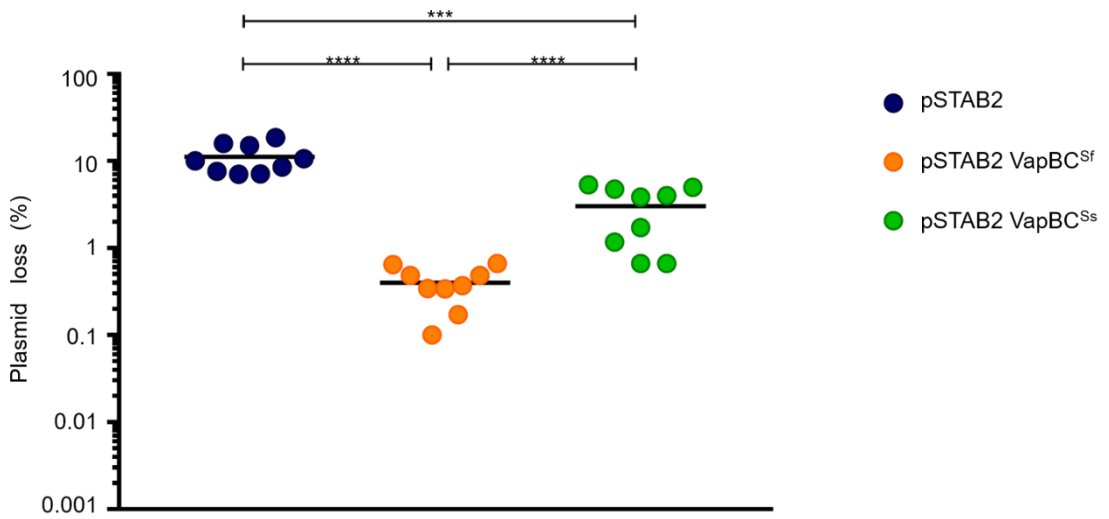


Figure 5.12 VapBC^{Sf} is more effective in reducing pSTAB2 loss than VapBC^{Ss} in *S. sonnei*

The ability of VapBC^{Sf} or VapBC^{Ss} to maintain pSTAB2 in *S. sonnei.* Results show the percentage of strains that have lost the *sacB*-kan^{r} cassette. Each dot represents results for a single colony (n = 9) for each strain. Each strain was tested on three independent occasions. The horizontal line shows the mean. One-way ANOVA with Tukey's multiple comparison statistical tests was performed. ****, $p < 0.0001$ and ***, $p < 0.001$.

5.12 VapBC^{Ss} is not effective at maintaining pSTAB2 in *E. coli.*

To investigate the interaction between tRNA^{fMet2} and the ability of VapBC^{Ss} to contribute to plasmid maintenance, pSTAB2 with VapBC^{Ss} was transformed into *E. coli* MG1655 and compared to derivatives with different tRNA^{fMet} profiles. In MG1655, VapBC^{Ss} did not significantly reduce plasmid loss compared to pSTAB2 with no insert (p = 0.3949, two-way ANOVA, Figure 5.13). Interestingly when pSTAB2 VapBC^{Ss} was introduced into MG1655 lacking tRNA^{fMet2} (MG1655Δ*metY*), there was also no significant difference in plasmid maintenance compared to pSTAB2 with no insert (p > 0.1400, two-way ANOVA, Figure 5.13) unlike pSTAB2 harbouring VapBC^{Sf} (Figure 5.5). In MG1655fMet1^{X4} and MRE600 there was also no significant difference in plasmid maintenance of pSTAB2 VapBC^{Ss} compared to empty pSTAB2 (p = 0.1462 and 0.6042 for MG1655fMet1^{X4} and MRE600, respectively, Figure 5.13). Taken together, these results demonstrate that VapBC^{Ss} is less effective at maintaining pSTAB2 than VapBC^{Sf} in *E. coli* irrespective of the tRNA^{fMet} profile.

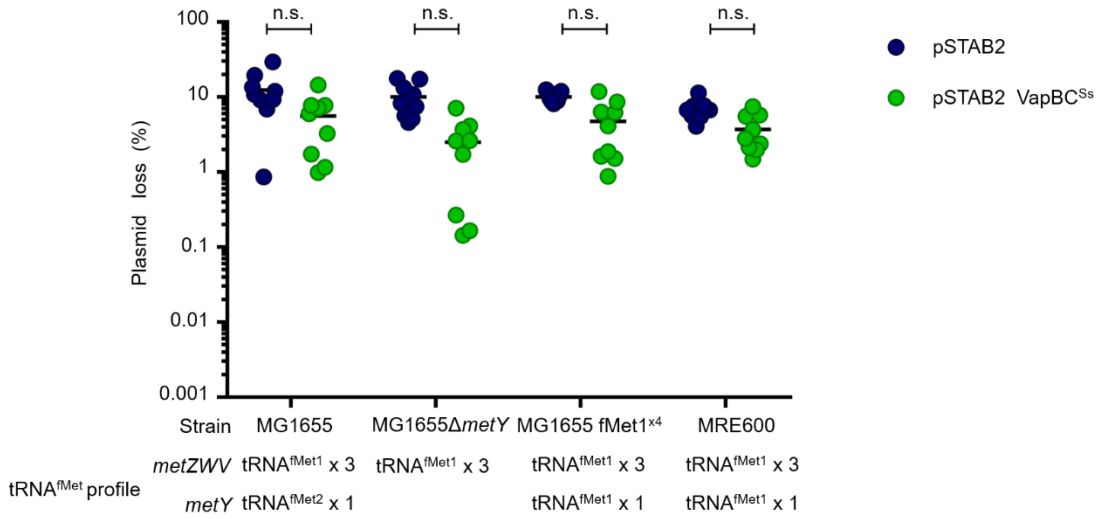


Figure 5.13 VapBC^{Ss} is not effective at maintaining pSTAB2 in *E. coli*

The ability of VapBC^{Ss} to maintain pSTAB2 in isogenic strains of MG1655 and MRE600 with different tRNA^{fMet} profiles. Plasmid loss was measured in a MG1655 mutants lacking tRNA^{fMet2} (MG1655Δ*metY*) or tRNA^{fMet2} replaced with tRNA^{fMet1} (MG1655 fMet1^{x4}) or MRE600 following 25 generations of growth at 37°C on LB agar. Each dot represents results for a single colony (n = 9) for each strain. Each strain was tested on three independent occasions. The horizontal line shows the mean. Two-way ANOVA with Tukey's multiple comparison statistical tests was performed. n.s., non-significant.

5.13 Discussion

Results in this chapter demonstrate that VapBC are able to maintain plasmids to varying extents in different backgrounds. This is due to $tRNA^{fMet}$ profile of the target of VapC, in *E. coli* and different species of *Shigella*. *E. coli* K-12 expresses two alleles of $tRNA^{fMet}$, with the presence of $tRNA^{fMet2}$ associated with reduced efficacy of VapBC from *S. flexneri* to maintain pSTAB2 (Figure 5.2). Further evidence demonstrating that that $tRNA^{fMet2}$ is responsible for this was obtained from analysis of isogenic strains (Figure 5.5). The target of VapC is initiator $tRNA^{fMet}$ which is essential for bacterial translation initiation (182). Translation requires the transfer of tRNAs through A, P, and E ribosomal sites (A for aminoacyl, P for peptidyl, and E for exit). The first amino acid of a polypeptide chain is always a methionine that enters the ribosome bound to the initiator $tRNA^{fMet}$. The initiator tRNA, $tRNA^{fMet}$ is essential and ensures initiation of translation from the Shine-Dalgarno site of the mRNA. In bacteria, the methionine on $tRNA^{fMet}$ is N-formylated, this selectively excludes the $tRNA^{fMet}$ during elongation (250). Even in the case of alternative start codons, these are all decoded by the $tRNA^{fMet}$ and translated as formylmethionine.

The biology of $tRNA^{fMet2}$ has not been well studied. The presence of adenine instead of N7-methyl guanine at position 46 is the only difference between $tRNA^{fMet1}$ and $tRNA^{fMet2}$ (242). N7-methyl guanine at position 46 (m7G46) is a common modification in tRNA, and this residue forms a hydrogen bond with G22 found in a C13–G22 base pair (251, 252). There are a number of tertiary base-base hydrogen bonding interactions, which serve to stabilise the three dimensional core of tRNA beyond the secondary structure (253). The G22 and G46 hydrogen bond is a base-backbone interaction which helps to neutralise positive charge on m^7G46 that is thought to stabilise the three dimensional core of tRNA (253). The substitution at this site with

adenine could affect this base pair interaction and stability of tRNA. Indeed, $tRNA^{fMet1}$ is thought to be more stable than $tRNA^{fMet2}$ with differences in the thermal stability of the dihydrouridine stem (254), this is supported by nuclear magnetic resonance spectra of the two $tRNA^{fMet}$ species (255).

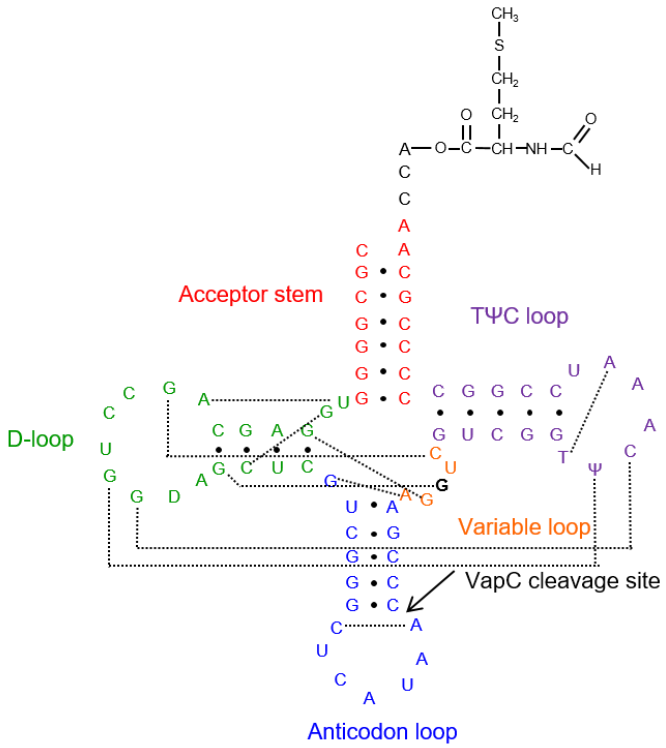


Figure 5.14 tRNA tertiary structure interactions

Secondary structure of $tRNA^{fMet}$. Dashed lines show the location of hydrogen bonds which stabilise the tertiary structure. Figure modified from Quigley and Rich (253).

Other reported differences include the two $tRNA^{fMet}$ species which differ in the rates at which they are aminoacylated, with the rate higher for $tRNA^{fMet2}$ (K_M of the reaction, 5 µM) being higher than $tRNA^{fMet1}$(K_M, 1.3 µM) (255). These differences suggest that the $tRNA^{fMet}$ might have distinct ability to bind the P site of the small subunit of the ribosome (256). Furthermore, G46 found on $tRNA^{fMet1}$ is methylated, but A46 found on $tRNA^{fMet2}$ is not methylated. This tRNA (m^7G46) modification is not essential for cell viability in *E. coli* (257), although post-transcriptional modification can reduce tRNA degradation (258).

Future experiments would be directed at understanding how $tRNA^{fMet2}$ confers reduced efficacy of $VapBC^{Sf}$. It is possible that VapC preferentially cleaves one of the $tRNA^{fMet}$ alleles. This could be assessed by performing *in vivo* cleavage assays (182); cellular $tRNA^{fMet}$ levels are measured by Northern blot analysis before and at time points after expression of VapC. The availability of isogenic strains with only $tRNA^{fMet1}$ or $tRNA^{fMet2}$ will allow the rates of degradation to be compared directly. Additionally it would be possible to perform *in vitro* assays, with synthesised tRNA and purified VapC (182). Furthermore, we could perform with VapC and $tRNA^{fMet1}$/$tRNA^{fMet2}$ binding assays and see if there is a differential recognition of the tRNAs (259, 260).

Despite the availability of a range of structures of PIN domain containing proteins as isolated nucleases or in eukaryotic proteins, the basis of the specific recognition of RNA substrates remains unknown and the basis of catalysis is poorly understood (185). So far there are no structures of PIN domains with a nucleic acid substrate. This might be the result of relatively weak or transient interactions between the PIN domains and their target RNAs (261). Potentially if $tRNA^{fMet2}$ is relatively resistant to cleavage by VapC, this substrate could be used to solve the structure of VapC with its

target. However, it is possible that $tRNA^{fMet2}$ is not even engaged by VapC, which would make it a poor candidate for structural studies.

The concept of anti-addiction factors has been discussed regarding chromosomal TA systems (262). For example, some chromosomal TA systems prevent PSK when a plasmid carrying a related TA system is lost (262). This 'anti-addiction' theory has been invoked to explain the diversity of chromosomal TA systems. Potentially $tRNA^{fMet2}$ also acts as an anti-addiction factor, by reducing the capacity of VapBC to stabilise plasmids. Future experiments will examine whether the different $tRNA^{fMet}$ profiles confer resistance against the acquisition and maintenance of VapBC containing plasmids. This could be analysed by performing toxicity assays with VapC, which assess the impact of inducing toxin expression of a toxin on *E. coli* viability with different $tRNA^{fMet}$ profiles (163). Furthermore, plasmid stability assays could be performed with mixed populations of *E. coli*.

Furthermore, these findings might offer insights into the evolution of *Shigella* from *E. coli* (9). Several studies have demonstrated that *Shigella* spp. are closely related to Group A and B1a and B1b *E. coli* and these strains do not have $tRNA^{fMet2}$ (133, 244). Indeed, $tRNA^{fMet2}$ has only been identified in strains of *E. coli* which are derived from or closely related to MG1655 K-12 which is a group A strain.

Table 5.1 tRNA^{fMet} profile in *E. coli* and *Shigella* spp.

Class	Strain	Phylo-group	*metZWV* operon	*metY* locus	
			tRNA^{fMet1}	tRNA^{fMet1}	tRNA^{fMet2}
Commensal *E. coli*	MG1655 K-12	A	3	-	1
Commensal *E. coli*	BL21	A	3	1	-
Commensal *E. coli*	MRE600	A	3	1	-
Commensal *E. coli*	SE11	B1	3	1	-
EAEC	55989	B1	3	1	-
ETEC	E24372A	B1	3	1	-
EHEC	11128	B1	3	1	-
EIEC	CFSAN029787	B1	3	1	-
Commensal *E. coli*	ED1a	B2	3	1	-
EPEC	E2348169	B2	3	1	-
UTEC	UT189	B2	3	1	-
Extracellular pathogenic *E. coli*	UMN026	D	4	1	-
Extracellular pathogenic *E. coli*	IA139	D	2	1	-
Extracellular pathogenic *E. coli*	SMS-3-5	D	3	1	-
EHEC	EDL933	E	3	1	-
EHEC	TW14359	E	3	1	-
EHEC	Sakai	E	3	1	-

The VapBC TA system is common to pINV in all *Shigella* spp.. VapBC has been shown to be necessary and sufficient for maintenance of pINV. *S. sonnei* however has a higher loss of pINV than *S. flexneri* (163). To investigate if there was a difference in the plasmid maintenance capacity of VapBC between the different species, I introduced VapBC from *S flexneri* or *S. sonnei* into pSTAB2 to directly compare the efficacies of the two VapBC systems. Results demonstrate that VapBC from *S. sonnei* has a reduced ability to retain pSTAB2 than VapBC from *S. flexneri* (Figure 5.10 and 5.12). Analysis of chimeric VapBCs demonstrated that VapC accounts for the difference between the species (Figure 5.11). The reason is not clear as the polymorphism is not near the active site or where VapB interacts with VapC. There several potential explanations for this result. First, it is possible that the substitution affects conformation of VapC alone; the structure of VapC alone might help to understand if this is true. Secondly, the activity of VapC might differ, either in rates of cleavage or substrate recognition and binding. This could be analysed by performing toxicity assays with VapC, which assess the impact of inducing toxin expression on *E. coli* viability (163). Differences in cleavage and binding could be assessed using *in vivo* and *in vitro* assays described above. Also, it is striking that $tRNA^{fMet2}$ influences the function of VapBC from *S. flexneri* but not *S. sonnei* (Figure 5.5 and 5.13). To investigate this further, pSTAB2 with chimeric VapBCs could be introduced into strains with different $tRNA^{fMet}$ profiles.

It is interesting that VapBC is polymorphic and so could be evolving with pINV for efficient plasmid maintenance, depending on life cycle of the bacterium. This work demonstrates that polymorphisms in VapC have significant effects on plasmid maintenance (Figure 5.11). Bioinformatic analysis reveals that there are further VapBC polymorphisms in *Shigella* spp. and closely related Enteroinvasive *E. coli* (EIEC) which

also have acquired pINV (Figure 5.15) (263). Polymorphisms in the VapB antitoxin are found in the C terminal which mediates antitoxicity so could have biological effects. The polymorphisms in VapC are not near the active site. It would be interesting to investigate whether these polymorphisms affect VapBC function using pSTAB2.

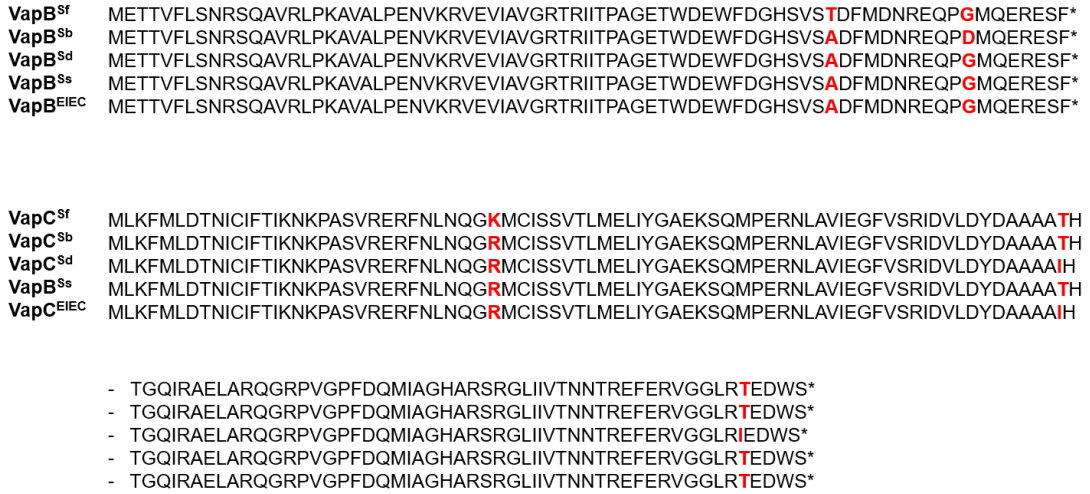


Figure 5.15 VapBC amino acid sequence alignments from EIEC and *Shigella* spp.

Amino acid alignment of VapB and VapC from EIEC and *Shigella* spp.. Noted in red are nucleotide or amino acid changes between sequences.

Furthermore, the tRNA^{fMet} profile is different between *Shigella* spp. which might affect VapBC function. This might explain the differential activity of the same VapBCs in different species of *Shigella* (Figure 5.10 and 5.12). *S. flexneri* has three tRNA^{fMet} genes while *S. sonnei* has four. One hypothesis is there is selection against the amount of tRNA^{fMet} which might help plasmid maintenance. Interestingly there are striking differences between EIEC which has recently acquired pINV and the *Shigella* spp.. EIEC only has tRNA^{fMet1}. *S. flexneri* and *S. dysenteriae* have lost one of the tRNA^{fMet1} so only have three tRNA^{fMet1} genes. Furthermore, aside from tRNA^{fMet1} and tRNA^{fMet2}, further alleles of the tRNA^{fMet} can be found in *Shigella* spp. (Table 5.2 and

Figure 5.16). *S. sonnei* and *S. boydii* have four tRNA^{fMet}, three tRNA^{fMet1} and polymorphisms are found in the remaining tRNA^{fMet} genes. *S. sonnei* and *S. boydii* potentially represent evolutionary intermediates in terms of tRNA^{fMet} profile.

Table 5.2 tRNA^{fMet} polymorphism profile in different *Shigella* spp.

			metZWV operon				*metY* locus			
Species	Strain	Phylo-group	tRNA^{fMet1}	tRNA^{fMet2}	tRNA^{fMet3}	tRNA^{fMet4}	tRNA^{fMet1}	tRNA^{fMet2}	tRNA^{fMet3}	tRNA^{fMet4}
EIEC	CFSAN029787	B1	3	-	-	-	1	-	-	-
S. boydii	B4 Sb227	S	3	-	-	1	1	-	-	-
S. boydii	B18 BS512	S	3	-	-	1	1	-	-	-
S. sonnei	Ss046	S	3	-	1	-	1	-	-	-
S. flexneri	2457T	S	2	-	-	-	1	-	-	-
S. flexneri	M90T	S	2	-	-	-	1	-	-	-
S. dysenteriae	D1 Sd197	S	2	-	-	-	1	-	-	-

tRNA^{fMet1} CGCGGGGTGGAGCAGCCTGGTAGCTCGTCGGGCTCATAACCCGAAGGTCGTCGGTTCAAATCCGGCCCCCGCAACCA
tRNA^{fMet2} CGCGGGGTGGAGCAGCCTGGTAGCTCGTCGGGCTCATAACCCGAAGATCGTCGGTTCAAATCCGGCCCCCGCAACCA
tRNA^{fMet3} GGCGGGGTGGAGCAGCCTGGTAGCTCGTCGGGCTCATAACCCGAAGGTCGTCGGTTCAAATCCGGCCCCCGCAACCA
tRNA^{fMet4} CGCGGGGTGGAGCAGCTTGGTAGCTCGTCGGGCTCATAACCCGAAGGTCGTCGGTTCAAATCCGGCCCCCGCAACCA

Figure 5.16 Nucleotide alignment highlighting polymorphisms in tRNA^{fMet} in *Shigella* spp.

Nucleotide alignments of tRNA^{fMet1}, tRNA^{fMet2}, tRNA^{fMet3} and tRNA^{fMet4}. Polymorphisms are highlighted in red.

tRNA^{fMet3} (C1G compared with tRNA^{fMet1}) is located in *S. sonnei metZ* although it is unclear whether this affects its function. Initiator tRNAs determinants are located in the anticodon stem, the acceptor stem, and the dihydrouridine stem. A significant feature that differentiates initiator tRNA from elongator tRNA, is the absence of Watson-Crick base pair between positions 1 and 72 in the acceptor stem (264); required for N-formylation of tRNA^{fMet}, which selectively excludes the tRNA^{fMet} from elongation during translation (250). Methionyl tRNA transformylase (MTF) formylates aminoacylated initiator tRNA, with the enzyme recognising tRNA that lacks a Watson-

Crick base pair between positions 1 and 72 base pair (256). Additionally, the absence of a base pairing between nucleotides 1 and 72 protects $tRNA^{fMet}$ against cleavage by peptidyl-tRNA hydrolase which recycles all N-blocked aminoacyl-tRNA molecules (256). In contrast to $tRNA^{fMet1}$ and $tRNA^{fMet2}$, $tRNA^{fMet3}$ has a G at position 1 which will form a base pair. Therefore, $tRNA^{fMet3}$ might not be formylated. VapC does not cleave methionine elongator tRNA, or other tRNAs (182). So $tRNA^{fMet3}$ could titrate VapC from $tRNA^{fMet1}$, making PSK less effective. It would be interesting to introduce $tRNA^{fMet3}$ into *S. flexneri* and perform plasmid loss assays using pSTAB2.

The two sequenced *S. boydii* strains have $tRNA^{fMet4}$ which has a polymorphism (C17T) located in the D loop of $tRNA^{fMet}$. Position 17 has not been studied in prokaryotes, although this position helps differentiate initiator from elongator tRNA in yeast (265). Perhaps again this tRNA could be recognised as an elongator tRNA rather than an initiator tRNA in *S. boydii.* Interestingly the $tRNA^{fMet4}$ was in different locations in different strains, one in the *metW* locus (in strain B4 SB227), and one in *metV* (in B18 BS512). It would be interesting to introduce $tRNA^{fMet4}$ into *S. flexneri* background and perform a plasmid loss assay using pSTAB2 with and without $VapBC^{Sf}$.

Results in this chapter highlight the importance of differences in the toxin and of TA system targets on plasmid maintenance function. Single nucleotide polymorphisms in TA systems affect the efficacy of plasmid maintenance. These changes could have profound effects on the stability of plasmids in different bacterial lineages, and changes could reflect adaptation of a plasmid to its host over time. Furthermore, it is possible that the profile of $tRNA^{fMet}$ for instance might influence the acquisition and fixation of horizontally acquired elements.

6 Conclusion

My thesis aimed to understand the molecular mechanisms of virulence in the important human pathogen, *S. flexneri*. This bacterium is a leading cause of bacillary dysentery world-wide, and is exclusively adapted to the human host (266). The bacterium has been studied extensively in the past, as it is able to invade into and manipulate host cell functions. However, at the start of my thesis, little was known about the intracellular phase in the infectious cycle of *Shigella*, particularly during replication within epithelial cells (2). This step is critical as epithelial cells sense the presence of bacteria in the cytoplasm, and initiate inflammatory responses (267).

My initial intention was to define the nutritional requirements of bacteria within this habitat by examining the capacity of individual mutants in a transposon library to survive and multiply within epithelial cells. Furthermore, I aimed to determine whether there was heterogeneity during intracellular replication. Recently developed methods, such as FD, have revealed diverse populations of bacteria within phagocytic cells, which make a significant impact on their fate (129). I therefore attempted to apply FD to *S. flexneri* to have a robust and rapid method to screen a library of mutants. However, my results highlighted several limitations with FD. For example, a low proportion of inoculum invade epithelial cells, and a large population of non-invasive, antibiotic treated bacteria (added to study intracellular bacteria only) was detected by flow cytometry, decreasing signal to noise ratio.

I circumvented this issue by changing the antibiotic used to kill extracellular bacteria and switching the selective marker in the plasmid used for FD. However, the choice of chloramphenicol proved problematic, and this antibiotic affected retention of pINV through unknown mechanisms. I did manage to find concentrations of

chloramphenicol which affected pINV stability less, but no selection was preferable. Finally, the signal from DsRed was sub-optimal in bacteria grown to mid-logarithmic phase, probably due to failure of maturation of the fluorophore following subculture. This was a significant setback, as it limited the number of divisions that FD could detect during growth within epithelial cells, and hence the sensitivity of the method. These limitations are likely to explain why plasmid-based FD has not been broadly applied to pathogens in non-phagocytic cells, and *in vivo* situations. As part of on-going work, I have developed a modified version of FD, in which the genes encoding rapidly maturing versions of the fluorophores are integrated in the genome in single copy; I also switched the fluorophores so that FD is based on dilution of GFP, rather than DsRed.

At this stage a paper was published (111) describing the analysis of auxotrophic *S. flexneri* mutants in epithelial cells as well as the results of metabolic flux of infected and un-infected cells. Therefore, I decided to change the focus of my studies to the virulence plasmid, pINV, and the basis of its maintenance in *Shigella* spp.. The mechanisms of plasmid replication and control of copy number was intensively investigated at the dawn of the age of molecular biology. Since then, there has been far less interest in plasmid biology, even though these extrachromosomal elements play a critical role in the development of AMR and virulence in many bacteria (135).

Previous work in the laboratory had demonstrated that temperature was an important factor in pINV maintenance. The main TA system responsible for retention of *S. flexneri* pINV at 37°C is VapBC, while at 21°C GmvAT makes a major contribution (163). While the reason for this is being investigated by others, I sought other conditions that might influence the role of TA systems in pINV maintenance. I explored

several parameters such as temperature stress, pH, oxygen, and nutrient limitation. I found that VapBC still has a significant role in these conditions. I could have examined several further stresses including oxidative or nitrosative stress, and the influence of short chain fatty acids. However, I decided to subject bacteria to a more complex and biologically relevant environment, looking at pINV maintenance during survival within phagocytes. Survival and virulence maintenance in these cells represents a key step in the lifecycle of *Shigella* (2). However, no plasmid loss was detected following infection of THP-1 derived macrophages. Working with phagocytic cells has advantages compared with epithelial cells, such as the active uptake of bacteria by macrophages increasing the number of intracellular bacteria. The limitation of using phagocytic cells is that *Shigella* can cause their death by necroptosis within a few hours following infection (51). This means that there is a limited time window for bacterial replication and therefore plasmid loss, reducing the limit of detection of this approach. It is likely that the time course of infection in macrophages was too short to observe any impact of TA systems on plasmid stability. Standard assays for plasmid instability (i.e. the appearance of CR- colonies, or using the dual marker system as above) are performed over 25 generations. Within macrophages, it is unlikely that there are more than 6 generations (assuming replication occurs every 37 min in a 5 hr infection) (111).

As a by-product of this work I found that the *Shigella* T3SS is necessary for intra-macrophage replication, which was a novel finding. The role of the T3SS became apparent, as the dual marker to detect instability of the plasmid was in the gene encoding the T3SS, MxiH. *mxiH*::*sk* did not replicate inside THP-1 derived macrophages. I therefore constructed an alternative strain with the dual marker in the PAI, but in a location that did not affect the T3SS. It is likely that the T3SS is required

for escape from the nascent phagosome, so following entry, bacteria are subjected to the toxic effects of lysosomal fusion (such as ROS, cationic peptides, proteases etc.). The implication of this result is that there will be strong selection for maintenance of the T3SS at steps beyond cell invasion, during replication in host cells. Given that this is a critical phase of amplification of the bacterial population in the GI tract, the population of virulent *Shigella* will expand once bacteria reach the epithelial surface and engage host cells.

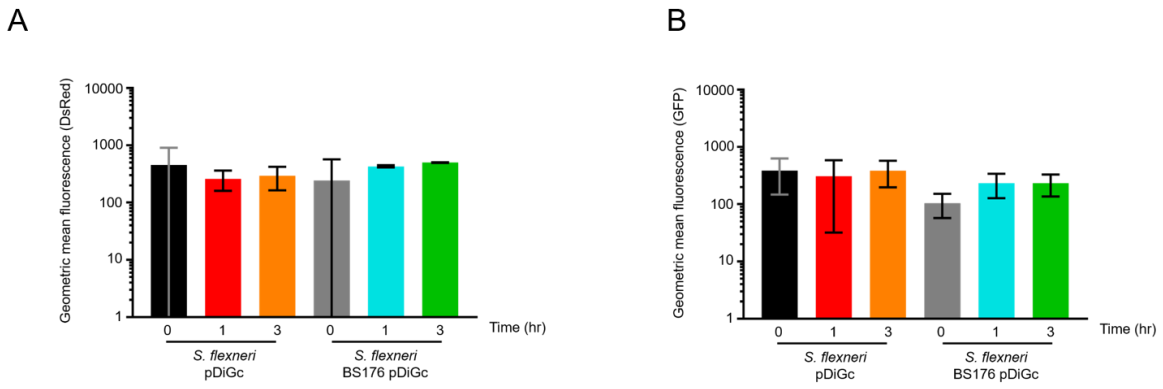
Following on from my work on environmental factors, the final chapter addressed the question of whether and how host genetic background can affect plasmid maintenance. This followed the striking observation that the VapBC TA system appeared unable to stabilise a plasmid in certain strains of *E. coli*, while it had a significant impact in *S. flexneri*. My results demonstrate that the profile of the target of VapC, $tRNA^{fMet}$ is a determinant of VapBC function in a bacterium. Specifically, the presence of the $tRNA^{fMet2}$ allele conferred relative resistance to VapBC. For this work, I developed and exploited a model plasmid, which enabled me to examine plasmid stabilisation systems individually. The mechanism(s) by which $tRNA^{fMet2}$ affects VapBC will be explored in the future. My main hypothesis is that this $tRNA^{fMet}$ is relatively resistant to cleavage by VapC; I will test this by examining the toxicity of VapC in various isogenic genetic backgrounds, and by undertaking *in vivo* cleavage assays, following the fate of $tRNA^{fMet}$ (by Northern blot analysis) in bacteria expressing exclusively $tRNA^{fMet1}$ or $tRNA^{fMet2}$ (182). Furthermore, the role of $tRNAf^{Met2}$ could pave the way for structural studies of a PIN domain protein (VapC) with its RNA target, although $tRNA^{fMet2}$ might or might not prove a suitable target for structural studies.

Interestingly the profile of $tRNA^{fMet}$ alleles varies in different strains of *E. coli*, and the reason for the evolution of $tRNA^{fMet2}$ is unclear. *Shigella* has emerged on four occasions from *E. coli* lineages which lack $tRNA^{fMet2}$; this might be because strains containing $tRNA^{fMet2}$ do not support fixation of VapBC containing plasmids due to their relative resistance to VapC. Therefore, $tRNA^{fMet2}$ might act as a host defence mechanism against parasitism by VapBC containing plasmids. This possibility is currently being addressed by examining the stability of plasmids in mixed populations of *E. coli*.

Finally, I found that a single amino acid substitution in VapC reduces the ability of VapBC from *S. sonnei* to stabilise the model plasmid, pSTAB2. The reasons for this are not obvious from inspection of the structure of the VapBC complex; the polymorphism is not located near the active site of VapC or in a region that interacts with the VapB antitoxin. It is possible that the substitution affects the conformation of the free toxin, and thereby its activity; studies of the VapC structure in isolation might address this possibility. Interestingly further polymorphisms were identified in VapBC from pINV in other species of *Shigella* and EIEC. Future studies could be undertaken to examine the effect of these differences on the maintenance of pINV.

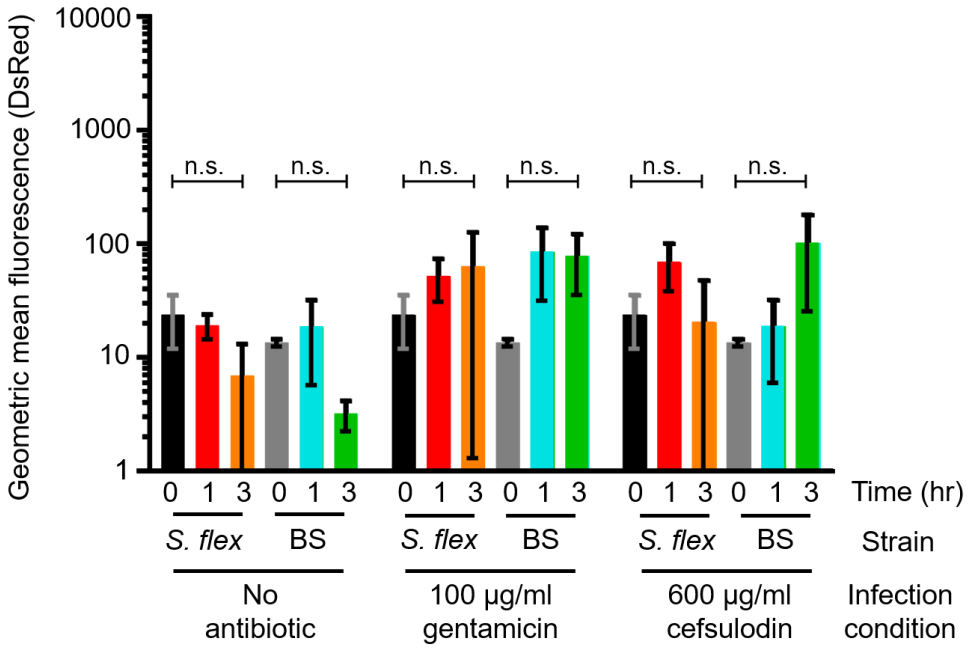
Appendix

Appendix 1 Geometric mean fluorescence of GFP and DsRed from HeLa infection with *S. flexneri* pDiGc



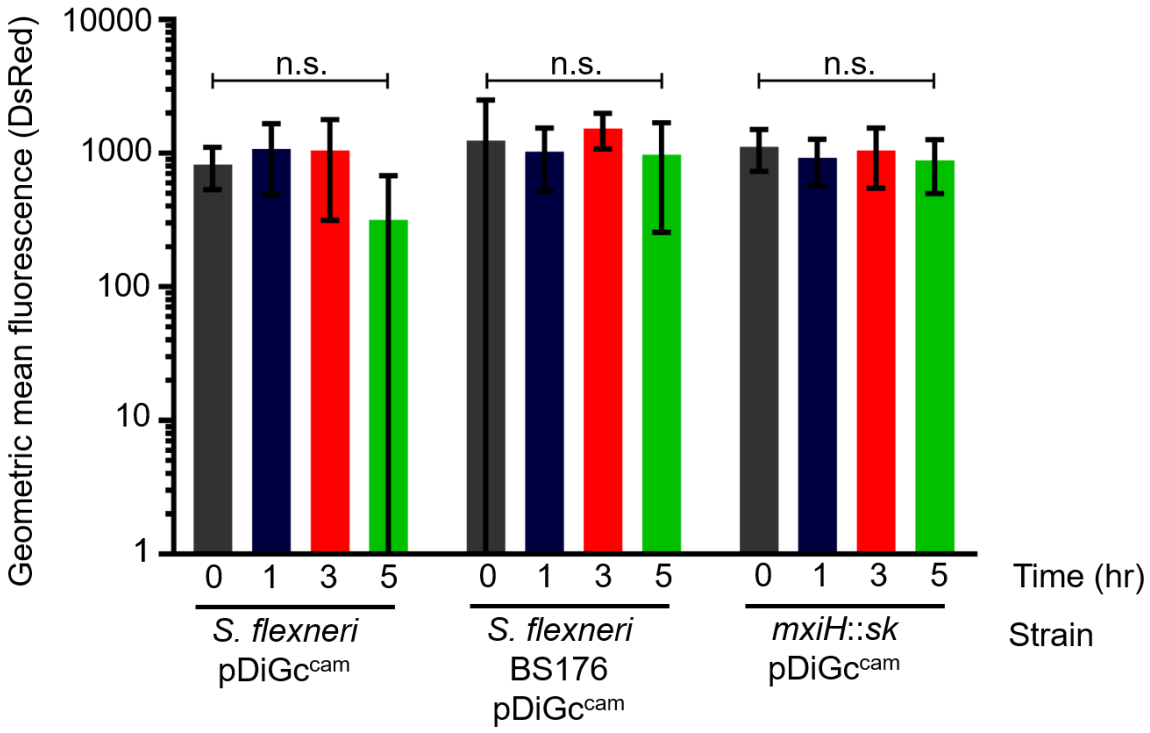
Supplementary data for Figure 3.6. (A) Results for the geometric mean fluorescence of DsRed mean show the mean +/- S.D. of two independent experiments. (B) Results for the geometric mean fluorescence of GFP mean show mean +/- S.D. of two independent experiments

Appendix 2 Geometric mean fluorescence of DsRed from HeLa infection with *S. flexneri* pDiGc^{cam}



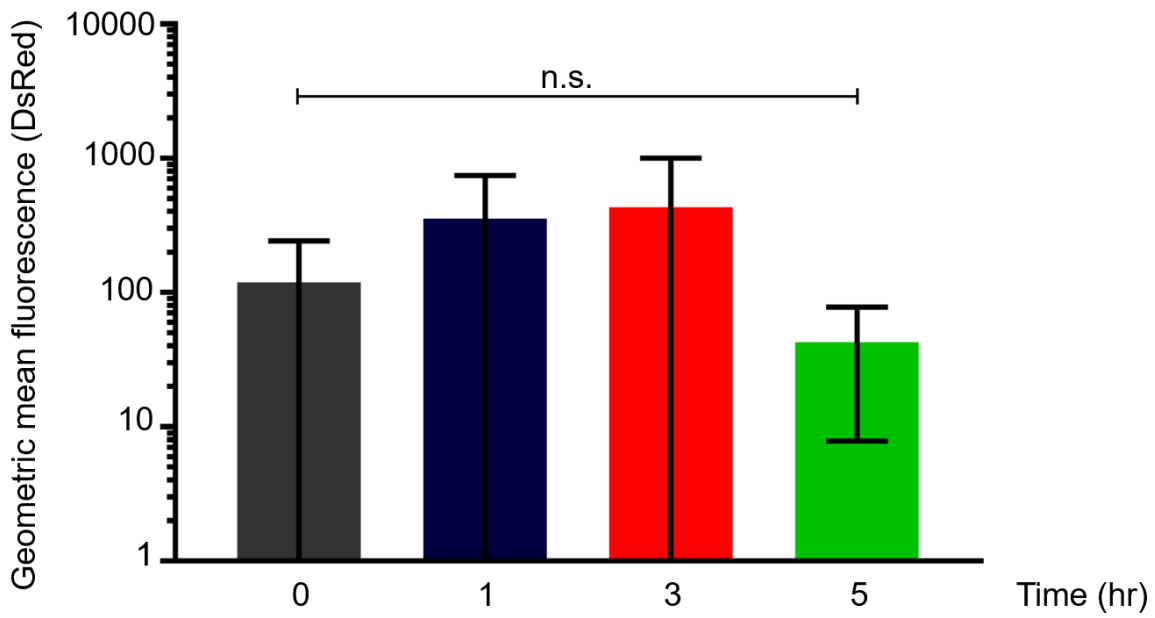
Supplementary data for Figure 3.11. Results for the geometric mean fluorescence of DsRed show mean +/- S.D. of three independent experiments. Two-way ANOVA statistical analysis with Tukey's multiple comparison was performed. n.s., non- significant.

Appendix 3 Geometric mean fluorescence of DsRed from THP-1 infection with *S. flexneri* pDiGc^{cam}



Supplementary data for Figure 4.7. Results for the geometric mean fluorescence of DsRed show mean +/- S.D. of three independent experiments. Two-way ANOVA statistical analysis with Tukey's multiple comparison was performed. n.s., non- significant.

Appendix 4 Geometric mean fluorescence of DsRed from Ig::*sk* THP-1 infection with *S. flexneri* pDiGc^{cam}



Supplementary data for Figure 4.11. Results for the geometric mean fluorescence of DsRed show mean +/- S.D. of three independent experiments. One-way ANOVA statistical analysis with Tukey's multiple comparison was performed. n.s., non- significant.

References

1. Labrec EH, Schneider H, Magnani TJ, Formal SB. Epithelial Cell Penetration as an Essential Step in the Pathogenesis of Bacillary Dysentery. J Bacteriol. 1964;88(5):1503-18.
2. Schroeder GN, Hilbi H. Molecular pathogenesis of *Shigella* spp.: controlling host cell signaling, invasion, and death by type III secretion. Clin Microbiol Rev. 2008;21(1):134-56.
3. Kotloff KL, Riddle MS, Platts-Mills JA, Pavlinac P, Zaidi AKM. Shigellosis. Lancet. 2018;391(10122):801-12.
4. Estimates of global, regional, and national morbidity, mortality, and aetiologies of diarrhoeal diseases: a systematic analysis for the Global Burden of Disease Study 2015. Lancet Infect Dis. 2017;17(9):909-48.
5. Liu J, Platts-Mills JA, Juma J, Kabir F, Nkeze J, Okoi C, *et al*. Use of quantitative molecular diagnostic methods to identify causes of diarrhoea in children: a reanalysis of the GEMS case-control study. Lancet. 2016;388(10051):1291-301.
6. DuPont HL, Levine MM, Hornick RB, Formal SB. Inoculum size in shigellosis and implications for expected mode of transmission. J Infect Dis. 1989;159(6):1126-8.
7. Holt KE, Thieu Nga TV, Thanh DP, Vinh H, Kim DW, Vu Tra MP, *et al*. Tracking the establishment of local endemic populations of an emergent enteric pathogen. Proc Natl Acad Sci U S A. 2013;110(43):17522-7.
8. Connor TR, Barker CR, Baker KS, Weill FX, Talukder KA, Smith AM, *et al*. Species-wide whole genome sequencing reveals historical global spread and recent local persistence in *Shigella flexneri*. Elife. 2015;4:e07335.
9. Lan R, Reeves PR. *Escherichia coli* in disguise: molecular origins of *Shigella*. Microbes Infect. 2002;4(11):1125-32.
10. Maurelli AT, Fernandez RE, Bloch CA, Rode CK, Fasano A. "Black holes" and bacterial pathogenicity: a large genomic deletion that enhances the virulence of *Shigella* spp. and enteroinvasive *Escherichia coli*. Proc Natl Acad Sci U S A. 1998;95(7):3943-8.
11. Anderson M, Sansonetti PJ, Marteyn BS. *Shigella* Diversity and Changing Landscape: Insights for the Twenty-First Century. Front Cell Infect Microbiol. 2016;6:45.
12. Chantemesse A WF. Sur les microbes de la dysenteriae épidémique. Bull Acad Med Paris. 1888;19:522–9.
13. Shiga K. Ueber den Erreger der Dysenterie in Japan. Zentralbl Bakteriol Mikrobiol Hyg. 1898(23):599-600.
14. Flexner S. The Etiology Of Tropical Dysentery. The British Medical Journal. 1900;2(2074): 917–20.
15. Sonne C. The bacteriology of atoxic dysentery bacilli (paradysentery bacilli). Zentralbl Bakteriol 1915;75:408–56.
16. Boyd JS. The antigenic structure of the mannitol-fermenting group of dysentery bacilli. J Hyg (Lond). 1938;38(4):477-99.
17. Shepherd JG, Wang L, Reeves PR. Comparison of O-antigen gene clusters of *Escherichia coli* (*Shigella*) *sonnei* and *Plesiomonas shigelloides* O17: *sonnei* gained its current plasmid-borne O-antigen genes from *P. shigelloides* in a recent event. Infect Immun. 2000;68(10):6056-61.
18. Peng J, Zhang X, Yang J, Wang J, Yang E, Bin W, *et al*. The use of comparative genomic hybridization to characterize genome dynamics and diversity among the serotypes of *Shigella*. BMC Genomics. 2006;7:218.
19. Yang F, Yang J, Zhang X, Chen L, Jiang Y, Yan Y, *et al*. Genome dynamics and diversity of *Shigella* species, the etiologic agents of bacillary dysentery. Nucleic Acids Res. 2005;33(19):6445-58.
20. McCormick BA, Fernandez MI, Siber AM, Maurelli AT. Inhibition of *Shigella flexneri*-induced transepithelial migration of polymorphonuclear leucocytes by cadaverine. Cell Microbiol. 1999;1(2):143-55.
21. Prunier AL, Schuch R, Fernandez RE, Maurelli AT. Genetic structure of the *nadA* and *nadB* antivirulence loci in *Shigella* spp. J Bacteriol. 2007;189(17):6482-6.

22. Prunier AL, Schuch R, Fernandez RE, Mumy KL, Kohler H, McCormick BA, *et al*. *nadA* and *nadB* of *Shigella flexneri* 5a are antivirulence loci responsible for the synthesis of quinolinate, a small molecule inhibitor of *Shigella* pathogenicity. Microbiology. 2007;153(Pt 7):2363-72.
23. Tominaga A, Lan R, Reeves PR. Evolutionary changes of the *flhDC* flagellar master operon in *Shigella* strains. J Bacteriol. 2005;187(12):4295-302.
24. Faruque SM, Khan R, Kamruzzaman M, Yamasaki S, Ahmad QS, Azim T, *et al*. Isolation of *Shigella dysenteriae* type 1 and *S. flexneri* strains from surface waters in Bangladesh: comparative molecular analysis of environmental *Shigella* isolates versus clinical strains. Appl Environ Microbiol. 2002;68(8):3908-13.
25. Cash BA, Rodo X, Emch M, Yunus M, Faruque AS, Pascual M. Cholera and shigellosis: different epidemiology but similar responses to climate variability. PLoS One. 2014;9(9):e107223.
26. Livio S, Strockbine NA, Panchalingam S, Tennant SM, Barry EM, Marohn ME, *et al*. *Shigella* isolates from the global enteric multicenter study inform vaccine development. Clin Infect Dis. 2014;59(7):933-41.
27. Levine MM, Kotloff KL, Barry EM, Pasetti MF, Sztein MB. Clinical trials of *Shigella* vaccines: two steps forward and one step back on a long, hard road. Nat Rev Microbiol. 2007;5(7):540-53.
28. Mao Y, Cui E, Bao C, Liu Z, Chen S, Zhang J, *et al*. Changing trends and serotype distribution of *Shigella* species in Beijing from 1994 to 2010. Gut Pathog. 2013;5:21.
29. Qiu S, Xu X, Yang C, Wang J, Liang B, Li P, *et al*. Shift in serotype distribution of *Shigella* species in China, 2003-2013. Clin Microbiol Infect. 2015;21(3):252 e5-8.
30. Hulland KR, Leontsini E, Dreibelbis R, Unicomb L, Afroz A, Dutta NC, *et al*. Designing a handwashing station for infrastructure-restricted communities in Bangladesh using the integrated behavioural model for water, sanitation and hygiene interventions (IBM-WASH). BMC Public Health. 2013;13:877.
31. Guerin PJ, Brasher C, Baron E, Mic D, Grimont F, Ryan M, *et al*. Case management of a multidrug-resistant *Shigella dysenteriae* serotype 1 outbreak in a crisis context in Sierra Leone, 1999-2000. Trans R Soc Trop Med Hyg. 2004;98(11):635-43.
32. Kotloff KL, Winickoff JP, Ivanoff B, Clemens JD, Swerdlow DL, Sansonetti PJ, *et al*. Global burden of *Shigella* infections: implications for vaccine development and implementation of control strategies. Bull World Health Organ. 1999;77(8):651-66.
33. Kotloff KL, Nataro JP, Blackwelder WC, Nasrin D, Farag TH, Panchalingam S, *et al*. Burden and aetiology of diarrhoeal disease in infants and young children in developing countries (the Global Enteric Multicenter Study, GEMS): a prospective, case-control study. Lancet. 2013;382(9888):209-22.
34. Baker KS, Dallman TJ, Ashton PM, Day M, Hughes G, Crook PD, *et al*. Intercontinental dissemination of azithromycin-resistant shigellosis through sexual transmission: a cross-sectional study. Lancet Infect Dis. 2015;15(8):913-21.
35. Shah N, DuPont HL, Ramsey DJ. Global etiology of travelers' diarrhea: systematic review from 1973 to the present. Am J Trop Med Hyg. 2009;80(4):609-14.
36. Cohen D, Bassal R, Goren S, Rouach T, Taran D, Schemberg B, *et al*. Recent trends in the epidemiology of shigellosis in Israel. Epidemiol Infect. 2014;142(12):2583-94.
37. Levine MM, DuPont HL, Formal SB, Hornick RB, Takeuchi A, Gangarosa EJ, *et al*. Pathogenesis of *Shigella dysenteriae* 1 (Shiga) dysentery. J Infect Dis. 1973;127(3):261-70.
38. Struelens MJ, Mondal G, Roberts M, Williams PH. Role of bacterial and host factors in the pathogenesis of *Shigella* septicemia. Eur J Clin Microbiol Infect Dis. 1990;9(5):337-44.
39. Miron D, Sochotnick I, Yardeni D, Kawar B, Siplovich L. Surgical complications of shigellosis in children. Pediatr Infect Dis J. 2000;19(9):898-900.
40. Melton-Celsa AR. Shiga Toxin (Stx) Classification, Structure, and Function. Microbiol Spectr. 2014;2(4):EHEC-0024-2013.
41. Flexner S, Sweet JE. The Pathogenesis of Experimental Colitis, and the Relation of Colitis in Animals and Man. J Exp Med. 1906;8(4):514-35.

42. Falkow S, Schneider H, Baron LS, Formal SB. Virulence of *Escherichia-Shigella* Genetic Hybrids for the Guinea Pig. J Bacteriol. 1963;86:1251-8.
43. Kopecko DJ, Washington O, Formal SB. Genetic and physical evidence for plasmid control of *Shigella sonnei* form I cell surface antigen. Infect Immun. 1980;29(1):207-14.
44. Sansonetti P, David M, Toucas M. Correlation between the loss of plasmid DNA and the transition from virulent phase I to avirulent phase II in *Shigella sonnei*. C R Seances Acad Sci D. 1980;290(13):879-82.
45. Sansonetti PJ, Kopecko DJ, Formal SB. Involvement of a plasmid in the invasive ability of *Shigella flexneri*. Infect Immun. 1982;35(3):852-60.
46. Sansonetti PJ, Kopecko DJ, Formal SB. *Shigella sonnei* plasmids: evidence that a large plasmid is necessary for virulence. Infect Immun. 1981;34(1):75-83.
47. Buchrieser C, Glaser P, Rusniok C, Nedjari H, D'Hauteville H, Kunst F, *et al*. The virulence plasmid pWR100 and the repertoire of proteins secreted by the type III secretion apparatus of *Shigella flexneri*. Mol Microbiol. 2000;38(4):760-71.
48. Venkatesan MM, Goldberg MB, Rose DJ, Grotbeck EJ, Burland V, Blattner FR. Complete DNA sequence and analysis of the large virulence plasmid of *Shigella flexneri*. Infect Immun. 2001;69(5):3271-85.
49. Maurelli AT, Baudry B, d'Hauteville H, Hale TL, Sansonetti PJ. Cloning of plasmid DNA sequences involved in invasion of HeLa cells by *Shigella flexneri*. Infect Immun. 1985;49(1):164-71.
50. Cornelis GR. The type III secretion injectisome. Nat Rev Microbiol. 2006;4(11):811-25.
51. Zychlinsky A, Prevost MC, Sansonetti PJ. *Shigella flexneri* induces apoptosis in infected macrophages. Nature. 1992;358(6382):167-9.
52. Ray K, Bobard A, Danckaert A, Paz-Haftel I, Clair C, Ehsani S, *et al*. Tracking the dynamic interplay between bacterial and host factors during pathogen-induced vacuole rupture in real time. Cell Microbiol. 2010;12(4):545-56.
53. Sansonetti PJ, Ryter A, Clerc P, Maurelli AT, Mounier J. Multiplication of *Shigella flexneri* within HeLa cells: lysis of the phagocytic vacuole and plasmid-mediated contact hemolysis. Infection and Immunity. 1986;51(2):461-9.
54. Lan R, Stevenson G, Reeves PR. Comparison of two major forms of the *Shigella* virulence plasmid pINV: positive selection is a major force driving the divergence. Infect Immun. 2003;71(11):6298-306.
55. Dorman CJ. Virulence Gene Regulation in *Shigella*. EcoSal Plus. 2004;1(1).
56. Parsot C, Ageron E, Penno C, Mavris M, Jamoussi K, d'Hauteville H, *et al*. A secreted anti-activator, OspD1, and its chaperone, Spa15, are involved in the control of transcription by the type III secretion apparatus activity in *Shigella flexneri*. Mol Microbiol. 2005;56(6):1627-35.
57. Parsot C. *Shigella* type III secretion effectors: how, where, when, for what purposes? Curr Opin Microbiol. 2009;12(1):110-6.
58. West NP, Sansonetti P, Mounier J, Exley RM, Parsot C, Guadagnini S, *et al*. Optimization of virulence functions through glucosylation of *Shigella* LPS. Science. 2005;307(5713):1313-7.
59. Formal SB, Oaks EV, Olsen RE, Wingfield-Eggleston M, Snoy PJ, Cogan JP. Effect of prior infection with virulent *Shigella flexneri* 2a on the resistance of monkeys to subsequent infection with *Shigella sonnei*. J Infect Dis. 1991;164(3):533-7.
60. Lindberg AA, Karnell A, Weintraub A. The lipopolysaccharide of *Shigella* bacteria as a virulence factor. Rev Infect Dis. 1991;13 Suppl 4:S279-84.
61. Schmidt H, Hensel M. Pathogenicity islands in bacterial pathogenesis. Clin Microbiol Rev. 2004;17(1):14-56.
62. Fasano A, Noriega FR, Liao FM, Wang W, Levine MM. Effect of *Shigella* enterotoxin 1 (ShET1) on rabbit intestine *in vitro* and *in vivo*. Gut. 1997;40(4):505-11.
63. Navarro-Garcia F, Gutierrez-Jimenez J, Garcia-Tovar C, Castro LA, Salazar-Gonzalez H, Cordova V. Pic, an autotransporter protein secreted by different pathogens in the *Enterobacteriaceae* family, is a potent mucus secretagogue. Infect Immun. 2010;78(10):4101-9.

64. Al-Hasani K, Navarro-Garcia F, Huerta J, Sakellaris H, Adler B. The immunogenic SigA enterotoxin of *Shigella flexneri* 2a binds to HEp-2 cells and induces fodrin redistribution in intoxicated epithelial cells. PLoS One. 2009;4(12):e8223.
65. Vokes SA, Reeves SA, Torres AG, Payne SM. The aerobactin iron transport system genes in *Shigella flexneri* are present within a pathogenicity island. Mol Microbiol. 1999;33(1):63-73.
66. Ingersoll MA, Zychlinsky A. ShiA abrogates the innate T-cell response to *Shigella flexneri* infection. Infect Immun. 2006;74(4):2317-27.
67. Purdy GE, Payne SM. The SHI-3 iron transport island of *Shigella boydii* 0-1392 carries the genes for aerobactin synthesis and transport. J Bacteriol. 2001;183(14):4176-82.
68. Luck SN, Turner SA, Rajakumar K, Sakellaris H, Adler B. Ferric dicitrate transport system (Fec) of *Shigella flexneri 2a* YSH6000 is encoded on a novel pathogenicity island carrying multiple antibiotic resistance genes. Infect Immun. 2001;69(10):6012-21.
69. Maurelli AT, Blackmon B, Curtiss R, 3rd. Temperature-dependent expression of virulence genes in *Shigella* species. Infect Immun. 1984;43(1):195-201.
70. Sereny B. Experimental *Shigella* keratoconjunctivitis; a preliminary report. Acta Microbiol Acad Sci Hung. 1955;2(3):293-6.
71. Tobe T, Nagai S, Okada N, Adler B, Yoshikawa M, Sasakawa C. Temperature-regulated expression of invasion genes in *Shigella flexneri* is controlled through the transcriptional activation of the *virB* gene on the large plasmid. Mol Microbiol. 1991;5(4):887-93.
72. Dorman CJ, McKenna S, Beloin C. Regulation of virulence gene expression in *Shigella flexneri*, a facultative intracellular pathogen. Int J Med Microbiol. 2001;291(2):89-96.
73. Falconi M, Colonna B, Prosseda G, Micheli G, Gualerzi CO. Thermoregulation of *Shigella* and *Escherichia coli* EIEC pathogenicity. A temperature-dependent structural transition of DNA modulates accessibility of *virF* promoter to transcriptional repressor H-NS. EMBO J. 1998;17(23):7033-43.
74. Porter ME, Dorman CJ. A role for H-NS in the thermo-osmotic regulation of virulence gene expression in *Shigella flexneri*. J Bacteriol. 1994;176(13):4187-91.
75. Tobe T, Yoshikawa M, Mizuno T, Sasakawa C. Transcriptional control of the invasion regulatory gene *virB* of *Shigella flexneri*: activation by *virF* and repression by H-NS. J Bacteriol. 1993;175(19):6142-9.
76. Di Martino ML, Falconi M, Micheli G, Colonna B, Prosseda G. The Multifaceted Activity of the VirF Regulatory Protein in the *Shigella* Lifestyle. Front Mol Biosci. 2016;3:61.
77. Mitobe J, Morita-Ishihara T, Ishihama A, Watanabe H. Involvement of RNA-binding protein Hfq in the osmotic-response regulation of *invE* gene expression in *Shigella sonnei*. BMC Microbiol. 2009;9:110.
78. Nakayama S, Watanabe H. Identification of *cpxR* as a positive regulator essential for expression of the *Shigella sonnei virF* gene. J Bacteriol. 1998;180(14):3522-8.
79. Pilla G, McVicker G, Tang CM. Genetic plasticity of the *Shigella* virulence plasmid is mediated by intra- and inter-molecular events between insertion sequences. PLoS Genet. 2017;13(9):e1007014.
80. Marteyn B, West NP, Browning DF, Cole JA, Shaw JG, Palm F, *et al*. Modulation of *Shigella* virulence in response to available oxygen *in vivo*. Nature. 2010;465(7296):355-8.
81. Campbell-Valois FX, Schnupf P, Nigro G, Sachse M, Sansonetti PJ, Parsot C. A fluorescent reporter reveals on/off regulation of the *Shigella* type III secretion apparatus during entry and cell-to-cell spread. Cell Host Microbe. 2014;15(2):177-89.
82. Battesti A, Majdalani N, Gottesman S. The RpoS-mediated general stress response in *Escherichia coli*. Annu Rev Microbiol. 2011;65:189-213.
83. Que JU, Casey SW, Hentges DJ. Factors responsible for increased susceptibility of mice to intestinal colonization after treatment with streptomycin. Infect Immun. 1986;53(1):116-23.
84. Anderson MC, Vonaesch P, Saffarian A, Marteyn BS, Sansonetti PJ. *Shigella sonnei* Encodes a Functional T6SS Used for Interbacterial Competition and Niche Occupancy. Cell Host Microbe. 2017;21(6):769-76 e3.

85. Johansson ME, Larsson JM, Hansson GC. The two mucus layers of colon are organized by the MUC2 mucin, whereas the outer layer is a legislator of host-microbial interactions. Proc Natl Acad Sci U S A. 2011;108 Suppl 1:4659-65.
86. Haider K, Hossain A, Wanke C, Qadri F, Ali S, Nahar S. Production of mucinase and neuraminidase and binding of *Shigella* to intestinal mucin. J Diarrhoeal Dis Res. 1993;11(2):88-92.
87. Sperandio B, Regnault B, Guo J, Zhang Z, Stanley SL, Jr., Sansonetti PJ, *et al*. Virulent *Shigella flexneri* subverts the host innate immune response through manipulation of antimicrobial peptide gene expression. J Exp Med. 2008;205(5):1121-32.
88. Sasakawa C. A new paradigm of bacteria-gut interplay brought through the study of Shigella. Proc Jpn Acad Ser B Phys Biol Sci. 2010;86(3):229-43.
89. Mounier J, Vasselon T, Hellio R, Lesourd M, Sansonetti PJ. *Shigella flexneri* enters human colonic Caco-2 epithelial cells through the basolateral pole. Infection and Immunity. 1992;60(1):237-48.
90. Sansonetti PJ, Arondel J, Cantey JR, Prevost MC, Huerre M. Infection of rabbit Peyer's patches by *Shigella flexneri*: effect of adhesive or invasive bacterial phenotypes on follicle-associated epithelium. Infect Immun. 1996;64(7):2752-64.
91. Ashida H, Ogawa M, Mimuro H, Kobayashi T, Sanada T, Sasakawa C. *Shigella* are versatile mucosal pathogens that circumvent the host innate immune system. Curr Opin Immunol. 2011;23(4):448-55.
92. Blocker A, Gounon P, Larquet E, Niebuhr K, Cabiaux V, Parsot C, *et al*. The tripartite type III secreton of *Shigella flexneri* inserts IpaB and IpaC into host membranes. J Cell Biol. 1999;147(3):683-93.
93. Senerovic L, Tsunoda SP, Goosmann C, Brinkmann V, Zychlinsky A, Meissner F, *et al*. Spontaneous formation of IpaB ion channels in host cell membranes reveals how *Shigella* induces pyroptosis in macrophages. Cell Death Dis. 2012;3:e384.
94. Suzuki T, Franchi L, Toma C, Ashida H, Ogawa M, Yoshikawa Y, *et al*. Differential regulation of caspase-1 activation, pyroptosis, and autophagy *via* Ipaf and ASC in *Shigella*-infected macrophages. PLoS Pathog. 2007;3(8):e111.
95. Suzuki T, Nakanishi K, Tsutsui H, Iwai H, Akira S, Inohara N, *et al*. A novel caspase-1/toll-like receptor 4-independent pathway of cell death induced by cytosolic *Shigella* in infected macrophages. J Biol Chem. 2005;280(14):14042-50.
96. Ashida H, Ogawa M, Kim M, Suzuki S, Sanada T, Punginelli C, *et al*. *Shigella* deploy multiple countermeasures against host innate immune responses. Curr Opin Microbiol. 2011;14(1):16-23.
97. Sansonetti PJ, Phalipon A, Arondel J, Thirumalai K, Banerjee S, Akira S, *et al*. Caspase-1 activation of IL-1β and IL-18 are essential for *Shigella flexneri*-induced inflammation. Immunity. 2000;12(5):581-90.
98. Kohler H, Rodrigues SP, McCormick BA. *Shigella flexneri* Interactions with the Basolateral Membrane Domain of Polarized Model Intestinal Epithelium: Role of Lipopolysaccharide in Cell Invasion and in Activation of the Mitogen-Activated Protein Kinase ERK. Infect Immun. 2002;70(3):1150-8.
99. Brotcke Zumsteg A, Goosmann C, Brinkmann V, Morona R, Zychlinsky A. IcsA is a *Shigella flexneri* adhesin regulated by the type III secretion system and required for pathogenesis. Cell Host Microbe. 2014;15(4):435-45.
100. Lafont F, Tran Van Nhieu G, Hanada K, Sansonetti P, van der Goot FG. Initial steps of *Shigella* infection depend on the cholesterol/sphingolipid raft-mediated CD44-IpaB interaction. EMBO J. 2002;21(17):4449-57.
101. Murillo I, Martinez-Argudo I, Blocker AJ. Genetic Dissection of the Signaling Cascade that Controls Activation of the *Shigella* Type III Secretion System from the Needle Tip. Sci Rep. 2016;6:27649.
102. Tran Van Nhieu G, Caron E, Hall A, Sansonetti PJ. IpaC induces actin polymerization and filopodia formation during *Shigella* entry into epithelial cells. EMBO J. 1999;18(12):3249-62.

103. Mounier J, Popoff MR, Enninga J, Frame MC, Sansonetti PJ, Van Nhieu GT. The IpaC carboxyterminal effector domain mediates Src-dependent actin polymerization during *Shigella* invasion of epithelial cells. PLoS Pathog. 2009;5(1):e1000271.
104. Niebuhr K, Giuriato S, Pedron T, Philpott DJ, Gaits F, Sable J, *et al*. Conversion of PtdIns(4,5)P(2) into PtdIns(5)P by the *S. flexneri* effector IpgD reorganizes host cell morphology. EMBO J. 2002;21(19):5069-78.
105. Garza-Mayers AC, Miller KA, Russo BC, Nagda DV, Goldberg MB. *Shigella flexneri* regulation of ARF6 activation during bacterial entry *0* an IpgD-mediated positive feedback loop. MBio. 2015;6(2):e02584.
106. Tran Van Nhieu G, Ben-Ze'ev A, Sansonetti PJ. Modulation of bacterial entry into epithelial cells by association between vinculin and the *Shigella* IpaA invasin. EMBO J. 1997;16(10):2717-29.
107. Bourdet-Sicard R, Rudiger M, Jockusch BM, Gounon P, Sansonetti PJ, Nhieu GT. Binding of the *Shigella* protein IpaA to vinculin induces F-actin depolymerization. EMBO J. 1999;18(21):5853-62.
108. Weiner A, Mellouk N, Lopez-Montero N, Chang YY, Souque C, Schmitt C, *et al*. Macropinosomes are Key Players in Early Shigella Invasion and Vacuolar Escape in Epithelial Cells. PLoS Pathog. 2016;12(5):e1005602.
109. Mellouk N, Weiner A, Aulner N, Schmitt C, Elbaum M, Shorte SL, *et al*. *Shigella* subverts the host recycling compartment to rupture its vacuole. Cell Host Microbe. 2014;16(4):517-30.
110. Campbell-Valois FX, Sachse M, Sansonetti PJ, Parsot C. Escape of Actively Secreting *Shigella flexneri* from ATG8/LC3-Positive Vacuoles Formed during Cell-To-Cell Spread Is Facilitated by IcsB and VirA. MBio. 2015;6(3):e02567-14.
111. Kentner D, Martano G, Callon M, Chiquet P, Brodmann M, Burton O, *et al*. *Shigella* reroutes host cell central metabolism to obtain high-flux nutrient supply for vigorous intracellular growth. Proc Natl Acad Sci U S A. 2014;111(27):9929-34.
112. Makino S, Sasakawa C, Kamata K, Kurata T, Yoshikawa M. A genetic determinant required for continuous reinfection of adjacent cells on large plasmid in *S. flexneri* 2a. Cell. 1986;46(4):551-5.
113. Bernardini ML, Mounier J, d'Hauteville H, Coquis-Rondon M, Sansonetti PJ. Identification of *icsA*, a plasmid locus of *Shigella flexneri* that governs bacterial intra- and intercellular spread through interaction with F-actin. Proc Natl Acad Sci U S A. 1989;86(10):3867-71.
114. Sansonetti PJ, Arondel J, Fontaine A, d'Hauteville H, Bernardini ML. OmpB (osmo-regulation) and *0.* (cell-to-cell spread) mutants of *Shigella flexneri*: vaccine candidates and probes to study the pathogenesis of shigellosis. Vaccine. 1991;9(6):416-22.
115. Egile C, Loisel TP, Laurent V, Li R, Pantaloni D, Sansonetti PJ, *et al*. Activation of the CDC42 effector N-WASP by the *Shigella flexneri* IcsA protein promotes actin nucleation by Arp2/3 complex and bacterial actin-based motility. J Cell Biol. 1999;146(6):1319-32.
116. Carpenter CD, Cooley BJ, Needham BD, Fisher CR, Trent MS, Gordon V, *et al*. The Vps/VacJ ABC transporter is required for intercellular spread of *Shigella flexneri*. Infection and Immunity. 2014;82(2):660-9.
117. Ogawa M, Yoshimori T, Suzuki T, Sagara H, Mizushima N, Sasakawa C. Escape of intracellular *Shigella* from autophagy. Science. 2005;307(5710):727-31.
118. Mostowy S, Sancho-Shimizu V, Hamon MA, Simeone R, Brosch R, Johansen T, *et al*. p62 and NDP52 proteins target intracytosolic *Shigella* and *Listeria* to different autophagy pathways. J Biol Chem. 2011;286(30):26987-95.
119. Baxt LA, Goldberg MB. Host and bacterial proteins that repress recruitment of LC3 to *Shigella* early during infection. PLoS One. 2014;9(4):e94653.
120. Dong N, Zhu Y, Lu Q, Hu L, Zheng Y, Shao F. Structurally distinct bacterial TBC-like GAPs link Arf GTPase to Rab1 inactivation to counteract host defenses. Cell. 2012;150(5):1029-41.

121. Burnaevskiy N, Peng T, Reddick LE, Hang HC, Alto NM. Myristoylome profiling reveals a concerted mechanism of ARF GTPase deacylation by the bacterial protease IpaJ. Mol Cell. 2015;58(1):110-22.
122. Ashida H, Mimuro H, Sasakawa C. *Shigella* manipulates host immune responses by delivering effector proteins with specific roles. Front Immunol. 2015;6:219.
123. Nataro JP, Seriwatana J, Fasano A, Maneval DR, Guers LD, Noriega F, *et al*. Identification and cloning of a novel plasmid-encoded enterotoxin of enteroinvasive *Escherichia coli* and *Shigella* strains. Infect Immun. 1995;63(12):4721-8.
124. Farfan MJ, Toro CS, Barry EM, Nataro JP. *Shigella* enterotoxin-2 is a type III effector that participates in *Shigella*-induced interleukin 8 secretion by epithelial cells. FEMS Immunol Med Microbiol. 2011;61(3):332-9.
125. Alberts BJ, A;Lewis,J;Raff,M;Roberts,K;Walter,P editor. Molecular biology of the Cell 5th ed. New York Garland Science; 2008.
126. Eisenreich W, Dandekar T, Heesemann J, Goebel W. Carbon metabolism of intracellular bacterial pathogens and possible links to virulence. Nat Rev Microbiol. 2010;8(6):401-12.
127. Lucchini S, Liu H, Jin Q, Hinton JCD, Yu J. Transcriptional adaptation of *Shigella flexneri* during infection of macrophages and epithelial cells: Insights into the strategies of a cytosolic bacterial pathogen. Infection and Immunity. 2005;73(1):88-102.
128. Pieper R, Fisher CR, Suh MJ, Huang ST, Parmar P, Payne SM. Analysis of the proteome of intracellular *Shigella flexneri* reveals pathways important for intracellular growth. Infect Immun. 2013;81(12):4635-48.
129. Helaine S, Thompson JA, Watson KG, Liu M, Boyle C, Holden DW. Dynamics of intracellular bacterial replication at the single cell level. Proc Natl Acad Sci U S A. 2010;107(8):3746-51.
130. Claudi B, Sprote P, Chirkova A, Personnic N, Zankl J, Schurmann N, *et al.* Phenotypic variation of *Salmonella* in host tissues delays eradication by antimicrobial chemotherapy. Cell. 2014;158(4):722-33.
131. Manina G, Dhar N, McKinney JD. Stress and host immunity amplify *Mycobacterium tuberculosis* phenotypic heterogeneity and induce nongrowing metabolically active forms. Cell Host Microbe. 2015;17(1):32-46.
132. Terskikh A, Fradkov A, Ermakova G, Zaraisky A, Tan P, Kajava AV, *et al*. "Fluorescent timer": protein that changes color with time. Science. 2000;290(5496):1585-8.
133. Lan R, Alles MC, Donohoe K, Martinez MB, Reeves PR. Molecular evolutionary relationships of enteroinvasive *Escherichia coli* and *Shigella* spp. Infect Immun. 2004;72(9):5080-8.
134. Schuch R, Maurelli AT. Virulence plasmid instability in *Shigella flexneri* 2a is induced by virulence gene expression. Infect Immun. 1997;65(9):3686-92.
135. Pilla G, Tang CM. Going around in circles: virulence plasmids in enteric pathogens. Nat Rev Microbiol. 2018.
136. Nordstrom K. Plasmid R1--replication and its control. Plasmid. 2006;55(1):1-26.
137. Brantl S. Plasmid Replication Control by Antisense RNAs. Phillips BEFaGJ, editor. Washington,DC: ASM press; 2004.
138. Ebersbach G, Gerdes K. Plasmid segregation mechanisms. Annu Rev Genet. 2005;39:453-79.
139. Pandey DP, Gerdes K. Toxin-antitoxin loci are highly abundant in free-living but lost from host-associated prokaryotes. Nucleic Acids Res. 2005;33(3):966-76.
140. Harms A, Brodersen DE, Mitarai N, Gerdes K. Toxins, Targets, and Triggers: An Overview of Toxin-Antitoxin Biology. Mol Cell. 2018.
141. Jaffe A, Ogura T, Hiraga S. Effects of the ccd function of the F plasmid on bacterial growth. J Bacteriol. 1985;163(3):841-9.
142. Gotfredsen M, Gerdes K. The Escherichia coli *relBE* genes belong to a new toxin-antitoxin gene family. Mol Microbiol. 1998;29(4):1065-76.
143. Gronlund H, Gerdes K. Toxin-antitoxin systems homologous with *relBE* of Escherichia coli plasmid P307 are ubiquitous in prokaryotes. J Mol Biol. 1999;285(4):1401-15.

144. Christensen-Dalsgaard M, Gerdes K. Two *higBA* loci in the Vibrio cholerae superintegron encode mRNA cleaving enzymes and can stabilize plasmids. Mol Microbiol. 2006;62(2):397-411.
145. Lehnherr H, Maguin E, Jafri S, Yarmolinsky MB. Plasmid addiction genes of bacteriophage P1: *doc*, which causes cell death on curing of prophage, and *phd*, which prevents host death when prophage is retained. J Mol Biol. 1993;233(3):414-28.
146. Szekeres S, Dauti M, Wilde C, Mazel D, Rowe-Magnus DA. Chromosomal toxin-antitoxin loci can diminish large-scale genome reductions in the absence of selection. Mol Microbiol. 2007;63(6):1588-605.
147. Lee KY, Lee BJ. Structure, Biology, and Therapeutic Application of Toxin-Antitoxin Systems in Pathogenic Bacteria. Toxins (Basel). 2016;8(10).
148. Gerdes K, Rasmussen PB, Molin S. Unique type of plasmid maintenance function: postsegregational killing of plasmid-free cells. Proc Natl Acad Sci U S A. 1986;83(10):3116-20.
149. Thisted T, Gerdes K. Mechanism of post-segregational killing by the *hok*/*sok* system of plasmid R1. Sok antisense RNA regulates *hok* gene expression indirectly through the overlapping mok gene. J Mol Biol. 1992;223(1):41-54.
150. Boggild A, Sofos N, Andersen KR, Feddersen A, Easter AD, Passmore LA, *et al*. The crystal structure of the intact E. coli RelBE toxin-antitoxin complex provides the structural basis for conditional cooperativity. Structure. 2012;20(10):1641-8.
151. Dienemann C, Boggild A, Winther KS, Gerdes K, Brodersen DE. Crystal structure of the VapBC toxin-antitoxin complex from *Shigella flexneri* reveals a hetero-octameric DNA-binding assembly. J Mol Biol. 2011;414(5):713-22.
152. De Jonge N, Garcia-Pino A, Buts L, Haesaerts S, Charlier D, Zangger K, *et al*. Rejuvenation of CcdB-poisoned gyrase by an intrinsically disordered protein domain. Mol Cell. 2009;35(2):154-63.
153. Afif H, Allali N, Couturier M, Van Melderen L. The ratio between CcdA and CcdB modulates the transcriptional repression of the ccd poison-antidote system. Mol Microbiol. 2001;41(1):73-82.
154. Goeders N, Van Melderen L. Toxin-antitoxin systems as multilevel interaction systems. Toxins (Basel). 2014;6(1):304-24.
155. Ogura T, Hiraga S. Mini-F plasmid genes that couple host cell division to plasmid proliferation. Proc Natl Acad Sci U S A. 1983;80(15):4784-8.
156. Fineran PC, Blower TR, Foulds IJ, Humphreys DP, Lilley KS, Salmond GP. The phage abortive infection system, ToxIN, functions as a protein-RNA toxin-antitoxin pair. Proc Natl Acad Sci U S A. 2009;106(3):894-9.
157. Short FL, Pei XY, Blower TR, Ong SL, Fineran PC, Luisi BF, *et al*. Selectivity and self-assembly in the control of a bacterial toxin by an antitoxic noncoding RNA pseudoknot. Proc Natl Acad Sci U S A. 2013;110(3):E241-9.
158. Masuda H, Tan Q, Awano N, Wu KP, Inouye M. YeeU enhances the bundling of cytoskeletal polymers of MreB and FtsZ, antagonizing the CbtA (YeeV) toxicity in *Escherichia coli*. Mol Microbiol. 2012;84(5):979-89.
159. Dy RL, Przybilski R, Semeijn K, Salmond GP, Fineran PC. A widespread bacteriophage abortive infection system functions through a Type IV toxin-antitoxin mechanism. Nucleic Acids Res. 2014;42(7):4590-605.
160. Wang X, Lord DM, Cheng HY, Osbourne DO, Hong SH, Sanchez-Torres V, *et al*. A new type V toxin-antitoxin system where mRNA for toxin GhoT is cleaved by antitoxin GhoS. Nat Chem Biol. 2012;8(10):855-61.
161. Aakre CD, Phung TN, Huang D, Laub MT. A bacterial toxin inhibits DNA replication elongation through a direct interaction with the beta sliding clamp. Mol Cell. 2013;52(5):617-28.
162. Jankevicius G, Ariza A, Ahel M, Ahel I. The Toxin-Antitoxin System DarTG Catalyzes Reversible ADP-Ribosylation of DNA. Mol Cell. 2016;64(6):1109-16.
163. McVicker G, Tang CM. Deletion of toxin–antitoxin systems in the evolution of *Shigella sonnei* as a host-adapted pathogen. Nature Microbiology. 2016;2:16204.

164. Mills JA, Venkatesan MM, Baron LS, Buysse JM. Spontaneous insertion of an IS1-like element into the virF gene is responsible for avirulence in opaque colonial variants of *Shigella flexneri* 2a. Infect Immun. 1992;60(1):175-82.
165. Payne SM, Finkelstein RA. Detection and differentiation of iron-responsive avirulent mutants on Congo red agar. Infect Immun. 1977;18(1):94-8.
166. Maurelli AT, Blackmon B, Curtiss R, 3rd. Loss of pigmentation in *Shigella flexneri* 2a is correlated with loss of virulence and virulence-associated plasmid. Infect Immun. 1984;43(1):397-401.
167. Gerdes K, Christensen SK, Lobner-Olesen A. Prokaryotic toxin-antitoxin stress response loci. Nat Rev Microbiol. 2005;3(5):371-82.
168. Tam JE, Kline BC. The F plasmid *ccd* autorepressor is a complex of CcdA and CcdB proteins. Mol Gen Genet. 1989;219(1-2):26-32.
169. Bernard P, Couturier M. The 41 carboxy-terminal residues of the miniF plasmid CcdA protein are sufficient to antagonize the killer activity of the CcdB protein. Mol Gen Genet. 1991;226(1-2):297-304.
170. Van Melderen L, Bernard P, Couturier M. Lon-dependent proteolysis of CcdA is the key control for activation of CcdB in plasmid-free segregant bacteria. Mol Microbiol. 1994;11(6):1151-7.
171. Madl T, Van Melderen L, Mine N, Respondek M, Oberer M, Keller W, *et al*. Structural basis for nucleic acid and toxin recognition of the bacterial antitoxin CcdA. J Mol Biol. 2006;364(2):170-85.
172. Bernard P, Couturier M. Cell killing by the F plasmid CcdB protein involves poisoning of DNA-topoisomerase II complexes. J Mol Biol. 1992;226(3):735-45.
173. Bernard P, Kezdy KE, Van Melderen L, Steyaert J, Wyns L, Pato ML, *et al*. The F plasmid CcdB protein induces efficient ATP-dependent DNA cleavage by gyrase. J Mol Biol. 1993;234(3):534-41.
174. Dao-Thi MH, Van Melderen L, De Genst E, Afif H, Buts L, Wyns L, *et al*. Molecular basis of gyrase poisoning by the addiction toxin CcdB. J Mol Biol. 2005;348(5):1091-102.
175. Arcus VL, Rainey PB, Turner SJ. The PIN-domain toxin-antitoxin array in mycobacteria. Trends Microbiol. 2005;13(8):360-5.
176. Pullinger GD, Lax AJ. A *Salmonella* dublin virulence plasmid locus that affects bacterial growth under nutrient-limited conditions. Mol Microbiol. 1992;6(12):1631-43.
177. Lobato-Marquez D, Molina-Garcia L, Moreno-Cordoba I, Garcia-Del Portillo F, Diaz-Orejas R. Stabilization of the Virulence Plasmid pSLT of *Salmonella Typhimurium* by Three Maintenance Systems and Its Evaluation by Using a New Stability Test. Front Mol Biosci. 2016;3:66.
178. Lobato-Márquez D, Moreno-Córdoba I, Figueroa V, Díaz-Orejas R, García-del Portillo F. Distinct type I and type II toxin-antitoxin modules control *Salmonella* lifestyle inside eukaryotic cells. Scientific Reports. 2015;5:9374.
179. Sayeed S, Reaves L, Radnedge L, Austin S. The stability region of the large virulence plasmid of *Shigella flexneri* encodes an efficient postsegregational killing system. J Bacteriol. 2000;182(9):2416-21.
180. Sayeed S, Brendler T, Davis M, Reaves L, Austin S. Surprising dependence on postsegregational killing of host cells for maintenance of the large virulence plasmid of *Shigella flexneri*. J Bacteriol. 2005;187(8):2768-73.
181. Winther KS, Gerdes K. Regulation of enteric *vapBC* transcription: induction by VapC toxin dimer-breaking. Nucleic Acids Res. 2012;40(10):4347-57.
182. Winther KS, Gerdes K. Enteric virulence associated protein VapC inhibits translation by cleavage of initiator tRNA. Proc Natl Acad Sci U S A. 2011;108(18):7403-7.
183. Arcus VL, Backbro K, Roos A, Daniel EL, Baker EN. Distant structural homology leads to the functional characterization of an archaeal PIN domain as an exonuclease. J Biol Chem. 2004;279(16):16471-8.
184. Arcus VL, McKenzie JL, Robson J, Cook GM. The PIN-domain ribonucleases and the prokaryotic VapBC toxin-antitoxin array. Protein Eng Des Sel. 2011;24(1-2):33-40.

185. Bendtsen KL, Xu K, Luckmann M, Winther KS, Shah SA, Pedersen CNS, *et al*. Toxin inhibition in *C. crescentus* VapBC1 is mediated by a flexible pseudo-palindromic protein motif and modulated by DNA binding. Nucleic Acids Res. 2017;45(5):2875-86.
186. Jurenas D, Garcia-Pino A, Van Melderen L. Novel toxins from type II toxin-antitoxin systems with acetyltransferase activity. Plasmid. 2017;93:30-5.
187. Cheverton AM, Gollan B, Przydacz M, Wong CT, Mylona A, Hare SA, *et al*. A *Salmonella* Toxin Promotes Persister Formation through Acetylation of tRNA. Mol Cell. 2016;63(1):86-96.
188. Helaine S, Cheverton AM, Watson KG, Faure LM, Matthews SA, Holden DW. Internalization of *Salmonella* by macrophages induces formation of nonreplicating persisters. Science. 2014;343(6167):204-8.
189. VanDrisse CM, Parks AR, Escalante-Semerena JC. A Toxin Involved in *Salmonella* Persistence Regulates Its Activity by Acetylating Its Cognate Antitoxin, a Modification Reversed by CobB Sirtuin Deacetylase. MBio. 2017;8(3).
190. Jurenas D, Chatterjee S, Konijnenberg A, Sobott F, Droogmans L, Garcia-Pino A, *et al*. AtaT blocks translation initiation by N-acetylation of the initiator tRNA(fMet). Nat Chem Biol. 2017;13(6):640-6.
191. Qian H, Yao Q, Tai C, Deng Z, Gan J, Ou HY. Identification and characterization of acetyltransferase-type toxin-antitoxin locus in *Klebsiella pneumoniae*. Mol Microbiol. 2018;108(4):336-49.
192. Bilous PT, Weiner JH. Dimethyl sulfoxide reductase activity by anaerobically grown *Escherichia coli* HB101. J Bacteriol. 1985;162(3):1151-5.
193. Kurylo CM, Alexander N, Dass RA, Parks MM, Altman RA, Vincent CT, *et al*. Genome Sequence and Analysis of *Escherichia coli* MRE600, a Colicinogenic, Nonmotile Strain that Lacks RNase I and the Type I Methyltransferase, EcoKI. Genome Biol Evol. 2016;8(3):742-52.
194. Hanahan D. Studies on transformation of *Escherichia coli* with plasmids. J Mol Biol. 1983;166(4):557-80.
195. Simon R, Priefer U, Puhler A. A Broad Host Range Mobilization System for *In vivo* Genetic-Engineering - Transposon Mutagenesis in Gram-Negative Bacteria. Bio-Technol. 1983;1(9):784-91.
196. Ferrieres L, Hemery G, Nham T, Guerout AM, Mazel D, Beloin C, *et al*. Silent mischief: bacteriophage Mu insertions contaminate products of *Escherichia coli* random mutagenesis performed using suicidal transposon delivery plasmids mobilized by broad-host-range RP4 conjugative machinery. J Bacteriol. 2010;192(24):6418-27.
197. Herrero M, de Lorenzo V, Timmis KN. Transposon vectors containing non-antibiotic resistance selection markers for cloning and stable chromosomal insertion of foreign genes in gram-negative bacteria. J Bacteriol. 1990;172(11):6557-67.
198. Norrander J, Kempe T, Messing J. Construction of improved M13 vectors using oligodeoxynucleotide-directed mutagenesis. Gene. 1983;26(1):101-6.
199. Guzman LM, Belin D, Carson MJ, Beckwith J. Tight regulation, modulation, and high-level expression by vectors containing the arabinose PBAD promoter. J Bacteriol. 1995;177(14):4121-30.
200. Kaniga K, Delor I, Cornelis GR. A wide-host-range suicide vector for improving reverse genetics in gram-negative bacteria: inactivation of the *blaA* gene of *Yersinia enterocolitica*. Gene. 1991;109(1):137-41.
201. Tsuchiya S, Yamabe M, Yamaguchi Y, Kobayashi Y, Konno T, Tada K. Establishment and characterization of a human acute monocytic leukemia cell line (THP-1). Int J Cancer. 1980;26(2):171-6.
202. Datsenko KA, Wanner BL. One-step inactivation of chromosomal genes in *Escherichia coli* K-12 using PCR products. Proc Natl Acad Sci U S A. 2000;97(12):6640-5.
203. Ramadoss NS, Zhou X, Keiler KC. tmRNA is essential in *Shigella flexneri*. PLoS One. 2013;8(2):e57537.
204. Ray K, Marteyn B, Sansonetti PJ, Tang CM. Life on the inside: the intracellular lifestyle of cytosolic bacteria. Nat Rev Microbiol. 2009;7(5):333-40.

205. Carayol N, Tran Van Nhieu G. The inside story of *Shigella* invasion of intestinal epithelial cells. Cold Spring Harb Perspect Med. 2013;3(10):a016717.
206. Mouton JM, Helaine S, Holden DW, Sampson SL. Elucidating population-wide mycobacterial replication dynamics at the single-cell level. Microbiology. 2016;162(6):966-78.
207. Bumann D. Heterogeneous host-pathogen encounters: act locally, think globally. Cell Host Microbe. 2015;17(1):13-9.
208. Heman-Ackah SM. Comparison of tetracycline action on *Staphylococcus aureus* and *Escherichia coli* by microbial kinetics. Antimicrob Agents Chemother. 1976;10(2):223-8.
209. Kohanski MA, Dwyer DJ, Collins JJ. How antibiotics kill bacteria: from targets to networks. Nat Rev Microbiol. 2010;8(6):423-35.
210. Burns JL, Jonas M, Chi EY, Clark DK, Berger A, Griffith A. Invasion of respiratory epithelial cells by *Burkholderia (Pseudomonas) cepacia*. Infect Immun. 1996;64(10):4054-9.
211. Renard C, Vanderhaeghe HJ, Claes PJ, Zenebergh A, Tulkens PM. Influence of conversion of penicillin G into a basic derivative on its accumulation and subcellular localization in cultured macrophages. Antimicrob Agents Chemother. 1987;31(3):410-6.
212. Tomasz A. The mechanism of the irreversible antimicrobial effects of penicillins: how the beta-lactam antibiotics kill and lyse bacteria. Annu Rev Microbiol. 1979;33:113-37.
213. Jacoby GH, Young KD. Cell cycle-independent lysis of *Escherichia coli* by cefsulodin, an inhibitor of penicillin-binding proteins 1a and 1b. J Bacteriol. 1991;173(1):1-5.
214. Jakobs S, Subramaniam V, Schonle A, Jovin TM, Hell SW. EFGP and DsRed expressing cultures of *Escherichia coli* imaged by confocal, two-photon and fluorescence lifetime microscopy. FEBS Lett. 2000;479(3):131-5.
215. Sorensen M, Lippuner C, Kaiser T, Misslitz A, Aebischer T, Bumann D. Rapidly maturing red fluorescent protein variants with strongly enhanced brightness in bacteria. FEBS Lett. 2003;552(2-3):110-4.
216. Sniegowski JA, Lappe JW, Patel HN, Huffman HA, Wachter RM. Base catalysis of chromophore formation in Arg96 and Glu222 variants of green fluorescent protein. J Biol Chem. 2005;280(28):26248-55.
217. Hale TL, Formal SB. Protein synthesis in HeLa or Henle 407 cells infected with *Shigella dysenteriae* 1, *Shigella flexneri* 2a, or *Salmonella typhimurium* W118. Infect Immun. 1981;32(1):137-44.
218. Figueira R, Watson KG, Holden DW, Helaine S. Identification of *salmonella* pathogenicity island-2 type III secretion system effectors involved in intramacrophage replication of *S. enterica serovar typhimurium*: implications for rational vaccine design. MBio. 2013;4(2):e00065.
219. Hebisch E, Knebel J, Landsberg J, Frey E, Leisner M. High variation of fluorescence protein maturation times in closely related *Escherichia coli* strains. PLoS One. 2013;8(10):e75991.
220. Shaner NC, Campbell RE, Steinbach PA, Giepmans BN, Palmer AE, Tsien RY. Improved monomeric red, orange and yellow fluorescent proteins derived from *Discosoma* spp. red fluorescent protein. Nat Biotechnol. 2004;22(12):1567-72.
221. Fauvart JMaM. Quantification of Persistence. Walker JM, editor. New York: Springer
222. Ogura T, Hiraga S. Partition mechanism of F plasmid: two plasmid gene-encoded products and a cis-acting region are involved in partition. Cell. 1983;32(2):351-60.
223. Evans SS, Repasky EA, Fisher DT. Fever and the thermal regulation of immunity: the immune system feels the heat. Nat Rev Immunol. 2015;15(6):335-49.
224. Abu Kwaik Y, Bumann D. Host Delivery of Favorite Meals for Intracellular Pathogens. PLoS Pathog. 2015;11(6):e1004866.
225. Christensen SK, Mikkelsen M, Pedersen K, Gerdes K. RelE, a global inhibitor of translation, is activated during nutritional stress. Proc Natl Acad Sci U S A. 2001;98(25):14328-33.
226. Miller TL, Wolin MJ. Pathways of acetate, propionate, and butyrate formation by the human fecal microbial flora. Appl Environ Microbiol. 1996;62(5):1589-92.
227. Di Russo Case E, Samuel JE. Contrasting Lifestyles Within the Host Cell. Microbiol Spectr. 2016;4(1).

228. Niu C, Yang J, Liu H, Cui Y, Xu H, Wang R, *et al*. Role of the virulence plasmid in acid resistance of *Shigella flexneri*. Sci Rep. 2017;7:46465.
229. Bosshart H, Heinzelmann M. THP-1 cells as a model for human monocytes. Ann Transl Med. 2016;4(21):438.
230. Daigneault M, Preston JA, Marriott HM, Whyte MK, Dockrell DH. The identification of markers of macrophage differentiation in PMA-stimulated THP-1 cells and monocyte-derived macrophages. PLoS One. 2010;5(1):e8668.
231. Magnusson LU, Farewell A, Nystrom T. ppGpp: a global regulator in *Escherichia coli*. Trends Microbiol. 2005;13(5):236-42.
232. Nagase T, Ishii S, Imamoto F. Differential transcriptional control of the two tRNA(fMet) genes of *Escherichia coli* K-12. Gene. 1988;67(1):49-57.
233. Kapoor S, Das G, Varshney U. Crucial contribution of the multiple copies of the initiator tRNA genes in the fidelity of tRNA(fMet) selection on the ribosomal P-site in *Escherichia coli*. Nucleic Acids Res. 2011;39(1):202-12.
234. Garcia-Pino A, Balasubramanian S, Wyns L, Gazit E, De Greve H, Magnuson RD, *et al*. Allostery and intrinsic disorder mediate transcription regulation by conditional cooperativity. Cell. 2010;142(1):101-11.
235. Jensen RB, Grohmann E, Schwab H, Diaz-Orejas R, Gerdes K. Comparison of *ccd* of F, *parDE* of RP4, and *parD* of R1 using a novel conditional replication control system of plasmid R1. Mol Microbiol. 1995;17(2):211-20.
236. Shim DH, Suzuki T, Chang SY, Park SM, Sansonetti PJ, Sasakawa C, *et al*. New animal model of shigellosis in the Guinea pig: its usefulness for protective efficacy studies. J Immunol. 2007;178(4):2476-82.
237. Fernandez MI, Thuizat A, Pedron T, Neutra M, Phalipon A, Sansonetti PJ. A newborn mouse model for the study of intestinal pathogenesis of shigellosis. Cell Microbiol. 2003;5(7):481-91.
238. Sevin EW, Barloy-Hubler F. RASTA-Bacteria: a web-based tool for identifying toxin-antitoxin loci in prokaryotes. Genome Biol. 2007;8(8):R155.
239. Wilbur JS, Chivers PT, Mattison K, Potter L, Brennan RG, So M. *Neisseria gonorrhoeae* FitA interacts with FitB to bind DNA through its ribbon-helix-helix motif. Biochemistry. 2005;44(37):12515-24.
240. Winther KS, Gerdes K. Ectopic production of VapCs from *Enterobacteria* inhibits translation and trans-activates YoeB mRNA interferase. Mol Microbiol. 2009;72(4):918-30.
241. Silva RM, Saadi S, Maas WK. A basic replicon of virulence-associated plasmids of Shigella spp. and enteroinvasive *Escherichia coli* is homologous with a basic replicon in plasmids of IncF groups. Infect Immun. 1988;56(4):836-42.
242. Ishii S, Kuroki K, Imamoto F. tRNAMetf2 gene in the leader region of the *nusA* operon in *Escherichia coli*. Proc Natl Acad Sci U S A. 1984;81(2):409-13.
243. Mandal N, RajBhandary UL. Escherichia coli B lacks one of the two initiator tRNA species present in *E. coli* K-12. J Bacteriol. 1992;174(23):7827-30.
244. Pupo GM, Lan R, Reeves PR. Multiple independent origins of *Shigella* clones of *Escherichia coli* and convergent evolution of many of their characteristics. Proc Natl Acad Sci U S A. 2000;97(19):10567-72.
245. Chaudhuri RR, Henderson IR. The evolution of the *Escherichia coli* phylogeny. Infect Genet Evol. 2012;12(2):214-26.
246. Zuo G, Xu Z, Hao B. *Shigella* strains are not clones of *Escherichia coli* but sister species in the genus *Escherichia*. Genomics Proteomics Bioinformatics. 2013;11(1):61-5.
247. Samhita L, Nanjundiah V, Varshney U. How many initiator tRNA genes does *Escherichia coli* need? J Bacteriol. 2014;196(14):2607-15.
248. Kenri T, Imamoto F, Kano Y. Construction and characterization of an *Escherichia coli* mutant deficient in the *metY* gene encoding tRNA(f2Met): either tRNA(f1Met) or tRNA(f2Met) is required for cell growth. Gene. 1992;114(1):109-14.
249. Walling LR, Butler JS. Structural Determinants for Antitoxin Identity and Insulation of Cross Talk between Homologous Toxin-Antitoxin Systems. J Bacteriol. 2016;198(24):3287-95.

250. RajBhandary UL. Initiator transfer RNAs. J Bacteriol. 1994;176(3):547-52.
251. Robertus JD, Ladner JE, Finch JT, Rhodes D, Brown RS, Clark BF, *et al*. Structure of yeast phenylalanine tRNA at 3 A resolution. Nature. 1974;250(467):546-51.
252. Kim SH, Sussman JL, Suddath FL, Quigley GJ, McPherson A, Wang AH, *et al*. The general structure of transfer RNA molecules. Proc Natl Acad Sci U S A. 1974;71(12):4970-4.
253. Quigley GJ, Rich A. Structural domains of transfer RNA molecules. Science. 1976;194(4267):796-806.
254. Crothers DM, Cole PE, Hilbers CW, Shulman RG. The molecular mechanism of thermal unfolding of *Escherichia coli* formylmethionine transfer RNA. J Mol Biol. 1974;87(1):63-88.
255. Daniel WE, Jr., Cohn M. Changes in tertiary structure accompanying a single base change in transfer RNA. Proton magnetic resonance and aminoacylation studies of *Escherichia coli* tRNAMet f1 and tRNAMet f3 and their spin-labeled (s4U8) derivatives. Biochemistry. 1976;15(18):3917-24.
256. Laursen BS, Sorensen HP, Mortensen KK, Sperling-Petersen HU. Initiation of protein synthesis in bacteria. Microbiol Mol Biol Rev. 2005;69(1):101-23.
257. De Bie LG, Roovers M, Oudjama Y, Wattiez R, Tricot C, Stalon V, *et al*. The *yggH* gene of *Escherichia coli* encodes a tRNA (m7G46) methyltransferase. J Bacteriol. 2003;185(10):3238-43.
258. Alexandrov A, Chernyakov I, Gu W, Hiley SL, Hughes TR, Grayhack EJ, *et al*. Rapid tRNA decay can result from lack of nonessential modifications. Mol Cell. 2006;21(1):87-96.
259. Robertson JM, Kahan M, Wintermeyer W, Zachau HG. Interactions of yeast tRNAPhe with ribosomes from yeast and *Escherichia coli*. A fluorescence spectroscopic study. Eur J Biochem. 1977;72(1):117-25.
260. Lill R, Robertson JM, Wintermeyer W. tRNA binding sites of ribosomes from *Escherichia coli*. Biochemistry. 1984;23(26):6710-7.
261. Senissar M, Manav MC, Brodersen DE. Structural conservation of the PIN domain active site across all domains of life. Protein Sci. 2017;26(8):1474-92.
262. Saavedra De Bast M, Mine N, Van Melderen L. Chromosomal toxin-antitoxin systems may act as antiaddiction modules. J Bacteriol. 2008;190(13):4603-9.
263. van den Beld MJ, Reubsaet FA. Differentiation between *Shigella*, enteroinvasive *Escherichia coli* (EIEC) and noninvasive *Escherichia coli*. Eur J Clin Microbiol Infect Dis. 2012;31(6):899-904.
264. Varshney U, Lee CP, RajBhandary UL. From elongator tRNA to initiator tRNA. Proc Natl Acad Sci U S A. 1993;90(6):2305-9.
265. Kapp LD, Kolitz SE, Lorsch JR. Yeast initiator tRNA identity elements cooperate to influence multiple steps of translation initiation. RNA. 2006;12(5):751-64.
266. Dupont N, Lacas-Gervais S, Bertout J, Paz I, Freche B, Van Nhieu GT, *et al*. *Shigella* phagocytic vacuolar membrane remnants participate in the cellular response to pathogen invasion and are regulated by autophagy. Cell Host Microbe. 2009;6(2):137-49.
267. Pinaud L, Samassa F, Porat Z, Ferrari ML, Belotserkovsky I, Parsot C, *et al*. Injection of T3SS effectors not resulting in invasion is the main targeting mechanism of *Shigella* toward human lymphocytes. Proc Natl Acad Sci U S A. 2017;114(37):9954-9.